INTERNATIONAL HYDROLOGICAL PROGRAMME

Ecohydrological processes in small basins

Sixth Conference of the European Network of Experimental and Representative Basins (ERB) Strasbourg (France), 24-26 September 1996

IHP/UNESCO - ERB - CEREG (ULP/CNRS)

PROCEEDINGS

Edited by

D. Viville
and
I.G. Littlewood

IHP-V | Technical Documents in Hydrology | No. 14
UNESCO, Paris, 1997

SC-97/WS/83

Preface

To mark the tenth anniversary of the Experimental and Representative Basin (ERB) Network, it is timely to give a brief review of ERB achievements before introducing the Proceedings of the Strasbourg Conference. The ERB Network was founded in 1986. The main aims of the Network are to bring together European scientists involved in catchment and hydrological processes research, to stimulate the exchange of information and results, and to encourage co-operation in research projects. Pursuit of these objectives is achieved through biennial ERB Conferences, the publication of a biannual Newsletter and the maintenance of a register of ERB catchments (ICARE — see later) operated by participating countries for long-term water balance studies and research into physical, hydrogeochemical and ecohydrological processes. Much of the work of ERB relates to small natural catchments but the development of methods for measuring, monitoring and assessing the impacts of environmental changes (e.g. afforestation, acidification, climate, land-use) on ecohydrological processes and systems at larger scales is a motivation for many of the projects carried out in ERB basins.

For the tenth anniversary of the ERB Network, which was founded in Aix en Provence in 1986, it was most appropriate that the Conference returned to France. Previous Conferences were:

- Aix-en-Provence (F), October 1986;
- 'Erosion and sediment transport', Perugia (I) October 1988 (Proceedings published in: Quad. Idronomia Montana [Special Issue], A.I.D.I., Fac. Di Agraria Univ. Padova);
- 'Hydrological research basins and the environment', Wageningen (NL) September 1990 (TNO Comm. on Hydrol. Res., Proc. and Informat. no. 44, The Hague, 347 pp);
- 'Methods of hydrological basin comparison', Oxford (UK) September 1992 (Institute of Hydrology Rep. no. 120, Wallingford, 198 pp);
- 'Assessment of hydrological temporal variability and changes', Barcelona (SP) September 1994 (Acta Geol. Hisp. [Special Issue] vol. 28 no. 2-3 [1993], Barcelona, 138 pp).

Copies of the Wageningen, Oxford and Barcelona conference proceedings are still available on request.

Each participating country provides a National Correspondent for the ERB whose nomination is supported and confirmed by the relevant Unesco International Hydrological Programme (IHP) Committee. Currently, the team of National Correspondents comprises:

Belgium	F. de Troch
Czech Republic	M. Tesar
France	D. Viville
Germany	A. Herrmann (ERB Coordinator, 1994 - 1998)
Italy	V. Anselmo
Poland	B. Wiezik
Romania	P. Mita
Russia	S. Zhuravin
Slovakia	P. Miklanek
Spain	F. Gallart
Switzerland	M. Spreafico
The Netherlands	P.Warmerdam
United Kingdom	I.G. Littlewood

The ERB Newsletter is published approximately twice yearly and distributed widely among hydrologists throughout Europe. The Newsletter provides information about national and international activities, projects, research findings and publications, as well as progress with the ERB Inventory of Catchments for Research in Europe (ICARE). ICARE provides a computer database of ERB Network basins (currently about 100 catchments in 13 countries), including their physical characteristics, instrumentation, available data, research aims and key publications. The database is maintained and continually updated by CEMAGREF in Lyon, France with information provided by the National Correspondents. Details of ICARE and ERB are available from http://wwwhh.lyon.cemagref.fr.

ERB Conference "Ecohydrological Processes in Small Basins"

These proceedings include 30 papers out of 29 oral and 15 poster presentations at the conference which were all invited for inclusion in this volume. The contributions cover current research carried out across south-west to Central Europe on ecohydrological processes in small basins and related topics. They focus mainly on the monitoring and modelling of soil-atmosphere interactions, runoff generation processes and water pathways, and water quality and hydrobiogeochemical behaviour at small basin scale. In this context, regionalisation and scale effects remain important unsolved problems which are frequently being discussed here, and probable effects of climate change on hydrological behaviour and mass budgets also. Accordingly, the selected Conference results published here largely fit many relevant discussions undertaken elsewhere, but they strictly concentrate on the process scale, with preference of both agricultural and forested basins. The main examples come from Spain, southern France, and Central Europe. ERB Network is encouraging working groups to get into contact and co-operate on joint scientific problems. Therefore, it is hoped that these Proceedings are of broad interest and help to establish new contacts. It may also encourage contributions to the next ERB Conference, "Catchment Hydrological and Biogeochemical Processes in Changing Environment", to be held in Liblice, Czech Republic, September 22-24, 1998.

Finally, I should like to thank the local organisers of the Conference from CEREG-CNRS at Louis Pasteur University in Strasbourg, including the scientific and technical staff for the excellent organisation, and especially Daniel Viville who played his co-ordinating role perfectly, and was always a most co-operative counterpart. These proceedings were possible due to the commendable efforts of authors, referees and of course of both co-editors Daniel Viville, Strasbourg and Ian Littlewood of the Institute of Hydrology in Wallingford.

Andreas Herrmann, ERB Coordinator (1994-1998)

Note from the Editors

These Proceedings comprise 30 papers presented orally as either full Papers or Posters at the Sixth Conference of the Experimental and Representative Basin (ERB) network, "Ecohydrological Processes in Small Basins", Strasbourg, September 24th - 26th, 1996. The Papers are grouped under four broad thematic headings corresponding to the four Sessions of the Conference:

Evapotranspiration components and modelling;
Surface water quality;
Runoff formation, discharge generation and water pathways; and
Runoff modelling.

Manuscripts were refereed for their technical and scientific suitability for publication by the Chairman of the Session in which the Paper or Poster was presented orally at Conference. The Editors are greatly indebted to the following Session Chairman for undertaking the review procedure:

A. Herrmann, Technical University, Braunschweig, Germany;
P.M.M. Warmerdam, Wageningen Agricultural University, The Netherlands;
P. Chevalier, ORSTOM, France; and
P. Miklanek, Institute of Hydrology SAS, Slovakia.

After the technical and scientific review of the Papers, the Editors prepared the Proceedings for camera-ready printing and publication by Unesco. Readers of the Proceedings are requested to bear in mind that the Papers are all by authors whose first language is not English. While this is a noteworthy achievement in itself, the Editors believe that the authors might agree that the written English was better in some manuscripts than in others. Editing for the readability of the written English was undertaken without returning the manuscripts to authors for final proof-reading, spending about the same amount of time on each Paper. While care has been taken to introduce a uniformity of style throughout the Proceedings, the editorial result may still be a little uneven in places. If, for example, non-standard phrases are still encountered in the Proceedings, readers are requested to bear in mind the practical limits on resources which could be made available for such aspects of preparing the Papers for publication. Any technical errors introduced at this stage of preparation of the Proceedings are the responsibility of the Editors.

Ian G. Littlewood, Institute of Hydrology, Wallingford, UK
Daniel Viville, CEREG (CNRS - Louis Pasteur University), Strasbourg, France

Contents

Evapotranspiration components and modelling

Surface water quality

Runoff formation, discharge generation, water pathways

Runoff modelling

Monitoring evapotranspiration and interception from grassland and forest patches overgrown in abandoned terraces at the Cal Parisa basin

P. Llorens, M. Abril, M.C. Salvany, R. Poch and F. Gallart

Institute of Earth Sciences, Barcelona, Spain

1. Introduction

The main geoecological adjustment observed in Mediterranean mountainous areas following the abandonment of agricultural lands is afforestation. The impact of this land cover change on water resources has not been sufficiently considered.

There is agreement among authors that forest cover gives higher water losses to the atmosphere than grassland (Bosch and Hewlett, 1982). Nevertheless, most of these studies were performed in temperate humid areas, with rainfall and weather regimes very different from Mediterranean ones.

The Cal Parisa basin, within the Vallcebre Experimental Catchment (ERBES030), was selected as representative of abandoned agricultural fields in Mediterranean mountainous areas (Llorens and Gallart, 1992). The climate is Mediterranean mountainous, with a mean annual precipitation of 850 mm and a mean annual temperature of about 9°C. After abandonment of agricultural fields spontaneous afforestation by scattered patches of pines has occurred increasing the forested area from 5% to 25% in the last 20 years.

One of the main purposes of the study at the Vallcebre catchments is to evaluate the consequences of land cover change on water resources in Mediterranean mountainous areas. The method used has two steps:

(a) analysis of the differences in water losses to the atmosphere between grassland and forest; and

(b) the development of techniques to generalize these results for modelling purposes.

2. Monitoring design and data obtained

Since 1989, the Cal Parisa basin has had a pluviometric and hydrological network comprising four rain recorders, one meteorological station and two hydrometric stations at the sub-catchment outlets.

Since 1992, soil water content profiles have been instrumented with six TDR stations (Rabadà, 1995). Each one has four probes at different depths below the soil surface (0-20cm, 20-40cm, 40-60cm and 60-80cm) that are read every week. Since 1995, these water content records are complemented with soil matric potential measurements following the filter paper method (Hamblin, 1981), and since 1996 these records are complemented with tensiometric measurements.

Two experimental plots were set up in 1993 to study hydrological processes in two representative areas.

(i) The grassed plot is located in an agricultural abandoned terrace, in the central part of the basin, and covered by mesophile grass. At this plot we can perform detailed analysis, at 5-minute steps, of the energy fluxes of the surface: net radiation, soil heat flux, sensible heat flux and latent heat flux,

allowing calculation of the actual evapotranspiration rates using the Bowen Ratio Energy Balance method (Bowen, 1926). The monitoring of complementary micrometeorological data at this plot (windspeed at 2 m and 10 m, albedo and soil temperature) allows calculation of potential and actual evapotranspiration rates using the Penman-Monteith method (Monteith, 1965) for hydrological modelling purposes.

(ii) The forested plot is located on a steep hillslope, covered by a dense monospecific *Pinus sylvestris* forest patch of overgrowth since earlier abandonment. Sets of rain recorders, throughfall collectors, stemflow rings and canopy wetness sensors are used to monitor forest rainfall interception (Llorens *et al.*, in press). Six trees are monitored to measure transpiration using Granier's (1985) sapflow measurement technique.

At the forested plot we record, at 5-minute steps, the water fluxes in the forest canopy which are necessary to determine the interception process; bulk precipitation, throughfall and stemflow. At this station we also perform detailed analysis, at 15-minute steps, of sapflow flux to determine the forest transpiration. The combination of the measured interception and transpiration rates give us information about the actual evapotranspiration rates of the forest patch.

(iii) In order to estimate the soil water available for the plants, as well as a field soil retention curve for each experimental plot, complementary measurements are made weekly with TDR, filters and tensiometers. These results are useful to complete the water balance and to check the information provided by the other methods.

3. Results

To illustrate the evaporative behaviour of the grassed and forested covers, periods of 20 days at the end of the summer (August 23 to September 11) for two consecutive years were selected as representative of different soil water content conditions. 1994 (Fig. 1) had an important drought during summer, as can be observed at the beginning of the selected period. 1995 (Fig. 2) had uncommon wet conditions during August.

The top graphs in Figs 1 and 2 show the following:

(a) Total bulk rainfall was 154 mm for the 1994 period and 191 mm for the 1995 period. Total interception losses were 21 mm in 1994 and 32 mm in 1995 representing 14% and 17% of total bulk rainfall respectively. These interception loss rates are representative of Mediterranean summer showers, characterized by short duration, high rainfall intensities and dry atmospheric conditions (Llorens *et al.*, in press).

(b) The evolution of soil water content during the two selected periods is representative of its observed behaviour for longer periods (Rabadà, 1995), and is characterized by a water content higher in the grassed plot than in the forested one, due to differences in the topographic situations, soil characteristics and interception losses.

In 1994, with drier soil conditions, differences in soil water content between the grassed and the forested plots are small (maximum differences are of about 20 mm). This period starts with a water content of about 200 mm for the two experimental plots and increases, after the summer showers, to about 340 mm for the two plots.

The same period in 1995 starts with a water content of about 310 mm in the grassed plot and 240 mm in the forested plot. The water content varies during the studied period following the rainfall inputs, but maintaining a difference of about 70 mm between the two plots (except for the measurement on August 23 where field observations indicated that greater differences are related to over-saturation conditions on the grassed plot).

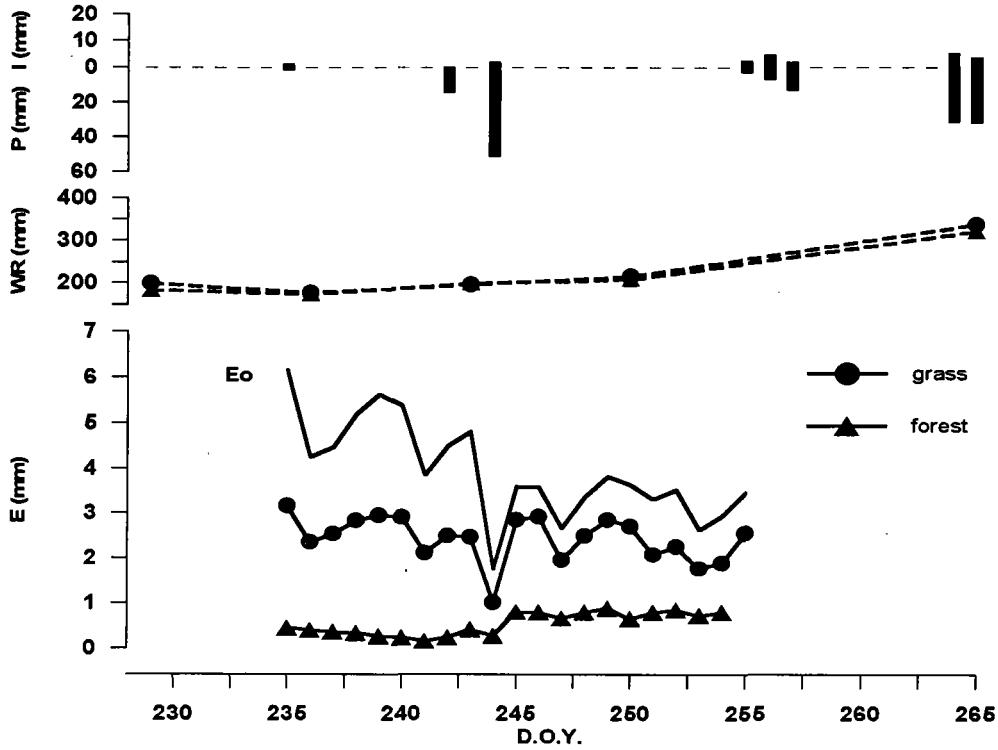

Figure 1: For the period 23 August - 11 September 1994. Top: rainfall and interception. Middle: soil water reserve for the grassed and the forested plots. Bottom: daily reference evapotranspiration and actual evapotranspiration for the same plots.

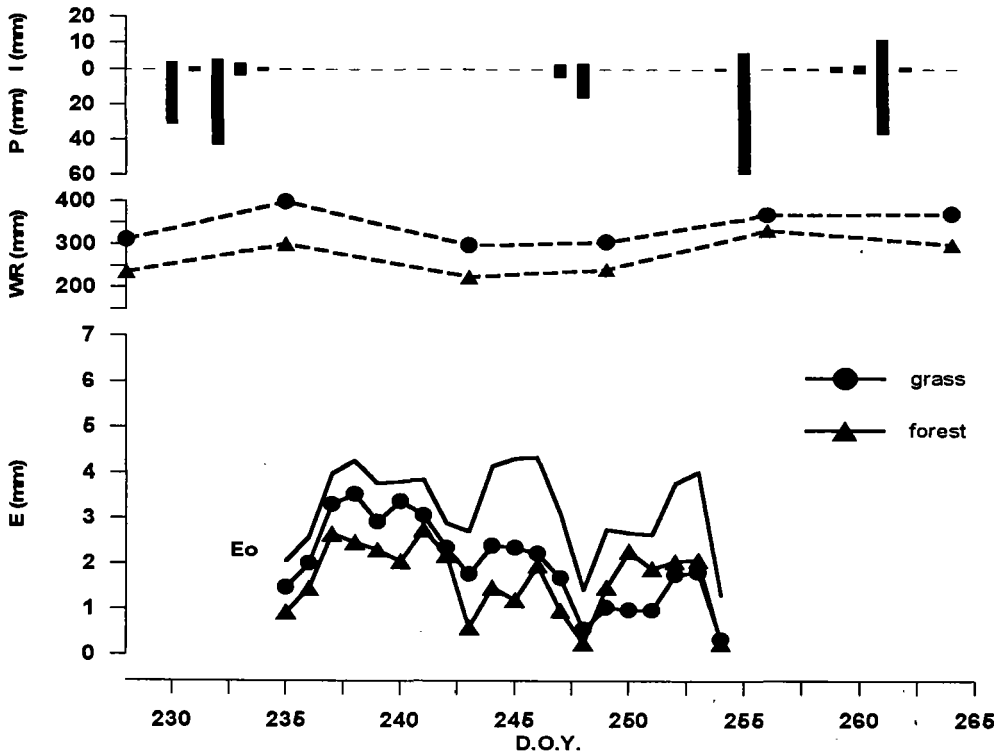

Figure 2: For the period 23 August - 11 September 1995. Top: rainfall and interception. Middle: soil water reserve for the grassed and the forested plots. Bottom: daily reference evapotranspiration and actual evapotranspiration for the same plots.

The bottom graphs in Figs 1 and 2 show the following for the studied periods:

(a) The mean daily reference evapotranspiration was 3.9 mm day^{-1} for 1994 and 3.2 mm day^{-1} for 1995. In 1994 it is possible to distinguish two periods: 23rd to 31st August, when mean daily reference evapotranspiration is about 5 mm day^{-1}; and 2nd to 11th September, when this value falls to 3.3 mm day^{-1}, similar to those registered in 1995.

(b) Mean actual evapotranspiration for grassland was 2.4 mm day^{-1} in 1994 and 2.0 mm day^{-1} in 1995, and the forest one was 0.6 mm day^{-1} and 1.7mm day^{-1}, respectively.

The results show that grassland is less sensitive to changes in soil water conditions than forest. Differences in mean grass actual evapotranspiration between the dry period in 1994 and the wet periods (in 1994 and 1995) are not significant, and its daily variability is mainly due to changes in evaporative demand.

In contrast, forest transpiration shows a low daily rate during the 1994 dry period, which more than doubles after the rain event of the 1st September. In the wet 1995 period, values are three times greater than corresponding values in 1994.

4. Discussion and conclusions

The water balance of the two observed periods allow us to describe the evapotranspiration behaviour of each kind of vegetation cover. The main differences observed between grassland and forest cover can be synthesized as follows:

It is interesting to note the importance of the interception process since it represents 15% of rainfall entering the system which will not be useful for vegetation. The mean interception loss for a whole year is 24%, and the values obtained for the studied periods are low due to the characteristics of the summer showers (Llorens *et al.*, in press).

The differences in soil water content between the grassed terrace and the forest patch during wet and dry periods are not of the same magnitude. During dry periods the difference in soil water content under both vegetation covers is not significant but the difference increases significantly during wetter periods.

Finally, it is important to consider the low sensitivity of grass to soil water stress and the significant response of the forest to the dryness of soils. For example during the 1994 dry period the forest was able to reduce transpiration by a factor of more than two, while the grass was not able to reduce transpiration at all. The forest water loss control acted also after the rainfall events. Even if forest transpiration increased, the daily values reflect the stress to which the trees have been subjected. This marked differences in tree transpiration shows the importance of the physiological control over water losses that can be performed by trees.

The selected examples presented here have allowed a detailed description of the differences in water losses to the atmosphere between grassed and forested areas, and can therefore assist in understanding the consequences of the reforestation of Mediterranean mountainous abandoned lands.

References

BOSCH, J.M. and J.D. HEWLETT (1982) 'A review of catchment experiments to determine the effect of vegetation changes on water yield and evapotranspiration'. *J. of Hydrology.*, 55: 3-23.

BOWEN, I.S. (1926) 'The ratio of heat losses by conduction and by evaporation from any water surface'. *Phys. Rev.*, 27: 779-787.

GRANIER, A. (1985) 'Une nouvelle méthode pour la mesure du flux de sève brute dans le tronc des arbres'. *Ann. Sci. For.*, 42(2): 193-200.

HAMBLIN, A.P. (1981) 'Filter-paper method for routine measurement of field water potential'. *Journal of Hydrology*, 53: 355-360.

LLORENS, P. and F. GALLART (1992) 'Monitoring a Small Basin Response in a Mediterranean Mountainous Abandoned Farming Area: Research Design and Preliminary Results'. *Catena* 19: 309-320.

LLORENS, P. , R. POCH, J. LATRON and F. GALLART (in press) 'Rainfall interception by a Pinus sylvestris forest patch overgrown in a Mediterranean mountainous abandoned area. Monitoring design and results down to the event scale'. *J. of Hydrol.*

MONTEITH, J.L. (1965) 'Evaporation and the environment'. In: State and movement of water in living organisms. *Symp. Soc. Ex. Biol.*, 19: 205-234.

RABADÀ, D. (1995) 'Dinàmica hidrològica d'una petita conca pirinaica de camps abandonats amb pinedes en expansió (Alt Berguedà, Barcelona)'. *Unpublished Ph. D. Thesis,* Universitat de Barcelona, 322p.

A new concept for canopy water storage simulation in a 30-years old spruce stand (Strengbach catchment, Vosges, France)

L. Pfister, D. Viville, G. Najjar, P. Biron, S. Richard and L. Fischer

Centre for Eco-Geographical Research Studies, Strasbourg, France

1. Introduction

The aim of this study is to obtain a better understanding of canopy storage dynamics in a spruce stand in the Strengbach catchment situated in the Vosges mountains, France. The main focus is on the relationship between throughfall and water stored on the canopy. In this context, a canopy water balance has been established. First, the balance was based on measurements made in the spruce stand. The influence of various factors such as wind speed or evapotranspiration on canopy drainage has been investigated. The water balance has been simulated by the means of a Rutter-type model that was mainly based on the use of a variable canopy storage concept. A balance based on measurements has been used to validate the simulated canopy water balance.

2. Site description and measurements

The study was undertaken in a 25 to 30-years old spruce stand in the Strengbach catchment (near Aubure, in the French Vosges mountains, 48°12'N and 7°12'E). Located at an altitude between 883 and 1146 m, this catchment receives a yearly rainfall input that varies from 1100 to 1600 mm (Viville *et al.*, 1993). The catchment is covered with conifers (80%) and beech (20%).

Measurements were made on a 322 m^2 plot, characterized by a density of 3400 trees ha^{-1} with a mean height of 12 m. Gross rainfall was measured by a tipping bucket pluviometer. Incident rainfall measurements are thus available every 30 minutes. Throughfall was collected by two gutters, each 4 m long and 0.125 m wide. The throughfall collected by this 1 m^2 area, and the stemflow captured by spiral gutters fixed at 1.3 m above the soil on 6 different trees, were connected to tipping bucket pluviometers. Both throughfall and stemflow data were recorded on a datalogger. Meteorological parameters (temperature, relative humidity, wind speed, global radiation) were measured on a 30 m high tower, situated close to the stand.

3. Results

3.1 Canopy water storage balance

Interception is mainly dependent on the amount of water already stored on the canopy. Quantifying interception requires the calculation of a balance of water input (incident rainfall) and output (throughfall, stemflow and evapotranspiration) for the canopy reservoir. In order to study the evolution of the water storage on the canopy, its level was determined every 30 minutes. As a balance of the real water quantities stored on the canopy is to be determined here, a couple of equipoise coefficients for incident rainfall, throughfall and stemflow are introduced. These coefficients are determined by the means of a method developed by Rutter *et al.* (1971). According to this method, a relationship between

incident rainfall and throughfall (and eventually stemflow) has to be characterized by a mathematical equation. The slope of the equation (a*x + b), named "a", helps to determine the equipoise coefficient "p": p = 1 - a.

The amount of water stored on the canopy at time t may be determined by Eq. (1).

$$storage_{(t)} = storage_{(t-1)} + p * Pi - [(Eg+Ect)-a * Pi] - (storage_{(t-1)}/Cs) * Ep \quad (1)$$

In Eq. (1): $storage_{(t)}$ and $storage_{(t-1)}$ are the total amount of water stored on the canopy (mm) at times (t) and half an hour ago (t-1) respectively; Pi is the gross incident rainfall (mm); Eg is throughfall (mm); Ect is stemflow (mm); Cs is canopy storage capacity (mm); Ep is potential evapotranspiration (mm); a is a coefficient for throughfall counterbalancing; and p is a coefficient for incident rainfall counterbalancing.

As the method only takes into account isolated amounts of rainfall that total at most the canopy storage capacity, the latter also has to be determined. For the studied spruce stand, the total amount of water intercepted by the previously completely dry canopy has been determined for several isolated rainstorms and can reach a maximum value of 6 mm (Biron, 1994; Pfister, 1995). The setting up of the canopy storage balance also requires evapotranspiration values to account for that major canopy drainage mechanism.

The study of the evolution of the water storage on the canopy from September 6th to 16th of 1994 has shown the role of at least one external factor influencing the canopy water balance (Fig. 1). Evapotranspiration, by emptying the water storage progressively. After having reached 14 mm on September 9th, intercepted water has been progressively evaporated from September 9th to 10th, as suggested by the high vapour pressure deficit values.

Canopy storage often was significantly greater than the theoretical canopy storage capacity (up to 8 mm above the canopy storage capacity fixed at 6 mm, on September 9th). From this point of view, the basic concept of a non-variable canopy storage capacity had to be revised. As a matter of fact, water quantities stored on the canopy pointed out the possibility of a maximum canopy storage variable in time. Without a variable maximum canopy storage, the water quantities stored on the canopy during the year of 1994 would not have been likely.

The new concept of canopy storage, proposed in this paper, is based on a temporally variable maximum storage. During an isolated rainfall event, the upper part of the canopy will be saturated. Once the canopy storage capacity has been reached, throughfall and stemflow appear. After the rain has stopped, the intercepted water is partially evaporated, while another fraction of it will move to lower sections of the canopy. The upper part of the canopy will then be able to intercept new rainfall again. By this, real water quantities stored by the canopy will be much more important than those assigned by the theoretical canopy storage capacity. As determined by a series of isolated rainfall events, canopy storage capacity induces a considerable error in the estimation of real maximum canopy water storage.

3.2 Modelling canopy storage balance

Simulation of canopy storage is supposed to permit a better understanding of the different processes that are guiding interception. For this simulation procedure, the main outlines of the Rutter (1971) interception model have been used. Based on canopy water storage, throughfall had to be simulated. The relationship between throughfall and canopy water storage has thus been introduced into the canopy storage model in terms of an equation.

In its application, this simulation reaches its limits very rapidly. The most important problem encountered was due to the weakness of the model in simulating storage significantly greater than the predefined canopy storage capacity. As the simple evaluation of canopy storage by means of measured values of gross rainfall, throughfall and evaporation has shown, canopy storage can exceed the theoretical canopy storage capacity. The simulation was limited by the non-variable canopy storage capacity that imposed a massive drainage of the canopy every time that this limitation was reached.

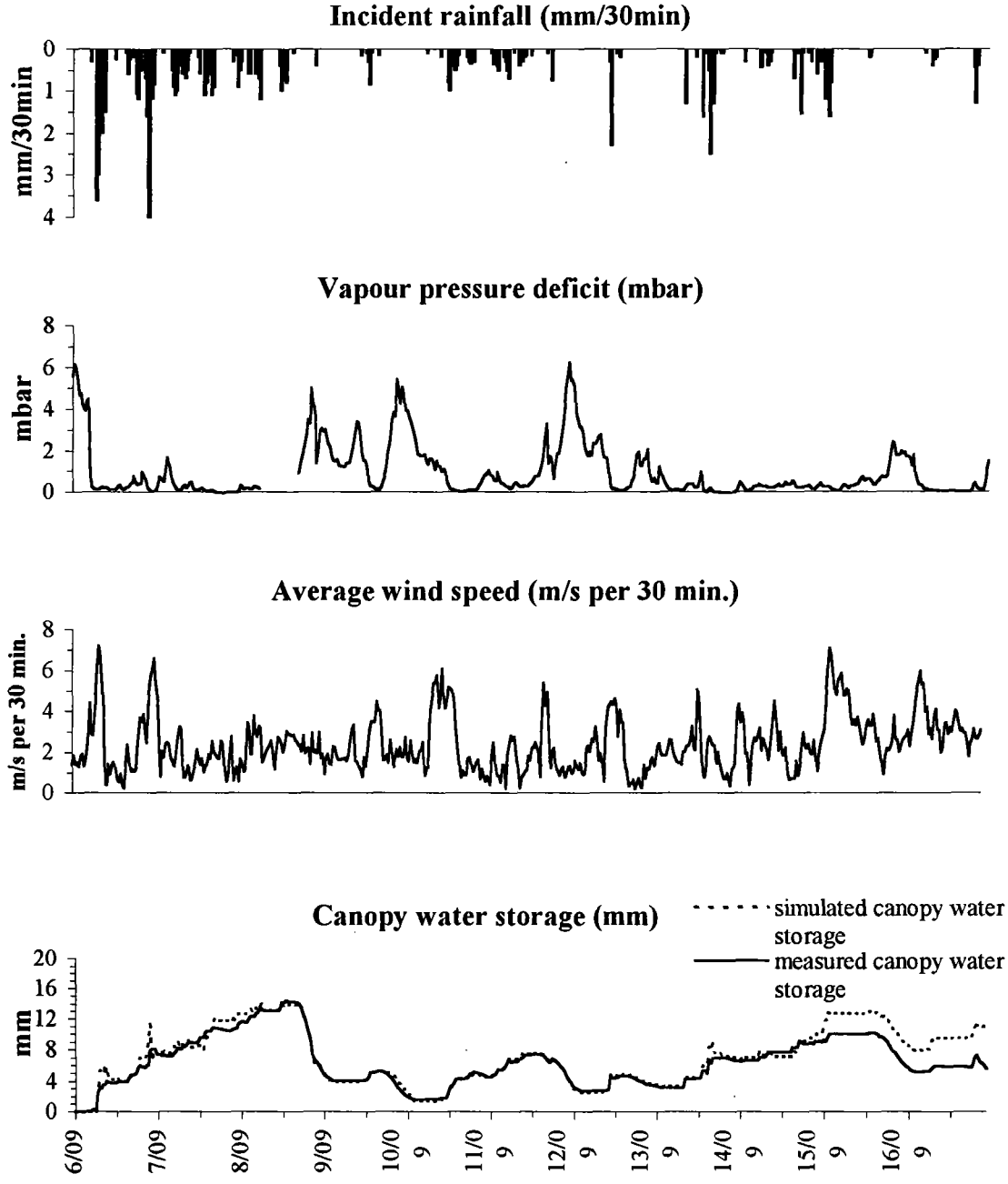

Figure 1: Incident rainfall, vapour pressure deficit, average wind speed and canopy water storage from September 6th to 16th.

The relationship between gross rainfall, canopy storage and drainage was then re-examined. It is very important to note here that the non-variable storage capacity of 6 mm has been established by the means of a series of isolated rainstorms, with a completely dry canopy at the beginning of each of these storms. So it can be said that this storage capacity is only representative of cases with very restricted conditions. But, in reality there might be a couple of rainstorms, separated by only a few minutes, so that the canopy is rarely completely dry. It is noted here that in order to analyse canopy storage dynamics, Jetten (1995) introduced a multi-level canopy reservoir concept. In this study concerning the Strengbach spruce stand, the drainage mechanism has been considered as being directly dependent on canopy storage values as well as rainfall sequences.

Considering the volume of intercepted water by the spruce canopy (up to 14 mm), the throughfall mechanism had first to be expressed in terms of the canopy storage. Thus, a relationship between water stored on the canopy and throughfall was established. For this purpose, data for the

period September 6th to 9th were chosen, because of the abundance of successive rainfall such that a complete drying up of the canopy did not occur.

At a 30 minute time step a classification of throughfall has been established in terms of canopy storage values, incident rainfall and wind speed. A representation of throughfall in terms of canopy storage was set up. In order to point out general tendencies, mean throughfall values were established for successive canopy storage classes of 0.5 mm width. This calculation was undertaken only for rainfall intensities between 0 and 4 mm/30 min. and wind speed less than 2 m/s in order to consider only throughfall generated by the filling up of the canopy reservoir and not by any external factors such as strong wind blasts. As shown by Fig. 2, four curves relating throughfall and canopy storage have thus been derived.

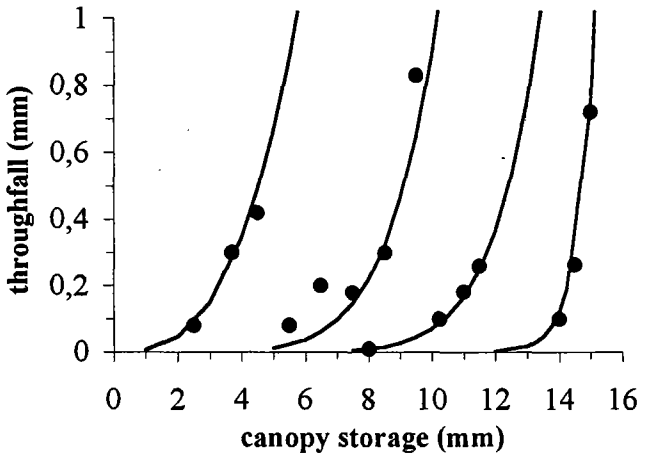

Figure 2: Measurement and adjustment of throughfall.

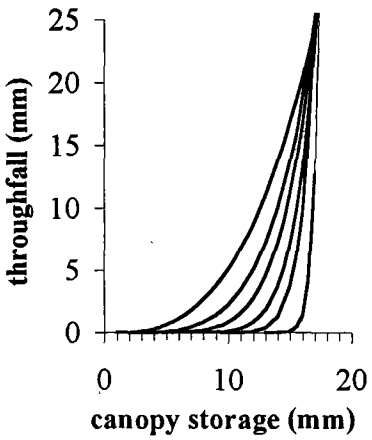

Figure 3: Extrapolation.

The results of this study indicate that there is a temporal variability of canopy storage capacity. Between two rainfall events, there might be enough time to drain the upper part of the canopy, in order to permit a partial interception of the rain that is falling on the canopy. Drainage towards the lower parts of the canopy, as well as the partial evaporation of the intercepted water, would enlarge considerably the canopy storage capacity, while the total amount of water stored on the canopy would be distributed in the lower parts of the canopy.

Until now, only four equations are available, valid for the period from September 6th to 9th. The next step was to find an expression of the variable storage capacity concept in terms of only one throughfall simulation equation which is valid for a large number of different rainfall events.

By extrapolating these curves for very high storage values, it appeared that they join for a canopy storage of about 17 mm and a throughfall of approximately 25 mm (Fig. 3). Of course, these values have absolutely no physical significance, each equation being valid only for a restricted amount of canopy storage. But nevertheless, the junction of those throughfall equations suggests that there is a link between them. It appears that there is a progressive evolution of the different parameters of a power type equation of the form given by Eq. (2), in which parameters c and d vary progressively

$$\text{throughfall}_{(t)} = c * x^{d}_{(t-1)}, \qquad (2)$$

By means of the four existing throughfall simulation equations a relationship between the evolution of both parameters (c and d) and the canopy storage was found. Consequently, having a given canopy storage, the coefficients c and d for the throughfall equation can be determined and thus the corresponding throughfall.

At this point, it is now possible to simulate the throughfall for a given rainfall input and previous canopy storage at any moment. In equation (1), throughfall (Eg) is thus replaced by the right hand side of Eq. 2.

$$\text{throughfall}_{(t)} = c * \text{storage}^{d}_{(t-1)} \quad (3)$$

It is now possible to simulate the dynamics of the canopy storage by means of only two different input variables; incident rainfall (input) and evapotranspiration (loss). The throughfall mechanism, which is a major component of the canopy water balance, is entirely simulated by equation (3).

As shown by the comparison between the simulated and the measured canopy storage evolution, the simulation was satisfactory (Fig. 1). Throughfall clearly appeared to be dependent on the dynamics of the water stored on the canopy, in the sense that the migration of intercepted rainwater to the lower parts of the canopy permits successive interception phases during a series of closely related rainstorms. Nevertheless, this simulation has also clearly shown at least one application limit in case of strong wind blasts. Indeed, on September 6th, 7th and 15th, strong wind blasts caused significant water quantities to fall down the canopy. This process which causes important throughfall values had already been described as a major drainage mechanism by Pook *et al.* (1991). Each time that there was high wind speeds, the canopy water storage was significantly over-estimated by the simulation (Fig. 1). As the simulation does not take into account the influence of strong wind blasts on the drainage mechanism, the important throughfall values that had occurred on September 6th, 7th and 15th, have not been calculated.

It can finally be said that the simulation gives a very good indication of the canopy storage evolution. Canopy drainage dynamics in terms of throughfall are estimated well by the simulation. The only severe restriction in the application of the simulation is due to high wind speeds.

4. Conclusion

The concept of a variable storage capacity thus appears to be a plausible explanation for canopy storage values exceeding largely the previously determined storage capacity of 6 mm. The comparison between measured and simulated canopy storage presented in this paper has clearly outlined the major influence of external factors (wind speed and rainfall intensity) on the throughfall process.

In the Strengbach spruce stand study, throughfall and canopy storage capacity turned out to be linked strongly. For two different periods, the dynamics of both the variable canopy storage capacity and throughfall have been clearly outlined. The use of several throughfall equations has permitted the simulation of the progressive drying-up of the canopy summit between two successive rainfall events. Intercepted water migrates progressively towards the lower parts of the canopy. The canopy summit will then be able again to intercept rainfall. In other terms, the canopy is considered as a single reservoir that is progressively filled by successive rainstorms. The application of the canopy storage dynamics model requires only two variables (incident rainfall and evapotranspiration), while throughfall is simulated by a single equation whose parameters are mainly dependent on the amount of water stored on the canopy.

References

BIRON, P. (1994) 'Le cycle de l'eau en forêt de moyenne montagne: flux de sève et bilans hydriques stationnels (bassin-versant du Strengbach à Aubure - Hautes-Vosges)'. *Thèse 3e cycle, Université Louis Pasteur,* Strasbourg, 240p.

JETTEN, V.G. (1995) 'Interception of tropical rain forest: Performance of a canopy water balance model'. *Hydrological Processes*, 10, 671-685.

PFISTER, L. (1995) 'Interception des précipitations dans quatre peuplements forestiers (épicéa, hêtre) du bassin-versant du Strengbach. Etude des processus et modélisation'. *Mémoire de DEA, Université Louis Pasteur* , CEREG-URA 95 CNRS, 97p.

POOK, E.W., P.H.R. MOORE and T. HALL (1991) 'Rainfall interception by trees of pinus radiata and eucalyptus viminalis in a 1300 mm rainfall area of southeastern New South Wales: II. Influence of wind-borne precipitation'. *Hydrological Processes*, 5, 143-155.

RUTTER, A.J., K.A. KERSHAW, P.C. ROBINS and A.J. MORTON (1971) 'A predictive model of rainfall interception in forests'. *Agric. Meteorol.*, 9, 367-384.

VIVILLE, D., P. BIRON, A. GRANIER, E. DAMBRINE and A. PROBST (1993) 'Interception in a mountainous declining spruce stand in the Strengbach catchment (Vosges, France)'. *Journal of Hydrology*, 144, 273-282.

Sap flow and micrometeorological measurements in the Strengbach catchment (Vosges mountains) for SVAT model validation

P. Biron [1], G. Najjar [1], D. Viville [1], A. Granier [2] and E. Dambrine [2]

[1] *Centre for Eco-Geographical Research Studies, Strasbourg, France*
[2] *Centre for Forestry Research, Nancy-Champenoux, Seichamps, France*

1. Introduction

The main objective of this research is to improve our knowledge about the processes of water and energy transfers in the "Soil Vegetation Atmosphere" system of middle mountain forest areas.

In forest ecosystems, evapotranspiration fluxes can be determined by the means of the complementary methods of (a) water and energy balances or (b) sap flow. Each method differs in its spatial and temporal resolution. Moreover, in middle mountain environments, topography controls the water and energy supplies. In such conditions, it can be difficult to apply energy and water balances (because, for example, of problems due to slope and exposure, conditions of air stability, soil heterogeneity, lateral fluxes) and xylem sap flow can provide an alternative method.

After assessing sets of complementary measurements, datasets are presented which allow the validation of the different water flux simulations.

2. Material and Method

In the framework of the ERB network and the REKLIP programme (an international project of climatology grouping scientific teams of three countries bordering the southern part of the Rhine valley in France, Germany and Switzerland), several intensive campaigns of measurements of forest evapotranspiration have been conducted in the Strengbach catchment (Najjar and Biron, 1995).

The study site is a dense 30 years old stand of spruce with a southern exposure (1050 m elevation, see Table 1). Projected leaf area index (LAI) was estimated using the relationship between sapwood area and leaf area (Oren *et al.*, 1986). Annual rainfall is about 1400 mm and annual average air temperature is 6°C (Viville *et al.*, 1993).

TABLE 1: Main characteristics of the study site

Mean tree height (m)	14.0
Leaf Area Index	5.6
Stand density (t/ha)	2350
Sapwood cross sectional area (m^2/ha)	31.9
Soil field capacity (m^3/m^3)	0.22
Soil wilting point (m^3/m^3)	0.11
Albedo	0.08

2.1 Sap flow measurements

During two consecutive summer periods (1994 and 1995), five trees were equipped with a sap flow measuring device (Granier 1985, 1987) in order to estimate transpiration.

This sap flow method measures the temperature difference ($\Delta T°C$)between two probes of 2 cm length inserted into the sapwood (20 cm apart vertically). The upper probe is heated continuously at constant power and the lower one remains at wood temperature as a reference. The sap flux density ($dm^3.dm^{-2}.h^{-1}$) is inversely proportional to the temperature difference between the two probes (ΔT is maximum at night, at zero sap flow).

The sensors were connected to a datalogger (Campbell Ltd, CR10) and to a power supply (car batteries). Measurements were taken every 10 seconds and half hourly means were stored for processing.

Total sap flow ($dm^3.h^{-1}$) was calculated for each tree by multiplying the sap flux density by the sapwood cross-sectional area (SA, dm^2) of the trees at the sensor level. SA was estimated using a relationship, given by Eq. (1), between tree circumference (C, cm) and SA which was established from a sampling of cores on the surrounding trees (Biron 1994, Lu *et al.* 1995):

$$SA = 0.00047 * C^{2.052} \qquad \text{where } r^2 = 0.97 \tag{1}$$

Stand transpiration (Tr, $mm.h^{-1}$) was estimated by Eq. (2)

$$Tr = SA_T \Sigma (F_{di} * p_i) \tag{2}$$

where SA_T was the plot sapwood area per unit of ground area (31.9 m^2/ha), F_{di} the mean sap flux density of the trees in the class of circumference i, and $p_i = SA_i/SA_T$ with SA_i the sapwood area of the trees in the class of circumference i.

2.2 Three-Propellers Eddy-Correlation measurements

A tower of 20 meters height was erected in 1994 in the study stand in order to make the energy balance measurements. The tower was instrumented for each summer period with a 3PEC (3 Propellers Eddy Correlation) device for the measurement of sensible heat flux. This device consists of a 3 D-Gill propeller anemometer and a thin wire thermocouple. Net radiation, global irradiance, and albedo were measured over the forest at 22 m height. Soil heat flux and the heat stored in the vegetation (G) were recorded using respectively soil fluxmeters and a Vaisala sensor which gave the variations of temperature and humidity at 10 m height. The measurement principles and the configuration of the devices are described by Bernhofer (1992).

The Eddy Correlation Energy Balance method used relies on the determination of the sensible heat flux H by Eq. (3)

$$H = \rho Cp \, (w'T') \tag{3}$$

where w is the vertical wind component and T the thermocouple temperature.

The latent heat flux (LE) is then calculated by the means of the forest energy balance given by Eq. (4)

$$Rn + G + H + LE = 0 \tag{4}$$

where Rn is the net radiation flux and G is the heat storage flux.

2.3 The SVAT models

The modelling of the soil water balance represents an interesting tool for the analysis of the water cycle in forested stands. We have used in this study two versions of the "Bilhyd" simple SVAT model (Granier *et al.*, submitted) which differ by the time step and the calculation procedures they use.

Daily time step model

This model only needs daily rainfall and Penman PET as input climatic data. It comprises a single soil reservoir composed of several horizontal layers. In each layer, water is absorbed by roots at a rate which is proportional to the root density distribution. The characteristics of the reservoir are determined by the soil water properties; the soil water storage at the wilting point defines the base of the reservoir. The soil water storage at the field capacity defines the value beyond which the drainage processes begin.

At a daily time step, we have used a linear regression based on experimental data to estimate throughfalls (T_h) from open-field rainfall (Pi) (Eq. 5).

$$T_h = 0.76 * Pi \qquad (r^2 = 0.96) \tag{5}$$

Previous measurements of sap flow have shown a strong dependency of spruce tree transpiration on potential evapotranspiration (PET) when soil water is not limiting. Under non-limiting soil water supply, the ratio Tr/PET was found to be close to 0.70-0.80 (Biron, 1994). Below a threshold of soil water content, transpiration rate was shown to decrease linearly.

This relationship has been calibrated from experimental data obtained in the same stand during the severe drought of summer 1990 (simultaneous recording of soil water content with a neutron probe and xylem sap flow measurements).

Hourly Time step model

The "Bilhyd" model uses hourly rainfall and standard climatic data for calculating the maximum transpiration according to the Penman-Monteith equation (i.e. net radiation or global irradiance, wind speed, air temperature and humidity).

The maximum canopy conductance (g_{cm}) was modelled in 1990 under non-limiting soil water conditions using the Penman-Monteith equation and sap flow data (Lu *et al.* 1995). It was assumed that vapour flux was equal to the stand sap flow. Then, a multiple regression (Eq. 6) was made using a non-linear model similar to the equation proposed by Lohammar *et al.* (1980):

$$g_{cm} = (Rg/Rg + 310))*(5.34 - 1.33 \ln (vpd)) \qquad r^2 = 0.70 \tag{6}$$

with g_{cm} in cm/s, the global irradiance (Rg) in $W.m^{-2}$ and air vapour pressure deficit (vpd) in hPa (100 * Pa).

Transpiration rate is controlled by a function of the soil water content as in the daily time step model. The soil water storage is monitored using a two-soil reservoirs system (Choisnel, 1992):

- a deep reservoir which is generally replenished during the autumn-winter-early spring period, the water content of this reservoir is time dependant as a function of the precipitations supply and of the trees transpiration, and
- a superficial reservoir replenished by rainfall prior to the deep one, and draining into it in the case of overflow.

This reservoir is variable in dimension and is created when a rainfall occurs after a drought period and if the deep reservoir is not full. If the drought is remaining, the superficial reservoir is emptied from the top. This two-soil reservoirs system provides two different levels of actual evapotranspiration regulation which permits simulation of evapotranspiration during successive dry and wet periods.

For the modelling of the rainfall interception, a canopy water balance is made as in the Rutter's model (Rutter *et al.*, 1971). The interception reservoir (RI) is filled up with the intercepted rainfall and is emptied by drainage (throughfall and stemflow) and by evaporation. This function has been calibrated and validated for each stand with experimental data over 7 years 1988-1995 (Viville *et al.*, 1993; Biron, 1994; Pfister, 1995).

3. Results

3.1 Hourly and daily variations of sap flux density

Fig. 1 displays an example of xylem sap flux densities (lower figure) measured on 5 trees on day 204 (July 23rd, 1995), in comparison with climatic factors (upper figure). It can be observed in Fig.1 that sap flux begins early in the morning at about 0600 hours only one hour after sunrise and reaches its maximum value at midday. In the afternoon, sap flow decreases simultaneously with global irradiance. At 2000 hours, there is practically no more sap flow. Sap flux densities exhibit a between-trees variability; the increase does not occur at the same time for all the trees and some display their maximum earlier than others (maximum values varying between 0.9 and 1.7 $dm^3.dm^{-2}.h^{-1}$).

This variability mainly depends on tree crown exposure and local soil water availability; lowest values are usually obtained for the suppressed spruce trees, highest for the dominant. Fig. 2 shows a 3-month time series of sap flux densities measured on the five selected trees. There is an important time variability of sap flow due to the high climate variability in mountainous area. There are also many days with no sap flow which correspond to rainy days with precipitation much higher than tree canopy saturation capacity. Sap flow has been continuously monitored over 4 months during the growing seasons of 1994 and 1995 with minimal maintenance. It appears to be a robust technique which permits long term measurements of tree transpiration in mountain conditions. It provides also a readily available database for the testing and the validation of our SVAT model.

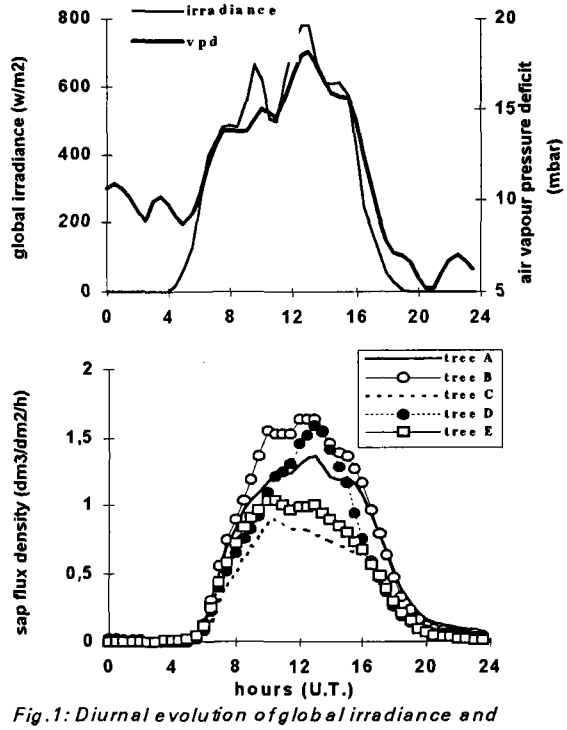

Fig.1: Diurnal evolution of global irradiance and air vapour pressure deficit (top) and of sap flux density measured on 5 trees (bottom)

3.2 Three-propellers eddy correlation - energy balance measurements (3PEC-EB)

An example of the daytime pattern of the energy balance components is given in Fig. 3 for 15 and 16 August 1994. Sensible heat flux measured by eddy correlation is approximately equal to 50% of the net radiation for a good soil water availability. The heat storage flux only represents 4% of the incoming net radiation but with a consistent time lag and a great inertia. Latent heat flux, calculated as the remaining energy, is less than 50% of the net radiation.

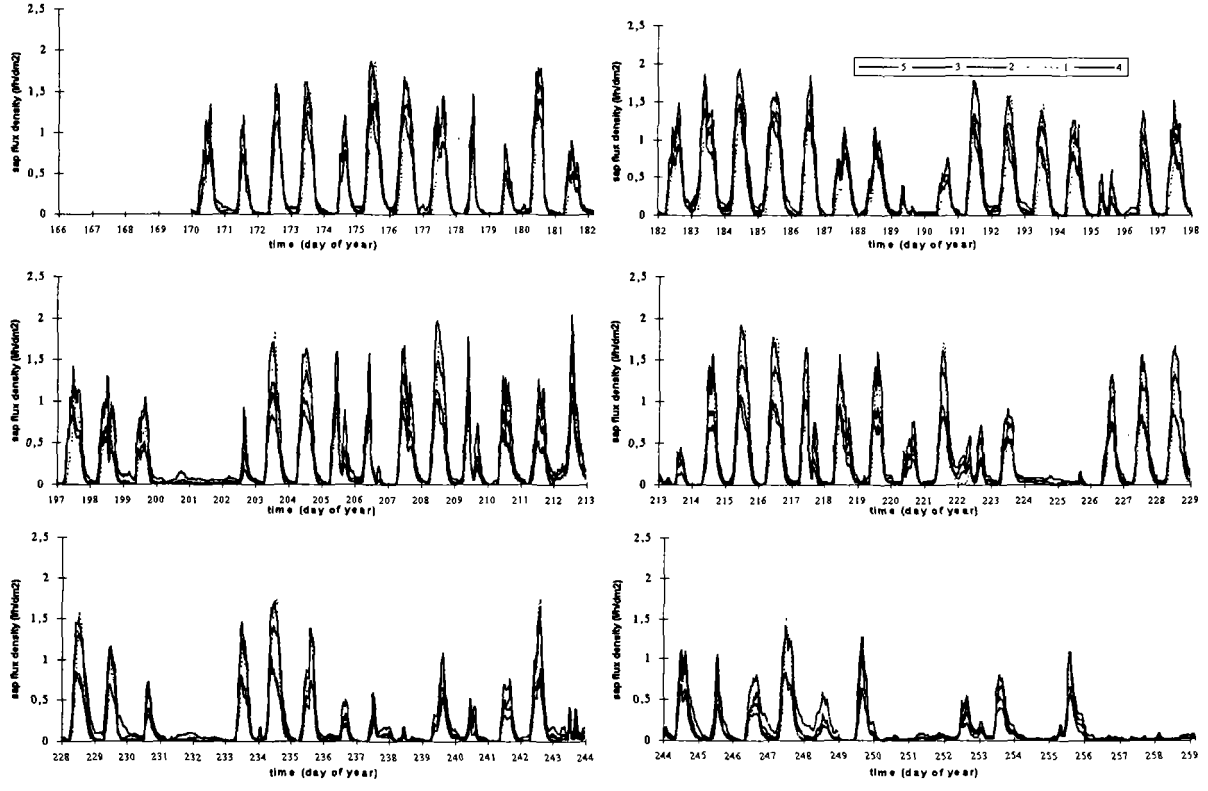

Fig.2: A 3 months time series of sap flux densities measured on 5 selected trees (Strengbach, 30 year old stand of spruce)

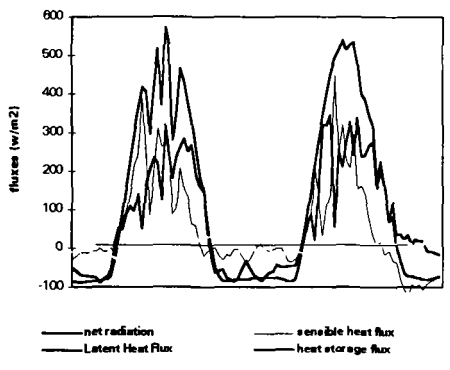

Fig.3: A 2 days time series of energy balance (Strengbach, 30 year old stand of spruce, 15-16th August 1994)

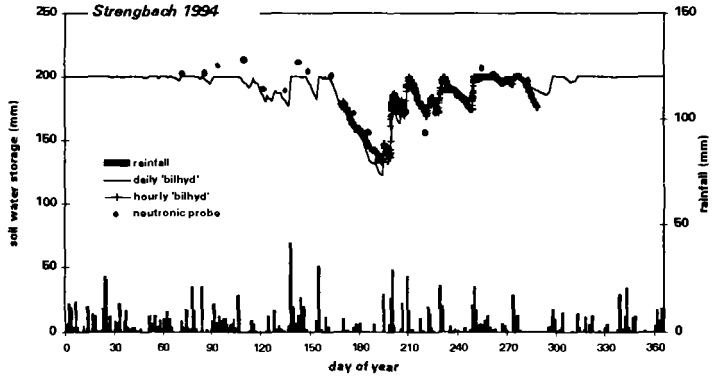

Fig.4: Simulations of the soil water storage by the 2 different versions of the "Bilhyd" model compared with the neutonic probe measurements (90 cm of soil depth)

3.3 Simulations of the soil water storage

Fig. 4 shows the soil water storage evolution in 1994 given by the two models in comparison with neutron probe measurements. During the major part of the year, especially in winter and autumn, the soil is at field capacity (none of these models calculates the soil water content above). During the short growing season, soil water content usually decreases rapidly but without reaching the wilting point. This behaviour is explained by the fact that the soil is characterised by a very coarse texture, high permeability and low retention capacity (Table 1). Nevertheless the simulations fit well the measurements and globally give very satisfactory results even if the hourly version of "Bilhyd" seems to be better during the drought periods.

3.4 Simulations of the stand transpiration

A comparison of a 10-day time series, for stand transpiration simulated by the hourly bilhyd with sap flow measurements is presented in Fig. 5.

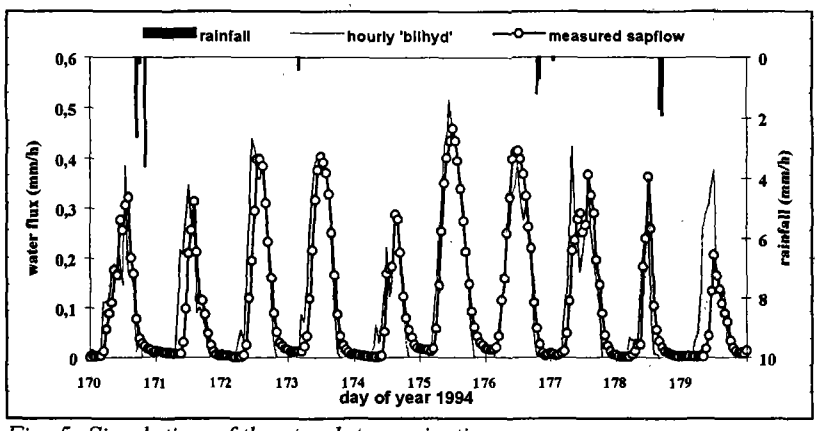

Fig. 5: Simulation of the stand transpiration.

A very good general agreement has been found especially for sunny days, but in contrast the worst results were obtained just after rainfall when the canopy was wet (days of year 171, 177, 179).

The simulations of the stand transpiration could be greatly improved after rainfall by taking into account respectively the proportions of transpiring and evaporating (wet) canopy.

3.5 Simulations of the Actual Evapotranspiration

For a 10-day period, Fig. 6 shows a comparison of actual evapotranspiration given by the 3PEC-EB method to the simulations of the model (Fig. 6).

Results show the occurrence of short-term peaks while simulated AET and sap flow provide smoother response curves. This is probably due to fast changes in the main wind direction. Sensible heat flux should be analysed as a function of the wind direction in order to take into account the contribution of each area. Furthermore, the 3PEC-EB technique appears to be inaccurate during rainfall; this can be clearly observed for days 229, 231.

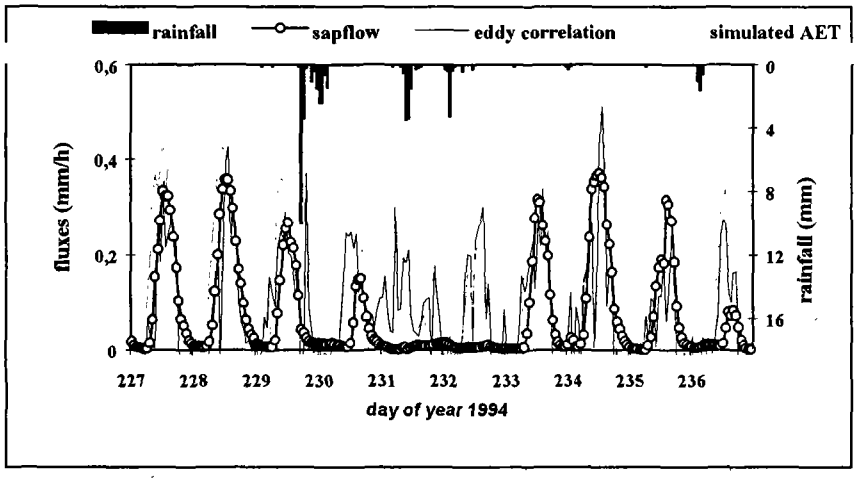

Fig. 6: Time courses of measured and simulated Actual Evapotranspiration.

But, after the rainfall, simulations seem to be very close to 3PEC-EB measurements and correspond to the estimation of the evaporation of the intercepted rainfall (days 232 and 236).

4. Conclusion

Micrometeorological methods such as eddy-correlation and energy balance are typically well suited for the average determination of global water vapour fluxes over large areas without discerning the different

components of the actual evapotranspiration, i.e. transpiration, soil evaporation, understorey evapotranspiration and evaporation of the rainfall intercepted by the vegetation.

The transpiration component of evapotranspiration is probably the most important term to determine. Nowadays, xylem sap flow measurements provide accurate determination of the stand transpiration separately from the whole AET. In a middle mountain environment, it appears to be the best method for this purpose.

With regard to the modelling, the hourly time step simulation seems to be more suitable with respect to the physically based processes but requires a reliable climatic database which is often difficult to obtain for long time series. On the other hand, a daily time step is more simple to use and is well suited to simulation over long periods.

Acknowledgements

This work has been supported by the French branch of the REKLIP programme (REgio - KLIma-Projekt).

References

BERNHOFER C. (1992) 'Estimating forest evapotranspiration at a non ideal site'. *Agric. For. Met.* 60, 17-32.

BIRON P. (1994) 'Le cycle de l'eau en forêt de moyenne montagne: flux de sève et bilans hydriques stationnels (bassin versant du Strengbach à Aubure - Hautes Vosges)'. *PhD thesis, Strasbourg University*, 244p + ann.

CHOISNEL E. (1992) 'Le calcul du bilan hydrique du sol: options de modélisation et niveaux de complexité'. *Sciences du Sol*, 30 (1): 15-31.

GRANIER A. (1985) 'Une nouvelle méthode pour la mesure du flux de sève brute dans le tronc des arbres'. *Ann. Sci. For.*, 42 (2): 193-200.

GRANIER A. (1987) 'Evaluation of transpiration in a Douglas-fir stand by means of sap flow measurements'. *Tree Physiol.* 3: 309-320.

GRANIER A., N. BREDA, P. BIRON and S. VILLETTE (submitted) 'A daily water balance model for long term studies of water stress duration and intensity in forest stands'. *For. Ecol. Man.*

LOHAMMAR T., S. LARSSON, S. LINDER and S.O. FALK (1980) 'Fast - simulation models of gaseous exchange in Scots Pine'. *Ecol. Bull.* (Stockholm) 32: 505-523.

LU P., P. BIRON, N. BREDA and A. GRANIER (1995) 'Water relations of adult Norway spruce (*Picea abies (L.) Karst.)* under soil drought in the Vosges mountains: water potential, stomatal conductance and transpiration'. *Ann. Sci. For.*52: 117-129.

NAJJAR G. and P. BIRON P. (1995) 'Campagne de mesures intensives 1994 sur le transect sud du fossé rhénan'. *Rapport de travail de la branche française de REKLIP-thème 4: Bilan hydrique-Bilan d'énergie,* 31p.

OREN R., K.S. WERK and E.D. SCHULZE (1986) 'Relationships between foliage and conducting xylem in *Picea abies (L) Karst'. Trees*. 1. 61-69.

PFISTER L. (1995) 'Interception des précipitations dans 4 peuplements forestiers (Epicea, Hêtre) du bassin-versant du Strengbach. Etude des processus et modélisation'. *Mémoire de DEA, Université Louis Pasteur,* CEREG (ULP/CNRS) Strasbourg, 97p + ann.

RUTTER A.J., K.A. KERSHAW, P.C. ROBINS and A.J. MORTON (1971). 'A predictive model of rainfall interception in forests. 1. Derivation of the model from observations in a plantation of corsican pine'. *Agric. Meteorol.*, 9: 367-384.

VIVILLE D., P. BIRON, A. GRANIER, E. DAMBRINE and A. PROBST (1993). 'Interception in a mountainous declining spruce stand in the Strengbach catchment (Vosges, France)'. *J. of Hydrol.*, 144: 273-282.

Sap flow measurement of floodplain forest of the Danube river

I. Meszaros and L. Molnar

Institute of Hydrology SAS, Bratislava, Slovakia

1. Transpiration of water from the forest ecosystem

Direct measurements of transpiration by floodplain forest were needed for monitoring the water requirements of vegetation cover under natural, and later also man-affected, hydrological regimes within the inundation area of the Gabcikovo hydraulic structure on the Danube river (Fig.1). The importance of direct and continuous measurements of transpiration depends upon the immediate assessment of water consumption by vegetation and, therefore, on the evaluation of disposable soil water resources and vegetation conditions.

Testing the equipment started during the second half of the vegetation season in 1990 on two representative plots in Gabcikovo (L01) and Kralovska luka (L06). Measurements on selected trees (oak-*Quercus robur L.* in Gabcikovo and poplar-*Populus* in Kralovska luka) continued during 1991 Monitoring of transpiration continued during the vegetation season in 1992 at the same sites and selected trees. Results have been published by Molnar and Meszaros (1991; 1992). In 1993, after the reservoir was filled, and the hydropower the vegetation season in 1994 and 1995 monitoring of transpiration continued at the same sites.

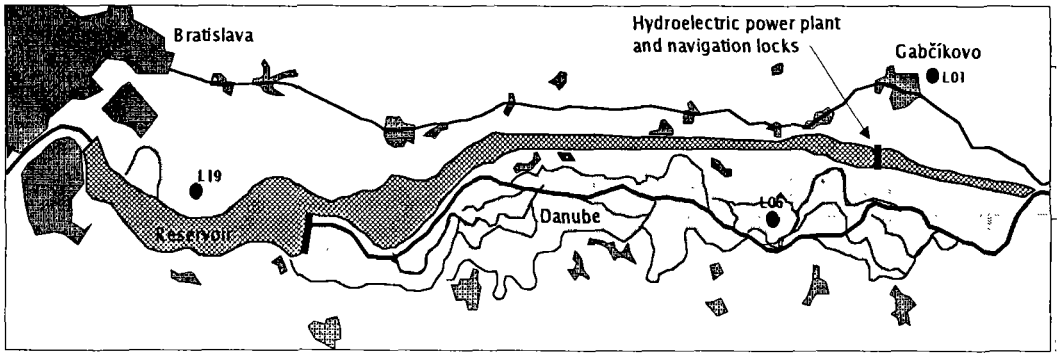

Fig.1: Scheme of the Gabcikovo hydraulic structure.

Sap flow was calculated at 20-minute time steps and related to hydrometeorological data measured near to the selected trees. The method of sap flow measurement described below has been tested, calibrated and used on different tree species and under different hydrological and/or morphological conditions. The flatland features of the Danubian floodplain forest are favourable for the use of the method. There are no problems with slope orientation, altitude and shading effect due to relief as in mountainous areas. It is easier, therefore, to find relationships between measured sap flow and corresponding meteorological characteristics. Calculation of a water balance always requires clear definition of the catchment area. In mountainous areas it is necessary to take account of both horizontal and vertical components of water fluxes, in comparison with floodplain areas where the horizontal part can be neglected since runoff occurs only exceptionally.

2. Method of measurements and equipment

The continuous measurement of sap flow within the stem of a selected tree is based on the heat balance method of Cermak *et al.* (1973). This non-destructive method depends on accurate measurements of the heat conductivity in the active xylem of a plant. For constant heating 5 electrodes are used. The electrodes are placed into the measured segment of a stem, so that the whole cambial profile is heated.

The temperature of the hydroactive xylem is measured by eight thermometers arranged in two levels just below and above the electrodes (Fig. 2). The recorded difference of temperature (up to 3 degrees of Celsius) or so-called cooling effect is related to the speed of sap flow in the hydroactive xylem, which allows estimation of the amount of water consumed for transpiration.

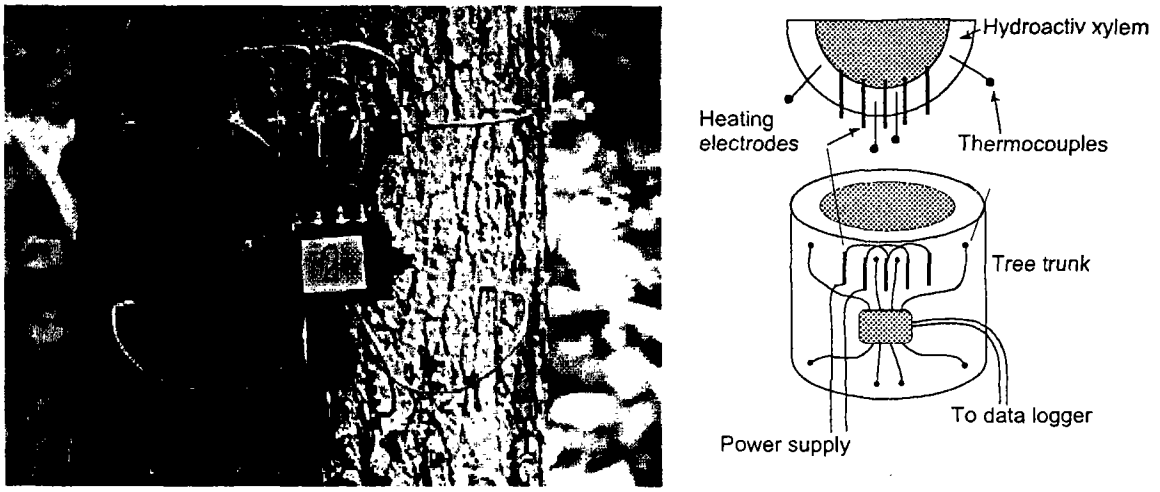

Fig.2: Measuring device applied on tree trunks

Recorded differences of the sap flow temperatures together with the power input, separation distance and number of electrodes, and finally the circumference of the tree, are input parameters for determination of the intensity of transpiration by the selected representative tree.

The actual sap flow Q_{wt} is result of separation according to the equation (1).

$$Q_{wt} = Q_{wt,rec} - Q_{wt,sep} \tag{1}$$

where : $Q_{wt,rec}$ recorded sap flow ($l.hr^{-1}$).
$Q_{wt,sep}$ separate night-time part of sap flow which represents heat losses ($l.hr^{-1}$).

The recorded sap flow $Q_{wt,rec}$ is calculated according to the equation (2).

$$Q_{wt} = \frac{P \cdot \Delta t}{\Delta T \cdot c_w} \cdot \frac{O_{bk}}{d \cdot (n-1)} \tag{2}$$

where
- P is wattage (W),
- Δt time interval (s),
- ΔT measured differences of sap temperature (°C),
- c_w specific heat of water 4 186.8 ($J.K^{-1}.kg^{-1}$),
- O_{bk} tree circumference without bark (cm),
- d distance of electrodes (cm),
- n number of electrodes.

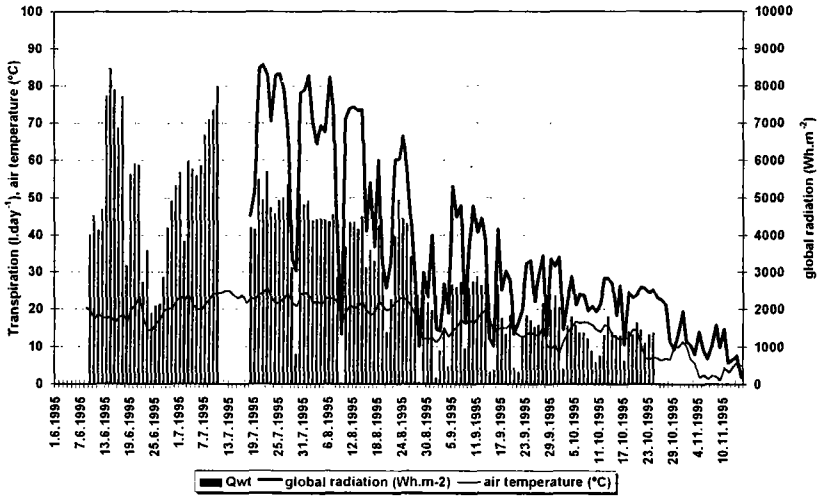

Fig.3: Transpiration Qwt, global radiation and air temperature in 1995 - Gabcikovo (L01).

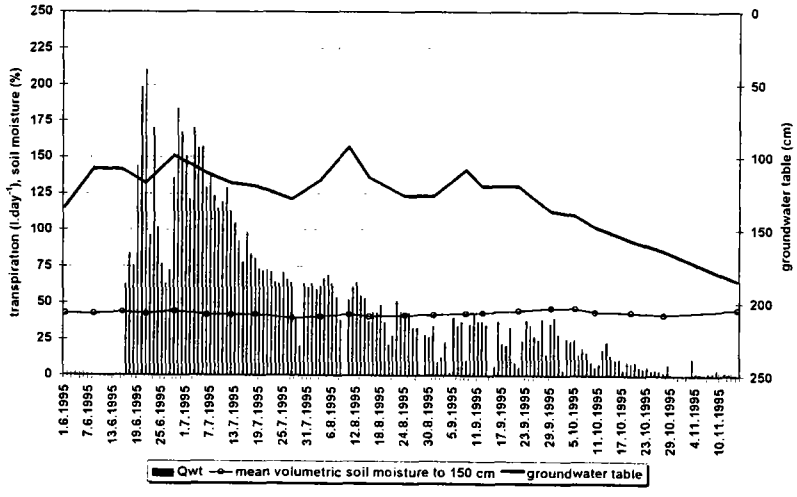

Fig.4: Transpiration Qwt, groundwater table and mean volumetric soil moisture to 150 cm in 1995, Kralovska luka (L06).

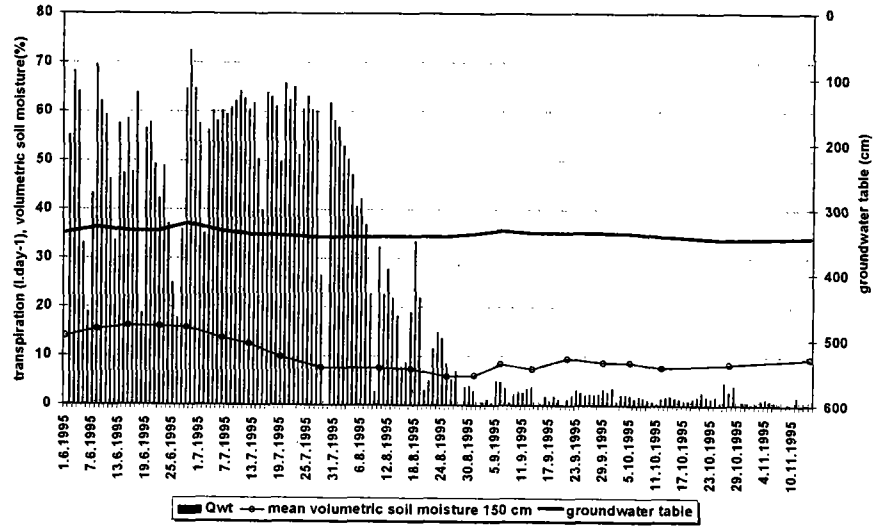

Fig.5: Transpiration Qwt, groundwater table and mean volumetric soil moisture to 150 cm in 1995 - Biskupice (L19).

3. Results

3.1 Interpretation of monitored data

Transpiration by the forest is the final product of the interrelation of different phenomena. The dominant diurnal variation of transpiration, with a daily maximum between 1200 hrs and 1500 hrs, is mainly determined by physiological processes within the vegetation and is considerably reduced by occasional rainfall. The transpiration intensity within a day also depends on solar radiation, air temperature, humidity and wind speed. Not all of these meteorological characteristics can be measured at all the sites selected for monitoring of transpiration. Therefore, the most relevant and easy measurable, the air temperature and global radiation over the canopy, were chosen and recorded.

In the case of floodplain forest, the most significant influence on transpiration is the availability of disposable soil water resources. Results obtained since 1991 show, that the basic seasonal variation of transpiration is governed by the vegetation cycle of deciduous forest, but substantially depends on the limiting soil water resources in Podunajske Biskupice (L19). On the other hand the results from the two permanent plots in Kralovska luka (L06) and Podunajske Biskupice (L19) show a dominant influence of meteorological characteristics on transpiration instead of soil water resources which are not a limiting factor at those sites. The groundwater table is within the reach of the root system of the trees. The close relationship between the diurnal variation of transpiration and global radiation is illustrated in Figures 3, 4 and 5. The diurnal variation of transpiration in a given day is dependent on rainfall and other meteorological conditions.

The significant ecological and also water resources management parameters are daily sums of transpiration of the selected tree species. As has been stated, daily sums of transpiration vary due to the characteristics of studied trees, to meteorology (e.g. rainfall) and disposable soil water resources.

3.2 Water balance

The water balance which included precipitation, runoff, soil water storage and evapotranspiration was calculated for Kralovska luka plot (L06) taking account of the infiltration to groundwater. The diurnal and seasonal variations of sap flow are shown in Fig. 6. Surface runoff from the flat study area was neglected. The cumulative actual evapotranspiration was calculated and compared with cumulative measured transpiration. The results show the dominant role of tree transpiration which, in the studied case, is 67% of the actual evapotranspiration and allows determination of the actual water resources for the studied forest ecosystem. The results mentioned above (Molnar and Meszaros, 1995) are shown in Figs. 7 and 8.

The water balance in its simplest form was estimated by equations (3) and (4).

$$P - R \pm \Delta W = E_e + E_t \qquad (3)$$

where
- P precipitation (mm),
- R surface and subsurface runoff (mm),
- ΔW change of soil water content (mm),
- E_e evaporation from the soil and shrubs transpiration (mm),
- E_t transpiration (mm).

$$\sum E_e + \sum E_t + I_g = \sum P \pm \Delta W \qquad (4)$$

where
- ΣE_e cumulative soil evaporation and shrubs transpiration (mm),
- ΣE_t cumulative tree transpiration (mm),
- I_g infiltration into / or from groundwater (mm),
- ΣP cumulative precipitation (mm),
- $\pm \Delta W$ changes of soil water content (mm),

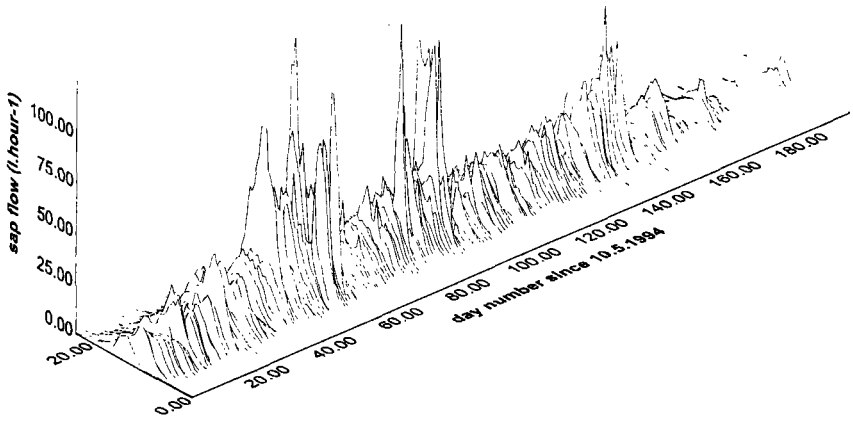

Fig.6: Diurnal and seasonal transpiration in 1994, since 10th May 1994.

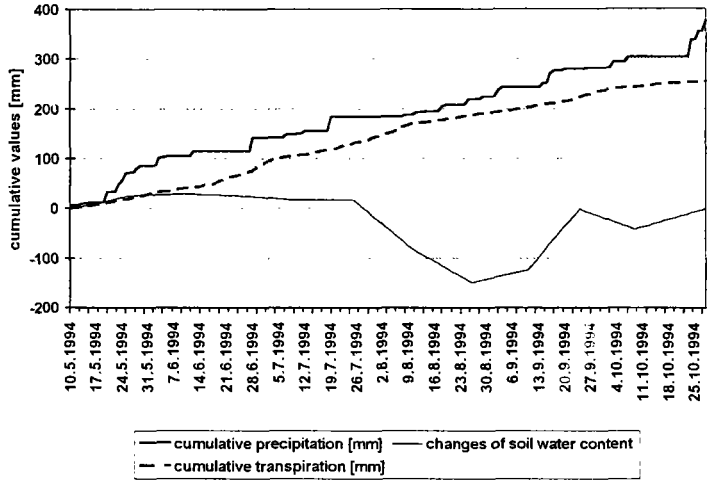

Fig.7: Cumulative water balance components - precipitation, transpiration and changes of the soil water content.

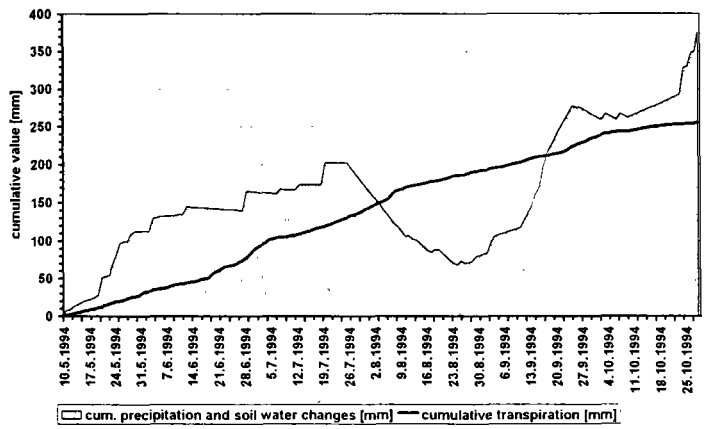

Fig.8: Cumulative evapotranspiration and infiltration (calculated by Eq.4) and cumulative transpirat n in (mm) during the period of 10th May to 28th October, 1984.

4. Conclusions

The monitored data led to the conclusion that the proper knowledge of diurnal and seasonal variations of transpiration by selected representative trees gives a unique opportunity to define the actual state of the studied forest ecosystem. The information presented in this paper can assist with optimization of the Gabcikovo water distribution system in real time, before damage to floodplain forests become visible.

References

CERMAK J., M. DEML and M. PENKA (1973) 'A new method of sap flow rate determination in tress'. *Biol. Plant.*, 15, pp. 171-178.

MOLNAR L. and I. MESZAROS (1991, 1992, 1993, 1994, 1995) 'Evaluation of disposable water resources of floodplain forest by continuous measurement of transpiration'. (In Slovak) *Technical Report*, IH SAS, Bratislava.

MOLNAR L. and I. MESZAROS (1995) 'The role of transpiration in the water balance of the Danube floodplain forest area'. *J.Hydrol. Hydromech.*, 43, 4-5, pp. 288-300.

Evapotranspiration from plant cover in the vegetation season

M. Tesar[1], M. Sir[1], J. Prazak[2] and J. Bucek[3]

[1] *Institute of Hydrodynamics, CAS, Prague, Czech Republic*
[2] *Institute of Thermomechanics, CAS, Prague, Czech Republic*
[3] *Czech Hydrometeorological Institute, Prague, Czech Republic*

1. Introduction

A long-term field experiment to estimate evapotranspiration losses during the vegetative season is described in this article. The paper presents a method for calculating evapotranspiration from plant cover, and the total output from below the root zone, with the aid of a hydropedological-balance model. The evapotranspiration loss component from the soil profile is calculated by means of the energy balance method. In this case the potential evapotranspiration was expressed as the need of water for the cooling of the vegetation cover. These methods are demonstrated in three localities (arable land, meadow and spruce forest) situated in the Sumava Mountains during the period 1983 to 1995.

2. Hydropedological-balance method

The uptake of water from the soil to the atmosphere (actual evapotranspiration) and the outflow of soil water to strata underlying the root zone were estimated with the aid of the hydropedological-balance method using time series of tensiometric measurements made at 2-day intervals and from daily precipitation. Retention curves were used to calculate soil moisture tensiometric data, and thus also the volume of soil water. Retention curves of individual soil horizons were determined by the inverse solution of Richards' equation (Sir *et al.*, 1988). The structure of the soil profile and the depth of the root zone were established with the aid of profile pits. By balancing precipitation and the volumes of water present in the root zone of the soil at 2-day intervals, the withdrawal of water from the root zone, designated LOSS, was obtained. Daily precipitation was measured in an adjacent open area. The analysis of tensiometric and precipitation data revealed that, during the balance period, several episodes occurred in which precipitation in combination with the actual soil moisture caused the outflow of soil water to strata underlying the root zone. The volume of water thus drained is termed OUTPUT. The amount of water taken up for transpiration was obtained by the equation T = LOSS - OUTPUT. In the given experimental areas there was no surface runoff.

3. Energy-balance method for estimation of potential evapotranspiration

The estimation of potential evapotranspiration ET from the vegetation cover during the growing season was evaluated as the water requirement for cooling. The calculation uses hourly values of air temperature and of global radiation totals. Properties of the vegetation cover are expressed in terms of two phenomenological constants, i.e. the effective absorptivity and the effective thickness of leaves (or needles). Both are obtained by calibration. Full description of the proposed method is given by Prazak *et al.* (1994, 1996).

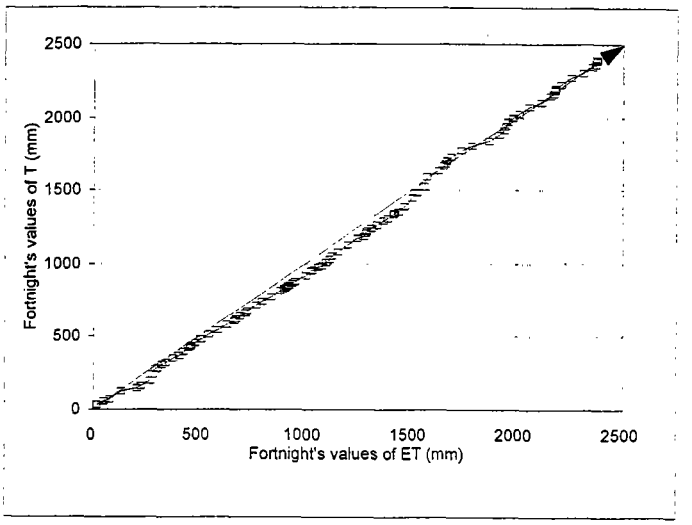

Figure 1: Double mass curve - field, vegetation seasons 1983-1991, 1993-1995.

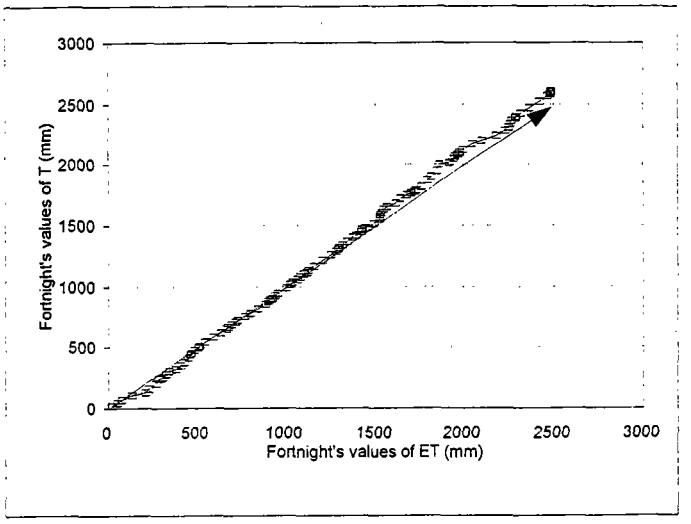

Figure 2: Double mass curve - meadow, vegetation seasons 1983-1991, 1993-1995.

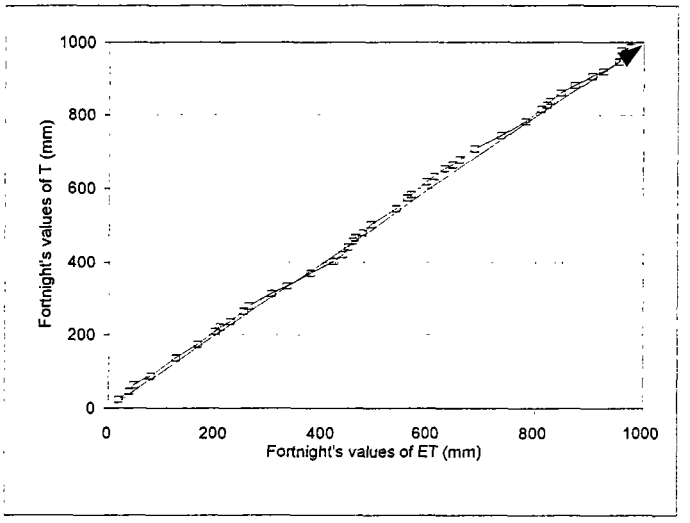

Figure 3: Double mass curve - forest, vegetation seasons 1985-1989.

4. Experimental site

The application of the proposed methods was demonstrated in three localities situated in the Zábrod and Liz experimental basins of the Institute of Hydrodynamics: grass cover (meadow) and arable land (field) land-use in the Zábrod area; and mature spruce (forest) land-use in the Liz area. Full descriptions of these three localities are given by Tesar (1991). These localities are in the Sumava Mountains which form the boundary between Bohemia, Germany and Austria.

5. Results

The hydropedological-balance and energy-balance methods were applied in three localities over the period 1983 to 1995. The results of both methods are mostly in a good harmony as can be seen from double mass curves (Figs. 1 to 3). These curves represent fortnightly totals of ET (evaluated as a need of water for cooling plants) aginst fortnightly totals of T (evaluated by the hydropedological-balance method as the withdrawal of water from the soil by the root system). It follows from the summary values ET and T, and from their difference against the precipitation total, that the proposed calculation method is quite applicable. Differences between ET and T do not exceed (a) 5% of the seasonal precipitation total for the forest locality, (b) 7% for the field locality and (c) 10% for the meadow locality. The largest differences appeared in the years 1992 and 1993 which were an extraordinarily dry and hot year, and a wet and cold year, respectively.

References

PRAZAK, J., M. SIR and M. TESAR (1994) 'Estimation of plant transpiration from meteorological data under conditions of sufficient soil moisture'. *J. Hydrol.*, 162, p. 409-427.

PRAZAK, J., M. SIR and M. TESAR (1996) 'Parameters determining plant transpiration under conditions of sufficient soil moisture'. *J. Hydrol.*, 183, p. 425-431.

SIR, M., M. KUTILEK, V. KURAZ, M. KREJCA and F. KUBIK (1988) 'Field estimation of the soil hydraulic characteristics'. *Soil. Technol.*, 1, p. 63-75.

TESAR, M. (1991) 'Water balance of the catchments with the agricultural parts' (In Czech). *PhD. Thesis,* Czech Technical University, Prague.

Soil water balance at a high-elevation site in the southern Black Forest

L. Zimmermann [1] and K.H. Feger [2]

[1] *Institute of Meteorology and Hydrology, Technical University of Dresden, Tharandt, Germany*
[2] *Institute for Soil Science and Forest Nutrition, University of Freiburg, Germany*

1. Introduction

Within the scope of the forest ecological project ARINUS the water balance was recorded on the scale of small catchments and experimental plots over a measurement period of eight years (Brahmer, 1990; Zimmermann, 1995). A physically deterministic soil water model was adapted to the experimental site Schluchsee, in order to get a high resolution of soil water balance in space and time. The purpose of this was two-fold. First, to have a base for the calculation of element fluxes in the soil. Second, to simulate the soil water balance in the years before measurements started (retrospective simulation). The latter was done to find potential causes of the occurrence of the montane tip-yellowing in Norway spruce in the late 1970s and the 1980s. Furthermore, soil water data could be compared with results from forest growth studies.

2. Material and methods

2.1 Site characteristics

The experimental site Schluchsee is situated on a wooded slope in the southern Black Forest (47°49'N, 8°6'E) at an altitude ranging from 1150 to 1290 m a.s.l.. The climate is cool-humid (average annual temperature 4.5°C, mean annual precipitation 1900 mm). About 30% of the annual precipitation falls as snow, leading to a snow cover for between four and six months (Brahmer, 1990).

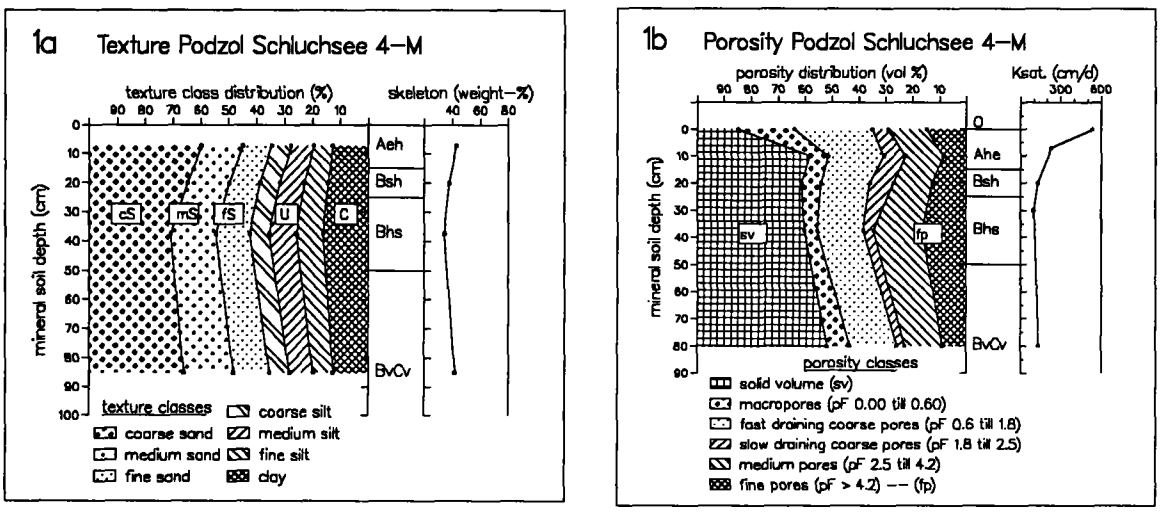

Fig. 1: (a) Texture and (b) porosity of a typical soil profile (catchment S4, mid-slope position).

The underlying bedrock consists of the extremely base-poor Bärhalde-granite. Through the coarse-grained weathering of the granite, loamy sands have developed with high gravel contents (40% - 60%), mainly fine (∅: 2 mm - 6 mm) (Fig. 1a). Saturated hydraulic conductivity reaches high values from 500 cm d^{-1} in the organic layer to 100 cm d^{-1} in the mineral soil due to the high percentage of large pores (Fig. 1b). The humic layer is a moder/raw-humus-type (thickness 5 cm). The present vegetation is second generation 60 years-old spruce. All of these properties favour podzolisation, so that mainly acid brown earth-podzols are found. Soil chemical properties show low pH-values and base saturation <5% throughout the profile (Feger, 1993). Available field capacity at 1 m depth is, on average, 130 mm but in addition there are roots in old beech root channels which reach beyond 1m depth. The soil physical properties, in combination with climatic conditions, mean that the site has, on average, sufficient water supply.

2.2 Instrumentation and measurement

Matric potential is measured with tensiometers within the stand. For the measurement of volumetric water content, TDR (time domain reflectrometry)-probes (Tektronix 1502B) are used. Open-field precipitation and other meteorological data are recorded at an adjacent site. More details of the methods and the experimental design are given in Zimmermann (1995) and Feger (1993). Texture, porosity and saturated hydraulic conductivity were measured with standard laboratory methods. Unsaturated conductivity was measured up to 160 cm WC with the one-step method (Zimmermann, 1991).

2.3. Modelling

For description of soil water flux, the modell WHNSIM (Huwe, 1990) was used which is based on an one-dimensional solution of the Fokker-Planck equation. The evapotranspiration part of the model was adapted to the forest situation. To calculate potential evapotranspiration PET, the Haude formula was used which was modified for forests (Brahmer, 1990). The use of the Haude-formula was of advantage for the retrospective simulation due to the simplicity of its meteorological input data (vapour deficit at 1400 hrs local time). In the model, litter interception was neglected. In order to get values for potential transpiration, daily values of PET (Haude) were reduced by interception. The daily loss of interception was found by the weekly measured difference between open-field precipitation and throughfall, which was distributed to single days according to the distribution of open-field precipitation and through comparison with canopy storage. Potential transpiration was divided between the different soil compartments according to fine root distribution and reduced to actual transpiration by a reduction function controlled by matric potential. For the winter season, a snow model driven by mean daily air temperature was used to simulate the meltwater discharge from the snow cover. Lower boundary condition matric potential at 1 m depth was interpolated from weekly measured values. For the years of the retrospective simulation, a gradient factor (Huwe, 1990) was used which was calibrated previously during the period of measurement and after all other calibrations had taken place.

For the calibration of the model, the saturated hydraulic conductivity was used with starting values from laboratory measurements. The aim of the calibration was to obtain a satisfactory agreement between the simulated and measured matric potentials. After calibration, the model was validated with data from another period of measurement.

For the retrospective simulation period (1962 - 1987) the meteorological input data (open-field precipitation, temperature and relative humidity) were found by regressions with data from surrounding stations of the German Meteorological Service. Throughfall in the period of the retrospective simulation was calculated by regressions, separately for summer and winter seasons, from open-field precipitation. In accordance with other studies (Mitscherlich, 1981), a change of canopy storage was not assumed in this age class of spruce. All assumptions for the retrospective simulation (interception, gradient factor) and the transfer of the meteorological data were tested by application to the measurement period.

3. Results and discussion

3.1 Matric potential and climatic conditions of the measurement period

In the measurement period there were wet (1988, 1993) as well as dry (1991, 1992, 1995) growing seasons, and years with moderate summer matric potentials (1989, 1990 and 1994). Peaks of matric potential in winter are caused by frost during times of little snow cover. During the measurement period open-field precipitation ranged from 1410 mm yr^{-1} to 2160 mm yr^{-1}. Interception reached 16% of open-field precipitation. During the measurement period, actual evapotranspiration averaged 520 mm yr^{-1}, with 42% of this amount due to actual transpiration. The high percentage of interception is in accordance with the high rainfall at this mountain range site. Average runoff was 1390 mm yr^{-1}, which agrees reasonably well with a seepage of 1338 mm^{-1} calculated for the plot scale. Given a long measurement period, a well-founded database which included different climatic conditions was available for the calibration and validation of the WHNSIM model.

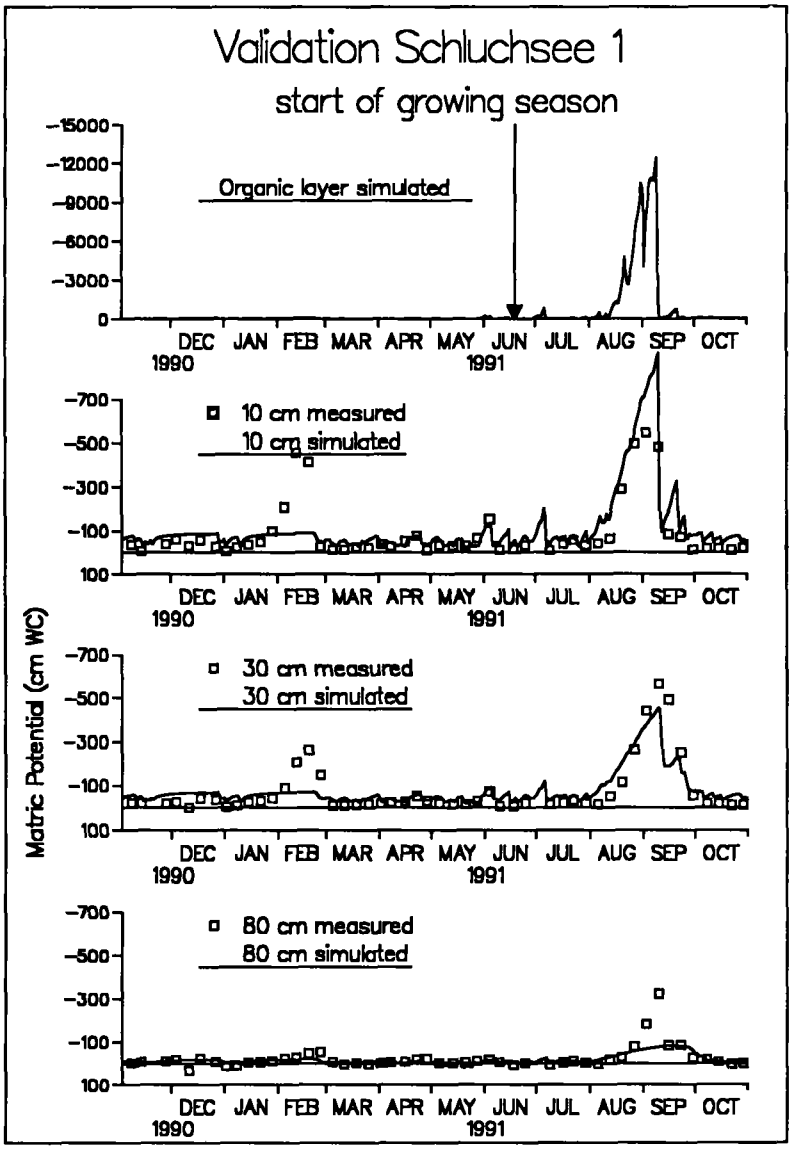

Fig. 2: Validation of the model WHNSIM by matric potentials of the hydrological year 1991 at plot S1.

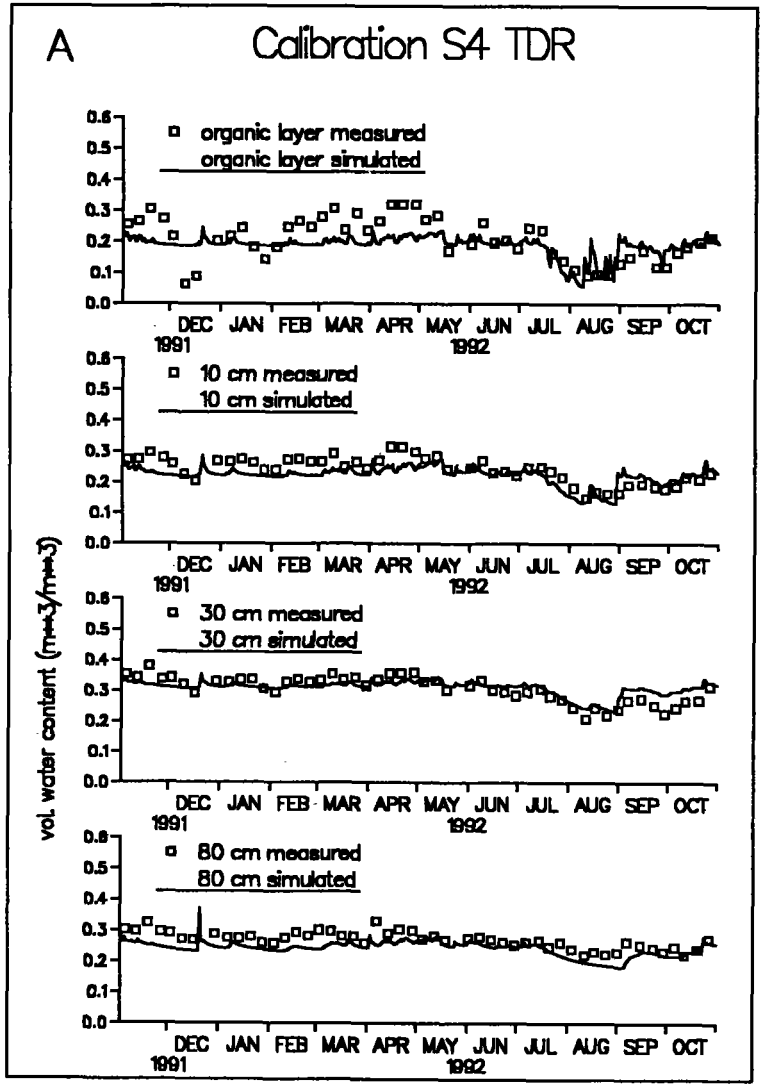

Fig. 3a: Volumetric water contents in the organic layer and 3 mineral soil depths at plot S4.

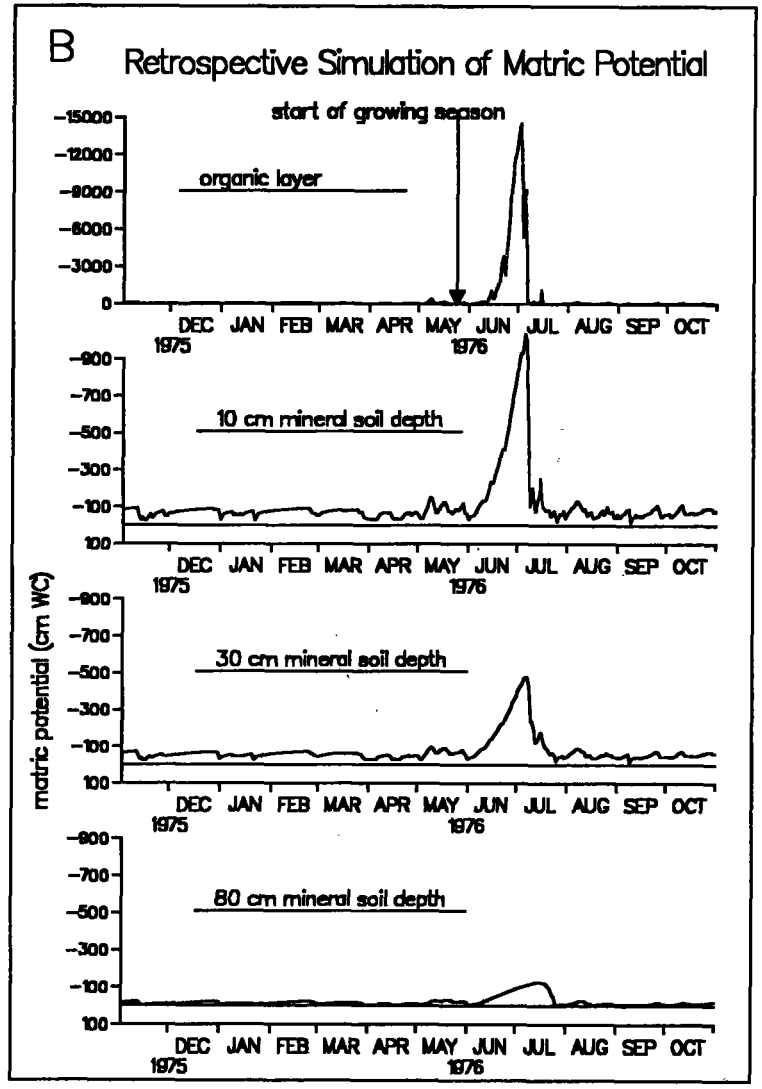

Fig. 3b: Retrospective simulation of matric potentials in the organic layer and depths in the mineral soil during the dry year 1976 at site Schluchsee.

3.2 Calibration and validation

For calibration, the hydrological year 1990 was taken as a typical dry year. All other years of measurement were used for validation. In the hydrological year 1991, for example, the simulation during the wet period shows a better fit to the measured matric potentials than in summer (Fig. 2). Especially in the re-wetting period, there is a retardation of the simulation after the peak of the summer dryness. This fast re-wetting can be explained by macropore flow (Zimmermann *et al.*, 1995) which cannot be taken into account by the model because of its underlying Fokker-Planck equation.

During the whole measurement period no matric potentials higher than 550 cm WC were measured in the upper mineral soil (10 cm depth) (Fig. 2). Thus transpiration was not reduced significantly (reduction of $T_{pot.}$ starting at 446 cm WC [pF=2.65]). For the organic layer on plot S4, the TDR-probes showed periods with much stronger drying out, reaching water contents around 10 Vol% (Fig. 3a). By fitting the pF laboratory curve to the values of $\Psi_M(\Theta)$ measured in the field, a fit of similar quality to that between simulated and measured water contents was reached (Fig. 3a). The marked variability of the measured water contents in the organic layer can be explained by its high variability of porosity (Zimmermann *et al.*, 1992). With this fitting the simulated matric potentials in the organic layer can also be used for interpretation.

The water balance of the catchment is a further control for the calculated water fluxes, especially of the calculated evapotranspiration (Zimmermann, 1995). The surplus of the balance lies within the error of the precipitation measurement of 10% - 15% in middle-range mountains (Sevruk, 1981). By comparing simulated seepage rates with the runoff from the catchment, the soil water model was additionally validated. The annual balances resulting from the comparison of seepage rates with runoff showed little non-systematic deviation.

3.3 Retrospective simulation and interpretation with respect to tip-yellowing

In the simulation period 1962 - 1986 only the years 1976, 1983 and 1985 revealed high matric potentials in the upper soil. In the years 1976 (Fig. 3b) and 1983 the dry period occurred early in the growing season compared to 1985 or the dry years of the measurement period 1990, 1991 and 1992. Since the mid-1980s a re-greening of needles has been observed at the Schluchsee site. Thus a summer drought occuring relatively late in the growing season seems to have no effect on tip-yellowing, whereas the years 1976 and 1983 coincided with the occurence of the needle yellowing.

In the literature, the yellowing is explained as magnesium (Mg) deficiency (Hüttl, 1991 ; Zöttl, 1995). The Schluchsee site has a latent magnesium deficiency, because Mg is mainly supplied from litter decomposition (Feger, 1993). The highest Mg content of the soil is found in the organic layer in which also 60% of the fine roots are concentrated (Raspe, 1992). During early summer when new shoots are formed the trees have a peak demand of nutrients, especially of Mg. A dry-out of the organic layer in this period can induce a shortage of Mg uptake by the shallow-rooting spruce and may therefore have a triggering effect for the occurence of tip-yellowing (Zimmermann, 1995; Zimmermann *et al.*, 1995).

The application of the soil water model described elucidates the potential of simulation models for interpreting physiological phenomena. The hypothesis of early summer drought induced bottle-necks for Mg supply will be tested on the site with a roof experiment during the years 1997 and 1998.

4. References

BRAHMER, G. (1990) 'Wasser- und Stoffbilanzen bewaldeter Einzugsgebiete im Schwarzwald unter besonderer Berücksichtigung naturräumlicher Ausstattungen und atmogener Einträge'. *Freiburger Bodenkundl. Abh. 25*, 295 S.

FEGER, K.H. (1993) 'Bedeutung von ökosysteminternen Umsätzen und Nutzungseingriffen für den Stoffhaushalt von Waldlandschaften'. *Freiburger Bodenkundl. Abh. 31*, 237 S.

HÜTTL, R. (1991) 'Die Nährelementversorgung geschädigter Wälder in Europa und Nordamerika'. *Freiburger Bodenkundl. Abh. 28*, 440 S.

HUWE, B. (1990) 'WHNSIM. Version 1. Ein Modell zur Simulation des Wasser-, Wärme- und Stickstoffhaushalts landwirtschaftlich genutzter Böden'. *Programmdokumentation*. Institut für Bodenkunde u. Standortslehre Fachgebiet Bodenphysik, Universität Hohenheim.

MITSCHERLICH, G. (1981) 'Wald, Wachstum und Umwelt, Bd. 2, Waldklima und Wasserhaushalt'. *Sauerländer Verlag*, 2. Aufl., Frankfurt, 365 S.

RASPE, S. (1992) 'Biomasse und Mineralstoffe der Wurzeln von Fichtenbestände (*Picea abies* Karst.) des Schwarzwaldes und Veränderungen nach Düngung'. *Freiburger Bdkdl. Abh. 29*, 197 S.

SEVRUK, B. (1981) 'Methodische Untersuchungen des systematischen Meßfehlers der Hellmann-Regenmesser im Sommerhalbjahr in der Schweiz'. *Mitt. Vers. Anstalt f. Wasserbau, Hydrologie u. Glaziologie*, ETH Zürich 52.

ZIMMERMANN, L. (1991) 'Räumliche Variabilität bodenphysikalischer Parameter in kleinen Experimentaleinzugsgebieten im Südschwarzwald'. *Diplomarbeit (unveröffentlicht)*, Institut für Bodenkunde und Waldernährungslehre, Universität Freiburg.

ZIMMERMANN, L. (1995) 'Der Bodenwasserhaushalt an einem Hochlagenstandort im Südschwarzwald'. *Freiburger Bdkdl. Abh. 35*, 206 S..

ZIMMERMANN, L., K.H. FEGER and G. BRAHMER (1992) 'Variabilität bodenphysikalischer Eigenschaften als Grundlage für Wasser- und Stoffbilanzen in Wassereinzugsgebieten im Kristallin-Schwarzwald'. *Allg. Forst- u. Jagdz. 163*, 187-195.

ZIMMERMANN L., S. RASPE, K.H. FEGER. and H.W. ZÖTTL (1995) 'Projekt ARINUS. IX.: Bodenwasserhaushalt an einem Hochlagenstandort - Messung, Modellierung und Bedeutung hinsichtlich der Mg-Mangelvergilbung'. *FZKA/PEF-Ber. 130*, 11-24.

ZÖTTL, H.W (1995) 'Waldschäden und Ursachen'. *Forst u. Holz 50*, 54-57.

Development of an evapotranspiration model from research studies in a small prealpine catchment

L. Menzel

Department of Geography, Federal Institute of Technology, Zürich, Switzerland

1. Introduction

In the recent past numerous hydrological and climate models for the simulation of water balance components related to climate conditions have been developed to operate on a meso-scale level (e.g. large river basins). Due to improved computer capacities and information systems, the areal and time resolution of these models is remarkable. On the other hand some of the included submodels often contain reveal simplifications or assumptions, which are not only caused by necessary optimizations in computing time. An example is the consideration of soil physical properties and the soil hydrology in General Circulation Models (GCM's), where the soil is usually regarded as a simple reservoir (e.g. Wild *et al.*, 1995). The lack of continuous and detailed measurements of soil moisture and related quantities complicates the comparison with real conditions (e.g. Garrat *et al.*, 1993) and the improvement of such models. Other processes, e.g. interception and evaporation of intercepted water from plant canopies, are often neglected. In hydrological models, aerodynamical and canopy resistance formulations to calculate evapotranspiration (e.g. Monteith, 1965; Shuttleworth and Wallace, 1985) are meanwhile widely in use (e.g. Braden, 1992). However, the meaning and importance of these parameters is often not well understood, and their estimation rarely improves the model results. This is the case especially tfor evapotranspiration which, as a decisive regulator of the water and energy balance, and therefore of great importance in studies on impacts of possible climate changes, has to be considered more carefully. The paper shows , that further detailed research studies in easily surveyed. surroundings like small catchments are needed. The development and improvement of physically based models for hydrological and ecological point studies and the collection of related data should contribute to improved regionalizations and create a link between modelers working at different scales.

2. Procedure

In the present work evapotranspiration is separated into its different processes. Thus, transpiration and interception evaporation are first modelled separately, as shown schematically in Figure 1. The modelling of transpiration is based on the Penman-Monteith equation, which is combined with a submodel to deliver canopy resistances. The interception model is based on a new method, which considers the non-uniform distribution of the intercepted precipitation inside the canopy. In a second step these two different processes are combined into evapotranspiration, using a weighting function of canopy wetness. Finally, areal evapotranspiration is calculated by application of the model in combination with interpolation techniques.

3. Field measurements

The experimental studies have been carried out in the prealpine research catchment of the Rietholzbach (Fig. 2), a small stream draining an area of 3.2 km^2 in the hilly terrain of eastern Switzerland (Koenig and Menzel, 1993). The climatic conditions of that region with approximately 1500 mm of yearly precipitation, and the dominance of dairy farming, lead to a vegetation cover which is 75% grassland.

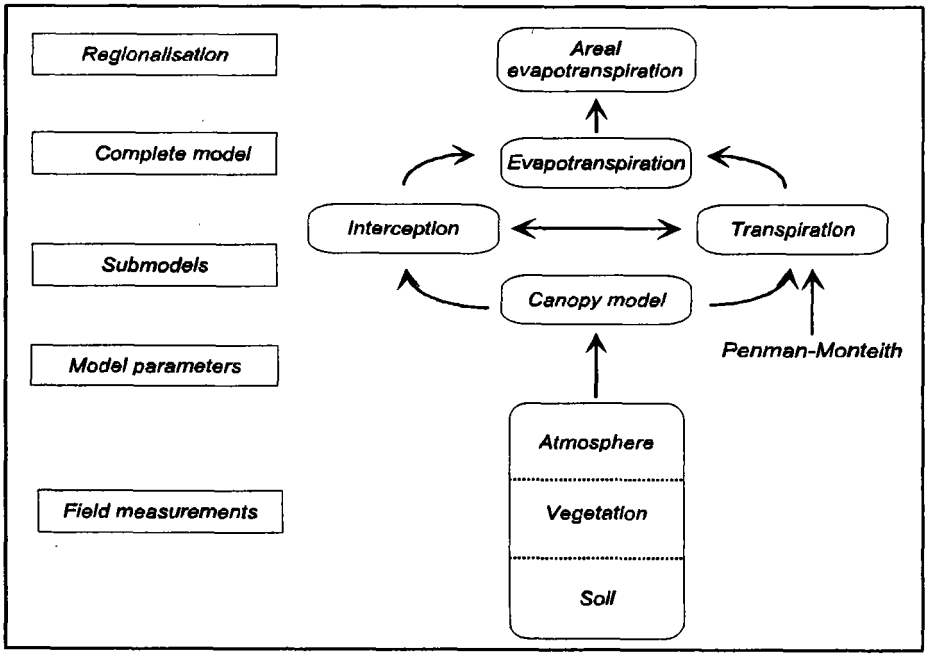

Figure 1: Simplified description of the evapotranspiration model.

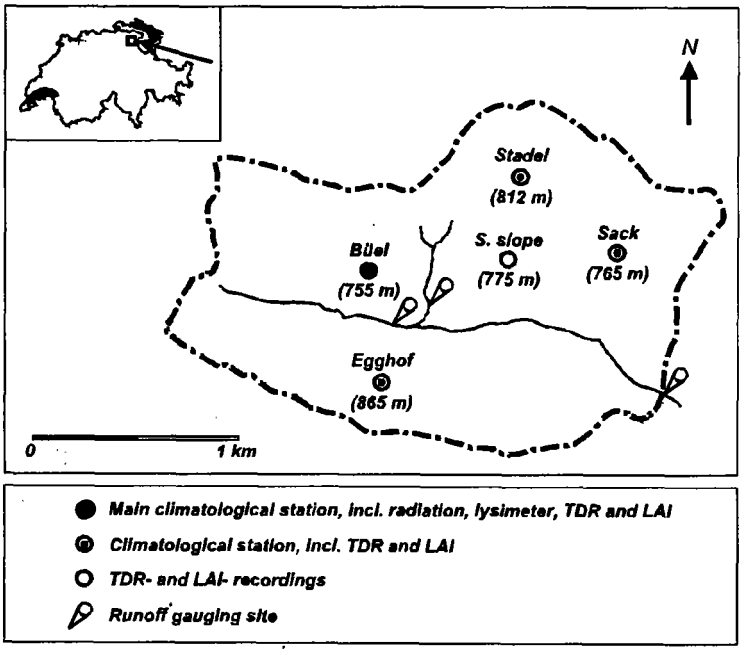

Figure 2: Overview of the hydrological research catchment Rietholzbach. Only the main measuring sites are shown.

The importance of this type of land-use for the regional hydrology was the main reason for the development of an evapotranspiration model for grassland. Besides long-term observations, including the operation of a large, grass-covered weighing lysimeter and detailed measurements of net radiation and its components, a special field programme was established in 1993 and 1994. It included hourly measurements of soil moisture with Time Domain Reflectometry (TDR) (Menzel, 1995) at different depths and locations. The phenological development of the grass cover has been recorded by weekly measurements of vegetation height, population density and leaf area index (*LAI*). All necessary measurements of meteorological variables, including precipitation, air and soil temperature, air humidity, windspeed and radiation, were carried out at 5-, 10- or 60-minute intervals at the lysimeter station and three supplementary stations at different locations of the catchment.

4. Model development

The interception submodel enables the division of the plant cover into an optional number of layers. The amount of intercepted water is calculated in relation to the storage capacity of the canopy (which is a function of the *LAI*) and the precipitation height. The derivation of storage capacities is based on field studies as well as on theoretical considerations. The distribution of the water into the different layers follows a derived relationship between vegetation height and cumulative *LAI*. The water is assumed to form individual droplets. The evaporation of the intercepted water thus follows the theory of heat and mass transfer for hemispheroids. Radiation and windspeed vary with height and distribution of the leaf area, which leads to different evaporation intensities between the single layers.

Another important element of the whole evapotranspiration model is the calculation of canopy resistances, following the investigations of Monteith *et al.* (1965). Numerous experiments, performed at the lysimeter site and under different weather conditions and soil moisture contents, finally showed a close relationship between calculated canopy resistances and *LAI*, soil water deficit of the uppermost 30 cm as well as air temperature. This relationship, derived by multiple regression, was applied to calculate daily values of evapotranspiration by the use of the Penman-Monteith-equation. Hourly values can also be computed when the daily value of the canopy resistance is divided into the individual hours, weighted by net radiation.

During intervals when the canopy is wet, transpiration and evaporation of intercepted water can occur, which is mainly determined by a relationship between the actual amount of intercepted water and the *LAI*. Other submodels serve to deliver data for the application of the Penman-Monteith equation, e.g. the soil heat flux, which is calculated by profiles of measured and modelled soil temperature and soil water content, or aerodynamic resistance as a function of wind speed and mean crop height.

5. Results

Table 1 shows a compilation of results from the interception submodel. The data refer to six-month periods (May-October) for the years 1993 to 1995. It can be seen that evaporation E_i of intercepted water amounts to more than one fifth of total evapotranspiration E_a from the investigated grassland. Considering selected months of the presented periods reveals a maximum percentage of E_a which is E_i of 45% (October 1994) and a the minimum of 2% (October 1995) due to very dry conditions. The ecohydrological importance of interception is further underlined by the calculated wetness durations, which are approximately 60% of the selected period in 1993 and 1994. Monthly extremes are found in October 1993 (82%) and October 1995 (16%), respectively.

TABLE 1 Half-yearly sums of measured evapotranspiration E_a, the modelled evaporation of intercepted water E_i, and the percentage of E_a which is E_i. Furthermore, half-yearly sums of precipitation P and percentages of rain duration P.d. and wetness duration W.d. over the respective period are listed.

May-October	E_a [mm]	E_i [mm]	E_i [%]	P [mm]	P.*d.* [%]	W.*d.* [%]
1993	413.1	86.5	20.9	928.7	16.1	60.0
1994	397.0	86.4	21.8	1009.9	16.9	59.6
1995	425.3	91.5	21.5	839.8	14.4	47.6

Besides the statistical analyses a more detailed view of modelled quantities is shown in Figure 3. For a day in July 1994, hourly modelled values of intercepted water storage *ISF* and evaporation E_i for three different layers are drawn together with measured precipitation and relative humidity (as one important factor influencing E_i). The lowest layer (relative crop height 0.3) can store the highest amount of water, because the leaf area is largest in that level. Also the intensity and the total amount of E_i reaches its maximum values in the lowest layer, which is mainly caused by the availability of water. The relatively low importance of E_i in the uppermost layer is therefore a consequence of restricted water supply.

In Figure 4, daily values of canopy resistances r_c and evapotranspiration E_a, derived from lysimeter measurements, are plotted against modelled data. The analyses have been limited to sunny days of the summers 1993 and 1994.

It can be seen that there is a high correlation between the datasets, confirming the applicability of the model. Furthermore, possible ranges of daily canopy resistances of grassland are shown. Even under the mentioned humid conditions considerable values of up to 600 s/m can occur, mainly as a result of dry soil conditions, in combination with relatively high air temperatures and low *LAI*-values.

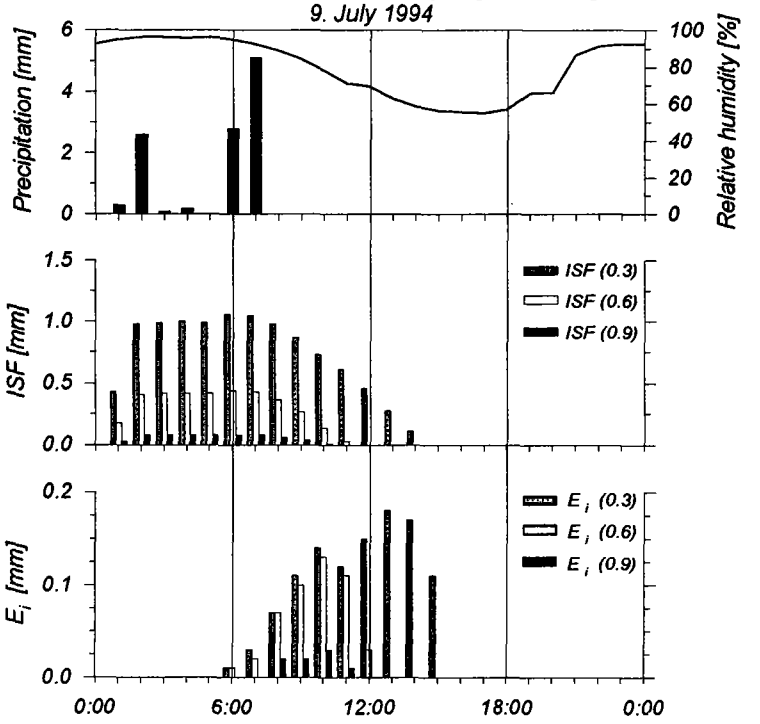

Figure 3: Hourly precipitation (bars), relative humidity (line) and modelled intercepted water storage ISF and evaporation E_i for July 9, 1994, which refer to three different layers at the levels 0.3, 0.6 and 0.9 of relative crop height. The measured, absolute crop height was 20 cm (LAI = 5.5).

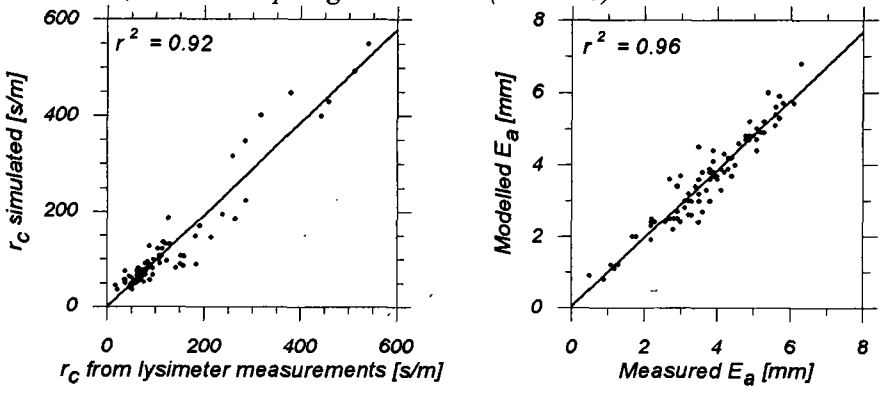

Figure 4: Comparison between daily canopy resistances r_c, derived by lysimeter measurements, and modelled values of r_c (left). On the right the comparison between daily measured values of evapotranspiration E_a and the modelled data is shown. The data refer to sunny days in summer 1993 and 1994.

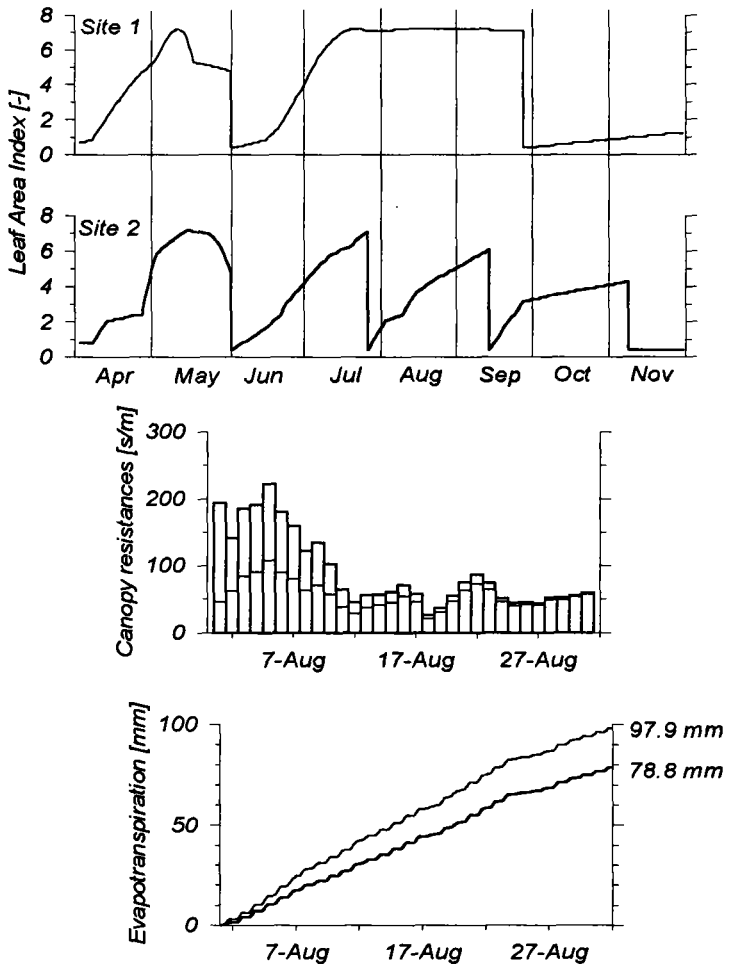

Figure 5: Differences in LAI-development at two sites in the research basin Rietholzbach during the vegetation period 1994. The consequences on modeling of canopy resistances and evapotranspiration are shown exemplary for the August 1994 (site 1: solid lines, site 2: grey lines).

Finally, Figure 5 shows the application of the evapotranspiration model to two different locations of the research catchment. Both sites are grass-covered, but site 1 is used less intensively, as can be seen by the comparison of the *LAI*-development throughout the vegetation period of the presented year 1994. Modeling of canopy resistances for August 1994 shows considerable differences between both sites, mainly caused by different vegetative developments. This has consequences for the computed evapotranspiration E_a, as can be seen by comparison of the two curves in Figure 5, which reflect the continuous accumulation of hourly values of E_a over the period of August 1994. Finally, there is a difference of approximately 20% in evapotranspiration between site 1 and site 2. For this example the net radiation measured on the valley floor at site 2 was also used for calculations for site 1, although the latter is located on a steep, southerly exposed slope. If the different radiation conditions are taken into account,the differences in calculated E_a between both sites are even larger.

6. Summary and conclusions

The objective of the study was to develop a model for the calculation of the evapotranspiration of grassland, which includes interactions between soil, vegetation and atmosphere. Simulations of the evaporation of intercepted water showed the great importance of this quantity under humid conditions and even in relatively low vegetation cover. As a next step it is planned to include the formation and evaporation of dew in the interception submodel. Another submodel provided canopy resistances; which are dependendent on soil moisture, vegetative development and air temperature. Based on the Penman-Monteith equation, hourly and daily evaporation rates have been calculated. The results are in good

agreement with lysimeter data, so that applications to different locations have been carried out. The results can be used to show the importance of parameters influencing evapotranspiration, e.g. land-use or topography. It is assumed that the processes described in the model can be used to make improvements towards simulations of evapotranspiration for different plant cover. Additional measurements in the high-alpine catchment of the Dischma river near Davos (Switzerland) serve to extend the model for applications in extremely inhomogeneous terrain with sparse plant cover.

Bibliography

BRADEN, H. (1992) 'Möglichkeiten zur Regionalisierung der Verdunstung.' In: H.B Kleeberg (Ed.), *Regionalisierung in der Hydrologie. Mitteilung der Senatskommission für Wasserforschung,* volume XI, 141-155. Deutsche Forschungsgemeinschaft, Weinheim.

GARRAT, J.R., P.B. KRUMMEL and E.A KOWALCZYK (1993) 'The surface energy balance at local and regional scales - a comparison of general circulation model results with observations.' *J. Clim.*, 6, 1090-1109.

KOENIG, P. and MENZEL, L. (1993) 'Die Forschung im Gebiet Rietholzbach. Eine Standortbestimmung.' In: D.Grebner (Ed.), *Aktuelle Aspekte in der Hydrologie*, of *Zürcher Geographische Schriften*, 53, 9-24. Geographisches Institut ETH, Zürich.

MENZEL, L. (1995) 'Bodenfeuchtemessung mittels Time Domain Reflectometry (TDR). Funktion und Anwendung.' *Berichte und Skripten,* 55. Geographisches Institut ETH, Zürich.

MONTEITH, J.L. (1965) 'Evaporation and environment.' In: G.Fogg (Ed.), *The state and movement of water in living organisms. Sympos. Soc. Exper. Biol.*, 19, 205-234. Society for experimental biology.

MONTEITH, J.L., G. SCEICZ and P.E. WAGGONER (1965) 'The measurement and control of stomatal resistance in the field.' *J. Appl. Ecol.*, 2, 345-355.

SHUTTLEWORTH, W.J. and J.S. WALLACE (1985) 'Evaporation from sparse crops - an energy combination theory.' *Quart. J. R. Met. Soc.*, 111, 839-855.

WILD, M., L. DÜMENIL and J.P. SCHULZ (1995) 'High resolution GCM simulations over Europe: Surface Processes'. *Report 176. Max-Planck-Institut für Meteorologie*, Hamburg.

A modular modelling system for calculatingevapotranspiration, soil water dynamics and groundwater recharge under various land-use systems

M. Wegehenkel

Institute of Landscape Modelling, Müncheburg, Germany

1. Introduction

Because of the important role of water balances within the general hydrologic cycle there are many computer models for simulating hydrological processes. These models calculate evaporation, transpiration, interception, capillary rise from groundwater into the unsaturated zone, percolation, soil water redistribution and groundwater recharge.

Ways of modelling processes of soil water dynamics in the unsaturated zone range from simple one-layer or multi-layer plate theory models up to simulation approaches based upon mathematical concepts like the well known Darcy, Darcy-Buckingham, Fokker-Plank or Richards' equations.

For the soil water modelling approach there are also many methods for calculating evapotranspiration depending on climate boundary conditions, crop type or land-use system and soil water status. The range here is from (a) simple calculation factors reducing potential evapotranspiration (PET) to actual evapotranspiration (AET) depending on the phenology of the actual crop and soil water status like the PET/AET coefficients from Sponagel (1980) up to (b) detailed complex so-called SVAT models (Soil-Vegetation-Atmosphere-Transfer), which simulate evapotranspiration with physically based modelling approaches like the Penman-Monteith equation (Monteith and Unsworth, 1990).

Every modelling approach mentioned above has its specific restrictions in application, and has different demands for input data and different model-dependent precision in the simulations results. Until now in many computer models soil, crop and atmospheric processes are incorporated in one single more or less complex main program and the components of such a program often cannot be replaced by alternative formulations without a modification of the source code of the program. Yet flexibility in using alternative submodels is essential to efficient research. These aspects lead to the concepts of modular modelling systems, which make it possible to construct a simulation structure adapted to the availability and precision of the input data as well as the objectives. Another requirement is an easy way to compare the results of different complex modelling approaches with such a system.

Until now there exist only a few modular modelling systems. The modular modelling system MMS is a system for hydrologic catchment simulation (Leavesley 1992). A modelling system especially for the purpose of nitrogen leaching in agroecosystems is Expert-N (Priesack and Engel, 1993). The modelling system MOBOWASI (**MO**dellverbund zur **BO**denwasser**S**Imulation) presented in this paper, was developed for flexible water balance modelling of locations and GIS-based regional calculations.

1.1 Components of the modelling system MOBOWASI

A short overview of the whole modeling system is given in Table 1. Within the modelling system any modules from the atmosphere, plant and soil sections can be linked to build a simulation structure for the purpose of water balance calculations

TABLE 1: Components of MOBOWASI

section	model, equation	input data	model outputs
atmosphere, potent. ET	acc. Haude (1955)	qs, plant specific coefficients	daily rate PET
"	acc. Turc (1961)	Rn , T_{mit}	"
"	acc. Penman (1948)	Rn, T_{mit}, qs, u	"
"	acc. Wendling *et al* (1991)	Rn, T_{mit}, qs, u	"
"	PENMAN-MONTEITH (Monteith and Unsworth 1990)	Rn, T_{mit}, qs, u	"
plant models	coefficients correcting PET/ AET acc. Sponagel (1980)	Crop type	"
"	semiempirical plant model acc. Koitzsch & Günther (1990), combined with a simple heat sum model	Crop type, T_{mit}	Plth, Rt, Sdg, Int, Ptrans
"	plant model acc. Stenitzer (1988) in connection with the PENMAN-MONTEITH approach	Crop type , T_{mit}, plant data	Plth, Rt, Sdg, Biom., Ptrans, Int, LAI
soil water dynamics	one layer plate-theory model acc. Renger *et al.* (1974a,b)	initial values Θ, FC, WP	Θ, AET, PERC
"	multiple layer plate theory model combined with a nonlinear storage routing technique acc. Glugla (1969)	initial values Θ, FC, WP, λ per soil compartment	Θ ,AET, Atrans, Int., PERC
"	DARCY-based model SAWAH (Ten Berge *et al* 1992)	initial values Θ, h(Θ)- and k(h) functions per soil compartment	Θ, AET, Atrans, Eva, Int., PERC, Q, CAP, INF

MOBOWASI has an interface to GIS, which facilitates model development, application analysis and visualization utilizing digital map information for spatially distributed systems. In this paper the results of a water balance calculation for one location and a regional simulation based on GIS-data are presented. The simulations were carried out with the following modules of the system (Table 1): a Darcy based soil water module Sawah (Ten Berge *et al.* 1992) with the Van Genuchten parametrization of the h(Θ) and k(h) functions; and a Penman-Monteith approach in connection with a plant model according to Stenitzer (1988)

The short descriptions in the following section give only the governing equations of the modules used in this study. A detailed documentation of the other modules can be found in the literature, which is specified in Table 1 above.

1.2 Penman-Monteith approach and plant model according to Stenitzer (1988)

For the calculation ofevapotranspiration a modified Penman-Monteith approach is used.

$$ET_p = \frac{\frac{Tf\ Rn + 0.864\ (e_s - e)}{R_a}}{Tf + 1 + \frac{R_c}{R_a}} \qquad (1)$$

$$Tf = e^{-0.296 + 0.053\ T_{mit}}$$

The aerodynamic resistance R_a is calculated here from wind speed for neutral atmospheric boundary conditions. The canopy resistance R_c is determined by a plant model according to Stenitzer (1988). Parameters for the plant model are available for winter and summer cereals, maize, potatoes, sugar beet and fodder seed. The model calculates the phenological stage of the crop based on the sum of photothermal units. The next step is the determination of different plant parameters which describe the interception of incoming global radiation into the canopy. With the help of these parameters assimilation and crop growth are calculated. Based on these calculations the actual canopy resistance is evaluated. The reduction of potential to actual evapotranspiration is controlled by the availability of soil water in the profile.

1.3 Soil water module

The soil water balance module SAWAH (Ten Berge *et al.*, 1992) is based on the numerical solution of the flux density and continuity equations. The flux density equation expresses the flux density (q) as a function of soil hydraulic conductivity and the gradient of the hydraulic head.

$$q = -k(h) \frac{\partial H}{\partial z} \qquad (2)$$

The rate of change of soil water over time t in the unsaturated zone follows from the continuity equation.

$$\frac{\partial \Theta}{\partial t} = - \frac{\partial q}{\partial z} + s \qquad (3)$$

These equations are solved numerically using explicit rectangular integration with an internal variable time step Δt using the parametrization of the k(h) and h(Θ) functions according to van-Genuchten (1980) .

2. Examples of simulation results obtained from the modelling system

2.1 Regional water balance simulation

In this section, a GIS-based regional simulation of water balance components for the 24.8 km^2 Agrarlandschaft Chorin catchment for the year 1993 is presented. This catchment is located in the moraine landscape of north-east Brandenburg. Here, several investigations and measurements of weather data, soil moisture, nutrient status of the soil and plant development stages were carried out with the main aim of calibrating and validating agroecosystem models with field measurements. For regional simulation for 1993, daily weather data of air temperature, wind speed, global radiation and air moisture were available. Furthermore in the GIS database a digital land-use map for 1993 and a digital soil map with soil texture types according to the MMK (MittelMaßstäblich landwirtschaftliche StandortKartierung, BGR, 1994) were used (Fig. 1).

The two maps presented in Figure 1 were overlayed within the GIS. The input parameters for the simulation were obtained from data models, which evaluate, for example, soil parameters like hydraulic conductivity k(h) and land-use parameters for the calculation of the plant model in connection with the Penman-Monteith formula from the digital map information.

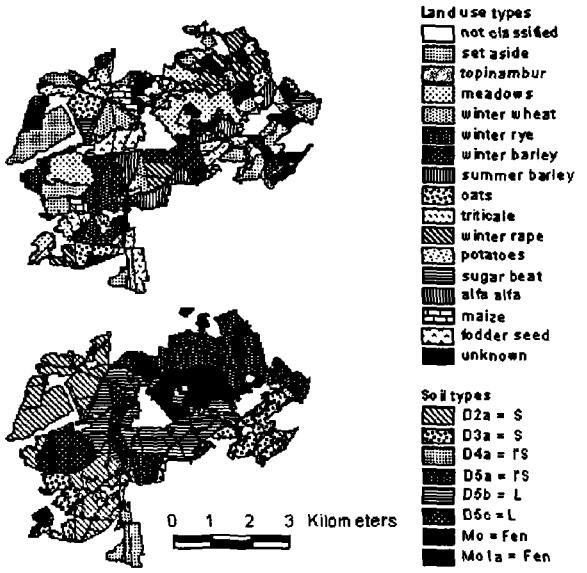

Figure 1: Soil map for the Agrarlandschaft Chorin catchment (BGR 1994) and the land-use map for 1993 based upon a classification from Dr. A.. Haberstock, Institute of Landuse systems, ZALF e.V.

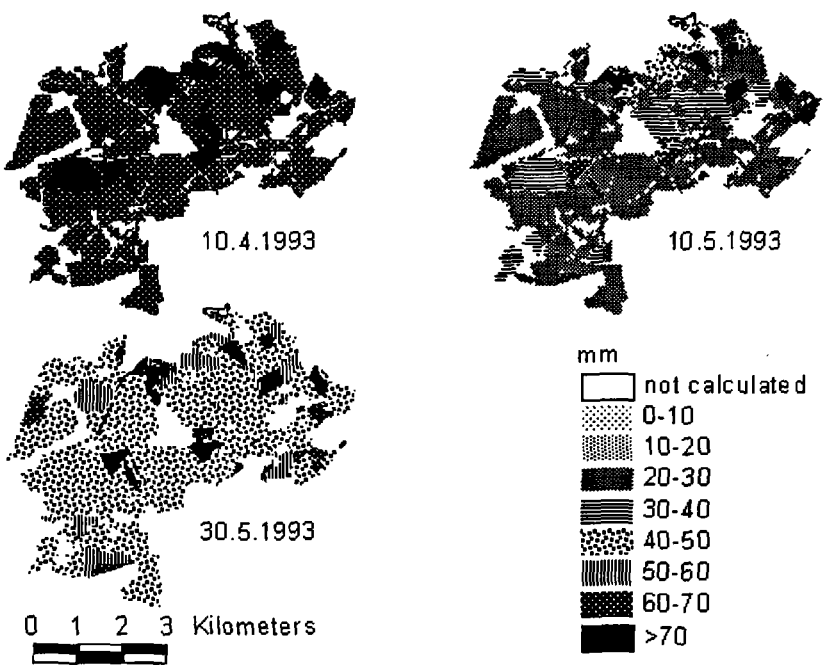

Figure 2: Dynamic changes of soil moisture (mm) 0-30cm for the year 1993 in the catchment Agrarlandschaft Chorin.

Evapotranspiration from crops, for which no plant parameters for the plant model were available, was calculated with the empirical correction factors PET/AET of Sponagel (1980). This affects 28% of the catchment area. The spatial discretization of the soil profiles was set to a value of 0.1 m and the time discretization of the simulation runs of the model was one day. The initial soil moisture conditions of the regional simulation were set to values corresponding to field capacity. With the help of the GIS-interface

the water balance components of each polygon were calculated by the modelling approach for the simulation period 1993 and stored within the GIS-database. As an example of GIS-based visualizing and analysing of modelling results, the regional distribution of dynamic soil moisture evolution through time is shown in Figure 2. The regional distribution of the soil moisture in the compartment 0-30cm shows great variations in space and time within the simulation period.

2.2 Water balance calculations for one location

Simulation results derived using the same modelling approach as used for the regional GIS-based calculations are presented in Fig. 3 for a test field near Hohenfinow located 10 km south-east of the catchment. The soil of this location is a loamy sand or a D3a1-soil according to the MMK classification (BGR, 1994). Daily weather data were available for the simulation period 1991 to 1995. The soil input data initial conditions, and the parameters for the plant model, were evaluated for this location in the same way as for theregional simulation.

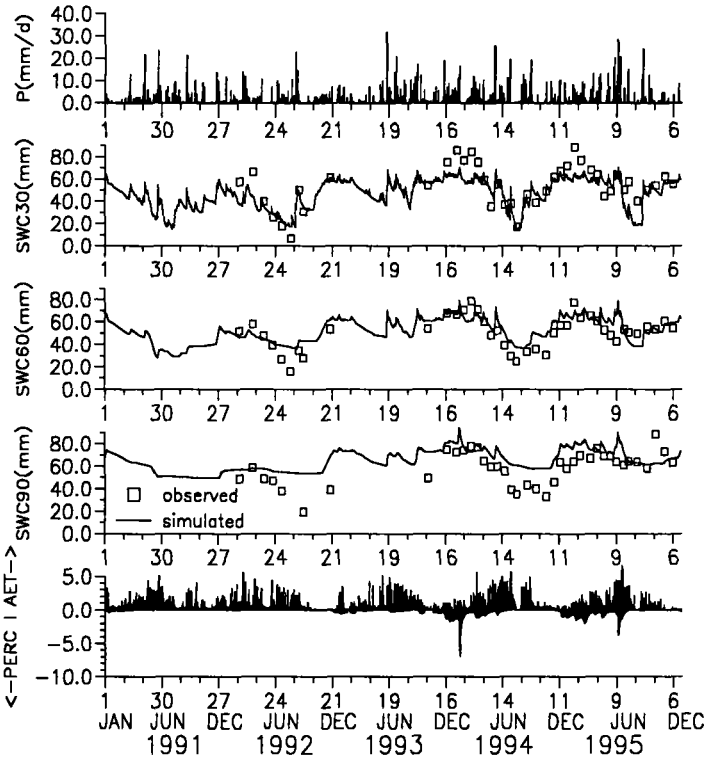

Figure 3: Simulation results for soil water balance of Hohenfinow 1991-1995, soil water content in mm in the compartments 0-30 cm, 30-60 cm and 60-90 cm below surface (SWC30, SWCF60, SWC90), precipitation (P), actual evapotranspiration (AET) and percolation (Perc) in mm d^{-1}.

The observed soil moisture values were measured gravimetrically from field soil samples. Although the model overestimates the soil water contents in the compartment 60-90 cm, the general variation of soil moisture is simulated quite well (Fig. 3). Therefore it can be assumed that the data models and the simulation structure work to a similar and sufficient precision for regional purposes.

2.3 Conclusions

Based upon the modelling system presented in this paper it is possible to build up a simulation structure for the calculation of water balance dynamics of different sites using the actual databases available and

according to specific objectives. Using a GIS-interface spatially distributed simulations are possible. The quality of such regional simulations depends on the kind and the scale of the digital maps used for such purposes and on the data models, which are employed to evaluate the input data for the simulations from the thematic contents of the underlying digital maps. The main problem is the validation of such spatially distributed simulations. The results of calculations for one location, undertaken with similar data models and the same simulation structure used for the GIS-based calculations, show a sufficient precision in simulating soil water content for a five year period. This leads to the assumption that the regional simulation approach also works quite well.

Bibliography

BGR (1994) 'Ergebnisse der Aufbereitung von Daten der Mittelmaßstäblichen Landwirtschaftlichen Standortkartierung (MMK) der ehemaligen DDR für länderübergreifende Bodenschutz.' *BGR, AußenstelleBerlin.*

GENUCHTEN M.TH. VAN (1980) 'A closed form equation for predicting the hydraulic conductivity of unsaturated soils'. *Soil Science Society of America Journal* 44: p.892-898.

GLUGLA G. (1969) 'Berechnungsverfahren zur Ermittlung des aktuellen Wassergehaltes und Gravitationsabflusses'. *Albrecht-Thaer-Archiv 13*, p.371-376.

HAUDE W. (1955) 'Zur Bestimmung der Verdunstung auf möglichst einfache Weise.' *Mitt. des Deutschen Wetterdienstes*, 11, Bad Kissingen.

KOITZSCH R. and R. GÜNTHER (1990) 'Modell zur ganzjährigen Simulation der Verdunstung und der Bodenfeuchte landwirtschaftlicher Nutzflächen'. *Arch. Acker-Pflanzenbau Bodenkd.* 24, p.717-725.

LEAVESLEY G. (1992) 'Modular Modeling System User's Manual Vol.One'. *University Colorado at Boulder, Center for Advanced Decision Support for Water andEnviromental Systems.*

MONTEITH J.L. and M.H. UNSWORTH (1990) 'Principles of environmental physics'. *Edward Arnold, New York.*

PENMAN H.L. (1948) 'Natural evaporation from open water, bare soil and grass.' *Proc.Roy. Soc. London A 193*, p.120-145.

PRIESACK E. and TH. ENGEL (1993) 'Modellierung des Wassertransportes im Modellsystem "EXPERT-N".' *Agrarinformatik* 24, p.33-40.

RENGER M., O. STREBEL and W. GIESEL (1974a) 'Beurteilung bodenkundlicher, kulturtechnischer und hydrologischer Fragen mit Hilfe von klimatischer Wasserbilanz und bodenphysikalischen Kennwerten 1.Bericht: Beregnungsbedürftigkeit'. *Z.f.Kulturtechnik u. Flurbereinigung* 15, H.3.

RENGER M., H. VOIGT, O. STREBEL and W. GIESEL (1974b) 'Beurteilung bodenkundlicher, kulturtechnischer und hydrologischer Fragen mit Hilfe von klimatischer Wasserbilanz und bodenphysikalischen Kennwerten 2.Bericht: Einfluß des Grundwassers auf die Wasserversorgung der Pflanzen'. *Z.f.Kulturtechnik u. Flurbereinigung* 15, H.3.

SPONAGEL H. (1980 'Zur Bestimmung der realen Evapotranspiration landwirtschaftlicher Kulturpflanzen. *Geol. Jahrbuch, Reihe F*, H.9 Hannover.

STENITZER E. (1998): Ein numerisches Modell zur Simulation des Bodenwasserhaushaltes und des Pflanzenertrages eines Standortes. *Mitt. aus der Bundesanstalt für Kulturtechnik und Bodemwasserhaushalt. Nr.31.*

TEN BERGE H.F.M., D.M. JANSEN, K. RAPPOLDT and W. STOL (1992): The soil water balance module SAWAH: description and users guide *Simulation Reports CABO-TT, No.22, Wageningen*

TURC L. (1961) 'Evaluation des besoins en eau d'irrigation evapotranspiration potentielle.' *Ann. Agron.* 12, 13.

WENDLING U., H.G. SCHELLIN and M. THOMÄ (1991) 'Bereitstellung von täglichen Informationen zum Wasserhaushalt des Bodens für die Zwecke der agrarmeteorologischen Beratung.' *Z. f. Meteorologie 41*, H. 6, p.1-16.

Main symbols

AET	=	actual evapotranspiration	mm d^{-1}
Atrans	=	actual transpiration	"
Biom.	=	biomass	kg ha^{-1}
CAP	=	capillary rise	mm d^{-1}
(e_s-e)	=	saturation deficit	g cm^{-3}
FC	=	field capacity	Vol%, mm dm^{-1}
$h(\theta)$	=	soil water suction versus water content	cm WS
INF	=	infiltration	mm d^{-1}
INT	=	interception	" "
H	=	soil water potential including gravitational potential	m
k(h)	=	soil hydraulic conductivity	m d^{-1}
LAI	=	leaf area index	m^2 m^{-2}
λ	=	empirical routing factor	mm^{-1}
N	=	precipitation	mm d^{-1}
PERC	=	percolation	"
PET	=	potential evapotranspiration	"
Plth	=	plant height	cm
q	=	flux density	m d^{-1}
qs	=	saturation deficit	%
Q	=	runoff	mm d^{-1}
R_a	=	aerodynamic resistance	s m^{-1}
R_c	=	canopy resistance	" "
R_{glob}	=	global radiation	J cm^{-2}
Rn	=	net radiation as evapotranspiration equivalent	mm d^{-1}
Rt	=	rooting depth	dm
Sdg	=	soil covering degree	%
Θ	=	soil water content	Vol%, mm dm^{-1}
T_f	=	temperature factor	
T_{mit}	=	average temperature of air	°C
u	=	wind speed	m s^{-1}
WP	=	wilting point	Vol%, mm dm^{-1}

Comparison of three soil-vegetation-atmosphere transfer models (EARTH, ISBA, SiSPAT) and application to a middle mountain site (Vosges, France)

S. Fouche-Roguiez[1] , G. Najjar[1], I. Braud[2], J. Noilhan[3] and B. Ambroise[1]

[1] *Centre for Eco-Geographical Research Studies, Strasbourg, France*
[2] *Laboratory of Hydraulic Transfers in the Environment, Grenoble, France*
[3] *Météo-France, Toulouse, France*

1. Introduction

In mountains, patterns of water and energy inputs are strongly controlled by spatial variations of different topographic features, e.g. elevation, slope, exposure to sunshine and wind, orographic shadows. These topographic effects on the water cycle have been studied within several nested research catchments in the Vosges massif (Ambroise, 1995; Ambroise *et al.*, 1995). One of the key remaining issues is to model correctly soil-vegetation-atmosphere transfers (SVAT) in such a temperate middle mountain environment.

As a first step, extensive data sets available at a reference site have been used to validate and compare three one-dimensional SVAT models of increasing complexity: EARTH (Choisnel, 1985), ISBA (Noilhan and Planton, 1989) and SiSPAT (Braud *et al.*, 1995). These models simulate water and energy surface budgets.

2. The Geisberg meteorological station

The Geisberg meteorological station, located near the small Ringelbach research catchment at Soultzeren (High-Vosges, France), is representative of a temperate middle mountain environment (Table 1). Standard meteorological data have been recorded every ten minutes (six minutes for precipitation) since 1987 (Table 2). Soil temperature, soil heat flux, net radiation, diffuse radiation and albedo have been measured since 1992. Soil water content and tension profiles down to 1 meter have been measured weekly during the summer period using a neutron probe and tensiometers.

TABLE 1: Site characteristics

	Geisberg Meteorological Station
Altitude	760 m
Latitude	48° 03'
Longitude	7° 06'
Aspect	South-South-West
Slope	8°

TABLE 2: Annual meteorological data for the year 1992 at the Geisberg station

	Annual value
Precipitation	1085 mm
Air temperature	8.4 °C
Air relative humidity	76 %
Global radiation	1281 $W.m^{-2}$
Wind speed	2.5 $m.s^{-1}$

The 1-m deep brown soil is coarse-textured and very permeable, with a high organic matter content in the upper layer. Undisturbed cores have been sampled every 5 cm in the soil; textural fraction, bulk density, water content, water retention at different tensions, hydraulic conductivity at saturation have been measured in the laboratory (Viville, 1985) (Table 3). Van Genuchten and Mualen models have been adjusted to define hydraulic conductivity and retention curves (Reutenauer, 1987; Reutenauer and Ambroise, 1992).

The catchment is covered by dense grassland pasture. The vegetation leaf area index has been measured during summer using a direct method. Root density values are available for a soil profile at a site with similar vegetation within the Ringelbach catchment (Humbert, 1977).

TABLE 3: Soil (1 m depth) and vegetation mean characteristics at the Geisberg station.

	Measured value
Soil moisture at saturation	0.483 $m^3.m^{-3}$
Soil moisture at field capacity	0.172 $m^3.m^{-3}$
Soil moisture at the wilting point	0.059 $m^3.m^{-3}$
Hydraulic conductivity at saturation	9.22 10^{-6} $m.s^{-1}$
Surface albedo	0.2
Leaf area index	6
Root density	1.35 10^5 $m.m^{-3}$

TABLE 4: Main vegetation parameters values used in the 3 models.

EARTH	*ISBA*	*SiSPAT*
Structural resistance 30 $s.m^{-1}$	Stomatal resistance 150 $s.m^{-1}$	Stomatal resistance 150 $s.m^{-1}$
		Plant resistance * 6.5 10^{12} $s.m^{-1}$
		Critical leaf water potential * -0.140 m

* Braud *et al.*, 1995

3. The Soil Vegetation-Atmosphere-Transfer Models

3.1 EARTH

This model has been developed by Choisnel (1985) for agroclimatological applications. It is a physically-based but very simple parametric model, using daily meteorological data; minimum and maximum air temperature and humidity, precipitation, global radiation and mean wind speed. It requires a few parameters including albedo, minimum surface resistance (Table 4), and an empirical parameter for surface humidity calculation.

Evapotranspiration is calculated using the Penman-Monteith formula. Soil is represented by two storages; a permanent storage and a temporary subsurface storage. The temporary storage is created near the surface when it is raining and when the soil is not at the field capacity. Water in this conceptual subsurface soil layer (i.e. temporary storage) is more available for evapotranspiration than water in the deep soil layer (i.e. permanent storage).

3.2 ISBA

This model (Noilhan and Planton, 1985) is used by Météo-France in numerical weather prediction models. It has already been tested in different climatic regions, but not yet in temperate mountains. Like EARTH, this parametric model has been developed with the aim of reducing as much as possible the number of parameters, while attempting to preserve as much as possible the representation of the physics. It uses the same meteorological data plus the atmospheric radiation. The time step of input data is typically one hour. It requires some additional parameters such as leaf area index (Table 3), the fraction of vegetation and the minimum stomatal resistance (Table 4).

Aerodynamic formulae are used to simulate three components of the evapotranspiration; bare soil evaporation, transpiration from leaves and evaporation of intercepted water. The soil is divided into two storages; a main storage, and a thin surface storage, to estimate surface moisture.

3.3 SiSPAT

This model (Braud *et al.*, 1995) is more sophisticated and more complex to use than the two others. It is a deterministic model solving the heat and water diffusion equations in soil. The main physical processes are represented with equivalent degrees of simplification for all the compartments. This model provides as complete a validation as possible for the various compartments. It requires the same meteorological forcing as ISBA and uses the same aerodynamic equations. One vegetation layer is considered and is characterized by the leaf area index (Table 3), and it also requires a shielding factor which partitions the incoming energy between the vegetation and the bare soil, a minimum stomatal resistance, a total plant resistance and a critical leaf water potential (Table 4). Turbulent transfers within the canopy and from bare soil are solved by using an approach derived from the two-source model of Shuttleworth and Wallace (1985).

In the soil, coupled heat and mass transfer dynamic equations are solved. Root uptake is modelled using an electrical analogue scheme with various resistances. The SiSPAT model is able to deal with non-homogeneous soils. Matric potential is continuous at the interface of the horizons.

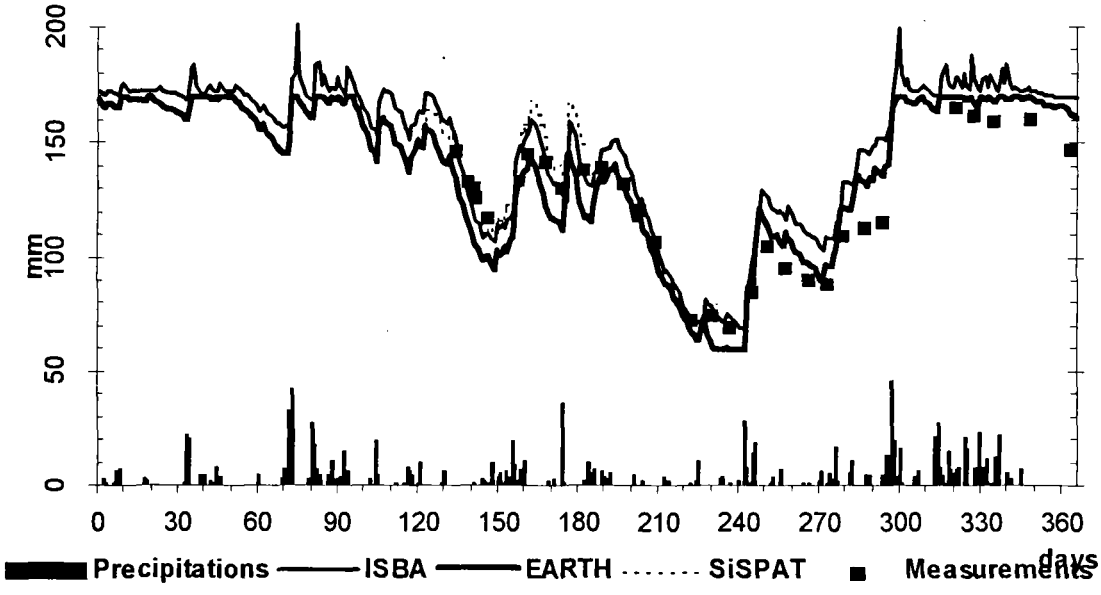

Figure 1: Daily soil water content simulations at the Geisberg station using EARTH and ISBA (year 1992), and SiSPAT (May-June 1992).

4. Results

EARTH and ISBA have been tested at the Geisberg meteorological station over the whole year 1992, while SiSPAT has been run over 2 months (May and June) of that year. A sensitivity analysis has been performed previously for EARTH and ISBA (Fouché *et al.*, 1994; 1995a; 1995b).

4.1 Daily results

The variation in soil water content through time simulated by the models is in reasonable agreement with measurements (Fig. 1). The first part of the year is rather well simulated by the two models. During summer, ISBA soil water simulation does not reach the wilting point, which is more realistic than EARTH simulation. In autumn simulated soil wetting-up by both models is faster than that observed. This phenomenon has been often observed on our sites; actual soil depletion in summer may slightly affect soil layers deeper than 1 m and these soil layers must be refilled before the upper soil layers.

Net radiation and evapotranspiration fluxes estimated by ISBA and EARTH (Fig. 2) are very similar, except that the EARTH model does not calculate soil water content above field capacity. So some differences occur in March and in November during dry periods.

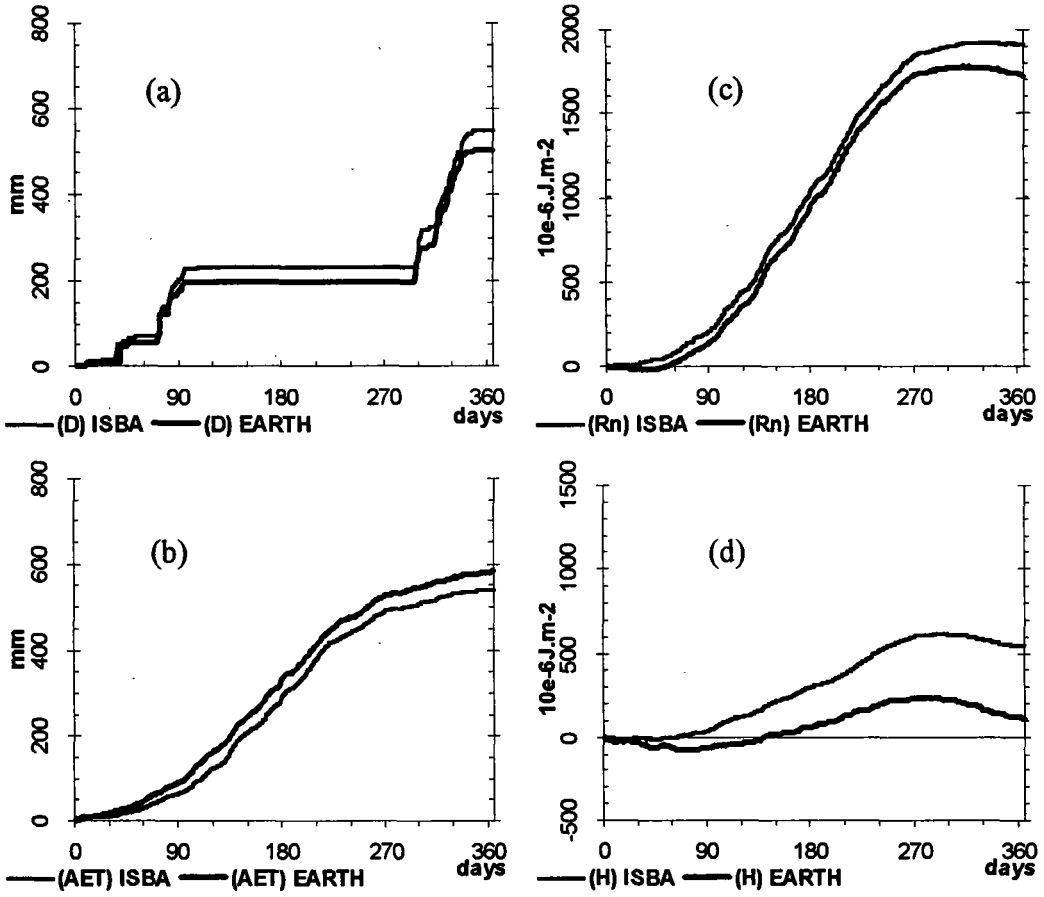

Figure 2: Daily cumulative simulations during 1992 at the Geisberg station using EARTH and ISBA. (a) drainage D, (b) total evapotranspiration AET, (c) net radiation Rn, (d) sensible heat flux H.

Sensible heat flux (Fig. 2) and soil heat flux (not shown) simulations are very different because the two models do not use the same formulae. ISBA considers a temperature gradient between the soil and the atmosphere while EARTH calculates soil heat flux and takes a sensible heat flux value in order to balance the energy budget. This serves as a reminder that the EARTH model has been derived for mainly for agroclimatological purposes while the ISBA model attempts to describe all the atmospheric fluxes with the same precision.

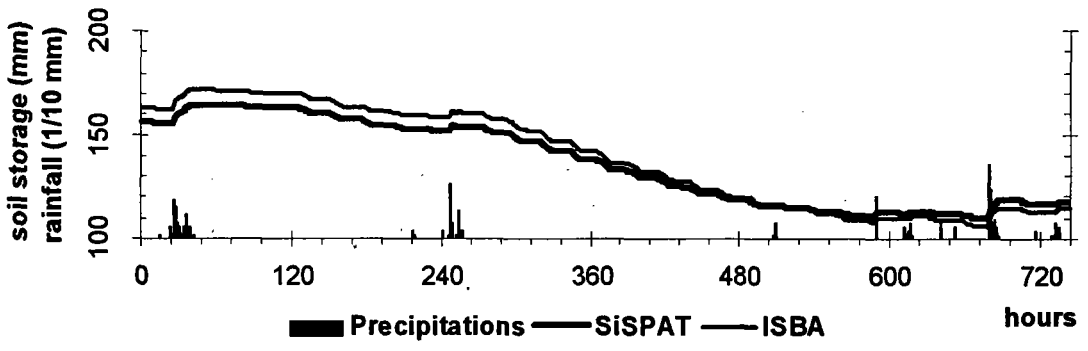

Figure 3: Hourly soil water content simulations during may 1992 at the Geisberg station using ISBA and SiSPAT.

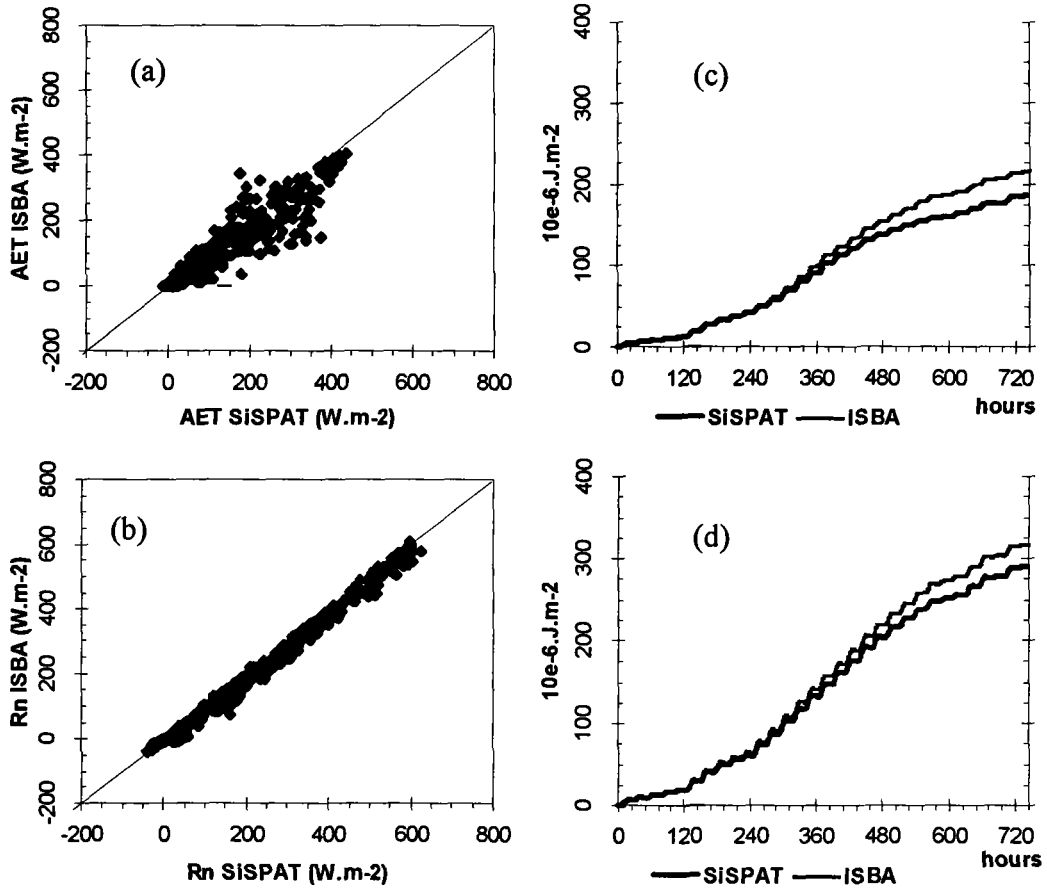

Figure 4: Hourly simulations of total evapotranspiration (a, c) and net radiation (b, d) during May 1992 at the Geisberg station using SiSPAT and ISBA: comparisons between hourly fluxes (a) and (b) and cumulative fluxes(c) and (d).

Both EARTH and ISBA seem to give reasonable estimations of the main water cycle components during the year 1992 at the Geisberg station even if water and energy budget partitions are not exactly the same (Table 5). The simulation of the soil moisture is satisfactory for the SiSPAT model during the two months of simulation (Fig. 1).

TABLE 5: Daily simulation results during 1992 at the Geisberg station

	ISBA model		*EARTH model*		*ISBA/EARTH*
Total or actual evapotranspiration AET (mm)	541	(50% P)	583	(54% P)	0.93
Potential evapotranspiration PET (mm)	-		787	(AET = 74%)	
Transpiration Etr (mm)	485	(90% AET)	-		
Drainage D (mm)	549	(50% P)	503	(46% P)	1.09
Net radiation Rn (10^{-6} J.m^{-2})	1911		1725		1.11
Latent heat flux (10^{-6} J.m^{-2})	1353	(71% Rn)	1440	(84% Rn)	0.94
Sensible heat flux H (10^{-6} J.m^{-2})	548	(29% Rn)	108	(6% Rn)	5.07
Soil heat flux G (10^{-6} J.m^{-2})	10	(0.5% Rn)	176	(10% Rn)	0.06
Mean surface temperature Ts (°C)	9.9		8.1		1.22

4.2 Hourly results

The SiSPAT model was initialised at the beginning of May 1992 with measured temperature and tension soil profiles. Its hourly simulations were compared with ISBA hourly results for May 1992, extracted from the whole year simulation.

Net radiation simulations (Fig. 4) are similar for the two models, with a slightly higher annual total using ISBA. Evapotranspiration (Fig. 4) simulations present some differences due on one hand to available energy and on the other hand to soil available water. In SiSPAT, soil water is extracted by roots at different levels and moves up to the leaf because of a pressure gradient calculated at each time step. In ISBA, evaporated water comes from the main soil storage acting like a bucket.

During this period, soil water content simulations (Fig. 3) are not very different because enough water is available for evapotranspiration. Atmospheric conditions control the amount of evaporated water. During dry periods, SiSPAT may give different results to ISBA because of the modelled extraction of water by roots in SiSPAT.

It is interesting to have tested this model during a long period (2 months) relative to the time step of calculation which may decrease to 1 second when it is raining. These results prove that a complicated model can run correctly for middle mountain conditions.

SiSPAT will be used for more precise simulations after a calibration using the results of a specific campaign (Regio Klima Projekt -REKLIP campaign in 1994).

5. Conclusion

Although no calibration has been performed, rather satisfactory results have been obtained using the 3 models for this specific site and year. Improvements could probably still be achieved by adapting these models in order to take into account the possible effects of lateral fluxes within sloping land. A further validation will be performed using data sets collected over several years and at several sites in the Ringelbach catchment, especially the water and energy fluxes measured during the REKLIP 94 Experiment.

In conclusion, the mechanistic SiSPAT model seems to provide a convenient tool for analysing physical processes within the soil-vegetation-atmosphere system at the stand scale during short periods, while the more simple parametric models EARTH and ISBA - which can more easily be coupled to distributed hydrological and meteorological models - seem to be useful to map water redistribution according to topography at the regional scale over long periods.

Acknowledgements

We thank E. Choisnel (Météo-France, Paris) for providing the EARTH model.
This study has been funded by:

- le Programme Climatique Régional transfrontalier franco-germano-suisse REKLIP/Phase 2 , Thème "Bilan d'énergie - bilan hydrique"
- le Programme de Recherche en Hydrologie PRH/INSU et le Programme "Exploitation Maximale des Données" EMD/INSU.

References

AMBROISE B. (1995) 'Topography and the water cycle in a temperate middle mountain environment : the need for interdisciplinary experiments.' *Agric. For. Meteorol.*, 73, 217-235.

AMBROISE B., A.V. AUZET, J. HUMBERT, J.L. MERCIER, G. NAJJAR, P. PAUL and D. VIVILLE (1995) 'Le cycle de l'eau en moyenne montagne tempérée: apport des bassins versants de recherche vosgiens (Ringelbach, Strengbach, Fecht).' *Ann. Géo.*, 581/582, 64-87

BRAUD I., A.C. DANTAS-ANTONINO, M. VAUCLIN, J.L. THONY and P. RUELLE (1995) 'A simple soil-plant-atmosphere transfer model (SiSPAT) development and field verification.' *J. Hydrol.*, 166, 213-250.

CHOISNEL E. (1985) 'Un modèle agrométéorologique opérationnel de bilan hydrique utilisant les données climatiques.' In : Perrier A.,Riou C. (eds) « *Les besoins en eau des cultures* », INRA, 115-132.

FOUCHÉ S. (1994) 'Modélisation du bilan hydrique stationnel dans le bassin versant du Ringelbach.' Projet de Fin d'Etudes ENSAIS, Mémoire de DEA Sciences de l'Eau ULP-ENGEES, CEREG, Strasbourg, 91 p.

FOUCHÉ S., G. NAJJAR and B. AMBROISE (1994) 'Test du modèle de bilan hydrique EARTH en un site de moyenne montagne tempérée : la Station Météorologique du Geisberg (Hautes-Vosges).' Actes de l'*Atelier de Modélisation de l'Atmosphère 1994*, Météo-France/CNRM, Toulouse, 29/11-1/12/1994, 57-64.

FOUCHÉ S., G. NAJJAR and B. AMBROISE (1995a) 'Validation of a 1-D Soil-Vegetation-Atmosphere-Transfer Model : the EARTH Model (Choisnel, 1985) in a temperate middle mountain environment (High-Vosges, France).' *European Geophysical Society, XX General Assembly*, Hambourg, 3-7 avril 1995 (poster).

FOUCHÉ S., G. NAJJAR, J. NOILHAN and B. AMBROISE (1995b) 'Testing of a Land Surface Parameterisation, the ISBA Model, in a Temperate Middle Mountain Environment'. *International Union of Geodesy and Geophysics, XXI General Assembly*, Boulder, Colorado, 3-7/7/1995 (oral communication).

HUMBERT J. (1977) 'Contribution à l'étude des transferts hydriques dans le système sol - plante - atmosphère.' *Thèse de 3ième cycle*, ULP Strasbourg, 194 p.

NOILHAN J. and S. PLANTON (1989) 'A simple parameterisation of land surface processes for meteorological models.' *Mon. Weather Rev.*, 117:536-549.

REUTENAUER D. (1987) 'Variabilité spatiale des propriétés physiques et hydriques des sols et des formations superficielles du bassin de la Fecht en amont de Turckheim (Haut-Rhin).' *Thèse de 3ième cycle*, ULP Strasbourg, 269 p.

REUTENAUER D. and B. AMBROISE (1992) 'Fitting the van Genuchten-Mualem model to observed hydraulic properties of coarse-textured soils in the Vosges Mountains of France.' In: M.T. van Genuchten, F.J. Leij, L.J Lund (Eds) "*Indirect Methods for Estimating the Hydraulic Properties of Unsaturated Soils*", University of California, Riverside (Ca, USA), 285-291.

SHUTTLEWORTH WJ. and J.S. WALLACE (1985) 'Evaporation from sparse crops - an energy combination theory.' *Quart J R Meteorol Soc* 111 : 839-855.

VIVILLE D. (1985) 'Variabilité spatiale des propriétés physiques et hydriques des sols dans le bassin versant du Ringelbach (Vosges granitiques).' *Thèse de 3ième cycle*, ULP Strasbourg, 158 p.

Variation of pH and concentration of nutrients and minerals during rain-events

H. Burch, P. Waldner and B. Fritschi

Swiss Federal Institute for Forest, Snow and Landscape Research, Birmensdorf, Switzerland

1. Introduction

Detailed information concerning actual forest damage in Europe is needed, specifically regarding the main processes on atmospheric deposition to forest ecosystems. In recent years, investigations on the composition of rainwater have been based on monthly, weekly or daily sampling periods (Verry, 1983; Klöti *et al.*, 1989; Mosello and Marchetto, 1996). To reduce the effects of evaporation and chemical reactions in samples left in the field for long periods, sampling on an event base has become increasingly common (Radojevic and Lim, 1995a; Khare *et al.*, 1996; Kennedy *et al.*, 1979).

In the published reports, a large variation in concentration of nutrients and minerals in precipitation during rain-events has been reported, usually with a peak of concentration at the beginning of an event. Data from sequential precipitation samplers give us more information to evaluate the deposition rate (flux and concentration) on an event basis. An Australian investigation showed that the most influential factors on the deposition rate were the season and the wind direction (Crockford *et al.*, 1996). It is mentioned in Khare *et al.* (1996), that during monsoon events in India, 50% of the total concentration of the ionic components is washed out in the first 7.2 mm of rain, based on 5 events in 1994. In terms of processes, a distinction is made between the mechanisms transferring material to cloud droplets before they begin their descent as a raindrop (rainout) and those processes transferring material to falling raindrops (washout). It is maintained that washout is the dominant process in the early part of an event, while rainout seems to determine the composition of the rain in the latter part of an event.

This information in Khare *et al.* (1996) does not explain the processes which are responsible for the variation in concentration during rain-events. As the particles in precipitation are composed of aerosols and gases in the atmosphere, they were fixed by raindrops or ice crystals during cloud condensation (rainout) or scavenged during rain-events (washout). The chemical composition of precipitation has also been reported in Fowler (1980), Prokop *et al.* (1996) and Baechmann *et al.* (1996).

The concentration of nutrients and minerals in precipitation is an essential factor affecting the biochemical processes at these locations. Not only the load but also the concentration of minerals and nutrients in wet deposition can be decisive in ecosystem processes. Recently, near real-time pH measurement within several rainstorms has been achieved, using a continuous flow system (Jennings *et al.*, 1992; Radojevic and Lim, 1995b; Tyree, 1981). The H^+ ion is a dominant element in wet deposition. Peaks in H^+ concentration can affect parts of natural ecosystems like the canopy (Schreiber, 1996), soilwater and root system, groundwater, lakes and aquatic wildlife.

2. Experimental and methods

This study is based on the following assumptions.

(i) Scavenging processes during rain-events are responsible for peaks in concentration of minerals and nutrients at the beginning of rain-events (washout), followed by decreasing concentrations in the latter part of the rain-events (rainout).
(ii) A maximum of acid particles in the atmosphere will be washed out at the beginning of a rain-event, leading to peaks in H^+ concentration and low pH values, followed by increasing pH values in the latter part of the rain-events (rainout).

The investigation area is situated in the Alptal valley, a rural region in the Swiss prealps with yearly precipitation amounts up to 2300 mm. Urban centres in the west (Schwyz, Zug, Luzern) are delimited by the mountain-ranges Mythen, Rigi and Rossberg (Burch, 1994). Rainwater samples (Table 1) have been collected at the climate station at 1220 m.a.s.l since 1973. Fischer-Riedmann (1995) calculated the nitrogen deposition at this climate station to be 16.3 kg (N) ha^{-1} yr^{-1} on average in 1993, including a measured quota of 19% for dry deposition.

TABLE 1: Equipment for wet-deposition measurements in the Alptal-valley (Canton of Schwyz)

Pos.	Equipment	Sampling-interval	from	to
1	bulk-deposition	weekly	Jun. 1973	Sep. 1996
2	wet only deposition (DEP)	weekly	Dec. 1988	Sep. 1996
3	sequential precipitation sampler (SPS)	5 mm / 10 mm precipitation	Oct. 1989	Jun. 1993
4	pH ombrometer (near real-time)	10 min.	Oct. 1989	Jun. 1993
5	pH analysis in the laboratory	weekly	Jun. 1990	Sep. 1996

2.1 Sequential precipitation sampler

To obtain accurate data concerning the variation of concentration in wet deposition, a new sampling apparatus that splits the precipitation into sequential samples was developed. This automatic 'wet' - only sequential precipitation sampler (SPS) was used from October 1989 to July 1993.

The SPS measured up to 6 rain-events during the usual maintenance interval of one week. A new rain-event is deemed to start after a dry period of at least 24 hours. During every rain-event, the first sample consisted of 5 mm; all other samples consisted of 10 mm of precipitation. To check the sampling device and the laboratory values, the load and the concentration of the weekly samples (DEP), from the 'wet'- only double bucket collector (WMO, 1994), were compared with the average concentration calculated from the sequential samples (SPS). The heated inlet funnel allowed measurement of snow-events in winter. In summer, the cooling system for the open rainwater-samples was not adequate to hold the water temperature at the proposed 4° C during hot periods.

In the laboratory, the samples were filtered (0.45 µm) and analysed by the following methods: ICP-MS (inductively coupled plasma - mass spectrometry) for concentrations of Ca, K, Mg, Na, Si, Al, Ni, P, S and Pb; IC (ion chromatography) for the ions NO_3, SO_4, PO_4 and Cl; and FIA (flow injected analysis) for NH_4.

2.2 Automatic measuring of the pH within rain-events by ombrometer

Close to the sequential precipitation sampler (SPS), an automatic near real-time pH-ombrometer was installed to measure the acidity of the rainfall at intervals of 10 minutes during rain-events. The pH electrode was calibrated biweekly with buffer solutions at pH 4 and pH 7. As the ombrometer was calibrated at regular intervals, the established precision is estimated at about 0.1 pH units.

3. Results and discussion

3.1 Variation of rain chemistry during rain-events

From 1989 to 1993, 685 samples were collected during 230 rain-events. The first 76 events have been analysed in detail (18% summer thunderstorms, 38% summer rain-events, 44% snow-events). Strong variations in concentration during rain-events have been measured in the sequential samples (SPS). Comparing this data with the weekly samples (DEP), the highest and the lowest concentration were found in the sequential samples (SPS). A report on the evaluation of the complete dataset and a detailed description of the instrumentation has been prepared by Waldner (1996).

A typical pattern during short thunderstorms is the high concentrations of nutrients (NO_3^-, NH_4^+) and minerals (Ca^{2+}) at the beginning of a rain-event, followed by a rapid decrease of concentration (Fig.1). The reason is the strong initial washout of the atmosphere by raindrops.

In summer rain-events, during which SO_4^{2-} concentrations exceed 2 mg/l, the same pattern as in thunderstorms, but at a lower level of concentration, can be recognised. This occurs during stable atmospheric conditions and at low wind velocities. When the SO_4^{2-}-concentration is below 2 mg/l, the concentration of other nutrients and minerals can increase during longer rain-events in combination with heavy winds (Figure 1). These winds can bring new nutrients and minerals from the surrounding area to supply the on-going precipitation processes.

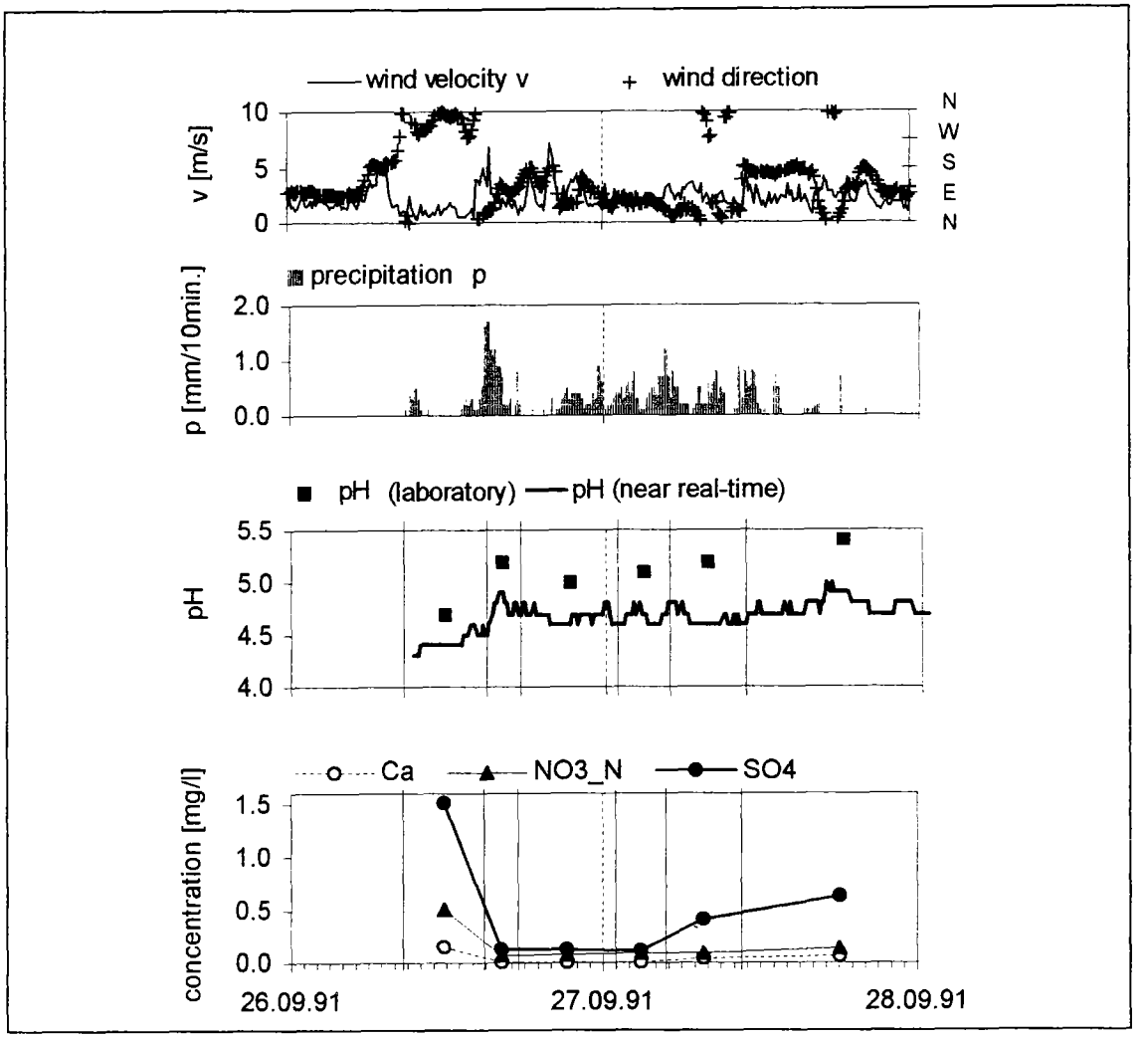

Fig. 1: Variation of concentrations (NO_3^--N, Ca^{2+}, SO_4^{2-}) and pH during the summer rain-event of 26/27 September 1991. During this rain-event, the sum of precipitation reached 64 mm with a maximum rainfall intensity of 1.7 mm/10 min.

During snow-events, the concentration of minerals and nutrients in the snowfall was mostly increasing or constant, independent of the SO_4^{2-} concentration. The total load of the wet deposition is higher in winter than in summer. However, the peaks in the concentration of minerals and nutrients are several times smaller in winter than in summer rain-events. Higher element concentration of snow compared to that of rainfall samples are explained by more efficient below-cloud scavenging of atmospheric constituents, especially aerosol particles, by snowflakes (Grosch and Georgii, 1989).

During rain-events, changes in concentration of minerals and nutrients showed generally the same trend in all cases investigated. Looking at some concentration ratios in wet deposition, other behaviours were recognised such as increasing Ca^{2+} content at the same time when the SO_4^{2-} concentrations are decreasing. Normally, the concentrations of minerals and nutrients during rain-events were inversely related to the pH.

This pattern can change if events with high Ca^{2+} concentrations occur after periods with low air-humidity and dry winds from the south. Such a typical rain-event was the scavenging of Saharan dust on 23 March 1990 (Schwikowski *et al.*, 1995), where initial pH values of 5.9 were observed in the Alptal valley, followed by pH values down to 5.2 in the next rainout of 39 mm in 10 hours (Waldner, 1996).

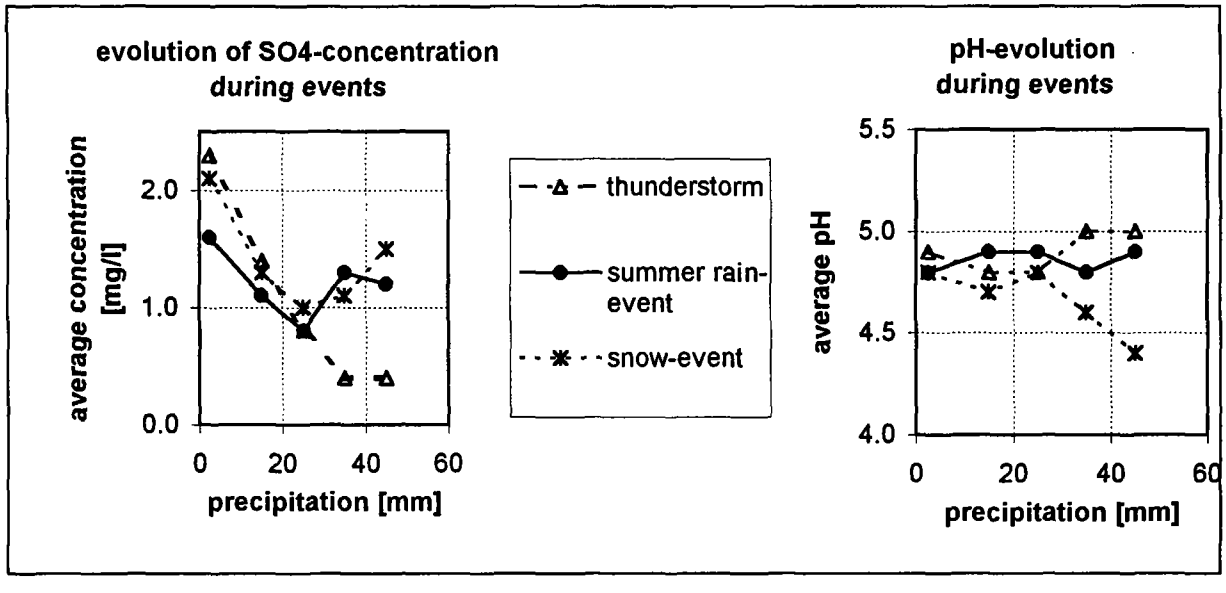

Fig. 2: Comparison of wet deposition within three types of rain-events (thunderstorm, summer rain-events and snow-events), using all 230 measured events. The average evolution of the SO_4 concentration (left) and the pH evolution (right) during events are shown for the first 45 mm of precipitation.

Figure 1 confirms the proposed assumptions, that a maximum of acid particles is washed out at the beginning of a rain-event, followed by lower concentrations at the end of an event, leading to low pH values at the beginning of an event. The hypothesis of an increase of the pH value in the rain after the initial peak was confirmed during thunderstorms, but not during snow-events. Based on a full analysis of the 230 events between 1989 and 1993, it was found that 28% of the total content of nutrients and minerals is washed out in the first 5 mm rain of thunderstorms. The corresponding data for snow-events and summer rain-events are 20 % and 13% respectively (Waldner, 1996).

3.2 Variation of pH during rain-events

The near real-time measurements with the pH-ombrometer in the Alptal valley showed a range between pH 3.8 and 6.7 with a weighted mean value of 4.75. The highest pH value (6.7) was observed during a short Saharan dust event (3.9 mm rain in 6 hours) of 9th March 1990 with a mean Ca^{2+} concentration of 4.3 mg/l. Analyses of all the precipitation samples in the laboratory between one and seven days later showed that these pH values were usually higher than the ombrometer data (Fig. 3). This shows a difficulty in determining the true value of the pH in precipitation, if the collected samples are not analysed for pH value during the event.

The pH of precipitation water depends on atmospheric processes like washout and rainout. It is a result of natural components like $CaCO_3$ from soil erosion and the acidic nature of gaseous (g) anthropogenic emissions like $NO_{x\,(g)}$ and $SO_{x\,(g)}$. The concentration of $SO_{x\,(g)}$ is not strongly correlated to the resulting pH or the concentration of SO_4^{2-} in precipitation water. On one hand, the SO_4^{2-} indicates an input of gaseous $SO_{x\,(g)}$ which leads to an acid reaction in precipitation water. On the other hand, if the SO_4^{2-} originates from the chemical decomposition of salts like $CaSO_4$, it does not indicate an acid input (Waldner, 1996).

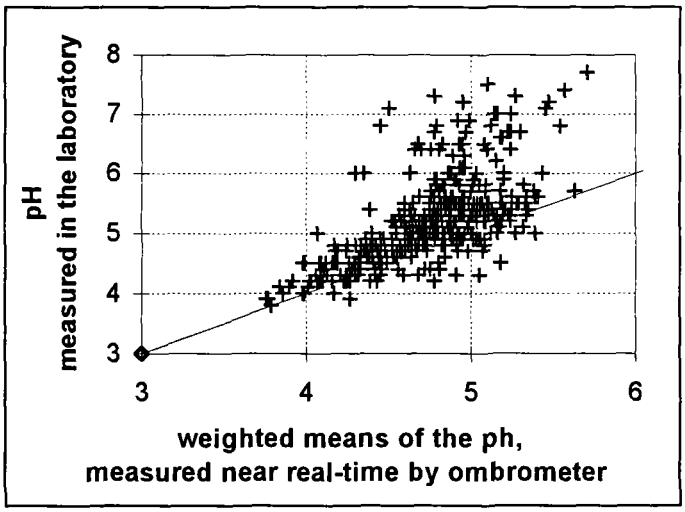

Fig. 3: pH-values in precipitation in the Alptal valley from 1989 to 1993. Comparison of the pH in the sequential samples analysed in the laboratory are shown against the mean, weighted by the sum of precipitation, of the single pH-values of the automatic pH-ombrometer during the corresponding sampling-period. (Unfortunately, the corresponding pH from the laboratory is missing for the highest pH (6.7) measured by ombrometer).

4. Conclusions

During the initial washout of rain-events, the proposed peaks in concentration of minerals and nutrients were verified. But during the final rainout, the proposed decrease of concentrations was confirmed only for thunderstorms and summer rain-events with a large initial impact of SO_4. The maximum specific deposition rate was observed during snow-events, followed by summer rain-events and thunderstorms.

A maximum of acid particles were scavenged by washout processes at the beginning of rain-events, leading to low pH values in the rain. After this early acid peak, the proposed increase of the pH values during rainout processes was only observed in thunderstorms. A different pattern was shown by rain-events affected by Saharan dust, leading to high pH-values in the early washout, followed by decreasing pH in the final rainout. The pH, measured in near real-time by an ombrometer, showed a range between 3.8 and 6.7 and was usually lower than the pH in the collected rain-samples.

During thunderstorms in the Alptal valley, 28% of the total load of elements and nutrients was washed out in the first 5 mm of a rain-event. The corresponding data for snow-events and summer rain-events were 20% and 13%, respectively. Based on the fact that increasing rainfall intensity generates increasing concentration of nutrients and minerals during rain-events, the 28% washout observed in the first 5 mm rain in the Alptal valley is in agreement with the 50% washout in the first 7.2 mm rain during more intensive monsoon events in India, as reported by Khare *et al.* (1996).

References

BAECHMANN K., P. EBERT, I. HAAG and T. PROKOP, (1996) 'The chemical content of raindrops as a function of drop radius'. *Journ. of Atmosph. Envir.*, Vol. 30: p. 1019 - 1025.

BURCH, H. (1994) 'Ein Rückblick auf die hydrologische Forschung im Alptal'. Hydrologie kleiner Einzugsgebiete, *Beitr. Hydrol. Schweiz* 35. SGHL/WSL-Report, CH-8903 Birmensdorf: p. 18-34.

CROCKFORD R., D. RICHARDSON and R. SAGEMAN, (1996) 'Chemistry of rainfall, throughfall and stemflow in a eucalypt forest and a pine plantation in south-eastern Australia'. *Journal of Hydrol. Processes,* Vol. 10/1: p. 6-11.

FISCHER-RIEDMANN A., (1995) 'Atmosphärische Konzentration und Deposition von N-haltigen Komponenten im Wald des hydrologischen Einzugsgebietes Erlenbach im Alptal'. *Diss. ETH Nr. 11035*, ETH-Zürich, 242 p.

FOWLER D., (1980) 'Removal of sulphur and nitrogen compounds from the atmosphere in rain and by dry deposition'. *Proc. of int. conf. ecol. impact acid precip.*, Norway, SNSF project: p. 22-31.

GROSCH S. and H.-W. GEORGII, (1989) 'Deposition by rain and snow - dry deposition on snow'. *Mechanisms and effects of pollutant-transfer into forests*, Kluwer academic publishers: p. 51-59.

JENNINGS M., T. PERKINS, M. HEMMERLEIN and R. KLEIN, (1992) 'Techniques for pollution monitoring in remote sites: I. Near real-time rainfall pH and depth'. *Water, Air and Soil Poll.*, Vol. 65: p. 237-244.

KENNEDY V., G. ZELLWEGER and R. AVANZINO, (1979) 'Variation of rain chemistry during storms at two sites in northern California'. *Water Resources Research*, Vol. 15, No. 3: p. 687-702.

KHARE P., S. KAPOOR, U. KULSHRESTHA, A. SAXENA, N. KUMAR, K. KUMARI and S. SRIVASTVA, (1996) 'Variation in ionic composition of precipitation collected by sequential sampling'. *Journal of Environ. Technol.*, Vol. 17: p. 637-642.

KLÖTI P., H. M. KELLER and M. GUECHEVA, (1989) 'Effects of forest canopy on throughfall precipitation chemistry'. *Proceedings of the Baltimore Symposium, May 1989. IAHS Publ.* 179: p. 203-209.

MOSELLO R. and A. MARCHETTO, (1996) 'Chemistry of atmospheric wet deposition in Italy: results from a five-year study'. *Ambio* Vol. 25, No. 1: p. 21-25.

PROKOP T., P. EBERT, M. KIBLER, A. MAINKA, B. TENBERKEN and K. BAECHMANN, (1996) 'Calculation of the in-cloud concentration of trace compounds in rain by sampling raindrops at the ground'. *Proc. of the 12th conference on clouds and precipitation, Zürich*, Vol. 2: p. 1114-1117.

RADOJEVIC M. and L. LIM, (1995a) 'Short-term variation in the concentration of selected ions within individual tropical rainstorms'. *Water, Air and Soil Pollution*, Vol. 85: S. 2363-2368.

RADOJEVIC M. and L. LIM, (1995b) 'A rain acidity study in Brunei Darussalam'. *Water, Air and Soil Pollution*, Vol. 85: p. 2369-2374.

SCHREIBER L., (1996) 'Wetting of the upper needle surface of abies grandis: influence of pH, wax chemistry and epiphyllic microflora on contact angles'. *Plant, Cell and Environment*, Vol. 19: p. 455-463.

SCHWIKOWSKI M., T. SEIBERT, U. BALTENSBERGER and H. W. GÄGGELER, (1995) 'A study of an outstanding Saharan dust event at the high-alpine site Jungfraujoch, Switzerland'. *Journ. of Atmosph. Envir.*, Vol. 29: p. 1829-1841.

TYREE S., (1981) 'Rainwater acidity measurement problems'. *Journ. of Atmosph. Envir.*, Vol. 5: p. 57-60.

VERRY E., (1983) 'Precipitation chemistry at the Marcell Experimental Forest in North Central Minnesota'. *Water Resources Research*, Vol. 19/2: p. 454-462.

WALDNER P, (1996) 'Variationen des pH und der Konzentration einiger Stoffe während Niederschlagsereignissen im Alptal für die Periode 1989-1993'. *Internal WSL-Report*, CH-8903 Birmensdorf, in press.

WMO, (1994) 'Guide to hydrological practices'. *Word Meteorol. Organisation. WMO-No. 168*: p. 113-114.

The estimation of pollutant loads from experimental microbasins during extreme hydrological events

A. Konicek, P. Miklanek and P. Pekarova

Institute of Hydrology SAS, Bratislava, Slovakia

1. Introduction

The influence of extreme runoff events upon nitrate concentrations and loads is studied in two microbasins in central Slovakia. In the first part of the study the water balance over a period of 30 years (1965 - 1994) for the experimental microbasins is evaluated and the influence of the vegetation cover upon the runoff is estimated. The second part gives a statistical analysis of the water quality data during the period 1986/87 - 1993/94. The influence of different land-use upon nitrate load is studied. The relation of the minimum and maximum discharge to the monthly nitrate concentrations in the streams, and the transported volume of the pollutants, was determined.

The land-use type and vegetation cover have a major influence on the hydrological regime and the water quality of the stream (Blazkova, 1994; Puech *et al.*, 1993; Gras *et al.*, 1993).

The objectives of this study are to

(i) analyse the long-term trends in time series of precipitation, discharge and temperatures measured at the two experimental microbasins Lesny and Rybarik, during the period 1965 - 1994,

(ii) investigate the impact of the type of vegetation cover on the hydrological regime of these microbasins, and

(iii) study the impact of type of vegetation cover on nitrate leaching from these microbasins.

2. Site description, field measurements

The experimental basin Mostenik in the Strázov highland was established in 1958 by the Institute of Hydrology, Slovak Academy of Sciences (IH SAS). The aim of the research was to study the water balance component processes in the middle mountainous areas. Since 1986, stream-, rain-, soil-, and ground- water quality have been studied in the following sub-basins of the Mostenik basin:

1. the Rybarik - an agricultural basin (potatoes, beet, cereals)
2. the Lesny - a forested basin (hornbeam).

The experimental microbasins Rybarik (0.12 km^2) and Lesny (0.086 km^2) are located in north-western Slovakia, about 10 km south-west of Povazská Bystrica (Konícek, 1996). The experimental basins are shown in Fig. 1. A brief physical and geographical description of these basins is presented in Table 1.

TABLE 1: Basic hydrological characteristics of experimental microbasins.

Basin	Area	Forest	Elev.a.s.l. aver. min/max	Precipitation	Runoff	Runoff coef.	Temperature
	(km^2)	(%)	(m)	(mm)	(mm)		(°C)
Rybarik	0.12	2.4	401 375/434	744.9	238.8	0.320	7.7
Lesny	0.086	100	380 350/416	732.5	163.4	0.223	7.7

Runoff monitoring began in 1958. The basins are equipped with water level recorders. For precipitation measurement, the standard rain gauge METRA (orifice 500 cm^2, height 1 m) was used. Precipitation in Lesny is the average of Rybarik and Kunovec (300 m to the south of Lesny). Other meteorological data were recorded at the meteorological station located in the basins.

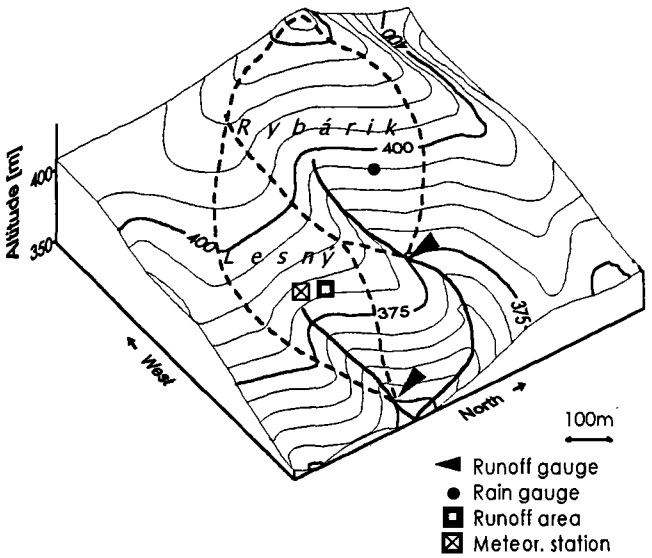

Fig.1 Scheme of the experimental basins and equipment

Water quality samples were taken manually every other day during 1986-1996. Three to five flood waves annually were sampled at intervals of between 5 and 10 minutes. Specific conductivity and pH were determined in situ, the anions Cl^- were analysed by titration ($AgNO_3$). NH^+_4, NO^-_2 and NO^-_3 were determined colorimetrically, and SO^{2-}_4 gravimetrically.

3. Analysis of the results

3.1.1 Long-term trends

During the last 15 years the hydrological situation in Slovakia has been considerably different from the long-term average. According to Majercakova and Sedik (1994), the whole period 1980 - 1990 was characterised by a rapid decrease of precipitation and river outflow. In some basins of southern Slovakia, this decrease represented about 40 % of the accepted hydrological average for 1931 - 1980. Simultaneously, a decrease of precipitation totals and an increase of annual temperatures occurred (Lapin *et al.*, 1994).

Figs. 2 and 3 show the situation in the microbasins Lesny and Rybarik. The hydrological years 1990/91 and 1992/93 were extremely dry. The hydrological year 1993/94 was above average in runoff volume and temperature. In that year, the annual mean temperature reached 10.3°C.

The linear regression equations representing the trends have the form:

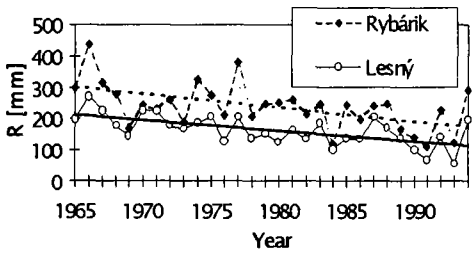

Fig. 2: Long-term trend of annual runoff.

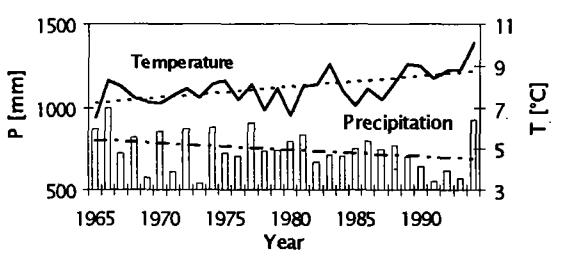

Fig. 3: Long-term trend of precipitation and temperature.

R_R	= 305.8 - 4.32 t	for the annual runoff depth in Rybarik microbasin,
R_L	= 212.3 - 3.47 t	for the runoff depth in Lesny microbasin,
P	= 808.7 - 4.148 t	for the annual precipitation,
T	= 7.147 + 0.0527 t	for the mean annual temperature,

where t is the number of the year (0, 1, 2, ...) since 1965.

The trend coefficient of decrease is very similar for both runoff and precipitation. It is slightly greater for runoff in the Rybarik agricultural basin. This may be connected with an increase in evaporation.

3.1.2 Impact of type of vegetation cover upon the hydrological regime

In the agricultural microbasin Rybarik, the annual average runoff was 1.46 times higher than in forested microbasin Lesny (see Fig. 2). Monthly maximum runoff was found during the snow-melt season in both microbasins: during February to March in the Rybarik; and during March - April in the Lesny.

Monthly minimum runoff occurred in September. During this month, the runoff coefficient was only 0.118 in Rybarik, and only 0.078 in Lesny. In Fig. 4, the annual runoff regime is shown.

The influence of vegetation cover on the runoff volume is shown in Fig. 5. In this Figure, the

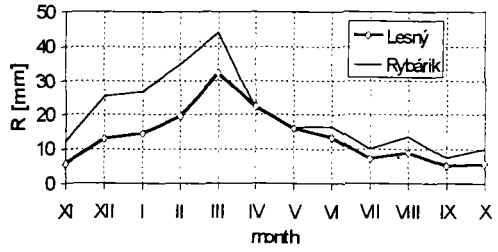

Fig. 4: Mean monthly runoff(average 1965 - 1994).

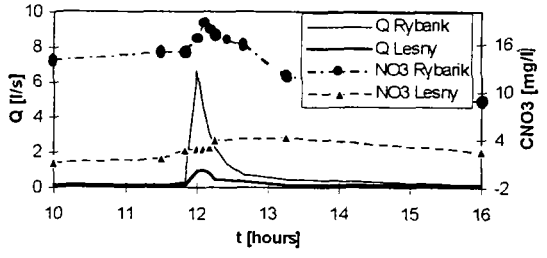

Fig. 5: Discharge and nitrate concentrations in Rybarik and Lesny (1. 8. 1991).

outflow wave observed in 10 minute steps is sketched for both microbasins with different land-use. The same precipitation event causes maximum discharges of 1.0 $l.s^{-1}$ in Lesny microbasin, and 6.6 $l.s^{-1}$ in the Rybarik microbasin (11.6 and 55 $l.s^{-1}.km^{-2}$ respectively).

3.2 Statistical analysis of the water quality data

In Table 2, basic statistical characteristics of observed time series of surface water quality data are given for both experimental microbasins. The Table illustrates the influence of agriculture on the quality of the stream water. Histograms of measured nitrate and chloride concentrations are given in Fig. 6.

TABLE 2: Conductivity, pH, nitrate (NO3), soluble matter (RL), sulfate (SO4), and chloride (Cl) concentrations

Rybarik	*conductivity*	*pH*	*NO3*	*RL*	*SO4*	*Cl*
			[mg l^{-1}]	[mg l^{-1}]	[mg l^{-1}]	[mg l^{-1}]
Mean	532.0	7.81	37.50	503	79.8	31.00
Standard Deviation	112.0	0.29	18.90	59	27.6	6.00
Minimum	50.0	6.30	10.00	204	31.0	4.00
Maximum	737.0	8.40	147.00	662	150.0	49.00
Lesny	*conductivity*	*pH*	*NO3*	*RL*	*SO4*	*Cl*
Mean	395.2	7.91	4.67	350	52.5	9.75
Standard Deviation	112.2	0.31	3.98	46	22.5	7.69
Minimum	95.0	6.10	0.25	250	37.0	0.90
Maximum	720.0	8.30	31.00	400	62.8	69.00

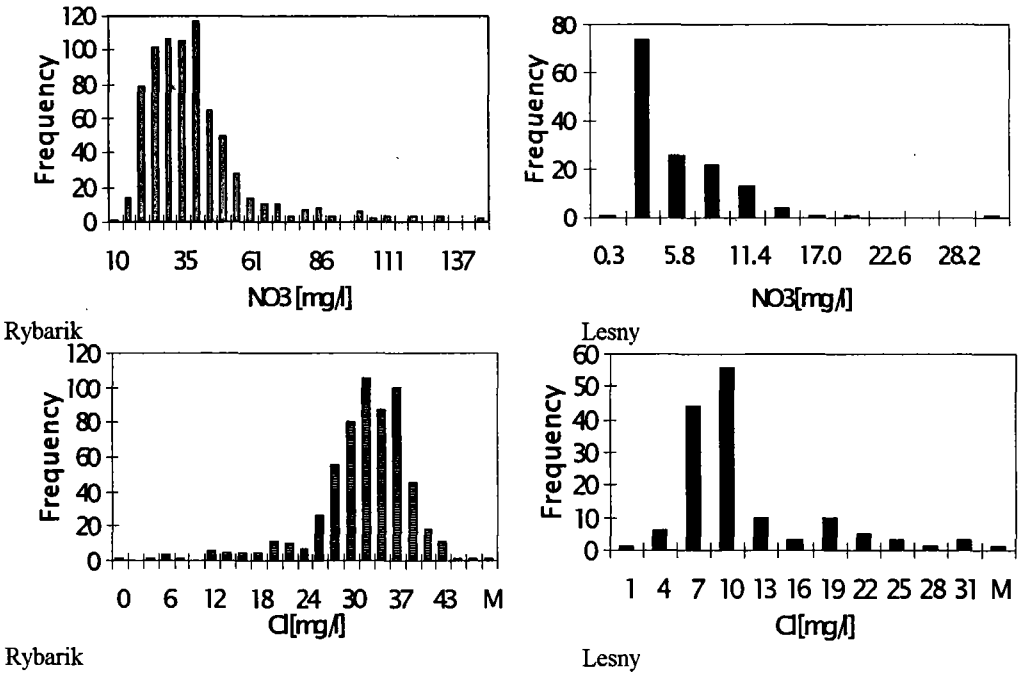

Fig. 6: Histograms of nitrate and chloride concentrations in the Rybarik and Lesny basins.

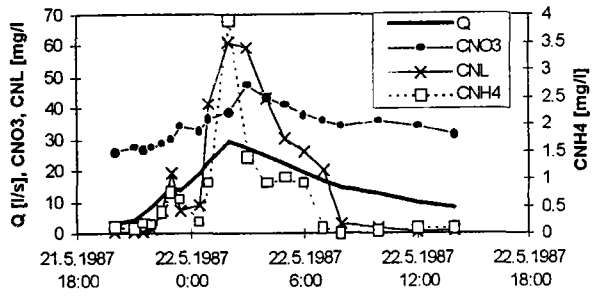

Fig. 7: Changes in Q, CNO3, CNH4 and insoluble matter (NL).

Pollutant concentrations during snow-melt and precipitation events reached higher values. There is an expressive dependence between discharge and any of NH_4^+, NO_2^-, NO_3^-, RL (soluble matter), NL (insoluble matter), and Cl water determinands in the Rybarik microbasin. In Fig 5, the discharge event during 1.8.1991 and the nitrate concentrations are shown. From Fig. 5, it can be seen that there is a time lag between nitrate concentration and discharge. The slow decrease of nitrate concentrations after the wave peak is caused by nitrate wash-out from the soil. In Fig. 7, the changes of discharge, NH_4^+, NO_3^-, and insoluble matter (NL) concentrations during the event 21st to 22nd May 1987 in Rybarik microbasin are given (the NL are given in thousands).

3.2.1 Estimation of monthly nitrate concentrations and nitrate specific yields

In Fig. 8, the temporal development of monthly nitrate concentrations and monthly runoff depths are given. Based on the monthly runoff depth R, the empirical relationships for calculating monthly nitrate concentrations and specific yields were estimated in Rybarik and Lesny microbasins (Pekarova *et al.*, 1995). The decrease of pollutants is connected with rapid decrease of fertiliser doses in recent years.
The following empirical relationships were used for calculating the monthly nitrate concentrations, empirical relationships of the form:

$$CNO3_{Rybarik} = 22.5\ R^{0.203} \quad [mg\ l^{-1}] \quad (1)$$

$$CNO3_{Lesny} = 2.336\ R^{0.203} \quad [mg\ l^{-1}] \quad (2)$$

For calculating the monthly nitrate specific yield Y from unit area, the following relationships were used:

$$Y_{Rybarik} = 0.162\ R^{1.203} \quad [kg.ha^{-1}.month^{-1}] \quad (3)$$

$$Y_{Lesny} = 0.0234\ R^{1.203} \quad [kg.ha^{-1}.month^{-1}] \quad (4)$$

In Table 3, the maximum, minimum and mean values of the monthly runoff depths, nitrate concentrations, and nitrate loads in Lesny and Rybarik microbasins (measured and calculated according to (1) - (4)) are given.

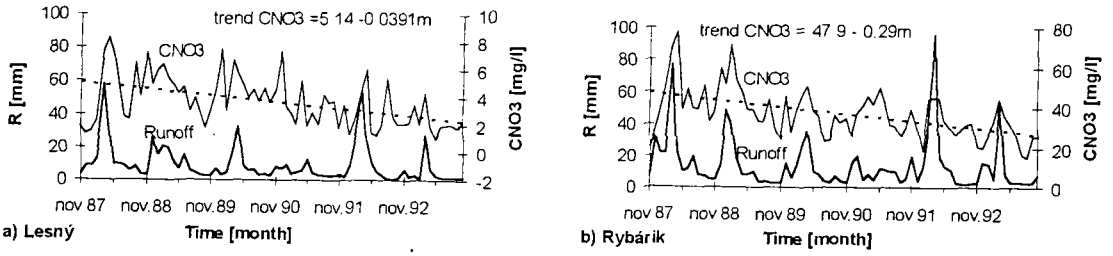

Fig. 8: Monthly runoff depths and weighedt average nitrate concentrations in:
a) Lesny microbasin, b) Rybarik microbasin.

Table 3: Maximum, minimum and mean values of the monthly runoff, nitrate concentrations and nitrate loads, Lesny and Rybarik microbasins

	Rybarik			Lesny		
	max. obs./cal.	min. obs./cal.	mean obs./cal.	max. obs./cal.	min. obs./cal.	mean obs./cal.
Runoff (mm)	96.1	1.8	14.9	58.5	0.5	9.35
Concentration ($mg.l^{-1}$)	77.9/56.8	15/25.3	35.4/36.1	7.5/6.3	1.0/1.5	3.6/3.3
Load ($kg.ha^{-1}.month^{-1}$)	39.4/39.3	0.29/0.33	4.46/4.46	2.6/2.9	.01/.01	.36/.34

4. Conclusions

Long-term observation of basic quantitative and qualitative elements of the runoff processes in both experimental basins has shown following results:

- Long-term (30 years) trends of precipitation and runoff decrease, and temperature increase were confirmed. The precipitation totals are decreasing by about 4 mm annually which corresponds with an equal decrease of mean annual runoff depth (4 mm). The mean annual temperatures have increased in last 30 years by 0.05°C yearly.
- The different land-use in the basins (agriculture and silviculture) is reflected in different annual runoff depth. The difference in runoff depths between the basins is about 75 mm, while the difference in precipitation is only 10 mm. The runoff regime expressed in monthly values is very similar in late spring and summer (April - September), while it is significantly different in autumn and winter months (October - March). The runoff depths in the agricultural basin are significantly higher during the seasons without crop growing.
- The relation between runoff and concentrations of selected determinands in the stream was also confirmed. Generally the concentrations of all determinands increase with runoff, excepted chlorides. In this paired basins study it is also related to land-use. Concentrations of stream water in the agricultural basin are generally higher than in the forest stream.

- The dependence between runoff and nitrate concentrations in both experimental basins allowed derivation of empirical relations for the estimation of both mean monthly concentrations and monthly specific yield per unit area from monthly runoff depths. The results were compared (Table 3).

Bibliography

BLAZKOVA, S. (1994) 'World-wide experience assessment of the deforestation influence upon runoff regime.' (In Czech.) In: *Vliv odlesneni na hydrologicky rezim v oblasti Jizerskych hor. Vyzkum pro praxi*. Sesit 28, VUV Praha

GRAS J.M., J.A. VEGA and S. BARA (1993) 'Six years of study on fast growing forest plantations catchments in the Northwest of Spain.' *Acta Geologica Hispanica*, v.28, No. 2-3, pp. 111-117.

KONÍCEK, A. (1996) 'Trends of basic water balance components in experimental basin Lesny during 1965 - 1994.' *J.Hydrol. Hydromech.*, 44, 4, pp. 252-260.

LAPIN, M., P. FASKO and V. ZEMAN (1994) 'Contribution to analysis of possible global warming impacts upon climate change in Slovakia.' (In Slovak.) *National Climate Programme of the Slovak Republic*, Bratislava, Vol. 2, pp. 37-77.

MAJERCAKOVA, O. and P. SEDIK (1994) 'The runoff change of the Slovak rivers.' (In Slovak.) *National Climate Programme of the Slovak republic*, Bratislava, Vol. 2, pp 109 - 137.

PEKAROVA, P., P. MIKLANEK and P. RONCAK (1995) 'Stream load and specific yield of nitrogen and phosphates from Slovakia.' *J.Hydrol. Hydromech.*, 43, 4-5, pp. 233-248.

PUECH, CH., P. VINE and J. LAVABRE (1993) 'Remote sensing techniques in the mapping of vegetation and their application to runoff evolution in burnt areas.' *Acta Geologica Hispanica*, v.28, No.2-3, pp.103-110.

Conference "Ecohydrological Processes in Small Basins", Strasbourg, 24 - 26 September 1996

Regionalisation of nitrate and pesticides in a small basin in south Germany

A. Rolke, S. Demuth, C. Leibundgut and H.-M. Rogg

Institute of Hydrology, University of Freiburg, Germany

1. Introduction

Increasing pollution of groundwater with contaminants, and progress in analytical detection of pesticides make it necessary to interpret the concentrations measured at monitoring stations. In the year 1990 the EC drinking water standards of 0.1 µg/l per pesticide component, 0.5 µg/l for the sum of all pesticide components, and 50 mg/l nitrate were introduced into the drinking water ordinance of Germany (BGBI 1). Therefore it is necessary to investigate the temporal development of contaminant concentrations and the effects of land-use and catchment characteristics on contaminant transport. The aim of the study is to show the relationship between atrazine and nitrate concentrations in groundwater and catchment characteristics, leading to a spatial interpretation of nitrate and atrazine concentrations.

2. Study area

The study area is a sub-basin of the Dreisam catchment, the Zartener Becken (Fig. 1). It is situated near the Black Forest in south-west Germany. The size of the sub-basin is 20 km^2 and it is filled with quartenary fluvioglacial gravels. The catchment is situated in a water protection zone and provides drinking water for the 147 000 inhabitants of the town Freiburg. The aquifer is overlain by bottom clay and loam of different depths deposited during floods (sandy-loamy silt to loam). On the lower terrace the thickness is more than 40 cm, and in the bottom of the valley it is less than 10 cm in places. The thickness of the loamy cover and the organic matter content are the determining factors for the storage availability and the sorptivity of the soils for organic substances. According to Glomb and Zwölfer (1990) the soils were classified into areas with low and high retention capacities for organic substances like atrazine. Only 4% of the area shows low retention capacities, and 10% shows high capacities. The soils with low to very low retention capacities are mainly situated in the valley bottom.

About 80% of the Zartener Becken is used for agriculture: 50% is used for grassland, 30% for arable land. On the arable land corn, maize and special cultures like strawberries are cultivated. Apart from the eastern part of the basin being used as grassland, there are no homogeneous land-use units.

Since 1987, 19 observation wells, 10 groundwater wells and 3 collector drains have been sampled regularly. The depth of the groundwater wells varies between 1 meter and 40 meters. The nitrate concentrations are monitored every two weeks and the pesticide concentrations at intervals of two or three months.

The average groundwater recharge from precipitation under residential areas is about 200 mm per year and under agricultural land about 320 to 450 mm per year (1959 - 1988). Close to the rivers, groundwater recharge is higher due to the infiltration of river water into the aquifer during the whole year (Ehrminger and Herdeg, 1992). According to Glomb and Zwölfer (1990), the annual groundwater recharge rate can be characterised as high to very high, compared to the medium water balance surplus of 320 mm per year (1959-1988). The nitrate retention capacity of the soils is calculated from the groundwater recharge rate and the field capacity of the soils. In the study area it may be characterised

as very low to medium with a groundwater recharge rate of 365 - 450 mm per year and a storage availability of 390 - 520 mm (Glomb and Zwölfer, 1990).

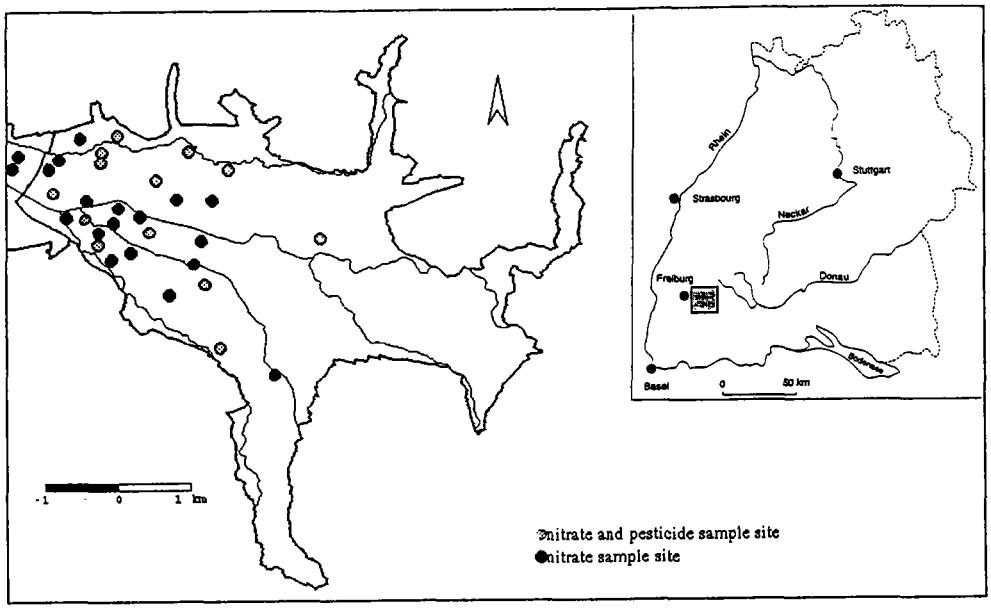

Figure 1: Study area

3. Spatial and temporal behaviour of atrazine, deethyl-atrazine and nitrate

To obtain the main contaminant load of the study area the spatial and temporal behaviour of the three contaminants atrazine, deethyl-atrazine and nitrate were examined. The time series showed that the deethyl-atrazine concentrations are mostly higher than the atrazine concentrations (Fig. 2). This is due to the higher mobility of the metabolite which is caused by a higher sorption of atrazine by mainly organic matter. Although the application of atrazine has been forbidden in the water protection zone since 1988, no decline of atrazine at most of the monitoring stations has been observed. Only at four monitoring stations has the concentration of deethyl-atrazine declined or increased during the period considered. However it can be stated that mostly the concentrations were higher in the years 1988 and 1991 and were lower in the year 1990. Therefore it is obvious that in general in the two years with high concentrations the maximum pesticide concentrations during the period 1988 to 1993 were measured. At all monitoring stations the maximum deethyl-atrazine concentrations occurred during the growing season (April to September). The monitoring stations in the north-east and south-west of the study area have a second maximum in the winter period (October to March). In the north of the basin maximum atrazin concentrations are found during the winter period, while in the south and the middle of the water protection zone maximum concentrations could be observed either in both periods or in the growing season. The fluctuations of the concentrations could be a result of the fluctuations of the groundwater recharge rate. The spatial differences due to the different coefficients of permeability of the aquifer in the northern and southern parts of the sub-basin result in different transport rates of contaminants from the surface where the water enters the aquifer.

Considering the number of data above the detection limit and above the EC drinking water standard, one can state that atrazine is found in 31% and deethyl-atrazine in 59% of the samples. But only 0.3% of the atrazine and 4% of the deethyl-atrazine samples exceed the EC drinking water standard of 0.1 µg/l. At nearly all monitoring stations 50% of the samples show an atrazine concentration below the detection limit. Of the samples taken from the monitoring stations receiving water from the southern part of the sub-basin, only 40% exceeded the detection limit. With regard

todeethyl-atrazine the same spatial behaviour can be observed. The samples taken in the south of the basin often exceed the standard of deethyl-atrazine, which is due to the low infiltration of river water into the aquifer, as shown by a study using environmental isotopes ($^{18}0$) and the groundwater model MODFLOW (Ehrminger and Herdeg, 1992). As a result, the two sampling sites with the smallest number of detections are strongly influenced by infiltrating water. The percentage difference of the frequencies of detection between the growing season and the winter period is not striking. Due to the different mobility of atrazine and its metabolite in the soil, the number of detections of atrazine is higher in the growing season, while for deethyl-atrazine the number of detections is higher in the winter period.

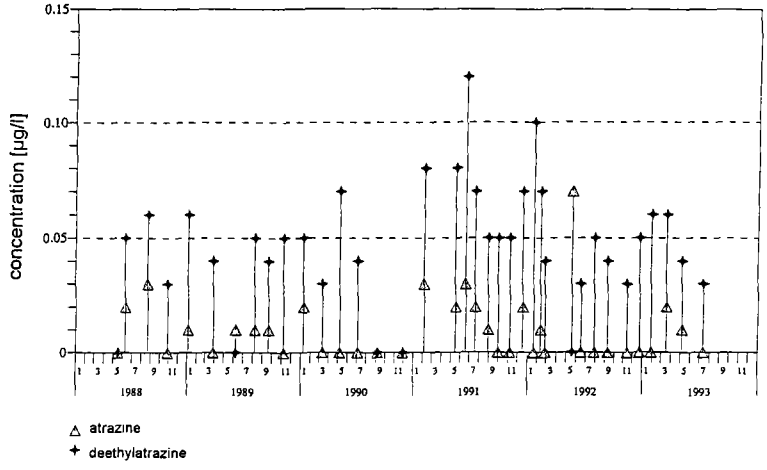

Figure 2: Example of a pesticide time serie 1988-1993

A one-factorial nonparametrical analysis of variance using rank-transformed data was performed to test if the medians of the pesticide concentrations show a significant statistical difference. As a result, the medians are statistically different (α = 5%). A multiple rank test (Tukey test, α = 5%) confirms that the groundwater in the south of the basin is more highly contaminated than in the north.

The nitrate concentrations were analyzed by visual inspection of the time series. The concentrations differ from year to year. At nearly all sample sites the amplitudes of the fluctuations are higher in the years 1987 and 1989 (Fig. 3). An interannual fluctuation of the nitrate concentrations is visible, especially in the years 1991 and 1992. Except for the wells near the western part of the river Dreisam, minimal concentrations were measured during summer and autumn. At 23 out of 31 stations maximum concentrations were detected at the beginning of the year. This is a result of the seasonal distribution of groundwater recharge in combination with the mineralisation and application of nitrate.

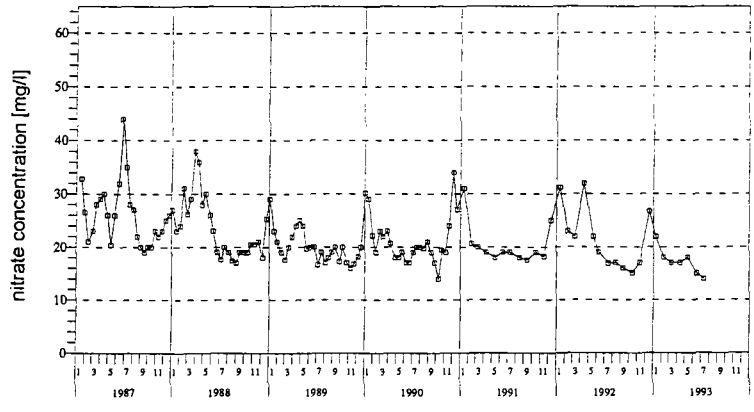

Figure 3: Example of a nitrate time serie (1987-1993)

The median concentration of nitrate is 16 mg/l and the groundwater can be characterised as relatively uncontaminated. The differences of the median concentrations between the years with minimal and maximal values are small: at 42% of the monitoring stations it is less than 5 mg/l, at 42% between 5 and 10 mg/l, and only at 16% it is more than 10 mg/l.

4. Regionalisation of atrazine and nitrate concentration

To regionalise the atrazine, deethyl-atrazine and nitrate concentrations, it was necessary to (1) model the groundwater flow and calculate the 'relevant areas of influence' of each groundwater monitoring station and of the inflow areas of wells, (2) overlay thematic maps, e.g. land-use maps, with the 'relevant areas of influence' using a GIS, (3) determine parameters of the atrazine and nitrate concentrations and the characteristics of the 'relevant areas of influence' and finally (4) perform a correlation analysis (Fig. 4).

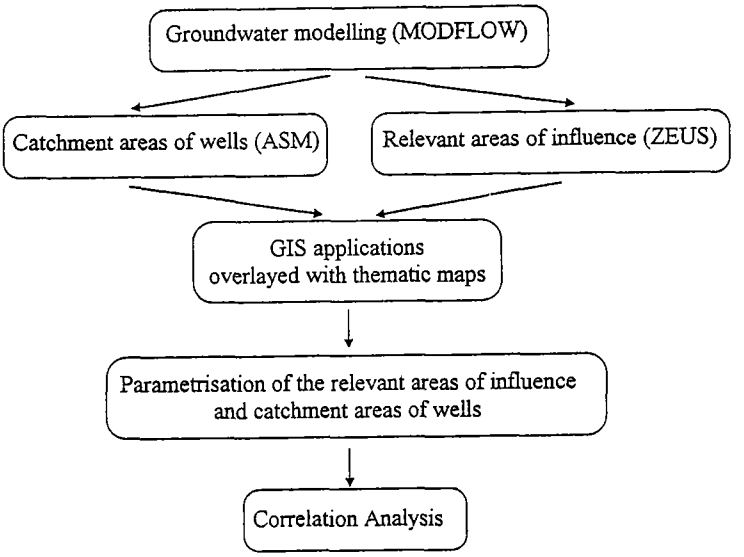

Figure 4: Scheme of the regionalisation

As a first approach, the average groundwater flow of the Zartener Becken was modelled under steady state flow conditions using MODFLOW (Donald and Harbaugh, 1984). The 'relevant areas of influence' are defined as areas where water infiltrates into the aquifer. The different 'relevant areas of influence' were calculated using an algorithm developed by the FAW (Forschungsinstitut für Anwendungsorientierte Wissensverarbeitung) in Ulm, Germany (1992). This algorithm is part of the ZEUS system (Central Advanced Environmental System). The pathways of the groundwater flow were constructed using the results of MODFLOW and the depths of the weep holes of the monitoring stations. Finally the result was projected onto the groundwater surface. However there are discrepancies between the calculated and the real groundwater flow due to uncertainties in modelling, dispersion effects and the inhomogenity of the aquifer. The inaccuracy can be reduced by calculating stream lines on both sides of the calculated pathway, choosing an opening angle of 4.5 degrees. Then the inflow areas of the wells were calculated with ASM (Aquifer Simulation Model, introduced by Kinzelbach and Rausch, 1989). The groundwater flow to the wells was simulated using the method of particle tracking. The data received from the groundwater model MODFLOW were taken as input data.

The application of a GIS helped to overlay the 'relevant areas of influence' and the inflow areas of the wells with thematic data such as land-use, retention capacity of soils with regard to pollutants (atrazine and nitrate) and groundwater recharge rates. To characterise the 'relevant areas of influence' and the inflow areas of the wells, the percentage of arable land, and an area-weighted average of classes of the filtration capacity, were created. The latter was subdivided into classes ranging from 1 (very low) to 5 (high). In addition, the two following parameters were created: an area-weighted average of classes of the groundwater recharge; and classes of the influence of infiltrating river water on the monitoring stations, according to the classes of Ehrminger and Herdeg (1992). As a measure for pesticide concentration the maximum and median atrazine and deethyl-atrazine concentrations were chosen. The samples were taken from 10 groundwater monitoring stations. The median and the maximum nitrate concentration of the 26 regularly sampled sites were used as a measure for the nitrate concentrations.

A correlation analysis was applied to detect relationships between the parameters of the 'relevant areas of influence' and the pesticide and nitrate concentrations. Therefore a Kendall τ-correlation (correlation on ranks) was calculated and tested two-sided with an α-error of 5%.

As a result, both the 'relevant areas of influence' and the catchment areas extend in the north of the basin from east to west. In the south of the basin they extend from south-east to north-west (Fig. 5).

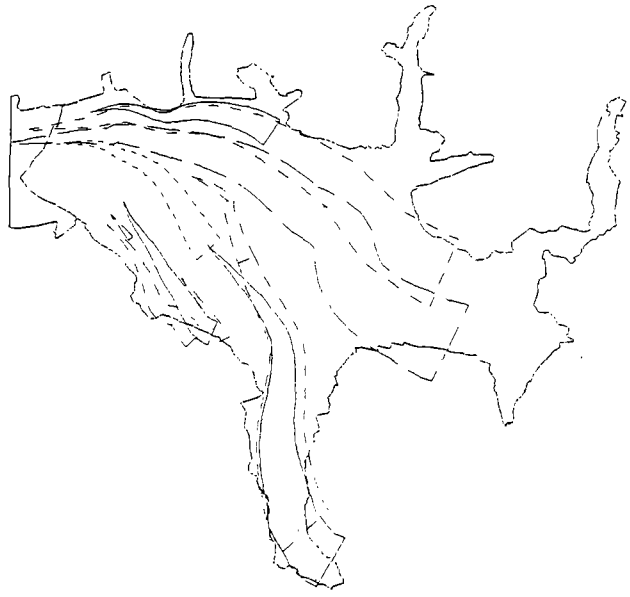

Figure 5: Examples of 'relevant areas of influence'

The correlation analysis between the characteristics of the 'relevant areas of influence' and the measured pesticide concentrations shows that the maximum atrazine concentrations only correlate significantly with the amount of infiltrating water. With increasing infiltration water the maximum of atrazine decreases, which is due to dilution effects ($\tau = 0.73$, $p = 0.009$).

Against all expectations there is a negative significant correlation between the median deethyl-atrazine concentration and the area of arable land ($\tau = -0.66$, $p = 0.01$). It can be explained by dilution effects, produced by the increase of the groundwater recharge rate with an increasing percentage of arable land in the 'relevant areas of influence'. Higher median concentrations of deethyl-atrazine were measured under soils with a higher sorption capacity for pesticides ($\tau = 0.51$, $p = 0.05$). As the application of atrazine has been prohibited since 1989, the detected atrazine in the samples is mainly desorbed from the soils. It has to be taken into consideration that in soils with a higher sorption capacity higher amounts of pesticides can be desorbed again. Finally, with an increasing groundwater recharge there is only a tendency for lower medians of deethyl-atrazine ($\tau = 0.50$, $p = 0.06$). This trend is not observed when calculating correlations while excluding the monitoring stations influenced by river infiltrations. Regarding the maximum deethyl-atrazine concentrations it can be concluded that there are the same statistical significant correlations and tendencies as are found for the median deethyl-atrazine concentrations.

With increasing percentage of grassland the median nitrate concentration decreases ($\tau = -0.38$, $p = 0.007$). And with increasing percentage of arable land the median nitrate concentration increases ($\tau = 0.34$, $p = 0.02$). Between maximum nitrate concentration and land-use there is no statistically significant correlation. The higher the minimum nitrate retention capacity, the lower are the measured maximum concentrations ($\tau = -0.32$, $p = 0.045$). The median nitrate concentration correlates significantly with the degree of infiltrating river water ($\tau = -0.42$, $p = 0.01$). When omitting the monitoring stations which are influenced by river infiltrations, there are high correlations between the average nitrate retention

capacity of the 'relevant areas of influence' and the maximum nitrate concentrations (τ = - 0.43, p = 0.01).

5. Conclusion

The study has shown that despite the prohibition of the application of atrazine since 1989, there are still traces of atrazine and its metabolite deethyl-atrazine detected in the groundwater wells and collector drains of the study area. There are also temporal variations of measured concentrations of atrazine and nitrate in the groundwater. Spatial variations in the amount of contaminant loads was found. Since the measured deethyl-atrazine concentrations are significantly higher than those of atrazine, more research is necessary to detect metabolites in groundwater and observation wells. The result of the regionalisation shows that correlations between the characteristics of both the 'relevant areas of influence' and the inflow areas of wells and the measured nitrate, atrazine and deethyl-atrazine concentrations can be found. The study indicated that some statistical parameters are more suitable for showing correlations with the characteristics of 'relevant ares of influence' and inflow areas of wells than others. The maximum concentration of atrazine is not suitable for the detection of correlations with parameters of the 'relevant areas of influence' and inflow areas of wells. The median concentration of deethyl-atrazine is a suitable parameter to show the influences of different land-use and of different filtration capacities on the measured concentrations. The median nitrate concentration shows the influence of different land-use on groundwater quality. On the other hand, the maximum nitrate concentration is a suitable parameter to detect the influences of the nitrate retention capacity of the soils on groundwater quality. Thus the regionalisation of contaminants using thematic maps and statistics is a promising method to indicate important ways for groundwater pollution.

The calculation of 'relevant areas of influence' is appropriate for areas where a steady state groundwater model is calibrated and different time series with long records are available. However, the method should be tested in other areas apart from the current study area. This would lead to a comparison of the present result with the results of other study areas with similar geological and pedological characteristics. A comparison with other contaminants in the area under study is not possible due to the lack of sufficient data above the reporting limit.

Acknowledgements

The research presented in this paper was financial supported by the local Water Supply Company (FEW) and the Förderverein Hydrologie at the Institute of Hydrology at the University of Freiburg.

6. Bibliography

DONALD, M.G. and A.W. HARBAUGH (1984) 'MODFLOW. A Modular Three-Dimensional Finite Difference Ground-Water Flow Model'. *U.S. Geological Survey, Open File Report 83-875.*

EHRMINGER, B. and U. HERDEG (1992) 'Abschlußbericht über die isotopenhydrologischen Untersuchungen und die erstellten Grundwassermodelle im Einzugsbereich des Wasserwerks Ebnet'. *Untersuchungen der Freiburger Energie- und Wasserversorgungs-AG und des Geologischen Landesamtes Baden Württemberg*, Freiburg i.Br..

GLOMB, G. and F. ZWÖLFER (1990) 'Grundwassermodell Zartener Becken. Bodenkundliche Untersuchungen'. *Unveröffentlichtes Gutachten des Geologischen Landesamtes Baden-Württemberg Nr. 0801.01/89-4765-Zw/Gg.*, Freiburg i.Br..

KINZELBACH, W. and R. RAUSCH (1989) 'ASM Aquifer Simulation Model'. *Programm-beschreibung,* Universität Kassel, Stuttgart.

Verordnung über Trinkwasser und über Wasser für Lebensmittelbetriebe (Trinkwasser-verordnung - TrinkwV) vom 12. Dezember 1990. *BGBl I*, S. 2613.

Mechanisms affecting streamflow and stream water quality: a new spectral analysis time series approach

J.-L. Pinault[1], H. Pauwels[1], V. Fritsche[1] and Ch. Cann[2]

[1] *Bureau of Geological and Minerals Research (BRGM), Orléans, France*
[2] *CEMAGREF, Rennes, France*

1. Introduction

Inverse methods can constitute a viable and effective alternative to conceptual models. They enable the calculation of physically realistic models without any compulsive hypothesis and are powerful enough to model complex interactions within a multimedia approach, thus enabling an actual description of hydrogeological phenomena. Powerful algorithms developed in signal processing theory are available, including multichannel spectral analysis of time series. Such a technique, coupled with an inverse method, allows the calculation of the unit hydrograph of the catchment as well as the impulse response of nitrate flux to rainfall.

Their application to the study of mechanisms affecting streamflow and stream water quality of the Coët-Dan catchment (Naizin, Brittany) is the purpose of this paper.

2. The model for streamflow

Streamflow $F(t)$ is the result both of groundwater flow down to the outlet and of overland flow; groundwater flow includes subsurface flow, seepage, and discharge of groundwater. Groundwater flow and overland flow are both discerned from their impulse responses to rainfall (their unit hydrographs), the former being a succession of phenomena that induces a relatively slow decrease of streamflow versus time (relaxation time being closely linked to water pathways) and the latter being very short. Thus, hydrograph separation into dominant quick and slow components of streamflow leads to:

$$F(t_i) = S \cdot \left[\Gamma_s * R_s + \Gamma_q * R_q\right](t_i) \qquad (1)$$

where * is the discrete convolution product (the convolution product of two functions h and g is: $[h * g](t_i) = \sum_{j=0,n} h(j\Delta) \cdot g(t_i - j\Delta)$, Δ is the time increment. t_0, $t_1 \cdots, t_m$ represent discrete time).

In addition

$S = \sum_{i=1,n} F(t_i) \Big/ \sum_{i=1,n} \left(R_s(t_i) + R_q(t_i)\right)$ is the catchment area where n is the length of time series.

The rainfall $R(t_i) = R_l(t_i) + R_s(t_i) + R_q(t_i)$ is decomposed into three components:

$R_l(t_i)$ = lost rainwater component, as a result of soil-water recharge

$R_s(t_i)$ = induces the slow component of streamflow (ground water flow down to catchment outlet)

$R_q(t_i)$ = induces the quick component of streamflow (overland and subsurface flow)

Γ_s and Γ_q are normalised impulse responses (area is unity):
Γ_s is the slow component of unit hydrograph
Γ_q is the quick component of unit hydrograph

The three components $R_l(t_i)$, $R_s(t_i)$, $R_q(t_i)$ of rainfall are such as:

$$R_l(t_i) = \mathrm{Inf}\{R(t_i), \Omega(t_i)\} \quad (2)$$

where $\Omega(t_i)$ is the effective rainfall threshold, the height of rainfall that corresponds to soil-water recharge, which is strongly influenced by evapotranspiration as well as water stored in the soil and in the vegetation.

In order to quantify the ability of the catchment to generate quick flow, its surface S is divided into two parts: $\alpha(t_i)\cdot S$ is responsible for overland and subsurface flows and $(1-\alpha(t_i))\cdot S$ for infiltration. The component of rainfall $R_q(t_i)$ that induces the quick component of unit hydrograph is expressed according to the relative area $\alpha(t_i)$ causing quick flow so that:

$$R_q(t_i) = (R(t_i) - R_l(t_i))\cdot \alpha(t_i) \quad (3)$$

Since this component is the result of overland and subsurface flows, it depends on vegetation conditions as well as on the water content of soil.

The symmetrical relationship linking the relative area $\alpha(t_i)$ and the component $R_s(t_i)$ of rainfall that induces the slow component of unit hydrograph is:

$$R_s(t_i) = (R(t_i) - R_l(t_i))\cdot (1-\alpha(t_i)) \quad (4)$$

The functions to be calculated are the normalised impulse responses Γ_s and Γ_q, the threshold of effective rainfall $\Omega(t_i)$ and the relative area causing the quick flow $\alpha(t_i)$. Numerical calculations are carried out by using multichannel spectral analysis (Pinault and Baubron, 1996), and an inverse method that has been developed iby Pinault and Fritsche (1997).

3. Field description and experimental method

3.1 Geologic and hydrogeologic situation

The Coët-Dan drainage basin (12 km^2) is located approximately 70 km south-west of Rennes and underlain by Brioverian schist (530Ma). It lies between the 700 and 800 mm annual rainfall isohyet. Due to the proximity of the Atlantic ocean, an oceanic climate is dominant. Excess rainfall may occur in winter. July and August are the only months during which rainfall is low. In winter, snow is extremely rare. In summer, rainfall is often the result of storm events.

Variations in mean temperatures are moderate throughout the year. Mean daily temperatures rarely exceed 25°C in summer, and rarely fall below 0 °C in winter.

The host rock below the surface mainly constitutes fissured schist. The top few meters consist of recent alluvia, weathered schist, and sandstone. Hydrological investigations revealed the occurrence of two aquifer zones corresponding to the top few meters of the bedrock and the unweathered bedrock respectively. Groundwater flow in the aquifers exhibits a vertical component that depends on topography [Hrkal *et al.*, 1992]. Shallow groundwater penetrates in places into the deep aquifer. Nevertheless, close to the river, and mainly during high-water periods, ascending flow from deep groundwater contributes to the recharge of the stream and the shallow aquifer. Overland flow from impermeable areas, subsurface flow from cultivated and uncultivated area, and groundwater discharge are the main contributions to the streamflow.

In this catchment, as in other places in Brittany (France), nitrate contamination of surface-water and groundwater due to intensive farming is a crucial problem. In the groundwater, large variations of

nitrate concentration with depth below the surface are observed. Contamination of shallow groundwater is high, comprising concentrations of up to 200 mg/l. Nevertheless, at deeper levels below 7-10 meters depth, where water circulates through fractures in the sound rock, nitrate concentrations decrease to a few mg/l. This decrease is partly interpreted as denitrification, i.e. biological transformation of nitrate into gaseous N_2 or N_2O (Pauwels *et al.*, 1996).

The principal mechanisms of transport of nitrate to the stream are subsurface flow from cultivated areas and shallow groundwater flow. There is a short-term decrease of nitrate concentration in stream water when effective rainfall events occur. Mean nitrate concentration weighted by flow is $\bar{c} = \sum_{i=1,n} c(t_i) \cdot F(t_i) / \sum_{i=1,n} F(t_i) = 63.8$ mg/l over the period from September 1992 to September 1995. The behaviour of nitrate flux in streamflow, i.e. the product of nitrate concentration and streamflow, provides a better insight into the mechanism of runoff generation than nitrate concentration, as is shown below.

3.2 Catchment instrumentation and data collection

CEMAGREF (Centre National du Machinisme Agricole, du Genie Rural, des Eaux et des Forets) has been extensively studying this catchment since 1970 (Cann, 1993, 1994; Cann and Villebonnet, 1993, 1994) because it is used as a reference basin for mechanisms leading to diffuse source pollution of agricultural origin that occurs in surface water and groundwater. The sampling strategy developed for this study was designed to provide data over a short period of time as well as on seasonal trends. Rainfall was measured by three pluviometers, but these were not generally in simultaneous use. The outlet of the catchment is equipped with notch wear, a limnigraph and a piezoresistive probe. Stream water samples are also regularly collected by an automatic sampler and analysed in a laboratory of CEMAGREF.

4. Analysis and discussion

4.1 Nature of flow and nitrate flux responses in streamflow in the Coët-Dan catchment

Figure 1a shows a comparison between streamflow rate at the outlet and the model calculated from relationship (1). The agreement between observed and computed streamflow is good, except for some features, the disparity being interpreted as the result of rainfall sampling errors. When two pluviometers are in use simultaneously, differences of up to 20 % are commonly observed, due to the vegetation. Such uncertainties may induce large errors in streamflow calculation, especially when the effective rainfall threshold $\Omega(t_i)$ is high. Another cause for disagreements between model outcome and observations results from the local character of heavy storms, which can make rainwater sampling, and the modelling of heterogeneous phenomena at watershed scale, more difficult.

High discharge rates occur in January as a result of autumn and winter rainfall, when the soil is becoming saturated. Particularly the autumn of 1994 was wet, leading to the flood in January 1995.

Figure 1b represents the Fourier Transform (order=3) of the effective rainfall threshold $\Omega(t_i)$ defined in formula (2). This threshold varies regularly from year to year. The highest values are reached in summer when soil water recharge is about 12 mm/8h.

Figure 1c shows the Fourier Transform (order=3) of the relative area $\alpha(t_i)$ causing the quick component of unit hydrograph as defined in relationships (3) and (4). In contrast to what was observed for the threshold $\Omega(t_i)$, the relative area $\alpha(t_i)$ strongly varies from year to year because its behaviour is tightly connected to saturation of soils. This phenomenon occurs at the end of autumn, especially after a rainy period, and $\alpha(t_i)$ increase can be very fast as shown in autumn of 1994. The maximum value of $\alpha(t_i)$ is reached in spring and it can overstep 40%. Water accumulates in soils of the lowest parts of the basin, producing overland flow.

The calculations carried out for nitrate flux $c(t_i)\cdot F(t_i)$ in streamflow and for rainfall decomposition are the same as those carried out for streamflow. Here again the input of nitrate flux is governed by rainfall because of leaching in soils. Rainfall is decomposed into three components such as:

$$R(t_i)\cdot\overline{c} = R_b(t_i)\cdot\overline{c} + R_s(t_i)\cdot c_s(t_i) + R_q(t_i)\cdot c_q(t_i) \qquad (5)$$

where $\overline{c}$ is the mean nitrate concentration in stream water. $c_s(t_i)$ and $c_q(t_i)$ are nitrate concentration in rain water in transit that induces slow and quick components of streamflow, respectively.

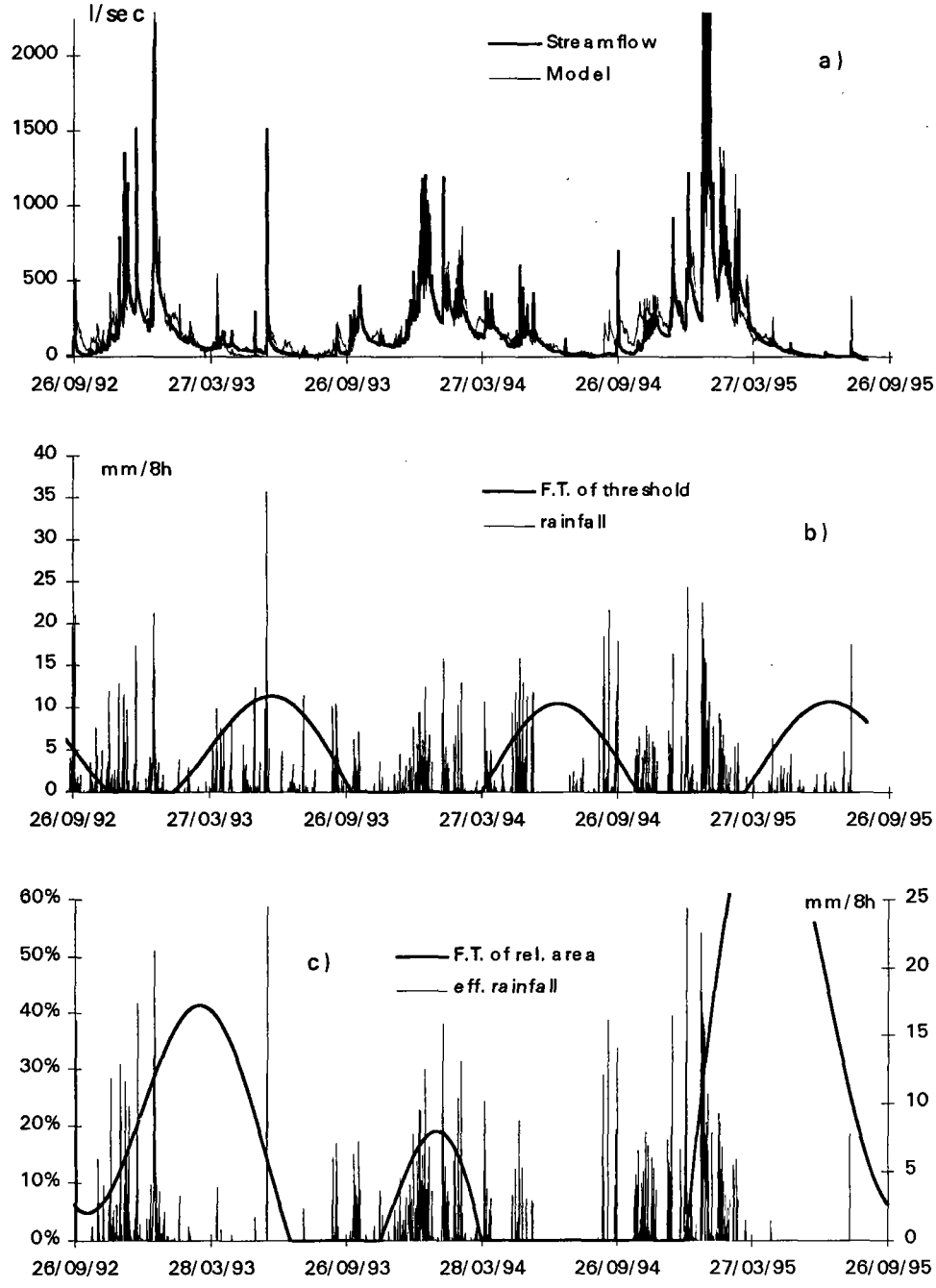

Figure 1
a) Observed and modelled streamflow
b) Fourier Transform of effective rainfall threshold
c) Fourier Transform of relative area causing quick component of hydrograph

The balance term $R_b(t_i)\cdot\bar{c}$ represents variations in nitrate flux inputs due to storage of nitrate in soil water or in vegetation, but also to manuring and to the mineralisation of organic matter in soils (initial nitrate concentration in rainwater is assumed to be zero). By dividing the two sides of (5) by $\bar{c}$, it becomes:

$R(t_i) = R_b(t_i) + R_s(t_i)\cdot\lambda_s(t_i) + R_q(t_i)\cdot\lambda_q(t_i)$

where $\lambda_s(t_i) = c_s(t_i)/\bar{c}$ and $\lambda_q(t_i) = c_q(t_i)/\bar{c}$.

The flow model remains virtually unchanged if $F(t_i)$, $R_i(t_i)$, $R_s(t_i)$ and $R_q(t_i)$ are replaced by $c(t_i)\cdot F(t_i)$, $R_b(t_i)$, $R_s(t_i)\cdot\lambda_s(t_i)$ and $R_q(t_i)\cdot\lambda_q(t_i)$, respectively.

Nitrate flux in stream water is:

$F(t_i)\cdot c(t_i) = S\cdot\left[\Gamma_s * (R_s\cdot\lambda_s) + \Gamma_q * (R_q\cdot\lambda_q)\right](t_i)$ where:

Γ_s and Γ_q are normalised impulse responses and

$S = \sum_{i=1,n} F(t_i)\cdot c(t_i)\Big/\bar{c}\cdot\sum_{i=1,n}\left(R_s(t_i)\cdot\lambda_s(t_i) + R_q(t_i)\cdot\lambda_q(t_i)\right)$.

New functions $\Omega(t_i)$ and $\alpha(t_i)$ are calculated in accordance with the new definitions.

The significance of threshold $\Omega(t_i)$ is as follows: when rainfall height is above this threshold, an input of nitrate occurs, the flux of which is $S\cdot\bar{c}\cdot\left[R_s(t_i)\cdot\lambda_s(t_i) + R_q(t_i)\cdot\lambda_q(t_i)\right]$.

The relative area $\alpha(t_i)$ causing the quick component of nitrate flux at the catchment outlet is such that:

$R_q(t_i)\cdot\lambda_q(t_i) = \left(R(t_i) - R_b(t_i)\right)\cdot\alpha(t_i)$ and

$R_s(t_i)\cdot\lambda_s(t_i) = \left(R(t_i) - R_b(t_i)\right)\cdot\left(1-\alpha(t_i)\right)$.

4.2 Mechanism of streamflow generation from analysis of impulse responses

The study of transport phenomena can be supported by analysis of impulse responses that are used in the models.

Figures 2a and 2b show the normalised impulse responses to rainfall of slow components of streamflow and nitrate flux at the outlet of the catchment. They represent the response of the hydrodynamic system after an effective rainfall event lasting exactly 8 hours (the sampling rate). Since impulse responses are normalised:

$\Gamma_{p,NO3}(t) > \Gamma_{p,flow}(t)$ for a particular lag t indicates nitrate enrichment of stream water

$\Gamma_{p,NO3}(t) < \Gamma_{p,flow}(t)$ indicates exhaustion of nitrate concentration

$\Gamma_{p,NO3}(t) = \Gamma_{p,flow}(t)$ indicates that nitrate concentration in streamflow is the mean concentration.

Because of sharp contrasts which affect nitrate concentration in various parts of the hydrosystem (rainwater, soil water, shallow and deep groundwater) a comparison of normalised impulse responses can be used to indicate water pathways.

Streamflow as well as nitrate flux are increasing quickly on the first day after rainfall event, and then decrease slowly over the next 20 days. The nitrate concentration in stream water is lower than the mean value for 5 days after the rainfall event: it is near zero during rainfall and then increases up to the mean value, due to both the dilution effect of rainwater and denitrification in wetlands. The nitrate recession of stream water lasts longer than the quick component of streamflow represented in Figure 2c (5 and 1 days respectively) and consequently it may occur in subsurface flow, the quick component of streamflow being the result of overland flow. Then, nitrate concentration remains very close to the mean value for two days, proving that mixing between subsurface water and highly nitrate contaminated shallow groundwater is efficient. Nitrate concentration in stream water is higher than the mean value between days 7 and 15, which can be explained by an increase in shallow-groundwater discharge into stream water. Later, nitrate concentration remains very close to the mean value. Deep groundwater

contributes to streamflow: stream water is the result of mixing of shallow and deep groundwater. After day 15, flow is nearly stationary, decreasing slowly until day 110.

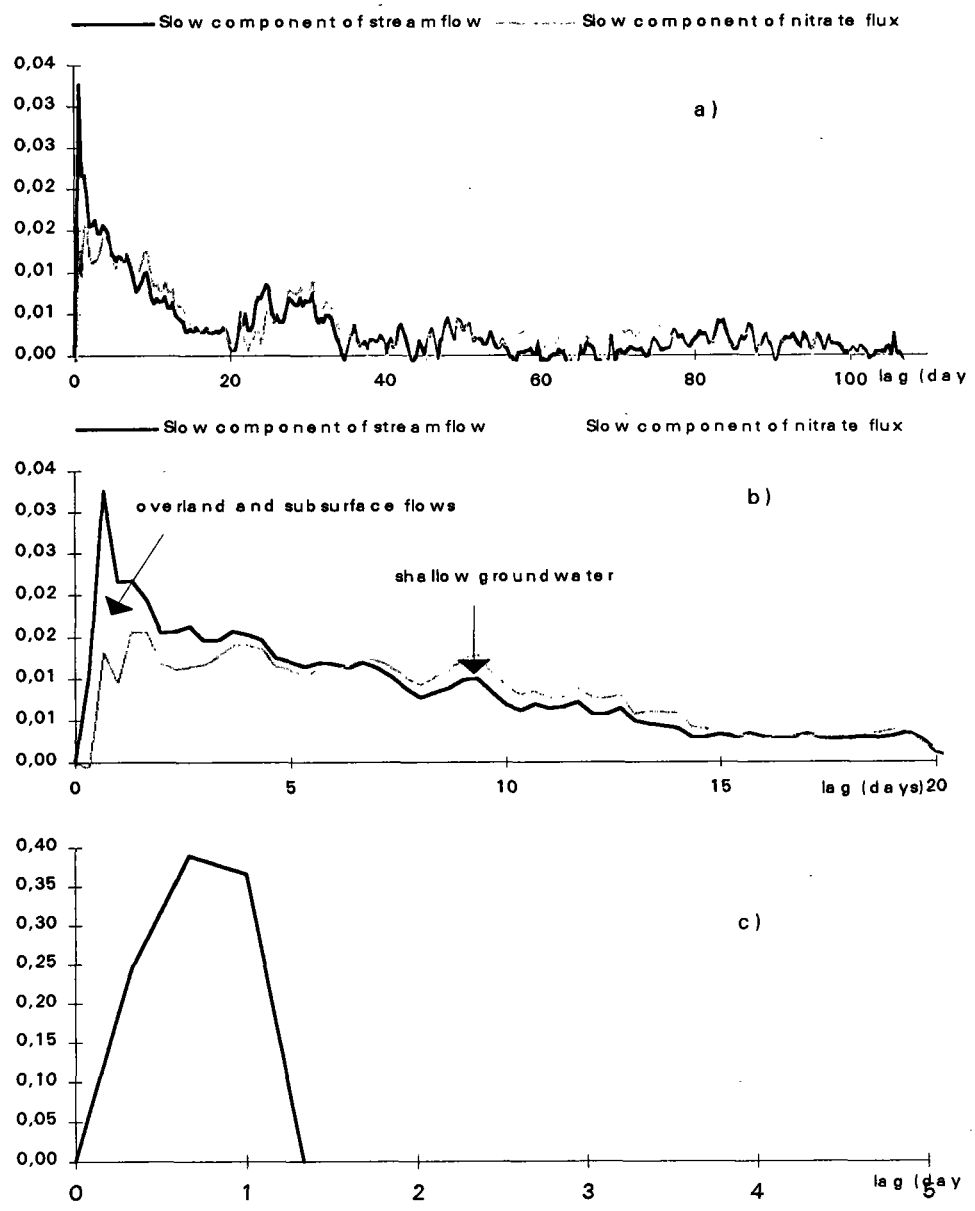

Figure 2 - Normalised impulse responses to rainfall
a) and b) slow components of streamflow and nitrate flux responses to rainfall
c) quick component of streamflow to rainfall (quick component of nitrate flux is the same)

5. Conclusions

The complementary application of hydrogeochemical and numerical analysis has resulted in greatly improved understanding of runoff generating processes in the Coët-Dan catchment. The global model, as expressed in formulae (1) to (5) proves to be efficient, since model outcomes are consistent with streamflow as well as nitrate flux observed at the outlet of the Coët-Dan catchment. Spectral analysis coupled with an inverse method have succeeded in producing estimation of response functions to rainfall on the catchment, and reflect the contribution of streamflow of relatively distinct pathways with different travel times.

Comparison of flow and nitrate flux impulse responses to rainfall defined how mixing of rainwater with soil water, shallow and deep groundwater occurs.

Future work is scheduled on modelling both nitrate and sulphate fluxes in stream in order to carry out the separation of the slow component of hydrograph into the responses to rainfall of shallow and deep groundwater discharge in streamflow.

Bibliography

CANN, C., 1993, Suivi de la qualité de l'eau - Etude menée sur le bassin versant expérimental du Coët Dan (Morbihan), *CEMAGREF,* Rennes.

CANN, C. and C. VILLEBONNET, 1993, Bassin de référence pour l'étude des transferts en milieu agricole intensif - bassin du Coët Dan (Morbihan*), CEMAGREF,* Rennes, 57p.

CANN, C., 1994, Etude de l'évolution des flux de phosphore apportés au littoral par le cours d'eau du Yar en baie de Lannion, *CEMAGREF,* Rennes, 136p.

CANN, C. and C. VILLEBONNET, 1994, Suivi de la qualité de l'eau - Etude menée sur le bassin versant expérimental du Coët Dan (Morbihan), 2eme année, *CEMAGREF,* Rennes.

HRKAL, Z., C. LANGEVIN, P. LEBRET, M. SINAN and M. STEENHOUDT, 1992, Bassin versant représentatif expérimental du Coët Dan (Naizin, Morbihan), *BRGM,* 52p.

PAUWELS, H., A. MARTELAT, P. LACHASSAGNE, J.-C. FOUCHER and O. LEGENDRE, 1996, Evolution des teneurs en nitrates dans l'aquifère du bassin versant du Coët Dan (Naizin, Morbihan*). Colloque Eaux souterraines en Région Agricole, Poitiers 9 -12 September 1996*, S4 81-S4 84.

PINAULT, J.-L. and J.-C. BAUBRON, 1996, Signal processing of soil gas radon, atmospheric pressure, moisture, and soil temperature data: A new approach for radon concentration modeling, *J. Geophys. Res.*, 101, B2.

PINAULT, J.-L. and V. FRITSCHE, 1997, Mechanisms affecting streamflow and stream water quality: a novel approach coupling spectral analysis of time series with an inverse method, *Water Res. Rech.*, in preparation.

The long-term forecast of monthly water quality in the Danube river

P. Pekarova [1], J. Pekar [2], P. Roncak [3]

[1] *Institute of Hydrology, SAS, Bratislava, Slovakia*
[2] *Department of Numerical and Optimising Methods, Comenius University, Slovakia*
[3] *Slovak Hydrometeorological Institute, Bratislava, Slovakia*

1. Introduction

During recent decades there has been an increasing demand for water quality monitoring of many rivers by regular measurements of various water quality parameters. Several qualitative as well as quantitative aspects must be considered in the analysis of the resulting data series. The long-term tendencies in water quality data series are of particular interest (Wolf, 1996; Velikov *et al.*, 1996; Pekarova and Miklanek, 1996).

This contribution deals with the choice of a suitable model for long-term prediction of monthly pollutant concentrations in surface water. Three models ARMA(p,q), ARIMA(p,q,d), as well as SARIMA(p,q,d)x$(P,Q,D)_L$ were tested. Due to the significant trend character and significant seasonality of the water quality data, the autoregressive model SARIMA was selected. The SARIMA model was applied to the prediction of monthly discharge, water temperature, nitrate, BOD, COD, dissolved oxygen, sulphate and chloride concentrations in the Danube river at two cross-sections: Bratislava - above the Gabcikovo water power station; and Komarno - below the Gabcikovo dam.

2. Time series analysis

2.1 Trend analysis

The Slovak part of the Danube River on the left river bank extends for about 172 km (from the mouth of the Morava river to the mouth of the Ipel). Among the water quality sampling sites along the river, the following five cross sections were considered (see Figure 1.):

1. The Danube River, Bratislava: a) left bank, b) middle, c) right bank, 1869 km;
2. The Danube River, Rajka, 1851 km;
3. The Danube River, Hrusov, 1842 km;
4. The Danube River, Medvedov;
5. The Danube River, Komarno: a) left bank, b) middle, c) right bank, 1764 km.

Fig. 1: Location of water quality sampling sites.

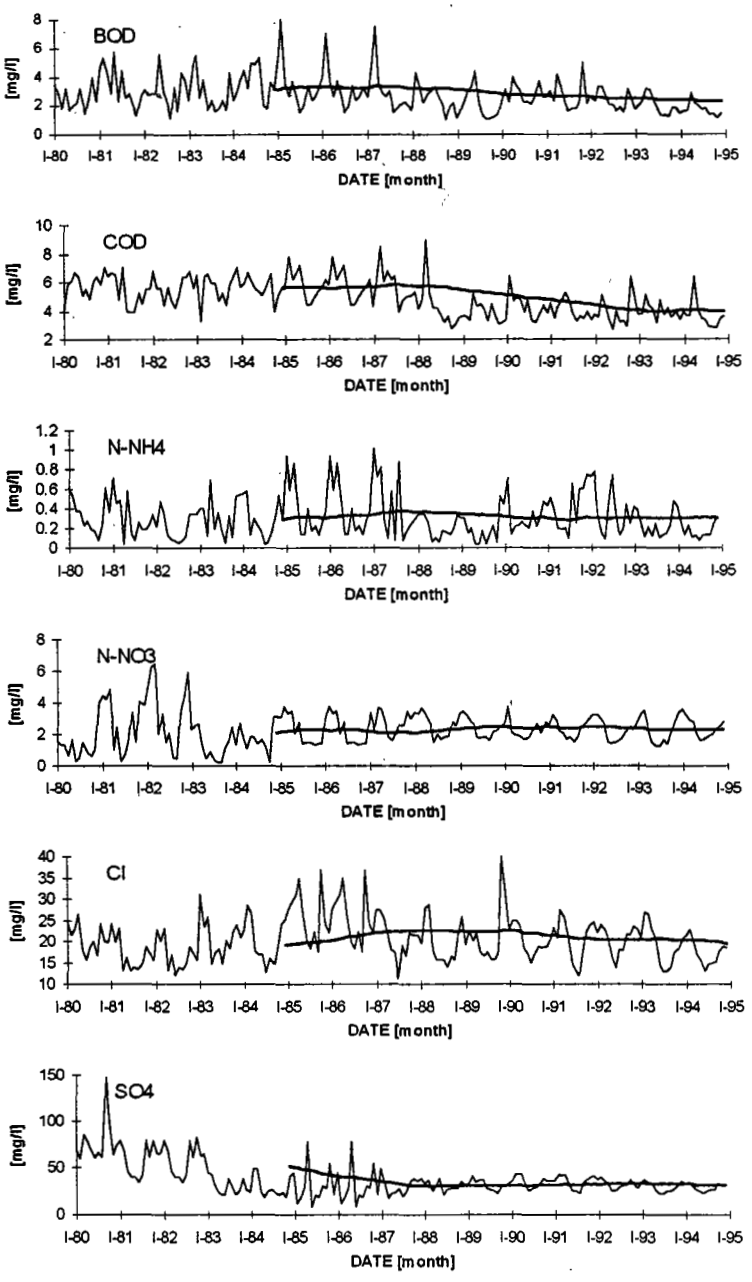

Fig. 2: Monthly courses of pollutant concentrations in Danube river at Bratislava - right bank. Moving average (m=60).

To apply a trend analysis the time series ought to be as long as possible. The trend analysis was based on monthly data measured at Danube-Bratislava cross - section during the period from 1980 to 1994. Between 1980 and 1989, samples were taken once a month, while during the years 1990-1994 the samples were taken every two weeks. The following data were collected: water temperature, pH, O_2, BOD, COD, TOC, NEL (non-polar extractable substance), Cl^-, $N\text{-}NH_4^+$, $N\text{-}NO_2^-$, $N\text{-}NO_3^-$, sulphates, total nitrogen, $P\text{-}PO_4^{3-}$, total phosphorus, chlorophyll-a, index saprobility, Cd, Pb, Cr, Cu, Zn, Hg, Ni, and As (Adamkova *et al.*, 1996, Borovickova and Durkovicova, 1996).

In Figure 2, the monthly measured concentrations of selected determinands in Danube River stream water at Bratislava are presented. In this figure, the five-year moving averages of the given time series are shown, as well. Since a similar trend occurred at all mentioned cross-sections, we can say that the water quality in the middle Danube has improved during the last decade. The most significant drop of concentrations occurs for sulphates.

2.2 Statistical analysis

The trend analysis showed that the given time series contain significant changes during the last fifteen years. To evaluate the recent Danube water quality, the last five year period was analysed separately. In Table 1, the main statistical parameters of the observed determinands of the Danube River at Bratislava (right bank) during the period from 1990 to 1994 are given.

TABLE 1: Basic statistical characteristics of measured pollutant concentrations in the Danube River at Bratislava - right bank, 1990 - 1994.

	T °C	pH	O_2 mg/l	BOD mg/l	COD mg/l	TOC mg/l	NEL mg/l	Cl^- mg/l	SO_4^{2-} mg/l
Average	11.20	8.04	9.99	2.32	3.97	12.00	2.40	19.02	31.24
Min	0.10	7.20	7.10	0.90	1.90	1.20	0.90	10.30	16.50
Max	23.10	8.60	13.50	7.90	9.25	66.00	4.10	34.50	48.00
Std.Dev	5.97	0.24	1.63	1.01	1.11	6.67	0.71	4.40	6.17
Median	11.50	8.00	10.10	2.10	3.80	11.00	2.36	18.80	31.00
	$N\text{-}NH_4^-$ mg/l	$N\text{-}NO_2^-$ mg/l	$N\text{-}NO_3^-$ mg/l	N-total mg/l	$P\text{-}PO_4^{3-}$ mg/l	P-total mg/l	chlor.-a mg/l	Ind.sap.	Col.bac. Ktj/l
Average	0.29	0.03	2.28	3.13	0.06	0.15	14.98	2.34	97.54
Min	0.04	0.01	1.04	1.55	0.01	0.05	0.79	1.75	5.00
Max	1.16	0.08	3.84	4.68	0.27	0.71	88.70	9.99	190.00
Std.Dev	0.23	0.01	0.70	0.85	0.04	0.08	16.52	0.99	44.80
Median	0.21	0.03	2.26	3.00	0.06	0.13	10.10	2.22	100.00
	Cd mg/l	Pb mg/l	Cr mg/l	Cu mg/l	Zn mg/l	Hg mg/l	Ni mg/l	As mg/l	
Average	0.14	3.48	1.59	4.25	0.03	0.20	2.62	1.42	
Min	0.00	0.00	0.00	0.00	0.00	0.00	0.00	0.00	
Max	1.41	40.30	12.20	34.10	0.15	1.00	15.10	6.30	
Std.Dev	0.28	8.23	2.40	6.44	0.03	0.19	2.88	1.25	
Median	0.06	1.40	1.00	3.10	0.02	0.20	1.90	1.00	

Significant changes of water quality did not occur along the river. The lowest pollutant concentrations during the period 1990 to 1994 were found at cross-section No. 2 - Rajka. In Figure 3 the average concentrations of BOD, COD, and total nitrogen at the five cross-sections along the Danube River are presented.

2.3 Seasonality

Both discharge and water quality change significantly during the year. In general, water quality decreases with decreasing discharge. In Figure 4, the seasonal variation in discharge in the Danube at Bratislava, and monthly temperature and concentrations of pollutants (averages 1990 to 1994), are shown.

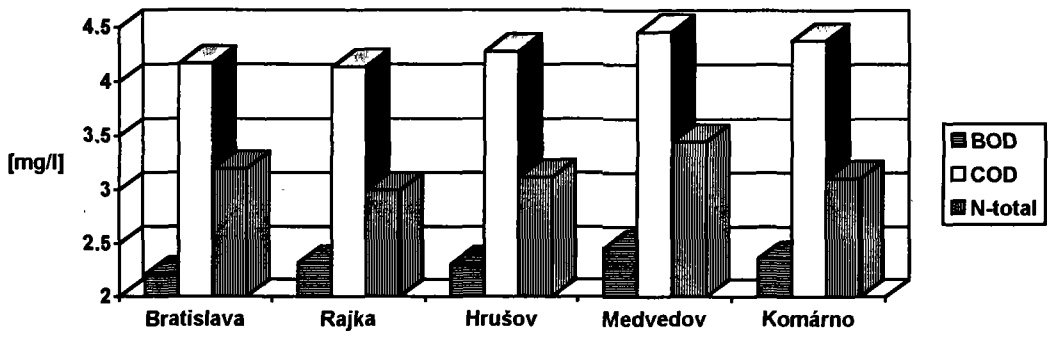

Fig. 3: Development of BOD, COD and total nitrogen along Danube; arithmetic mean of two-weekly values (1990 - 1994).

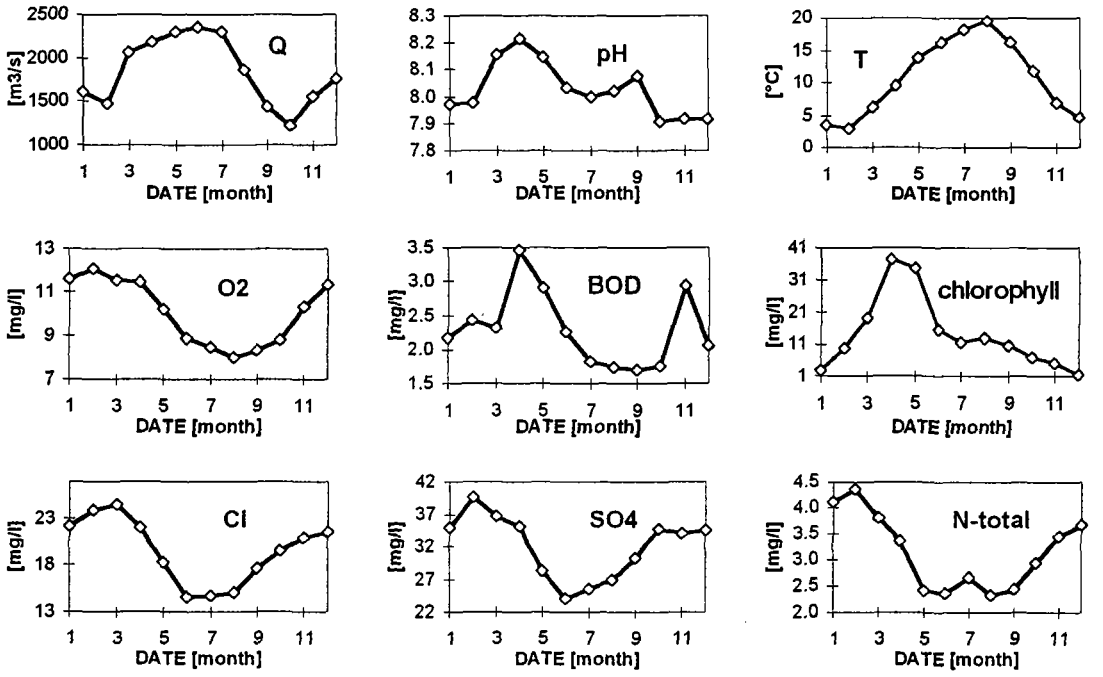

Fig. 4: Seasonal variations in discharge, monthly temperature and concentrations of selected determinands (averages 1990 - 1994) in the Danube River at Bratislava.

3. Modelling results

3.1 ARIMA modelling approach

The Box - Jenkins models represent a reasonable method to describe the periodical time series with essential stochastic behaviour. These models are highly flexible and are able to model stochastically the seasonality as well as trends, in a better way than the classical time series analysis techniques. The basic component of these models is an independent and normally distributed random variable E_t (Mendel *et al*, 1995; Nachazel, 1984; Szolgay, 1985; Prochazka, 1984).

ARMA(p,q) model of the orders p and q can be defined as a combination of the autoregressive (AR) and moving-average (MA) processes of the form

$$Y_t = \varphi_1 Y_{t-1} + \ldots + \varphi_p Y_{t-p} + E_t + \Theta_1 E_{t-1} + \ldots + \Theta_q E_{t-q}\,, \qquad (1)$$

where: E_t - independent and normally distributed random variable with zero mean m = 0 and variance σ_E^2,

Θ_i - parameters of MA polynomial of the order q,

φ_i - parameters of AR polynomial of the order p.

In operator form, the model can be written as:

$$\varphi(B)\, Y_t = \Theta(B)\, E_t\,, \qquad (2)$$

where: B - the backward shift operator defined as $BY_t = Y_{t-1}$

Θ - the regular MA operator of the order q,

φ - the regular AR operator of the order p.

To construct the ARIMA(p,d,q) model, stationarity of the analysed series (Y) is not required. Instead of original series it operates with the series (Z) of the first or higher order differences. For the differences of the first order, it holds:

$$Z_t = Y_t - Y_{t-1}, \quad Z_{t-1} = Y_{t-1} - Y_{t-2} \quad , \ldots, . \tag{3}$$

The generalised operator form is:

$$Z_t = \nabla^1 Y_t = (1-B)Y_t \quad , \tag{4}$$

where ∇^1 is the backwards difference operator.

The final form of the ARIMA model can be written as:

$$\varphi(B)\, \nabla^d Y_t = \Theta(B)\, E_t. \tag{5}$$

In the Box-Jenkins methodology, the seasonality and the trend can be modelled stochastically. To construct the seasonal model, successive models for each month are constructed (i.e., first the model of January data, then of February, etc.)

The general form of the SARIMA(p,d,q)x(P,D,Q)$_L$ model takes the form:

$$\varphi(B)\, \varphi(B^{12})\nabla^d\, \nabla^D_{12}\, Y_t = \Theta(B)\Theta(B^{12})E_t, \tag{6}$$

where ∇^D_{12} is the seasonal backwards difference operator,

φ is the regular SAR operator of the order p,

Θ is the regular SMA operator of the order q.

3.2 SARIMA model identification

To identify this model, it is necessary to analyse the particular components of the time series as follows (Pekar and Pekarova, 1996):

a) identification of trend (differencing order d) and of seasonality (seasonal differencing order D);
b) model type (AR, MA, ARMA) selection and the model order determination;
c) estimation of model parameters; and
d) model verification.

3.3 Modelling results

The monthly values of determinands for the period 1990 to 1994 were treated as a time series and used for forecasting purposes.

To construct the models, data from the graphic record of original observed series were used as well as the estimated autocorrelation (Figure 5) and partial autocorrelation functions of observed series. To search for periodicity (or seasonality), periodograms of the observed time series were constructed. In Figure 6, the periodogram of total nitrogen in Danube at Bratislava is given.

If it was necessary, the trend (non-stationarity) of the series was removed by differencing of the first order (d=1). The seasonal differencing was of the first order (D=1) in all cases. The models considered were

SARIMA(1,1,1)x(1,1,1)$_{12}$,
SARIMA(1,1,1)x(1,1,0)$_{12}$, and
SARIMA(0,1,1)x(1,1,1)$_{12}$.

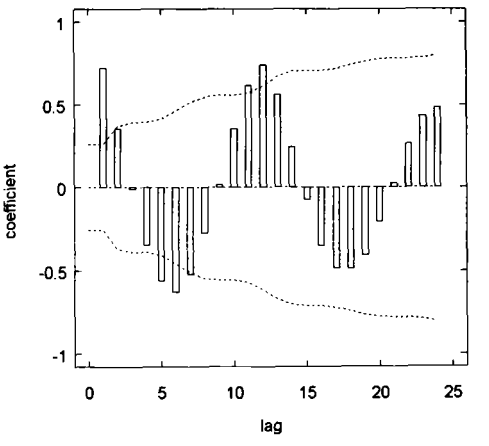

Fig. 5: ACF patterns for the origina series of nitrogen.

It is clear (Figure 7), that the distribution of some measured concentrations is not Gauss-normal (e.g. the BOD concentrations are from a log-normal distribution). Since the ARIMA models assumes uses elements which are normal distributed, a logarithmic transformation was applied to the input time series before prediction.

Table 2 shows the estimated parameters φ_1, Θ_1, φ_I and Θ_I of SARIMA models for the Danube River at Bratislava - right bank for: discharge, water temperature, BOD, O_2, chlorophyll-a, $N\text{-}NO_3^-$, Cl^- and SO_4^{2-}.

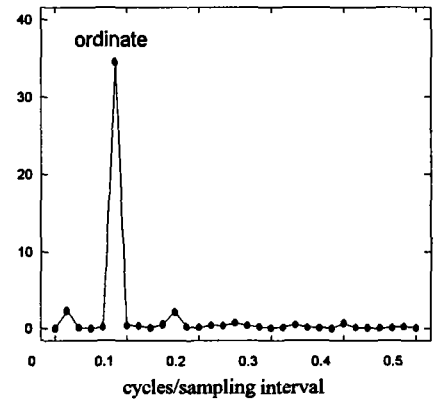

Fig. 6: Periodogram of nitrogen, (Danube: Bratislava - middle, 1990 - 1994).

TABLE 2 Parameters of SARIMA models, Danube Bratislava right bank

Determinand	φ_1	Θ_1	φ_I	Θ_I	estim. white noise std.	logarithmic transformation
Discharge	0.342	1.03	-0.673	0.897	0.22	yes
Temperature	-0.365	0.927	-0.913	-	1.35	no
BOD	-	0.912	0.519	0.897	0.221	yes
O_2	-	0.899	-0.565	0.695	0.023	yes
chlorophyll	0.833	0.671	-	0.780	0.288	yes
$N\text{-}NO_3^-$	0.352	0.943	-0.641	-	0.15	yes
Cl^-	0.106	0.726	-0.890	-	0.117	yes
SO_4^{2-}	0.394	0.953	-0.77	-	3.08	yes

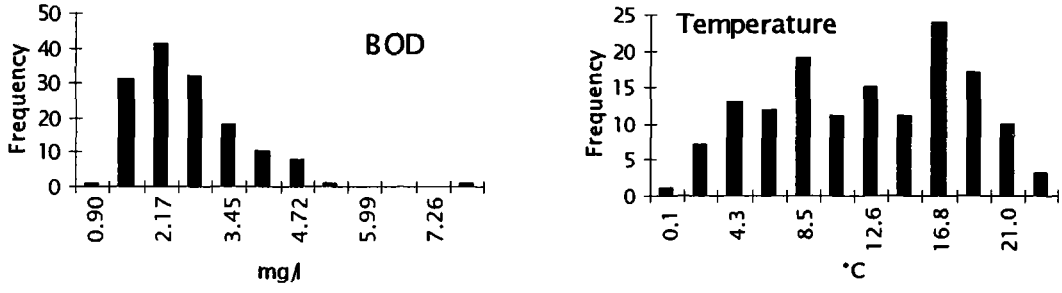

Fig. 7: Histograms of measured BOD concentrations (log-normal distribution) and water temperature (normal distribution) in the Danube at Bratislava - right bank, 1990-1994.

4. Conclusions

From time series analysis of the monthly concentrations of selected determinands it follows that water quality in the middle part of the Danube River has improved during the last decade.

Figure 8 shows plots of predicted values of determinands by SARIMA models pertaining to the years 1995, 1996, 1997 and 1998. In spite of the shortness of the water quality time series used, and because these series were considerably influenced by decreasing trends (except for water temperature where there was an increase), the obtained results are satisfactory. It might be expected that the real

values will not show such rapid decreases as those predicted by the SARIMA models. The forecasting performance of the SARIMA model was found to be satisfactory.

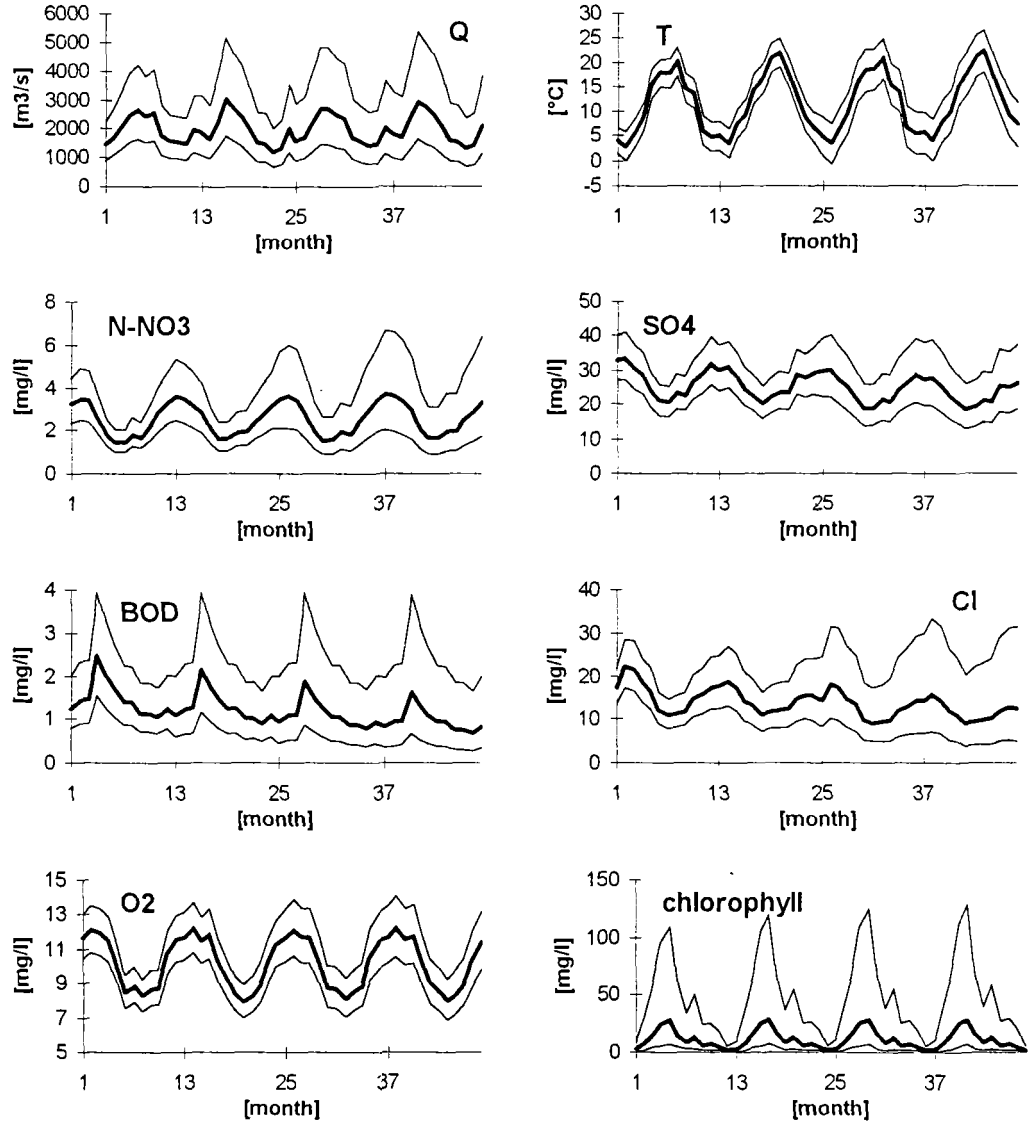

Fig. 8: Prediction of selected determinands, (bold line), 48 months ahead, Danube Bratislava-right bank, (1 denotes Jan 1995), 95% upper and lower limits.

5. Bibliography

ADAMKOVA, J., J. GAVORA and P. RONCAK (1996) 'Ecotoxicological methods as the part of water quality monitoring'. *In Proceedings of XVIIIth Conference of the Danube Countries on hydrological forecasting and hydrological bases and water management data.* TU Graz, Austria, Vol.2, E73-78.

BOROVICKOVA, A. and D. DURKOVICOVA (1996) 'Changes in Danube water quality in the area affected by the Gabcikovo dam project.' *In Proceedings of XVIIIth Conference of the Danube Countries on hydrological forecasting and hydrological bases and water management data.* TU Graz, Austria, Vol.2, E79-84.

MENDEL, O., P. PEKAROVA and S. KROG (1995) 'Long-term monthly runoff computation using the ARIMA model.' In *Proc. International Symp. Runoff computations for water projects.* St.Petersburg, Russia, Oct.-Nov.

NACHAZEL, K. (1984) 'On some problems concerning the deviation of statistical characteristics of average monthly flow series and their mathematical models.' *J. Hydrol. Hydromech.*, 32, 1, 3-31. (In Czech).

PROCHAZKA, M. (1984) 'The comparison of different methods of determination of order of autoregressive model by synthetic streamflow generation.' *J. Hydrol. Hydromech.*, 32, 2, 139-147. (In Czech).

PEKAR, J. and P. PEKAROVA (1996) 'Some problems of long-term prediction of monthly runoff and pollutant concentrations in the Vah river.' *In Proceedings of full paper of the conference: Environmental statistics and earth science*, (Ed. by: Horova, I., Jureckova, J. and Vosmanský J.), Masaryk U Brno, Czech Republic, 131-135.

PEKAROVA, P. and P. MIKLANEK (1996) 'The balance of pollutant loads by Slovak rivers into the Danube River. ' *In Proceedings of XVIIIth Conference of the Danube Countries on hydrological forecasting and hydrological bases and water management data.* TU Graz, Austria, Vol.2, E85-90.

SZOLGAY, J. (1985) 'A simple stochastic model of daily flows.' *J. Hydrol. Hydromech.*, 33, 142-155.

VELIKOV, B., M. MACHKOVA, D. DIMITROV and I. MILUSHEV (1996) 'Tendencies in the Dynamics of the Hydrochemical Parameters in the Danube Waters, its Tributaries and Groundwater in Bulgarian Part of the River Basin'. *In Proceedings of XVIIIth Conference of the Danube Countries on hydrological forecasting and hydrological bases and water management data.* TU Graz, Austria, Vol.2, E9-16.

WOLF, B. (1996) 'Water quality of the River Danube in Bavaria'. *In Proceedings of XVIIIth Conference of the Danube Countries on hydrological forecasting and hydrological bases and water management data.* TU Graz, Austria, Vol.2, E25-30.

Spatial and temporal patterns of runoff generation processes in mountainous Mediterranean basins (Vallcebre, Catalonia)

J. Latron, P. Llorens and F. Gallart

Institute of Earth Sciences, Barcelona, Spain

1. Introduction

The Vallcebre catchments were selected in early 1989 to analyze the hydrological consequences of land abandonment as well as the hydrological and sediment yield behaviour of badland areas.

The description and characterisation of runoff generation mechanisms from field observations and hydrograph analysis is the first step in the construction of a perceptual model of the functioning of the Vallcebre catchments. Sediment concentrations in stream water, as well as measurements of soil moisture and phreatic levels, provide supplementary information that help in constructing a perceptual model that will be used in further validation of the internal functioning of hydrological models.

The aim of this paper is to discuss differences between the hydrological functioning of two sub-basins with different land cover and extent of badland areas, paying attention to the transition between a period with water deficit and a period with water excess observed in summer 1995.

2. The study area

The Vallcebre catchments are located in the headwaters of the Llobregat river, in the southern margin of the Pyrenees, at altitudes between 1100 m. and 1700 m a.s.l.. The bedrock is dominated by red clayey mudrocks with massive limestone beds. The climate of this area is mountainous Mediterranean with a mean annual temperature of about 9° C and with about 850 mm of mean annual precipitation. The main rainy seasons are autumn and spring, but short intense rainstorms usually occur during late August and early September. Most of the hillslopes below 1600 m a.s.l. have been terraced in the past for cultivation and are now used for cattle stockbreeding or forestry.

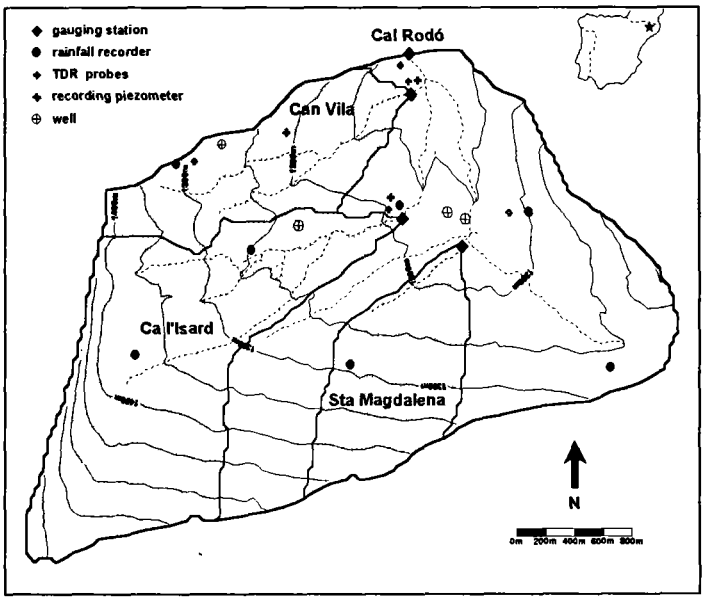

Figure 1: General arrangement of the measuring network.

The clayey characteristics of the bedrock, the steep topography, as well as winter freezing and summer rainstorms, have led to the formation of badland areas. These surfaces play a significant role in sediment production (Balasch *et al.* 1992) and also in the hydrological response (Latron and Gallart, 1995).

2.1 Instrumental set-up

The instrumentation of the research catchments began in 1989, and sought to analyze the hydrological and sediment yield consequences of land-use changes as well as the dynamics of badland areas (Llorens and Gallart, 1992, Balasch *et al.*, 1992). The research design (Fig. 1) consists of a set of 6 small catchments (4 of which are nested), with areas ranging from 14 to 400 ha. The pluviometric and weather network consists of 10 rain recorders, one weather station and one Bowen Ratio station.

The Can Vila sub-basin (0.59 km^2) was selected in early 1995 to study the behaviour of non-degraded areas, including forested hillslopes, abandoned agricultural terraces, meadows and some farming fields. This basin was selected to substitute the Cal Parisa catchments where water balance is problematic.

The Ca L'Isard sub-basin (1.0 km^2) was selected in 1990 to study the hydrological and sediment yield behaviour of basins covered with significant surface of badlands. This basin is 1 km^2 in area, and the three main landscape units are 12 ha of badland surfaces, 29 ha of old agricultural terraced fields, patchily forested, and 59 ha of forested hard bedrock outcrops with shallow soils. This basin is provided with an automatic pumping sampling device, an infra-red backscattering turbidity meter, and a ultra-sonic solids meter sensor.

Soil water content has been measured with TDR method at five points in the Can Vila and Ca'L'Isard basins since early 1995. The measuring design consists of 0.5 m long probes, vertically inserted in the soil, that are read every week. This design is intended to give a simple but practical assessment of soil water storage used for both runoff generation and plant evapotranspiration studies.

Phreatic levels are measured weekly at six wells. Continuously recording piezometers have been installed in the basins in late 1995, after the summer period studied in this paper.

2.2 Hydrological functioning of the basins

Early studies in the Cal Parisa terraced catchment (Llorens, 1991) showed that during dry periods this basin is insensitive to intense rainstorms, and that runoff is only produced when a water storage threshold is reached, following the appearance of some saturated areas. Soil moisture measurements with TDR demonstrated that this threshold corresponds to a soil water storage of 280 mm (about 60% of soil saturation) (Gallart *et al.* in press b).

Field observations, as well as the study of hydrographs and sediment concentrations at the Ca L'Isard station, demonstrated that badland surfaces produce significant Hortonian runoff in response to intense summer rainstorms, and that during dry periods they are the only runoff sources (Latron and Gallart, 1995). During wet periods, stream sediment concentrations are diluted by the clean water contributed by areas well protected against erosion by dense vegetation cover (Gallart *et al.*, in press a).

3. Results

The data obtained at the Can Vila and Ca L'Isard basins since May 1995 until June 1996 have been analyzed and compared in order to improve understanding of the role of basin water status on runoff generation, as well as the modifications introduced by the badland areas.

3.1 Correlation analyses

A series of correlation analyses has been performed using the weekly measurements of soil water content and phreatic levels, as well as runoff coefficients and rainfall depth and intensity of the events, observed in the Can Vila and Ca L'Isard basins during the study period.

3.1.1 Soil water content and phreatic levels

If all the observations available on soil moisture and phreatic levels at 50 points and including a short drought period are used, there is positive and significant correlation. Nevertheless, if the measurements obtained during the dry period (20 points) are separated from the readings obtained during the wet

period, a clear distinction appears between soil moisture and phreatic levels: soil moisture readings are only well correlated during wet conditions, whereas phreatic levels are better correlated during dry conditions than during wet ones.

This result demonstrates that any information on soil moisture or phreatic level is sufficient to classify the overall status of the basin between a dry or a wet condition, but soil moisture and phreatic water behave in a different manner when they are analyzed with more precision. During wet conditions soil moisture values vary within a wider range than during dry conditions, whereas phreatic levels show much smaller oscillations during wet periods than during dry ones.

If the correlations between individual soil moisture measuring points and phreatic levels are analyzed, it appears that the comparisons are not consistent for different wetness conditions; some soil moisture points that are relatively well correlated with phreatic levels during the wet periods are among the worst correlated with them during dry ones.

These findings are slightly different to the soil moisture patterns observed in Cal Parisa during the wet-dry transitions (Gallart *et al.*, in press b).

3.1.2 Runoff coefficients

A correlation coefficients matrix has been built to compare rainfall depths, rainfall intensities and runoff coefficients for 19 events measured at the two stations, together with the antecedent averaged soil moisture and the phreatic level at one measuring point (Table 1).

TABLE 1: Correlation coefficients between Soil moisture (S. M.), Phreatic level (Ph. L.), Precipitation total (P. T.), Precipitation intensity (P. I.), Runoff coefficient at Can Vila (R C Vila), and Runoff coefficient at Ca L'Isard (R C Isard). Coefficients in bold are significant at the 0.01 level and coefficients underlined at the 0.05 level.

	S. M.	Ph. L.	P. T.	P. I.	R C Vila	R C Isard
S.M.	**1.00**	**0.74**	0.44	-0.22	0.55	**0.60**
Ph. L.	**0.74**	**1.00**	-0.47	**-0.68**	**0.70**	**0.62**
P.T.	0.44	-0.47	**1.00**	**0.66**	**0.57**	**0.66**
P.I.	-0.22	**-0.68**	**0.66**	**1.00**	-0.49	-0.37
R C Vila	0.55	**0.70**	**0.57**	-0.49	**1.00**	**0.98**
R C Isard	**0.60**	**0.62**	**0.66**	-0.37	**0.98**	**1.00**

Table 1 demonstrates first that precipitation of high intensity occurs during dry periods of low phreatic level and soil moisture, whereas higher magnitude precipitation shows the same coincidence with low phreatic levels but occurs over somewhat wetter soils.

Runoff coefficients confirm the main role of saturation mechanisms (good positive values with phreatic level and negative ones with rainfall intensity), but this behaviour is more evident at Can Vila than at Ca L'Isard, where runoff coefficients are more related to rainfall total and less negatively related to rainfall intensity. This small difference is consistent with a moderate contribution of Horton runoff from badland areas in the Ca L'Isard basin.

3.2 Behaviour of the catchments during the summer 1995 events

Fig. 2 shows rainfall, runoff, runoff coefficients and water table depths measured in the Can Vila basin during the summer of 1995. Water storage in the basin at the beginning of the series of heavy rainfall events (29 July) was relatively high, compared with the usual summer conditions, but sufficiently low to give a very low runoff coefficient (0.7%). Subsequent rainfall events produced higher runoff coefficients (up to 30 %), in response to the increasing water status of the basin. The lack of good correlation between high runoff coefficients and phreatic levels on the graph is attributed to the high dynamics of the water table during the events; this was the reason for starting the continuous measurements of the piezometric levels.

Fig. 3 shows the suspended sediments concentrations and the runoff coefficients measured at the

Ca L'Isard station for the same events of the former figure. This graph demonstrates that runoff coefficients successively increase, at the same time that the slopes of the sediment concentration - discharge relationships decrease. The individual plots of the events show a nearly linear sediment concentration - discharge relationship, with sustained concentrations during the recession limb and without any sediment exhaustion effect. The progressive decrease of the slopes of the events are therefore attributed to a dilution effect, consistent with the increasing runoff coefficient, rather than to a sediment exhaustion effect that is only observed at the end of the wet season (Regüés *et al.*, 1995).

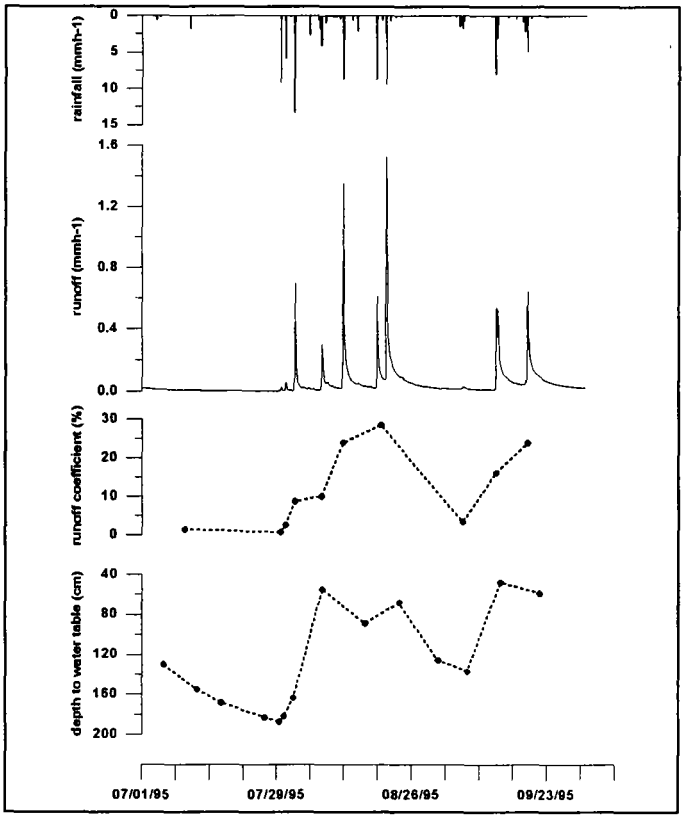

Figure 2: Summer 1995 events at the Can Vila station.

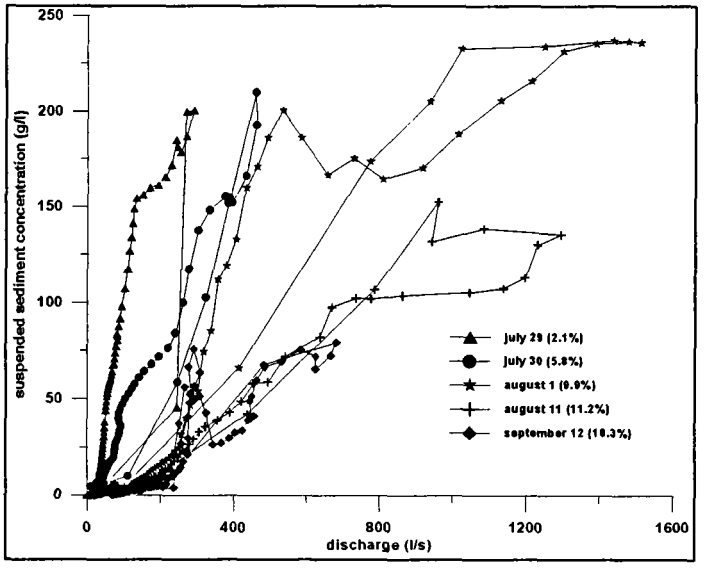

Figure 3: Summer 1995 suspended sediment concentrations at the Ca L'Isard station.

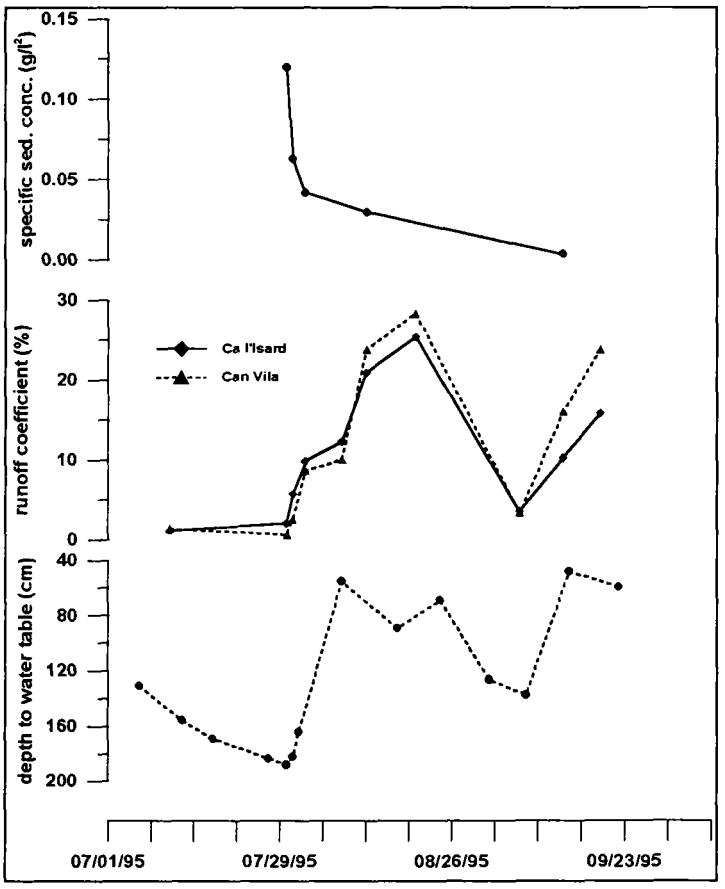

Figure 4: Comparison of the responses of Can Vila and Ca L'Isard sub-catchments during the Summer 1995 events

Fig. 4 summarizes the comparison between the two former graphs. Runoff coefficients are higher in Ca L'Isard than in Can Vila at the beginning of the wet period, the difference being almost constant. During this period, there is a decrease of the slope of the sediment concentration - discharge plot (specific sediment concentration in the graph).

4. Conclusion

The data analyzed confirm the major role of saturation mechanisms in the runoff generation of these basins, as well as the possibility of a good relationship between the basin water status, measured through the phreatic levels, and the runoff coefficients.

The relationships between local soil moisture values and phreatic levels deserve further analysis, taking into account the situation of the measuring points within the catchment as well as the physical properties of the individual soil profiles.

The comparison between the Ca L'Isard and Can Vila basins demonstrates that badland areas are far more important in terms of sediment than in terms of runoff production. The Horton runoff generation mechanisms active in these degraded areas can not be considered as a benefit because the small amount of runoff is overcompensated by the very low quality of the water produced.

Acknowledgements

This work was funded by the European Commission (Project VAHMPIRE, ENV4-CT95-0134), and the CICYT (Project PROHIDRADE, AMB95-0986-C02-01). The contributions of J. Latron and P. Llorens were possible thanks to a training contract from the UE (EV5V-CT94-5222) and a post-doctoral research contract funded by the Ministerio de Educación y Ciencia, respectively.

References

BALASCH, C., X. CASTELLTORT, P. LLORENS and F. GALLART (1992) 'Hydrological and sediment dynamics network design in a Mediterranean mountainous area subject to gully erosion'. in: Erosion and sediment transport monitoring programmes in river basins, Bogen, J., Walling, D.E. and Day, T. (Ed.), *IAHS Pub. no.* 210: 433-442.

GALLART, F., J. LATRON and D. REGÜÉS (In press, a) 'Hydrological and sediment transport processes in the research catchments of Vallcebre (Pyrenees)'. *in: Modelling erosion by water*, J. Boardman and D. Favis-Mortlock (Eds.). ANSI NATO Series.

GALLART, F., J. LATRON, P. LLORENS and D. RABADÀ (in press, b) 'Hydrological functioning of Mediterranean mountainous basins in Vallcebre, Catalonia: some challenges for hydrological modelling'. *Hydrological Processes, special issue TOPMODEL.*

GALLART, F., P. LLORENS and J. LATRON (1994) 'Studying the role of old agricultural abandoned terraces on runoff generation in a Mediterranean small mountainous basin'. *J. Hydrol.*, 159: 291-303.

LATRON, J. and F. GALLART (1995) 'Hydrological response of two nested small Mediterranean basins presenting various degradation states'. *Phys. Chem. Earth,* 20 (3-4): 369-374.

LLORENS, P. (1991) 'Resposta hidrològica i dinàmica de sediments en una petita conca pertorbada de muntanya mediterrània'. *Unpublished phD thesis,* Universitat de Barcelona, pp 277.

LLORENS, P. and F. GALLART (1992) 'Monitoring a Small Basin Response in a Mediterranean Mountainous Abandoned Farming Area: Research Design and Preliminary Results', *Catena*, 19: 309-320.

LLORENS, P. , J. LATRON and F. GALLART (1992) 'Analysis of the role of agricultural abandoned terraces on the hydrology and sediment dynamics in a small mountainous basin (High Llobregat, Eastern Pyrenees)'. *Pirineos*, 139: 27-46.

REGÜÉS, D., G. PARDINI and F. GALLART (1995) 'Regolith behaviour and physical weathering of clayey mudrock in a gullied area, as dependent on seasonal weather conditions'. *Catena*, 25: 199-212.

Runoff generation in a small catchment under silvo-pastoral land-use in south-west Spain

A. Ceballos and S. Schnabel

Department of Geography, University of Extremadura, Cáceres, Spain

1. Introduction

Research has been carried out in the Guadalperalón catchment (35.4 ha) in Extremadura, Spain, since 1990 in order to understand the hydrological and sedimentological processes operating in areas with the so-called *dehesa* land-use system. It consists of openly spaced evergreen woodland, generally *Quercus* species, with silvo-pastoral exploitation. The interest of this investigation lies in the economical and ecological importance of this land-use type within the Iberian Peninsula, and in other Mediterranean countries. *Dehesas* represent about 50% of agriculturally used land in the provinces of south-west Spain.

The project includes studies of overland flow and soil erosion at hillslopes, as well as gullying and discharge production in the main channel. The present paper focuses on runoff at the catchment outlet and investigates:

(a) the relation between rainfall characteristics and discharge;
(b) the causes of temporal variability in annual runoff coefficients; and
(c) the importance of antecedent moisture conditions for the catchment hydrology in the area.

2. The study area

The study basin is located 25 km north-east of the city of Cáceres (Fig. 1). It is situated on a peneplain with slope gradients in the order of 10 to 25%. The substrate is exclusively formed by schists. The climate is Mediterranean, with atlantic and continental influences. Mean annual precipitation amounts to 510 mm. The annual rainfall distribution shows a dry season lasting from June to September and a wet season from October to March. Annual rainfall is highly variable, as illustrated by the 20 and 80 percentiles of 328 mm and 650 mm respectively. The intensity of rainstorms is lower than at the Mediterranean coast. For example, a 30-minute maximum intensity of 55.5 mm h^{-1}, has a recurrence interval of 50 years (Schnabel, in press), whereas for Barcelona a value of 117.6 mm h^{-1} is reported (Elias Castillo and Ruiz Beltran, 1979).

The hillslope soils are shallow (10 cm - 30 cm), with a silty loam texture and low organic matter content. Their structure is poorly developed and can be classified as Leptosols. The valley bottoms are formed by fluvio-colluvial sediments, composed of silty sands and gravels with a thickness of 1 m to 2 m. The soils found in this area are also poorly developed (Regosols), but their porosity is higher than on hillslopes. In the lower part of the main valley fluvial erosion in the form of gullies takes place.

In the catchment, areas with a tree cover of *Quercus ilex* alternate with areas lacking oaks. In the treeless zones, where rock outcropping is frequent, shrubs of the species *Lavandula pedunculata* are dominant and the herbaceous cover is very poor. On hillslopes, where trees are growing, pasture is dominant. The valley bottoms are densely covered by herbaceous plants and trees are absent (Fig. 1). The land is grazed by sheep and to a minor degree by cattle and pigs.

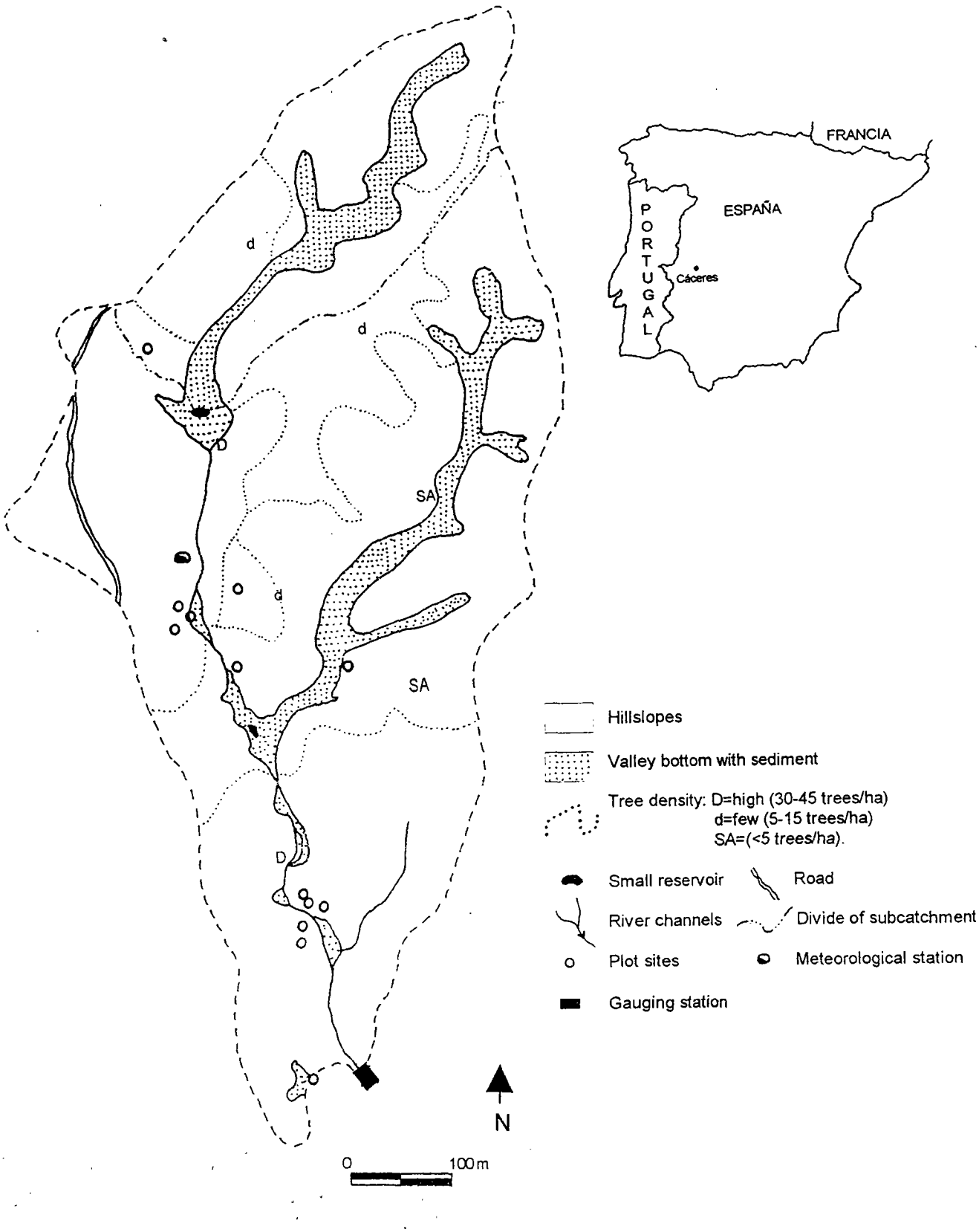

Fig. 1: Map of the Guadalperalón catchment showing the location of instruments, valleys filled with fluvio-colluvial sediments, and tree density.

3. Methods

Since the autumn of 1990 runoff and soil loss from hillslopes have been measured on an event basis at 27 open plot sites (0.5 m wide, Gerlach type troughs), distributed in the catchment according to five established soil-vegetation units (Gómez and Schnabel, 1992; Schnabel, in press). Rainfall is registered automatically with a tipping-bucket device of 0.2 mm resolution in intervals of 5 minutes. Since 1994, six additional simple pluviometers have been distributed in the area in order to study the spatial variability of rainfall. Runoff is determined at the outlet of the basin using the relationship between water depth and discharge. The gauging station consists of an H-flume (U.S. Department of Agriculture, 1979) with a capacitance depth sensor (UNIDATA). A datalogger registers mean water depth at intervals of 5 minutes.

During the last hydrological year (September until August) porosity, density and water content of the soils were measured. For soil moisture the gravimetric method (Martínez Fernandez and López Bermúdez, 1996) was applied. Samples were taken from the upper 5 cm using a metal cylinder with a volume of 98.1 cm^3.

4. Results and discussion

Discharge data are available since the hydrological year 1991. There is a lack of data for the year 1994 due to technical problems with the datalogger.

During the three years with a complete set of data, flow was observed at the catchment outlet only 10 times per year, on average. Rainstorms of 9 mm with moderate intensity, i.e. a maximum 10-minute intensity of about 25 mm h^{-1}, generate runoff, even under dry antecedent moisture conditions. Rainfall events of moderate or high intensity and amounts of up to 25 mm produce channel flow of short duration (three hours or less) with a lag time (peak rainfall to peak discharge) of only 5 to 10 minutes. Figure 2 shows the hydrograph of an event, which occurred during April 1993 when the soils in the catchment were dry. A rainfall of 20.4 mm with a maximum 5-minute intensity of 33.6 mm h^{-1} produced a total discharge of 280.7 m^3. Peak flow (295.0 l s^{-1}) was registered only five minutes after the precipitation peak. The relatively high runoff coefficient (5%) in comparison with the other events is related to the fact that maximum rainfall was observed at the end of the storm.

The reason for the quick response of discharge in the channel is Hortonian type overland flow production (Horton, 1940) at hillslopes caused by the low infiltration capacity of the soils. However, most of the catchment runoff coefficients are lower than 5%, and contrast with the higher values observed at the plot scale (Schnabel, in press). For the study basin it could be shown that with increasing scale (from micro-plots to the whole catchment) the hydrological processes become more complex, because the importance of each of the operating factors is difficult to determine (Ceballos *et al.*, 1996).

On an annual basis the runoff coefficients for the catchment are even lower (Table 1), with the exception of 1995. From September 1995 until February 1996 the output represented 18.3% of the total precipitation. These differences are probably related with variations of rainfall. The area suffered a drought lasting from 1991 until 1994 . The year 1994 was exceptionally dry with only 331.5 mm of precipitation, an amount lower than the 0.2 percentile. However, the runoff coefficient of 1994 is slightly higher than the previous ones (Table 1). These small variations are due to the characteristics of individual storm events. In the case of 1994 one event with 40.8 mm of precipitation (12.3% of the annual total) accounted for 55% of the annual discharge amount.

The prolonged drought ended in the middle of November 1995 with a delayed rainy season (usually starting in September) and the commencement of an exceptionally humid period, registering 533.2 mm of rainfall until February. This amount exceeds the long-term mean by 200 mm. By the end of December almost 150 mm of rain caused moisture saturation of the catchment. Precipitation falling afterwards produced a period of uninterrupted channel flow. During a period of 52 days (from the end of December until the middle of February) the runoff coefficient reached a value of 27.9%. The high

discharges are clearly related to moisture saturation of the area. Water content reached values of 24.3% at hillslopes and 34.3% at colluvial sites and the valley bottom. In the centre of the valley bottom values between 40% and 50% were determined, i.e. complete saturation.

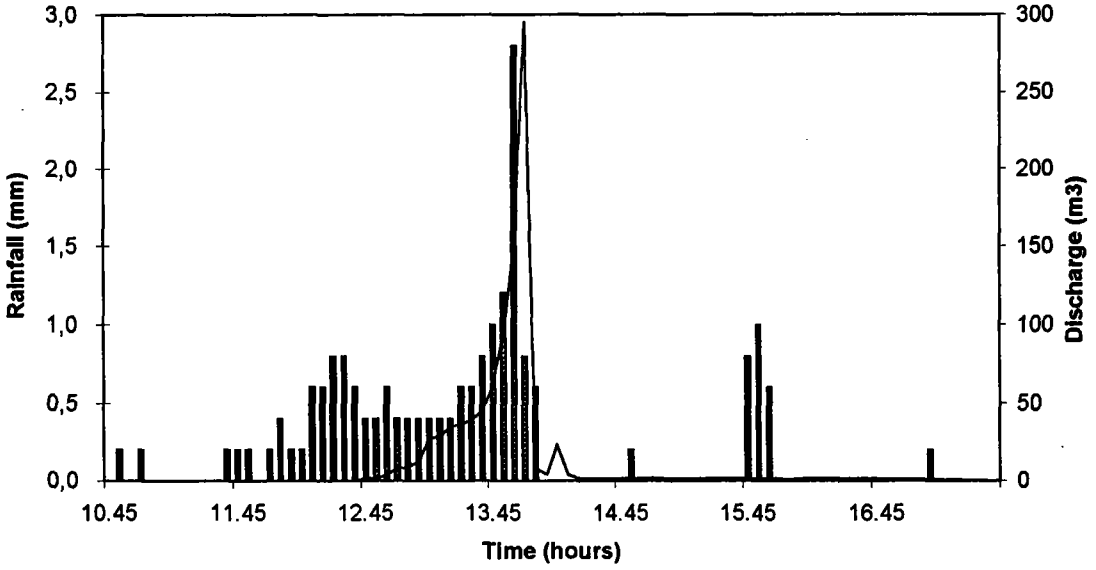

Fig. 2: Rainfall and discharge produced during 24.4.1993.

TABLE 1: Precipitation and runoff coefficients during the observation period (* - from September 1995 until February 1996).

Year	Precipitation (mm)	Runoff Coefficient (%)
1991	386.0	1.0
1992	372.8	1.3
1993	528.7	---
1994	331.5	2.9
1995*	533.2	18.3

During 1991 and 1992 the average runoff coefficient at hillslopes amounted to about 12%, whereas the coefficient for the whole basin was 1.1%. The mean runoff coefficient of plots located at colluvial footslopes is estimated to be about 2.0% (Schnabel, in press). This indicates that most of the surface water running down the hillslopes is reinfiltrated at colluvial sites and the valley bottom, where the soils are deeper and have a higher porosity. Furthermore, the slope gradients are lower. The topographic control over soil moisture was demonstrated by Zhang and Berndtsson (1988), who divided the study area into subareas such as valley bottoms and hillslopes.

Runoff is usually of the Hortonian type. Only when large amounts of rainfall cause saturation of the valley bottoms does discharge reaches high values, as in the case of winter 1995. Hortonian overland flow is generally found in arid and semiarid environments, whereas other types of surface flow, such as saturation overland flow or return flow (Kirkby, 1985), are associated with humid or subhumid climates (Dunne and Leopold, 1978). However, in the study area continuous rainfall produces water saturation of the soils and hence generates saturation overland flow. Then the sediment-filled valley bottoms and concave colluvial areas produce flow in the manner as described by the partial-area concept (Dunne and Black, 1970). The size of the saturated area depends on soil humidity, which is related to the intensity and duration of rainstorms (Lavee and Yair, 1990) and the topography (Zhang

and Berndtsson, 1988). In Guadalperalón return flow is observed at points where subsurface flow is produced.

The frequently found discontinuities of surface runoff occur at the contact between Leptosols (slopes) and Regosols (valley bottom), which can easily be detected by pedological and botanical evidences, similar to those reported by Yair and Lavee (1985) and Prosser and Melville (1988). Lavee and Yair (1990) showed that in small arid catchments flow discontinuities are due to the short duration of rainstorms and the soil surface properties.

The existing poor relationship between rainfall characteristics (e.g. amount and intensity) and discharge at an event basis (Fig. 3) is explained by the complexity of the hydrological processes. The importance of antecedent moisture conditions as one of the controlling factors of streamflow response demonstrates the necessity of studying the relationship between soil moisture and runoff. The first measurements of soil water content in the Guadalperalón study catchment were made in 1995 with the gravimetric method. Because of its high variability in time and in space, it was decided to start monitoring with a less destructive method. In the future soil moisture will be determined with a TDR.

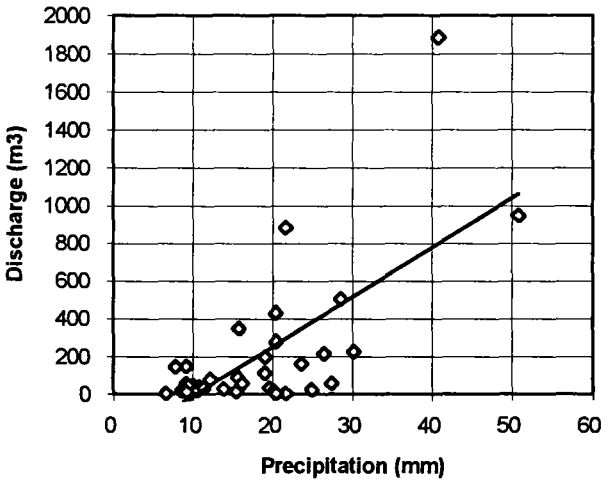

Fig. 3: Relationship between rainfall amount and discharge for 36 events with line of best fit (R^2 = 0.46, SE 269.6).

5. Conclusions

Investigations carried out in the Guadalperalón study catchment demonstrate the existence of a complex relationship between runoff from hillslopes and discharge production in the main channel. Although Hortonian overland flow, producing high peak discharges and low runoff coefficients, is the most frequent runoff type, saturation overland flow is also produced. It is shown that the concept of partial-area contribution to runoff can also be valid for small basins in semiarid environments, where discontinuities are produced by variations of soil characteristics and topography. The dominant type of surface flow during an event is largely controlled by variations of rainfall.

Acknowledgements

This investigation is carried out within the projects AMB 92/0580 and AMB95/0986, funded by the COMISIÓN INTERMINISTERIAL DE CIENCIA Y TECNOLOGÍA (CICYT). Funds were also provided by the Junta de Extremadura and the Fondo Social Europeo.

References

CEBALLOS, A., S. SCHNABEL and A. CERDÀ (1996) 'El efecto de la escala sobre los procesos de escorrentía superficial. In GRANDAL, A. and PAGÉS, J. (Eds): *IV Reunión de Geomorfología*, pp. 91-102.

DUNNE, T. and R.D. BLACK (1970) 'Partial-area contribution to storm runoff in a small New England watershed'. *Water Resources Research*, vol. 6: 478-490.

DUNNE, T. and L.B. LEOPOLD (1978) 'Water in Environmental Planing'. By W.H. Freeman and Company.

ELIAS CASTILLO, F. and L. RUIZ BELTRAN (1979) ' Precipitaciones máximas en Expaña'. *Ministerio de Agricultura*, Madrid.

HORTON R.E. (1940) 'An approach toward a physical interpretation of infiltration capacity'. - *Proceedings of the American Society for Soil Science*, vol. 5: 399-417.

KIRKBY, M.J. (1985) 'Hillslope hydrology'. In: Anderson, M.G. and Burt, T.P. (Eds*): Hydrological Forecasting*, pp 37-75. John Willey and Sons Ltd.

LAVEE, H. and A. YAIR (1990) 'Spatial variability of overland flow in a small arid basin'. Erosion; Transport and Deposition Processes (Proceedings of the Jerusalem Workshop). *IASH Publ.* n°189: 105-120.

MARTÍNEZ FERNÁNDEZ, J. and F. LÓPEZ BERMÚDEZ (1996) 'Métodos para el estudio de las propiedades hídricas de suelos y formaciones superficiales'. *Cuadernos Técnicos de la S.E.G.*. Geoforma Ediciones, Logroño.

PROSSER, I.P. and M.D. MELVILLE (1988) 'Vegetation communities and the empty pore space of soils as indicators of catchment hydrology'. *Catena*, vol. 15: 393-405.

SCHNABEL, S. (in press) 'Untersuchungen zur räumlichen und zeitlichen Variabilität hydrologischer und erosiver Prozesse in einem kleinen Einzugsgebiet mit silvo-pastoraler Landnutzung (Extremadura, Spanien)'. - *Berliner Geographische Abhandlungen 63*, Institut für Geographische Wissenschaften, Berlin.

SCHNABEL, S., and D. GÓMEZ AMELIA (1992) 'Procesos sedimentológicos e hidrológicos en una pequeña cuenca bajo explotación de dehesa en Extremadura'. In: F. LÓPEZ BERMUDEZ *et al.* (Eds.): *Estudios de Geomorfología en España*, pp. 55-63.

U.S. DEPARTMENT OF AGRICULTURE (1979) 'Field Manual of Research in Agricultural Hydrology'.*Agriculture Handbook*, No. 224.

YAIR, A. and H. LAVEE (1985) 'Runoff generation in arid and semi-arid zones'. In: Anderson, M.G. and Burt,T.P. (Eds): *Hydrological Forecasting*. pp 183-220. John Willey and Sons Ltd.

ZHANG, T. and R. BERNDTSSON (1988) ' Temporal patterns and spatial scale of soil water variability in a small humid catchment'. *Journal of Hydrology*, vol.104:.111-128.

Water pathways and streamflow generation in the Noor catchment

R. Dijksma, H.A.J. van Lanen and B. van de Weerd

Department of Water Resources, Wageningen Agricultural University, The Netherlands

1. Introduction

In 1991 a research project was started to investigate the hydrogeological system of the Noor catchment, including the relationship between recharge, groundwater heads, spring flow and stream flow of the Noor brook. The impacts of groundwater abstractions from the Margraten Plateau in the Noor catchment were explored (van Lanen *et al.*, 1995). In the context of this project the water pathways (overland flow, interflow, base flow) were estimated. A detailed survey was carried out to observe the geological framework. Furthermore precipitation, groundwater levels, spring flow and streamflow, and their chemical compositions have been measured. The objective of this paper is to discuss water pathways and associated streamflow generation in the Noor catchment.

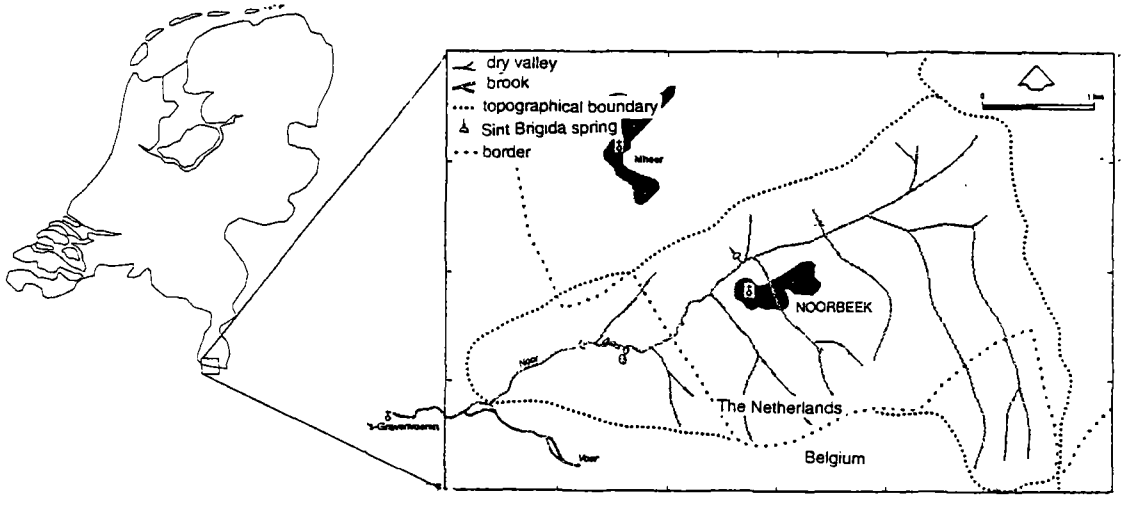

Fig. 1: The Noor catchment in the south-east of The Netherlands.

2. Description of the Noor catchment

The Noor catchment (10.6 km^2) is located in the south-east of The Netherlands and north-east of Belgium in the centre of the triangle formed by Maastricht, Aachen and Liège (Fig. 1). The elevation varies between 240 m a.s.l. in the south-east and 91 m a.m.s.l. at the outlet in 's-Gravenvoeren (B). The Noor brook starts as the Sint-Brigida spring in Noorbeek at 138 m a.s.l. and flows into the Voer, which is a tributary of the river Meuse. The Noor brook has a length of 3 km and drains a dissected chalk plateau, which has steep slopes to the valley (max. 20%). Folded Paleozoic shales and sandstones (BC) form the impermeable base. The consolidated rocks are discordantly overlain by subhorizontal Upper-Cretaceous

deposits (Fig.2), i.e. silty clay loam with thin sandstone layers (Vaals Formation, FvV) and chalk (Gulpen Formation, FvG), which form a multi-aquifer system. In the catchment, groundwater levels occur at shallow depths (<0.50-1.0 m below surface) in the narrow valley and at deep levels (30-40 m below surface) under the plateau. Permanent grassland, arable land and forest cover 62%, 35% and 1% of the area respectively.

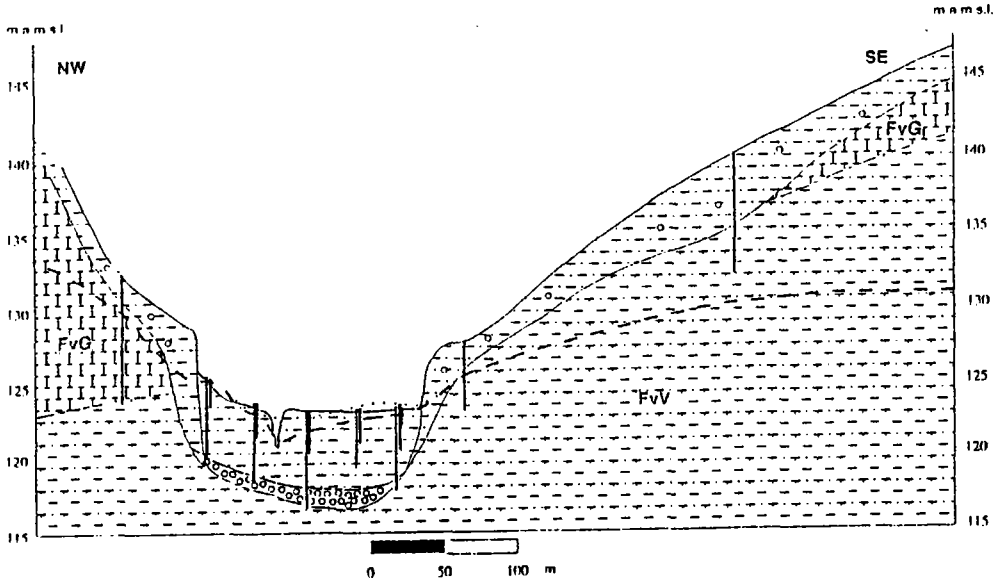

Fig.2: Geological cross section.

Streamflow may consist of overland flow, interflow and baseflow. Rainfall simulation studies in the Noor catchment and similar adjacent catchments showed that overland flow rarely occurs on agricultural land (van Lanen *et al.*, 1993). Some overland flow from the village of Noorbeek, unpaved roads in the valley and from the wet valley (minor area) will only feed the Noor brook. So, precipitation excess (precipitation minus evapotranspiration) in this catchment will either flow as interflow or baseflow to the Noor. In flat areas (90% of the catchment) precipitation excess will move vertically through the thick unsaturated zone to the watertable. Interflow (temporarily saturated flow in the unsaturated zone) is expected not to be a major process in this chalk catchment (Van Lanen *et al.*, 1993).

3. Methods

Precipitation excess at a particular location and time depends on meteorological data (precipitation and reference-crop evapotranspiration), crop characteristics (rooting depth and potential evapotranspiration), soil characteristics (hydraulic properties and rootable depth) and hydrological conditions (water table depth). The precipitation (P) and reference crop evapotranspiration (E_{ref}) data were obtained from the stations Bergenhuizen and Beek, respectively, for '10-day' periods. The Bergenhuizen precipitation station is located 2 km north-east of Noorbeek. The Beek Meteorological station is at Maastricht airport, approximately 13 km north of Noorbeek. Crop factors were used to compute potential evapotranspiration (E_{pot}) from the reference crop evapotranspiration. The available soil moisture for permanent grassland, arable land and forest was estimated to be 75, 250 and 175 mm, respectively, based on soil type and rooting depth. Deep groundwater tables, where no capillary rise occurs, cover about 90% of the catchment. In the Noor catchment eight different units of land-use and watertable depth were distinguished. Precipitation excess (Table 1) was computed for hydrological summers (April-September) and winters (October-March).

Groundwater levels were measured once a month, using tubes with a filter screen. Streamflows were measured with sharp-crested V-notches in the (north and south) springs and with a broad-crested weir at the outlet of the catchment.

TABLE 1: Areal precipitation, potential evapotranspiration and precipitation excess

Period	P (mm)	E_{pot} (mm)	P-E_{pot} (mm)	Prec. Excess
Apr 92-Sep 92	450	487	-37	10
Oct 92-Mar 93	387	114	273	262
Apr 93-Sep 93	462	459	3	3
Oct 93-Mar 94	510	96	414	414
Apr 94-Sep 94	377	476	-99	25

4. Results

The average chemical composition of surface water, derived from samples collected on both rainy and dry days in the Noor brook, is similar to the groundwater composition and significantly differs from rainwater composition (Table 2). This implies that the Noor brook is predominantly fed by groundwater (base flow) and not by a rain-type water (overland flow and interflow) (Jansen and Verhagen, 1991).

TABLE 2: Average chemical composition of precipitation, groundwater and surface water

	n	pH	Ec	SiO_2	K^+	Na^+	Ca^{2+}	Mg^{2+}	NH_4^+	Cl^-	NO_3^-	SO_4^{2-}	$H_2PO_4^-$	HCO_3^-
Precipitation	8	6.2	85	0.4	1.0	1.4	1.6	0.3	1.5	1.6	4.8	12.7	0.5	5.6
Groundwater	153	6.3	601	39.3	3.1	7.2	120	5.1	1.2	15.0	13.2	50.6	0.9	323
Surface water	231	7.6	650	42.6	2.1	6.5	133	4.0	0.1	17.1	44.3	47.8	0.2	306

Eventually precipitation excess will feed the saturated groundwater zone. The estimated travel time in the unsaturated zone is at least some years. Nevertheless, groundwater levels will respond on precipitation excess, i.e. groundwater recharge, after about 70 days in the areas with deep groundwater tables.

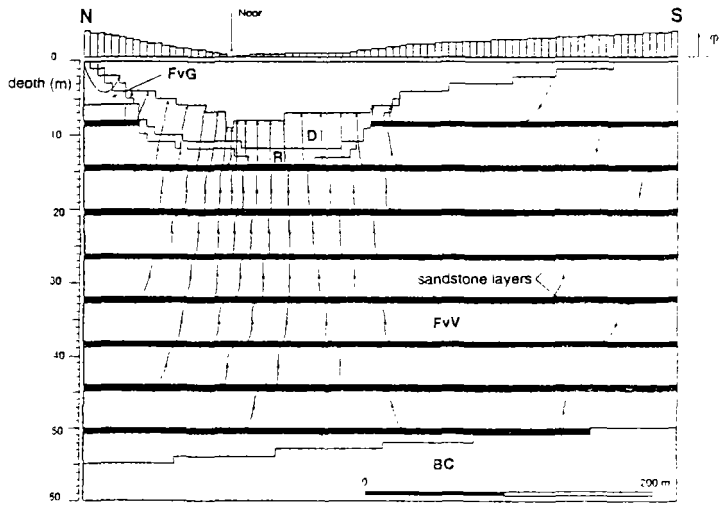

Fig. 3: Simulation of groundwater flow.

After a water particle reaches the water table, it will flow through the Gulpen Formation (FvG) and mostly through the Vaals Formation (FvV). The permeability of the chalk varies with depth; the

upper layer has a significantly higher permeability than the lower layers because of weathering processes. The bottom chalk layer has a permeability of about 1 m/day, whereas the overlying layer (intermediate chalk layer) has a somewhat higher permeability, e.g. between 3 and 5 m/day. The silty layers of the Vaals Formation do not allow substantial horizontal groundwater flow. The interbedded fractured sandstone layers (thickness 0.1 m - 0.2 m), however, act as horizontal groundwater drains. Some simulation results, obtained with a steady-state saturated groundwater flow model, are given in Figure 3 (Engelen and Jones, 1986). This simulation shows that groundwater in the Vaals Formation will preferentially flow through the sandstone layers. The simulated travel times for water particles to flow through the saturated zone from the water divide to the Noor brook is at least 9 years.

TABLE 3: The contributions of the Sint-Brigida spring, other springs, and seepage areas to the discharge of the Noor brook.

	27 February 1992		3 November 1993		1 April 1994	
	(m^3/d)	(%)	(m^3/d)	(%)	(m^3/d)	(%)
Sint-Brigida spring	26	1	285	10	2480	32
north springs	640	24	640	22	1085	14
south springs	870	32	812	28	1122	14
drainage of seepage areas	1151 [1)]	43	1174 [1)]	40	3133 [1)]	40
Noor at outlet	2687	100	2911	100	7820	100

[1)] Difference between discharge at the outlet and total spring flow

Groundwater is discharged in springs and seepage areas. The Noor brook starts as a chalk spring, i.e. the Sint-Brigida spring. Downstream, the Noor is fed by a number of tributaries which collect water from a large number of small springs and some seepage areas. Table 3 gives the contributions of the Sint-Brigida spring and the total discharge of springs and seepage areas to the streamflow of the Noor.

In the period 1992-1994, spring flow and streamflow substantially increased because of a high precipitation excess compared to the previous period 1990-1991. The precipitation excess in the 1993/94 winter resulted in a rise of deep groundwater levels of 5 m and more. Figure 4 shows the groundwater level at the plateau in observation well WP98 and the associated Sint-Brigida spring flow. The increased precipitation excess clearly affects deep groundwater levels and spring flow. Drainage of seepage areas also increased. As a result, the discharge at the outlet increased from 0.25 mm/d to 0.8 mm/d (Fig 5).

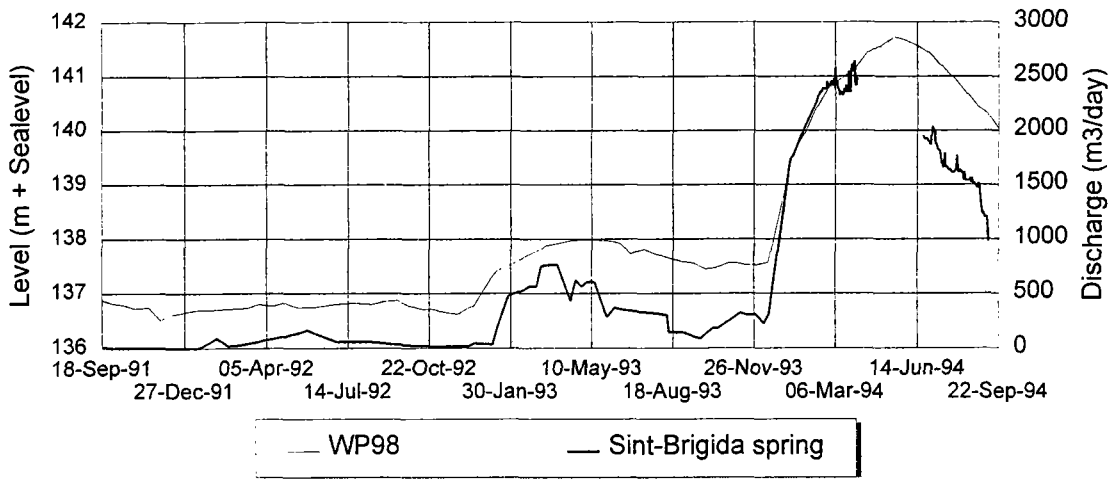

Fig. 4: Groundwater level at the plateau (WP98) and Sint-Brigida spring flow.

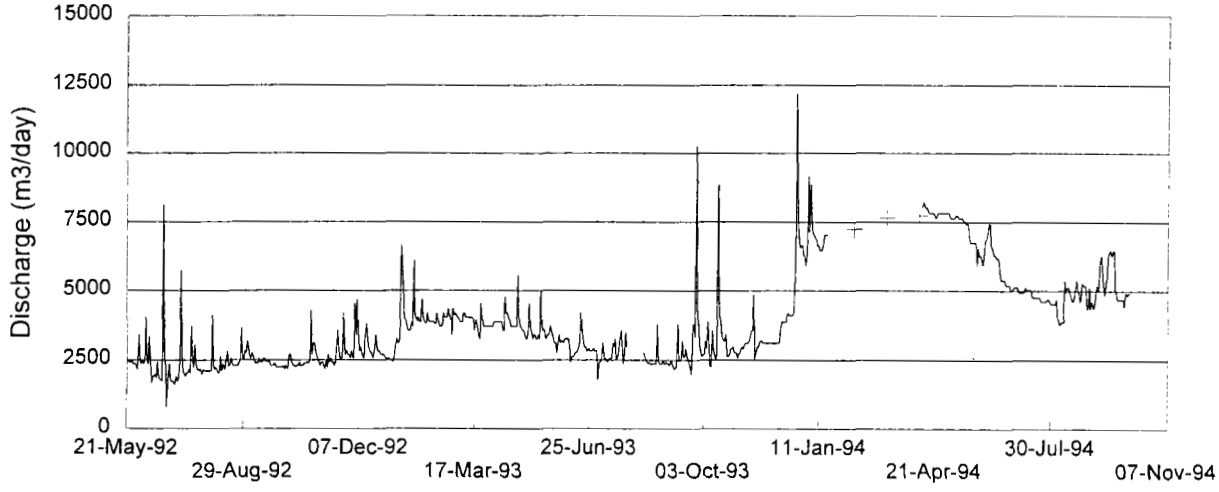

Fig. 5: Daily discharge of the Noor at the outlet.

During dry periods (e.g. 1990 - 1991), groundwater levels drop several meters, resulting in a diminishing Sint-Brigida spring flow. Obviously, the groundwater level is then below Sint-Brigida spring level (138 m a.m.s.l.). Water pathways are then diverted to the lower part of the Noor valley, leaving some discharge to the downstream springs and seepage areas.

Groundwater follows different flow paths in the multiple aquifer system (Fig. 3). If the upper part of the chalk becomes saturated, groundwater levels can quickly respond as a result of groundwater recharge (Van Lanen *et al.*, 1993). These effects are indicated by the difference in response on precipitation excess between north and south springs (Fig. 6). Under dry conditions north springs contribute half as much to the Noor discharge as south springs. After high precipitation rates the ratio increases; the north springs react while south springs still remain constant. Probably, the upper part of the chalk, with the higher permeability, becomes saturated north of the brook (Fig. 2) resulting in a quick groundwater response on a high precipitation excess. The springs at the south react, on average, a few days later to precipitation. Table 3 indicates an increase of the discharge of the Noor at the outlet.

The hydrograph of the Noor catchment (Fig. 5) shows peaks as a result of overland flow and a quick response of ground-water flow especially from the north springs. Incidentally the daily streamflow is 0.5 mm/d - 0.75 mm/d higher than in the previous or following days. In Figure 7 the streamflow of the Noor brook during one particular day is given, i.e. 14 October 1993. Two clear peaks can be recognized as a result of a daily rainfall of 30.4 mm.

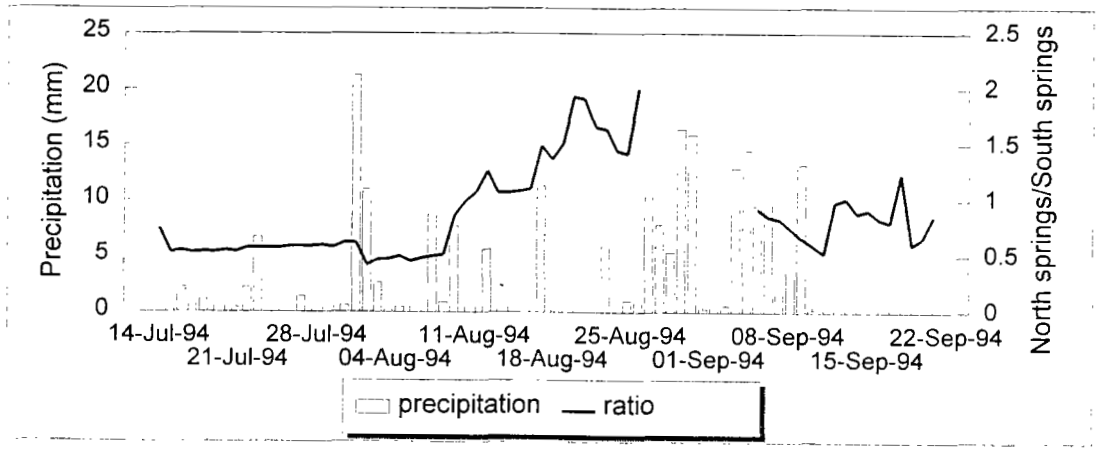

Fig. 6: Ratio between north and south springs.

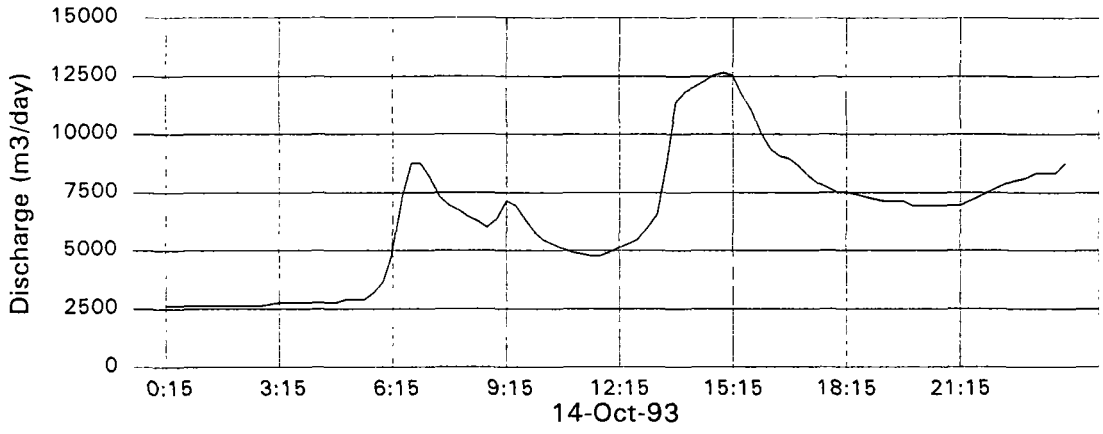

Fig. 7: Short-term discharge variations at the outlet.

Baseflow increased from 0.25 mm/d to 0.75 mm/d on 14 October 1993. Additionally, two peaks were measured. The volume of these two peaks is approximately 2000 m^3 , equal to 0.2 mm. This is only a minor part of the rainfall, i.e. 0.3%. Overland flow can account for this small quantity.

5. Conclusions and discussion

In the Noor catchment, which consists of a chalk aquifer with deep water tables, overland flow rarely occurs. Rainfall simulation and the chemical composition of surface water support this conclusion. Furthermore, hydrograph analyses show that the overland flow is very small. Interflow is likely not to prevail. However, the different response of the discharge of north and south springs shows that if the upper part of the chalk becomes saturated, a quick reaction to precipitation may occur. Nevertheless, this is only a minor part of total (annual) discharge. So, the streamflow of the Noor predominantly consists of deep groundwater. This baseflow is strongly related to the annual groundwater recharge. In the period 1992-1994 baseflow nearly doubled because of the groundwater recharge in the winter 1993/1994. During dry periods the streamflow comes from groundwater which generally has flowed through the chalk (Gulpen Formation) and the underlying silty clay loam with thin sandstone layers (Vaals Formation). During wet periods a minor quantity of overland flow and water which quickly flows through the chalk is added to this baseflow.

Bibliography

ENGELEN, G.B. and G.P. JONES (1986) 'Developments in the analyses of groundwater flow systems'. *International Association of Hydrological Sciences*, 356 pp.

JANSEN, I.M.H. and S.M.L. VERHAGEN (1991) 'Onderzoek naar de aanvulling van het grondwater door neerslag en de effecten hiervan op de stijghoogten van het grondwater en afvoer in het Hofdal'. *MSc. thesis Hydrogeology*, Wageningen Agricultural University, 65 pp.

LANEN, H.A.J., M. HEIJNEN, T. DE JONG and B. VAN DE WEERD (1993) 'Nitrate concentrations in the Gulp catchment: some spatial and temporal considerations'. *Acta Geologica Hispanica* 28 (2-3): 65-73.

LANEN, H.A.J. VAN, B. VAN DE WEERD, R. DIJKSMA, H.J. TEN DAM and G. BIER (1995) 'Hydrogeologie van het stroomgebied van de Noor en de effecten van grondwaterstandonttrekkingen aan de rand van het Plateau van Margraten (in Dutch)'*Report 57*, Wageningen, 152 pp.

Major hydrological processes in a farmed catchment of the Mediterranean area

M. Voltz[1], P. Andrieux[1], R. Bouzigues[1], R. Moussa[1], O. Ribolzi[2], C. Joseph[3] and W. Trambouze[1]

[1] *Soil Science Laboratory, Montpellier, France*
[2] *Soil Science Laboratory, Avignon, France*
[3] *Geofluids Laboratory, Montpellier, France*

1. Background situation and objectives

The Mediterranean environment is known for its fragility, the result of often unproductive soils, limited water resources that are subject to considerable year-to-year variability, and a rainfall pattern characterized by heavy downpours that sometimes cause devastating flooding. In the agricultural domain there is consequently only a small range of products that are viable in non-irrigated systems. The political decisions of the European Union with regard to agricultural orientation are at the same time necessitating major transformations in Mediterranean agrosystems. Thus, there are two changes occurring in the Languedoc region:

1) Intensification on suitable soils of traditional activities such as viticulture and non-irrigated arboriculture, with greater recourse to potentially extremely polluting agricultural practices. According to Munoz (1992) grapevines receive 51% of all pesticides employed in French agriculture.
2) A policy of grubbing up vines (127,722 ha in Languedoc-Roussillon between 1975 and 1994), after which the land is most often abandoned and sometimes converted to annual crops needing more water, with a major modification in all cases to the soil surface features and water requirements.

This has led the Soil Science Laboratory of the French National Institute for Agricultural research (INRA) in Montpellier, in association with the laboratories mentioned above, to develop a research project called the Allegro-Roujan Project to study water and pollutant flows in the Mediterranean wine-growing area (for more details see Voltz *et al.*, 1994).

The project has two main scientific objectives: identification and quantification of the spatio-temporal distribution of water and pollutant flows in the Mediterranean viticultural agrosystem; and development of a distributed hydrological model able to represent the complex operation of a primarily man-made agrosystem.

Only the results connected with the first objective will be developed in the present paper.

2. Site and basic experimental design

The experimental site is a 91 ha catchment located in the Hérault administrative department in south-France (43°30' N, 3°19' E). The main crop is grapes. The site is primarily man-made, with terraced slopes and a major network of ditches collecting the runoff water. In geological terms, the substrata derive from marine, lacustrine or fluvial sediments (Fig. 1 According to the F.A.O. soil classification system, the main soil types are luvisols, regosols and camb. ols.

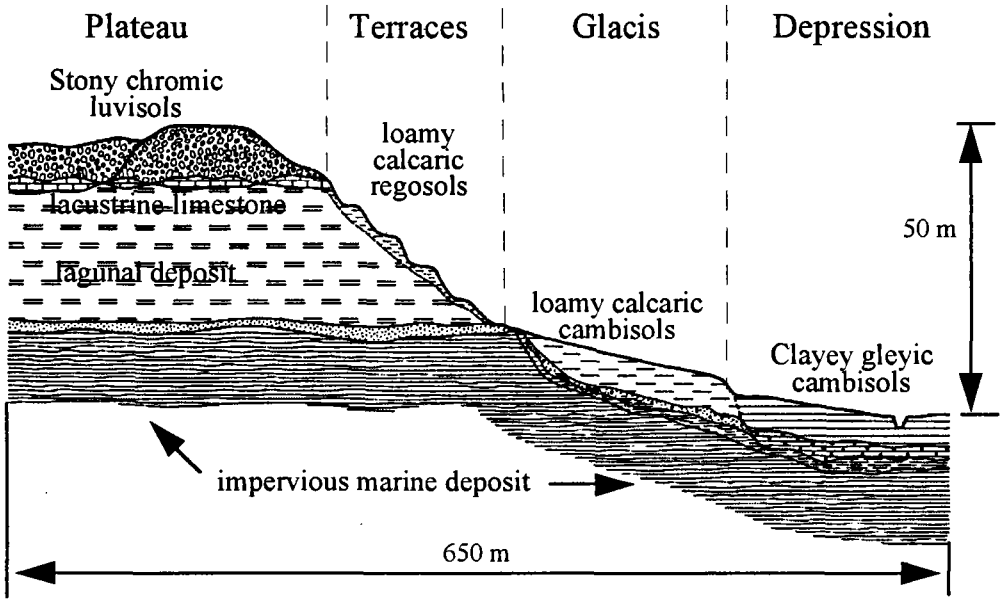

Figure 1: Transversal section of the Roujan catchment.

The climate is sub-humid Mediterranean, with a prolonged dry season. Average annual rainfall is 650 mm and average annual Penman potential evapotranspiration is 1090 mm. There is a large year-to-year variability in rainfall. Maxima of monthly precipitation are registered in February and October. Average summer (June - August) precipitation are 84 mm. Rainfall mainly occurs as storm events with an average rainfall intensity of 31 mm/h and maximum intensity of 110 mm/h, as measured over time steps of 5 min.

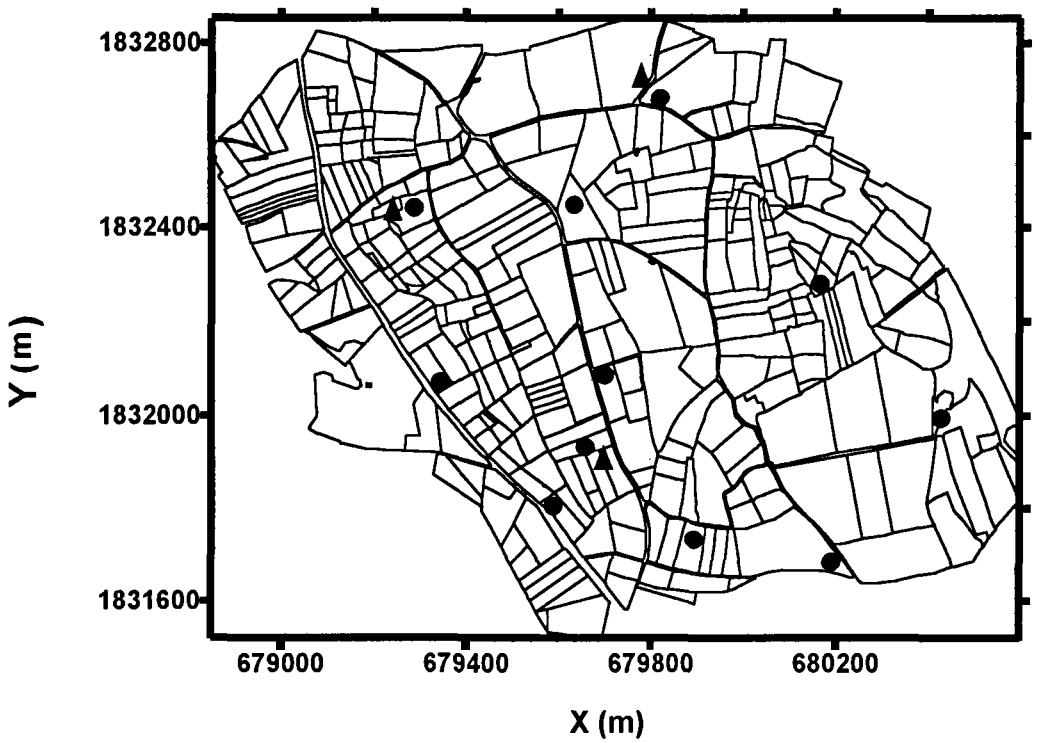

Figure 2: Basic monitoring design: ▲ location of flow gauges and water samplers; ● location of rain gauges. The X and Y axis correspond to Lambert zone III coordinates.

The basic hydro-meteorological equipment has been in place since May 1992 (Fig. 2). It consists of a rainfall measurement network (thirteen raingauges), a piezometric measurement network

(fourteen sites), a system for monitoring water flows, suspended substances and pesticides at the outlets of the catchment and from two fields with different agricultural practices, and a network of eight sites to monitor soil moisture and soil water potential.

3. Main results

Fig. 3 shows that the streamflow at the outlet of the catchment is clearly event-dominated. This is typical of the hydrological cycle in the Mediterranean zone.

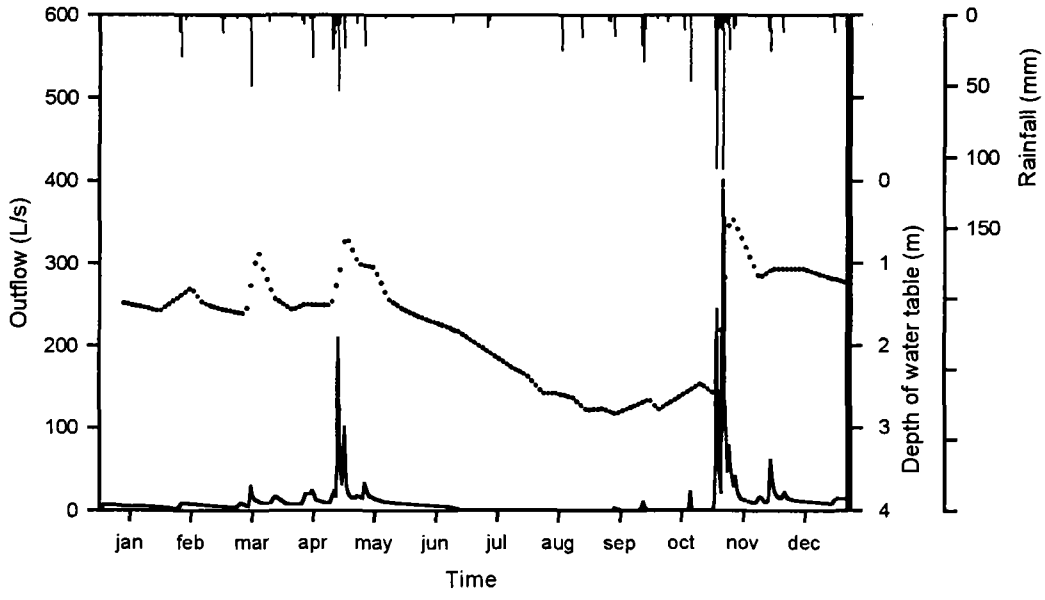

Figure 3: Daily outflow (—), *rainfall* (l) *and water table depth* ("") *in the Roujan catchment in 1993.*

Analyzing the general characteristics of runoff events from 1992 to 1995 showed that the event outflow varied from 0 to 38% of rainfall with a lag time of 30 to 60 min between the onset of rainfall and the peak flow. The duration of the events was between 6 and 12 hours. The catchment's very short times of response to rainfall pulses suggest that flows during rainfall are primarily dominated by Hortonian overland flow. This was confirmed by hydrochemical tracing (Ribolzi, 1996) which showed on some events that up to 80% of the peak flow was due to overland flow. The predominance of overland flow is very closely linked to the climatic and soil characteristics (heavy rainfall, capped soils) of the catchment, but also and above all to farming methods (sparse crops, and tillage practices producing relatively impermeable soil surfaces). This produces intense runoff processes at the field scale. Andrieux *et al.* (1996) measured runoff volumes amounting to 70% of rainfall at the outlet of an uncultivated field.

Despite the event-dominated nature of outflow, some seasonal characteristics are apparent. Three periods can be distinguished. The first corresponds to the period during which the water table in the depression of the basin is high, namely from October to May. In that instance, the network of ditches drains the water table, which produces a permanent, although minor, baseflow. In this first period, when high intensity rainfall occurs, outflow of the catchment reacts directly. The second period is summer during which rainfall is rare, the water table falls and baseflow ceases. In that situation, the intense summer storms of the Mediterranean climate rarely affect the catchment's outflow. This is either because soil moisture is low and thus no runoff is produced at the field scale, or because field runoff is captured by the ditches and reinfiltrates to the water table. The third period corresponds to the transition

between the dry and wet periods. It is very short, as can be seen in Fig. 3. The first main rainfalls in autumn replenish the water table of the depression in less than one or two days.

Closely linked with runoff processes is the transport of pesticides. In effect, the surface water of the catchment was shown to be severely polluted by pesticides used for controlling weeds and fungis in the vineyards (Lennartz *et al.*, 1996). At the scale of the whole catchment, it was observed that the rapid transit of runoff flows routed pollutants from the field edges to the outlet very quickly, except in summer situations of intensive water table replenishment (Voltz *et al.*, 1996).

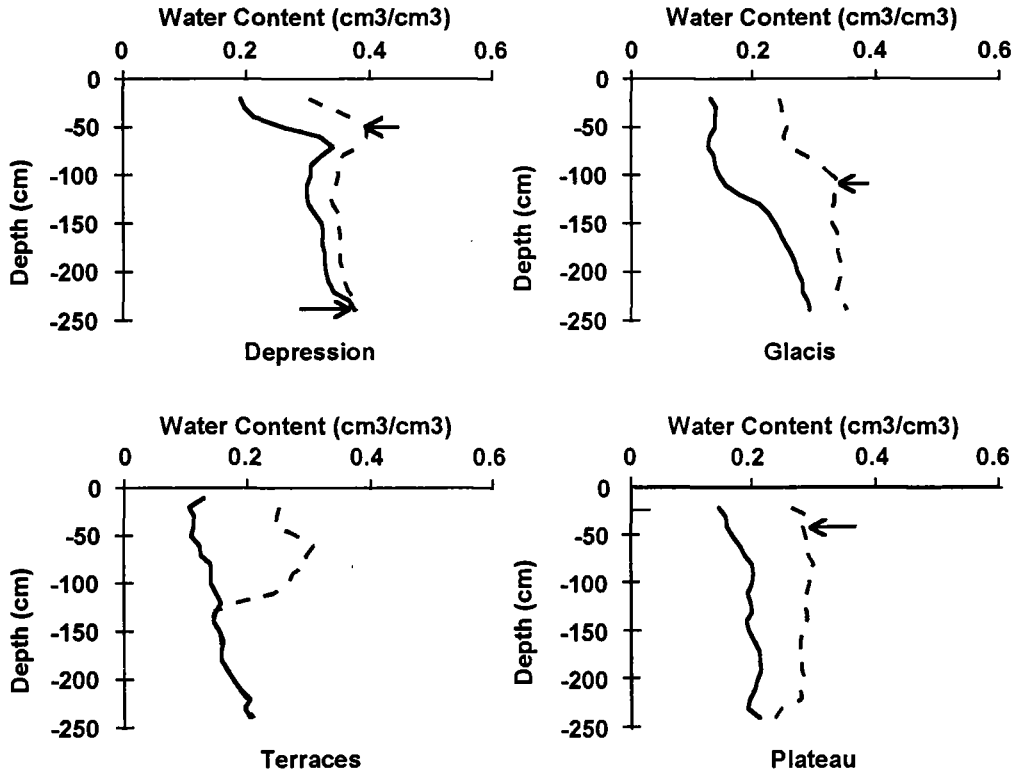

Figure 4: Minimum and maximum observed water content profiles in the four catchment sections in 1993. The arrows indicate the depth of the water table at the time of measurement of the profiles.

Fig. 4 illustrates the difference in soil water dynamics between the four compartments of the catchment. Clearly, the variation in soil moisture along the hillslope is very different from that observed previously in humid regions (Dunne, 1978). There is no regular increase in soil saturation from the plateau of the catchment to the depression. A water table develops on the plateau during the rainy periods which falls to a depth of 5 m during summer. Water from the plateau is mainly drained by the ditches and is thus routed directly to the depression. Consequently, in spite of their mid-slope position, the water dynamics of the terraces are almost only influenced by intercepted rainfall. In addition, as surface runoff is highest on the terraces because of their capped soils, infiltration is limited and the soil remains dry. Conversely, downhill, in the depression and the glacis (see Fig. 1), a general watertable exists due to the reinfiltration of runoff and drained water from the plateau and the terraces. The soils of the depression remain close to saturation around the year.

Finally, it should be noted that the most important flux in the hydrological cycle of the catchment is evapotranspiration. At the annual scale, during the three years of survey, outflow was 32% of total rainfall, which indicates that total evapotranspiration represents almost two thirds of the annual rainfall. As vine vegetation is of limited duration, the annual rates of evaporation and transpiration in the catchment are of the same order of magnitude (Trambouze, 1996).

4. Conclusion

The hydrological cycle in this farmed catchment under a Mediterranean climate is dominated by intense and short rainfall events and by evapotranspiration fluxes. In contrast to northern catchments, Hortonian overland flow is the major process, whereas subsurface flow and saturation-excess overland flow are insignificant. The considerable temporal variability of soil water conditions in the Mediterranean climate increases the effect of initial conditions on hydrological response, an effect already recognized in other situations.

The variability of water flow processes within the catchment is complex. It depends on topographical position, the geometry of sedimentary materials and the variability of soil surface features resulting from agricultural activities. One can observe a fragmented and discontinuous variability both of the areas contributing to the runoff and of the soil water regimes.

The network of human-made ditches appears to serve various purposes with regard to water flows. It accelerates runoff by concentrating flows and avoiding natural obstacles. If the water table is high, the network drains the water table, and thus provides a basic water flow that is intermittent in annual terms. If the water table is low, replenishment of the water table occurs by reinfiltration of the runoff water through the bottom of the ditches.

5. Acknowledgement

The research in the Roujan catchment was funded by INRA (AIP Valorisation et protection des ressources en eau and AIP Ecopol).

6. References

ANDRIEUX, P., X. LOUCHART, M. VOLTZ and T. BOURGEOIS (1996). Déterminisme du partage infiltration-ruissellement sur parcelles de vigne en climat méditerranéen. *Documents du B.R.G.M.* 256, Editions B.R.G.M., Orléans, pp. 7-11.

DUNNE, T. (1978). Field studies of hillslope flow processes. *In Hillslope Hydrology*, M.J. Kirkby (Ed.), Wiley & Sons, New York, pp. 227-293.

LENNARTZ, B., X. LOUCHART, M. VOLTZ and P. ANDRIEUX (1996). Diuron and Simazine losses to runoff water in mediterranean vineyards as related to agricultural practices. *Submitted to Journal of Environmental Quality.*

MUNOZ, J.F. (1992). Méthodologie d'étude des produits phytosanitaires. *Thèse de doctorat*, Université de Lyon, 175 p.

RIBOLZI, O. (1996). Etude des mécanismes de genèse des crues par le traçage naturel (chimique et isotopique) sur un bassin versant méditerranéen cultivé (Roujan, Hérault, France), *Thèse de doctorat*, Université de Marseille III, 191 p.

TRAMBOUZE, W. (1996). Bilan hydrique de la vigne à l'échelle de la parcelle: caractérisation et modélisation. *Thèse de doctorat*, ENSA de Montpellier, 190 p.

VOLTZ, M., P. ANDRIEUX, C. BOCQUILLON and S. RAMBAL, (1994). Le site atelier ALLEGRO, Languedoc. *Actes du Séminaire National Hydrosystèmes, Paris 10-11 mai 1994.* Ed. CEMAGREF, pp. 121-129.

VOLTZ, M., B. LENNARTZ, P. ANDRIEUX, X. LOUCHART, L. ROGER and M. LUTTRINGER (1996). Transfert de produits phytosanitaires dans un bassin versant cultivé méditerranéen: analyse expérimentale et implications pour la modélisation. In *Proceedings of GIP Hydrosystèmes-GFP congress, Nancy, 22-23 mai 1996*, CEMAGREF Editions, Antony, (in press).

A water balance study in a small representative mountainous forested basin

C. Etzenberg [1], G. Müller [2] and G. Peschke [1]

[1] *International Graduate School, Zittau, Germany*
[2] *University of Technology, Dresden, Germany*

1. Introduction

In recent years the importance of water balance studies has increased markedly. This is primarily due to the following.

- Given expected climatic changes and the ongoing changes in land-use, the temporal variability of water budget elements, including the occurrence of extreme events (floods and low-flows), plays an important role (Famiglietti and Wood, 1997; Kauifez-Bogataj and Hocevar, 1994; Wolock and Hornberger, 1991).
- The spatial variability of water budget elements, and particularly scale issues, are important factors in the coupling of hydrological and meteorological models (Braun *et al.*, 1996; Famiglietti and Wood , 1997).
- The connection of water and energy balances, especially in the complex soil-vegetation-atmosphere system, requires an extensive database (Arain *et al.*, 1996; Famiglietti and Wood, 1997; Hetsch and Heilig, 1981).
- The variability of runoff as a water balance element, and streamflow as the medium for solution and transport of substances in biogeochemical cycles, must be investigated to assist with integration of ecosystem mass budgets (Gerke, 1987; Wolock and Hornberger, 1991).

These tasks require intensive and detailed investigations, which are not realizable in all catchments. The best conditions for calculating complete water balances are given by small representative and research basins. Only such areas offer the possibility of establishing the necessary large experimental effort involving continuous long-term observation for the interdisciplinary work of hydrologists together with other natural scientists. Such catchment studies can be used, for example, to investigate the relationship between forest and water (Peschke, 1996; Peschke *et al.*, 1990, 1995; Swanson *et al.*, 1987).

Concerning the importance of detailed water balance studies for the solution of ecosystem problems, this paper presents and discusses the long-term water balance of a representative basin possessing excellent experimental equipment. Special attention will be given to the temporal variability of the runoff component of the water balance.

2. The experimental basin

Experimental investigations have been carried out in the small mountainous basin of the Wernersbach brook. It is situated in eastern Germany near Dresden in the Tharandter Wald (basin centre latitude 50°58′ N, longitude 13°28′ E). Its altitude is from 322 m to 424 m above sea level, and its area is 4.6 km^2. The climatic conditions are typical for the continental-maritime transition zone (Peschke *et al.*, 1990). Slightly-sloping hillsides are characteristic, with steeper slopes only locally important.

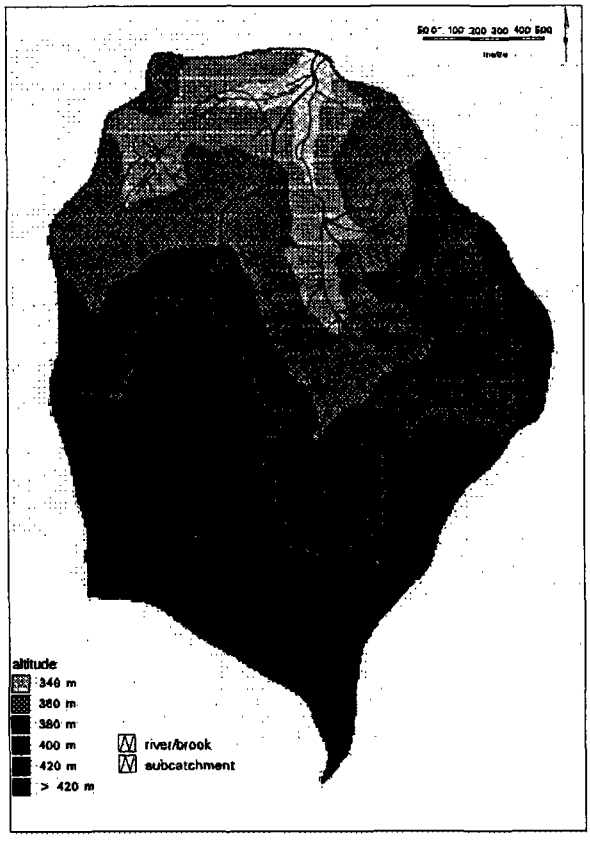

Fig. 1: The Wernersbach basin with river network, elevation zones and sub-basins.

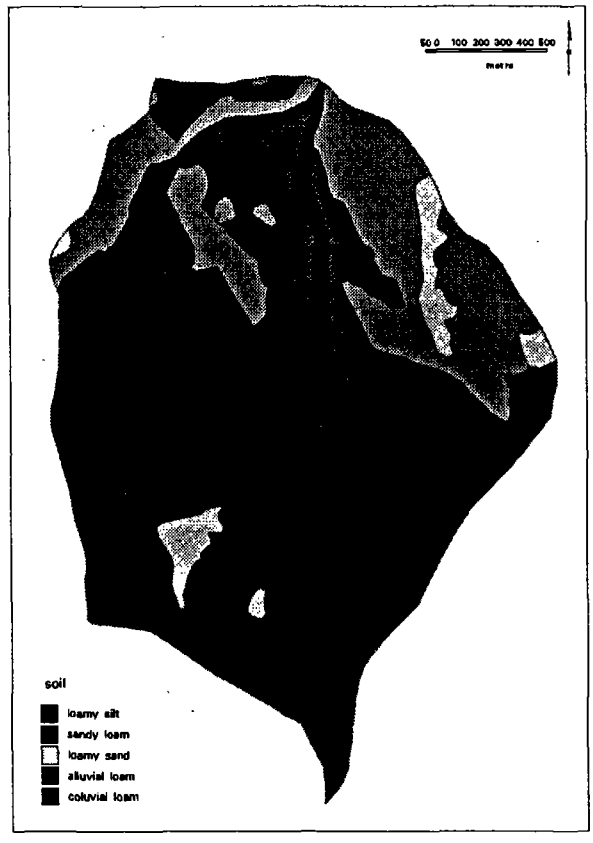

Fig. 2: Soil classes in the Wernersbach basin.

The geological structure is heterogeneous. The predominant rock is porphyry, but Cretaceous formations are also typical in this catchment. The soil cover mainly consists of cohesive weathering products of porphyry (loamy grit, loam) and loamy Pleistocene deposits (Fig. 2). Because of frequent shallow soil profiles, the skeletal portion of the soil exerts a control on hydraulic conductivity and therefore the conditions of runoff generation. Sandy soils with good infiltration properties and a small storage capacity occupy only a small part of the catchment.

The two main streams are Wernersbach and Triebenbach, but we can also subdivide the catchment into five subsystems (Fig. 1). Because of the low hydraulic conductivity of the soils in the basin there is a dense system of artificial ditches to drain the forested areas. The basin is completely used by forestry. Spruce (*Picea abies(L.) Karst*) of different ages dominate, partly mixed with deciduous trees.

The natural conditions of the basin offer excellent possibilities to study the water balance in its spatial and temporal variability, and an efficient measuring network and a long-term data base are available. Since the late 1960s we have measured at two stations all meteorological variables affecting the water cycle. In addition, precipitation is measured at six sites within the basin. Streamflow output for the whole basin and for four sub-basins are observed continuously. Further hydrological variables are measured in the sub-basins, e.g. soil moisture at 13 points, soil suction in two measuring fields, groundwater level at three points and spring outflow at 22 sites.

3. Results and discussion

The average 27-year water balance of the entire Wernersbach basin is presented in Table 1. The large amount of evapotranspiration is conspicuous. This is caused not only by the forest canopy, but also by the high water storage capacity of the loamy soil. Figure 3 presents the interannual distribution of (a) precipitation with maxima in summer and winter and (b) runoff with a maximum value in spring during snowmelt. The individual annual precipitation fluctuates between 1190 mm (1974) and 570 mm (1982), while the corresponding variation of runoff amounts to 453 mm (1981) and 85 mm (1991). However, the considerable dynamics of the precipitation and runoff water balance elements become evident in Table 2, which shows large differences between monthly values. The reason for these considerable fluctuations in the water balance is the variable weather in the research area due to the macro-scale synoptic situation. The atmospheric circulation above Saxony is dominated by the westerlies of the middle latitudes: In front of frequent eastwards moving cyclones warm air from the sub-tropic regions streams northwards, while cold air from sub-polar regions moves southwards behind the cyclones resulting in frequent and abrupt weather changes. Cloudiness and precipitation are non-seasonally distributed and show considerable variability.

TABLE 1: Average annual water balance of the Wernersbach basin (1969 - 1995).

		P	ET	R
year	mm	850	609	241
	%	100	72	28
summer	mm	457	367	90
(V - X)	%	100	80	20
winter	mm	393	242	151
(XI - IV)	%	100	62	38
summer/year	%	54	60	37
winter/year	%	46	40	63

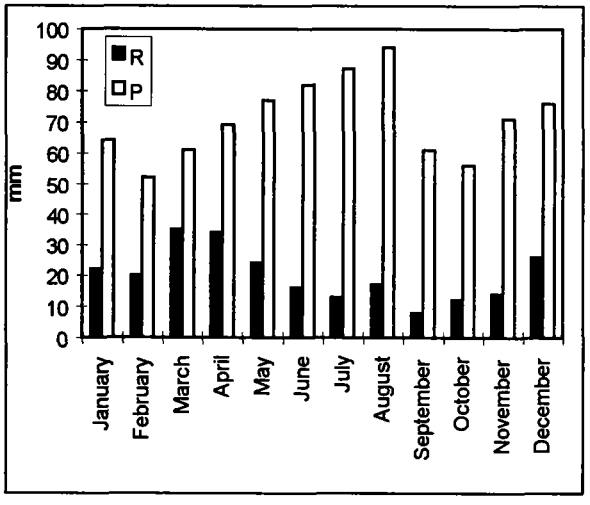

Fig. 3: Average monthly precipitation and runoff in the Wernersbach basin (1969 - 1995).

Tables 2 and 3 present (a) the maxima and minima of annual and monthly precipitation and (b) runoff extremes. It may be clearly seen that times of greatest runoff rarely occur in the year or month of the highest precipitation. This fact demonstrates that other factors, especially the catchment characteristics, ultimately determine the actual distribution of precipitation in the various components of the water balance. According to the results of our investigation of flood hydrographs and low-flow hydrographs we find that the catchment response really depends on the event-specific interaction of precipitation and basin features. These are not only the individual features of the area such as morphology, soil characteristics and so on, but the catchment moisture state is also very important.

Figures 5 and 6 show characteristic flood hydrographs observed under different meteorological and soil moisture conditions in the catchment. These figures make it clear, that the interaction of precipitation features (intensity and duration) and the current soil moisture of the basin has a strong effect on the kind, form and intensity of the catchment response. During very wet periods the catchment features are less important than the actual precipitation features. The resulting floods reflect the course of the precipitation event and have a large runoff volume (Fig. 5a and 6). If very intensive precipitation falls on a very dry basin (typical for rain events in summer), a rapid increase in the amount of discharge is observed; but the volume of the resulting flood remains minimal because of the rapid decrease, as seen in Figure 5b.

TABLE 2: Variability of annual and monthly precipitation in the Wernersbach basin (1969 - 1995)

annual precipitation

year	P [mm]	year	P [mm]
1974	1190	1983	800
1981	1186	1993	797
1995	1131	1971	747
1980	1101	1984	741
1970	1066	1985	736
1977	1026	1989	685
1987	942	1975	684
1978	941	1969	682
1986	930	1976	676
1979	920	1972	661
1994	886	1990	645
1973	862	1991	636
1988	854	1982	570
1992	853		

monthly precipitation extremes

month	year: P_{min} [mm]	year: P_{max} [mm]
January	1990: 15.7	1976: 172.7
February	1972: 9.4	1988: 117.4
March	1974: 17.9	1994: 152.2
April	1988: 16.9	1980: 173.1
May	1990: 12.7	1978: 187.9
June	1994: 40.4	1977: 167.8
July	1971: 15.5	1980: 240.3
August	1976: 39.5	1983: 192.0
September	1982: 10.9	1978: 136.5
October	1979: 11.2	1974: 190.6
November	1986: 14.0	1995: 125.1
December	1972: 15.4	1974: 203.5

TABLE 3: Variability of annual and monthly runoff in the Wernersbach basin (1969 - 1995)

annual runoff

year	R [mm]	year	R [mm]
1981	453	1971	208
1987	453	1992	186
1980	443	1985	172
1995	390	1975	170
1974	374	1982	164
1970	351	1983	153
1979	317	1993	142
1977	310	1984	133
1978	285	1972	127
1988	273	1989	124
1986	270	1976	117
1994	253	1990	99
1973	226	1991	85
1969	209		

monthly runoff extremes

month	year R_{min} [mm]	year R_{max} [mm]
January	1970: 1.9	1976: 68.3
February	1991: 3.4	1980: 63.7
March	1991: 6.0	1988: 104.5
April	1991: 4.3	1970: 113.6
May	1976: 3.9	1978: 73.4
June	1983: 2.3	1995: 73.5
July	1976: 1.3	1980: 96.3
August	1976: 1.0	1977: 67.0
September	1976: 1.2	1995: 47.7
October	1976: 1.7	1974: 55.9
November	1982: 2.3	1995: 56.6
December	1982: 3.6	1974: 114.6

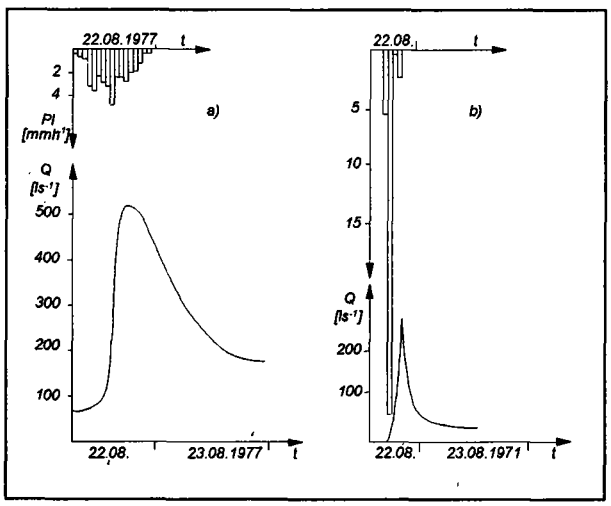

Fig. 5: Connection between precipitation and runoff and the dominating influence of
a) the soil water content in the basin before rain
b) rain intensity.

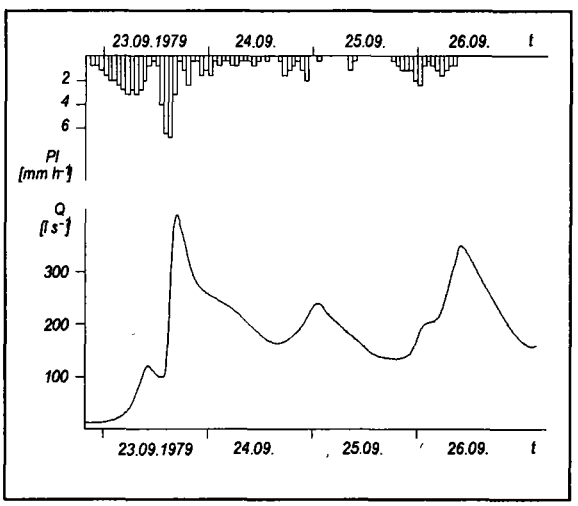

Fig. 6: The main reason for this flood event in September 1979 in the Wernersbach basin was the increasing soil moisture during the extended rain event.

The type and frequency of the flood events (and dry periods as well) can alter the average annual course of the basin's runoff and its proportion of the total water balance. The temporal course of the basin runoff is determined by the runoff contributions from the different parts of the catchment and the kind and intensity of the resulting runoff components.

In the Wernersbach basin are found nearly all runoff components typical of the low mountain area (Fig. 7). On average, slow runoff components predominate, and surface runoff makes up a relatively small part of the average runoff in the Wernersbach basin (Peters *et al.*, 1995; Robinson *et al.*, 1995). During flood events caused by high intensity rain, surface runoff as Horton overland flow is very important for rapid catchment response. However, runoff can also occur from saturated areas around the rivers, caused by long periods of rainfall of a medium intensity. The interflow and base flow in the Wernersbach basin can be considered as components which are generated at different soil depths and somewhat later become part of the runoff. The runoff volume from these sources varies according to the size of the contributing area.

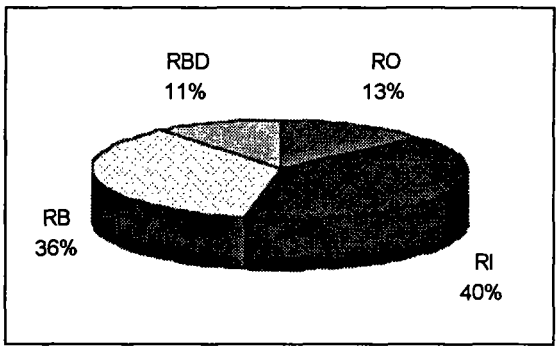

Fig. 7: Percentage of different runoff components in the Wernersbach basin (average of 1968-1990): RO (overland flow), RI (interflow), RB (base flow), RBD (delayed base flow).

Whether or not the land is forested has an influence on both the runoff generating catchment features and the effective precipitation input. Very generalized statements about the effects of forest on runoff emphasize its leveling effect on the catchment water balance (Otto, 1994). But if we look at the flood hydrographs in the Wernersbach basin, the short time between the peak of the precipitation event and discharge is conspicuous (Fig. 5). Large variations occur in the water balance (Table 1) as well as in the characteristic average discharge values of the basin (Table 4). Between the lowest in our catchment measured discharge value NNQ and the highest one HHQ there is a factor of 16.350. So we can see that the influence of forest is secondary to the influence of other runoff-generating features and cannot be proven explicitly in this basin.

TABLE 4: Characteristic mean and extreme discharge values [l s^{-1}] of the Wernersbach basin.

05.08.1990	annual series 1968 - 1995			23.07.1980
lowest low water discharge NNQ	**mean low water discharge MNQ**	**mean discharge MQ**	**mean high water discharge MHQ**	**highest high water discharge HHQ**
0.3	10	35	286	6 540

The aim of our research in the Wernersbach catchment was not to generate a comparison with an unforested one, but rather to investigate the interaction between forest and water under actual conditions on the area. The results in different parts of the Wernersbach basin show that forest increases all the infiltration-influencing features and impedes the generation of surface runoff. But, whether or not a general reduction of runoff and a corresponding increase in evapotranspiration and groundwater take effect in the entire basin, depends on both the specific characteristics of the soil profile and the groundwater level.

4. Conclusions

Water balance studies in representative basins provide important information about catchment responses, which are also applicable at larger scales.

For catchment response and the formation of the water balance elements, the particular combination of influencing factors plays an important role. The temporal and spatial variability of precipitation and catchment features should not be studied separately, because both are decisive for the distribution of the water balance elements. Therefore investigations into runoff generation and concentration conditions, runoff components and extremes are necessary. Only such detailed studies make it possible to (a) identify the factors which influence water balance elements and (b) quantify the changes in the relationship between water balance elements as a result of changing land-use and changing climatic conditions. We are also able to interpret and quantify the mass cycles if we know (a) the source areas of runoff and other water balance components in a particular time or under specific conditions in the basin and (b) how the interactions between the elements of the soil-vegetation-atmosphere-system influence mass transport and transformation.

References

ARAIN, A. M., J. MICHAND, W. J. SHUTTLEWORTH, and A. J. DOLMAN, (1996) 'Testing of vegetation parameter aggregation rules applicable to the Biosphere-Atmosphere Transfer Scheme (BATS) and the FIFE site'. *J. Hydrol.* 177, 1-22.

BRAUN, P., T. MOLNAR, and H.-B. KLEEBERG, (1996) 'Das Skalenproblem bei der rasterorientierten Modellierung hydrologischer Prozesse'. *DGM*, 40, 83-90.

FAMIGLIETTI, J. S., and E. F. WOOD, (1997) 'Evapotranspiration and runoff from large land areas: Land surface hydrology for atmospheric general circulation models'. *Surv. Geophys.*, 12, 179-204.

GERKE, H., (1987) 'Untersuchungen zum Wasserhaushalt eines Kalkbuchenwald-Ökosystems und zur Wasserbewegung in flachgründigen Böden'. *Ber. Forschungsz. Waldökosysteme/Waldsterben, Reihe A*, Bd. 27.

HETSCH, W. and K.-H. HEILIG, (1981) 'Der Wasserhaushalt von Fichten in Abhängigkeit von Boden und Atmosphäre'. *Z. Pflanzenernähr. Bodenk.* (144), 317-330.

KAIFEZ-BOGATAJ, L., and A. HOCEVAR, (1994) 'Assessment of climate change effects on productivity of a beech stand in Slovenia using simulation methods'. *Agricultural and Forest Met.* (72) 1-2, 47-56.

OTTO, H.-J., (1994) 'Waldökologie'. Stuttgart, Verlag E. Ulmer.

PESCHKE, G., (1996) 'Water balance study of a single tree and a spruce stand'. Proc. of IUFRO-Conf.: *Conference on Effects of Environmental Factors on Tree and Stand Growth. Berggießhübel 1996.*

PESCHKE, G., K. MIEGEL, CH. ETZENBERG, and H. HEBENTANZ, (1990) 'On the spatial variability of hydrologic processes in a small mountainous basin'. In: *Hydrology in Mountainous Regions. Proc. of Lausanne Symposia 1990.*

PESCHKE, G., M. ROTHE, J. SCHOLZ, C. SEIDLER, M. VOGEL, and W. ZENTSCH, (1995) 'Experimentelle Untersuchungen zum Wasserhaushalt von Fichten [Picea abies (L.) Karst]'. *Forstw. Cbl.* 114, 326-339.

PETERS, D. L., J. M. BUTTLE, C. H. TAYLOR, and B. D. LAZERTE, (1995) Runoff production in a forested, shallow soil, Canadien Shield basin'. *Water Resour. Res.*, Vol. 31 (5), 1291-1304.

ROBINSON, J. S., M. SIVAPALAN, and J. D. SNELL, (1995) 'On the relative roles of hillslope processes, channel routing, and network geomorphology in the hydrologic response of natural catchments'. *Water Resour. Res.*, 31 (12), 3089-3101.

SWANSON, R. M., P. Y. BERNIER, and P. D. WOODARD (Eds.), (1987) 'Forest hydrology and water management'. *Proc. of Intern. Symp., Vancouver, Canada, IAHS Publ.* No. 167.

WOLOCK, D. M., and G. M. HORNBERGER, (1991) 'Hydrological effects of changes in atmospheric carbon dioxide levels'. *J. Forecast.*, 10, 105-116.

The forest effect on floods in small mountainous catchments: some results from the experimental catchments of Draix, France

N. Mathys, M. Meunier and S. Brochot

Division of Erosion Protection, CEMAGREF, Grenoble, France

1. Introduction

The forest effect on runoff is usually assessed as important, especially on peakflows. This opinion has lead many countries to plan afforestation works to prevent flooding. In France, at the end of the 19th century, a large programme of afforestation of steep mountain slopes was undertaken with this purpose in mind. Most often, one observes that forests reduce flood runoff but some observations after forest fellings show no modification of peak discharge and even sometimes a reduction (Humbert and Najjar, 1992). The forest effect is not always apparent, and for periods of very high rainfall, forest cover may not be able to reduce runoff. The basin saturation threshold seems to be the most important factor in flood runoff formation (Cosandey, 1991). The experimental basins of Draix (south Alps, France) allow a comparison because the two catchments of nearly 1 km² have homogeneous but different vegetation covers. Vegetation cover may be the most important factor which controls their hydrological behaviour. This report will summarize work which has focused on the comparison of forested and bare catchments.

2. Experimental basins of Draix : Laval and Brusquet catchments

Located 15 km north-east of Digne (South Alps, France), these basins have been equipped since 1982 for the measurement of rainfall, streamflow and both bedload and suspended solids transport. Both are situated on black marls and have badlands morphology. One of these basins, Brusquet, was afforested at the end of the last century by the "restauration des terrains en montagne (RTM)" service in a programme of erosion prevention. It is now covered with a pine forest and can be compared to the Laval catchment, which has nearly the same surface area, but which has almost no vegetation cover, neither herbaceous nor forest.

TABLE 1: Characteristics of the two basins

Name	Area (km²)	No vegetation area (%)
Laval	0.86	78
Brusquet	1.08	13

3. Comparison between floods in forested and unforested catchments

The comparison is only based on flood events, not on continuous data. Rainfall is recorded with tipping bucket raingauges at two points in each basin, near the outlet and near the crest, and discharge is measured at the outlet of the catchment, so that the catchment-scale effect of forest cover may be apparent. First, parameters or characteristics of each flood such as the runoff, the runoff coefficient, concentration time and lag time are compared for each pair of floods in the two different catchments or for the two series. Secondly, erosion processes and sediment yield of the two basins are compared. Finally, because two simple rainfall-runoff models, defined in the hydrosedimentological model ETC

(Brochot and Meunier, 1996), were calibrated on Laval and Brusquet flood events, the differences in the calibrated parameters can be related to forest cover.

3.1 Runoff threshold

On these small Mediterranean mountainous catchments, there is little or no baseflow. Thus, discharge before a flood is not indicative of the initial conditions of the basins. Mean annual rainfall is 850 mm with two main rainy periods in April-May and September-October. July and August rainfalls are mainly due to 1 to 3 storms of 30 mm to 60 mm. Some falls of rain, especially after a dry period, do not produce any variation of the discharge. When observations of rainfall depths which do or do not cause runoff are plotted against dry period duration, "rainfall threshold curves" can be defined as shown in Figure 1. It is interesting to note that in the Laval basin, most falls of rain greater than 9 mm can cause runoff, whereas at Brusquet after a long dry period even 25 mm of rain may not. The maximum threshold is about 9 mm for Laval and about 30 mm for Brusquet. The maximum value is reached after five days in the first case and after more than thirty days in the second case. This means that rain which falls in the period before the event has no influence on Laval runoff after a short time. These curves will be used in hydrological modelling to predict initial conditions. Points which do not fall on the right side of Laval curve are due to short periods of rain of high intensity. The Brusquet catchment has no reaction to this kind of rainfall.

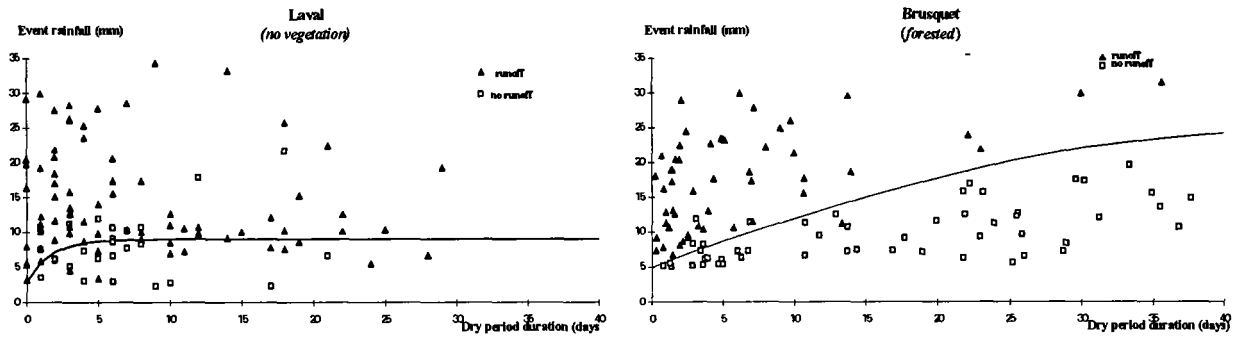

Figure 1: Threshold rainfall curves for Laval and Brusquet

3.2 Peakflows and hydrographs shapes

When hydrographs produced by similar rainfall on the two basins are compared, it is apparent that most peaks are delayed and reduced in the basin with denser vegetation as shown below in Figure 2. Laval hydrographs closely follow rainfall intensity variations and often have several peaks, whereas Brusquet is much less sensitive to these variations and its hydrographs have much more regular shapes. Time of concentration determined from many rainfall-runoff graphs is from 15 to 30 minutes for Laval and about 1 to 2 hours for Brusquet, though the shapes and slopes of the catchments are similar. For Laval and Brusquet respectively: the range of altitude is 350 m and 400 m; the shape index ($0.28*\text{perimeter}/\text{area}^{0.5}$) is 1.25 and 1.2; the slope of the main drain is 18% and 21%; and the mean slope of the main channel 4.5% and 6%.

When rainfall depth on the two sites is similar, peak discharges can be compared: all of the 21 cases of this kind have a Laval to Brusquet ratio higher than 2:1. In 16 cases it is higher than 5:1 and in 8 cases it is higher than 10:1. When all the floods of the test period are taken into account, it is difficult to make a direct comparison as the volume of rainfall during the storms which cause a large number of these floods may be very different. Nevertheless, for 78% of simultaneous flood events, Brusquet peak discharges are lower than 1/5 of Laval peak discharges. If the exponential statistic law is adjusted to the highest peak discharges of the observation period (Figure 3), the ten-year return period flood is about ten times less at Brusquet than at the Laval catchment. Up until the end of 1993, the most important peaks registered were 510 l/s at Brusquet and more than 6000 l/s at Laval.

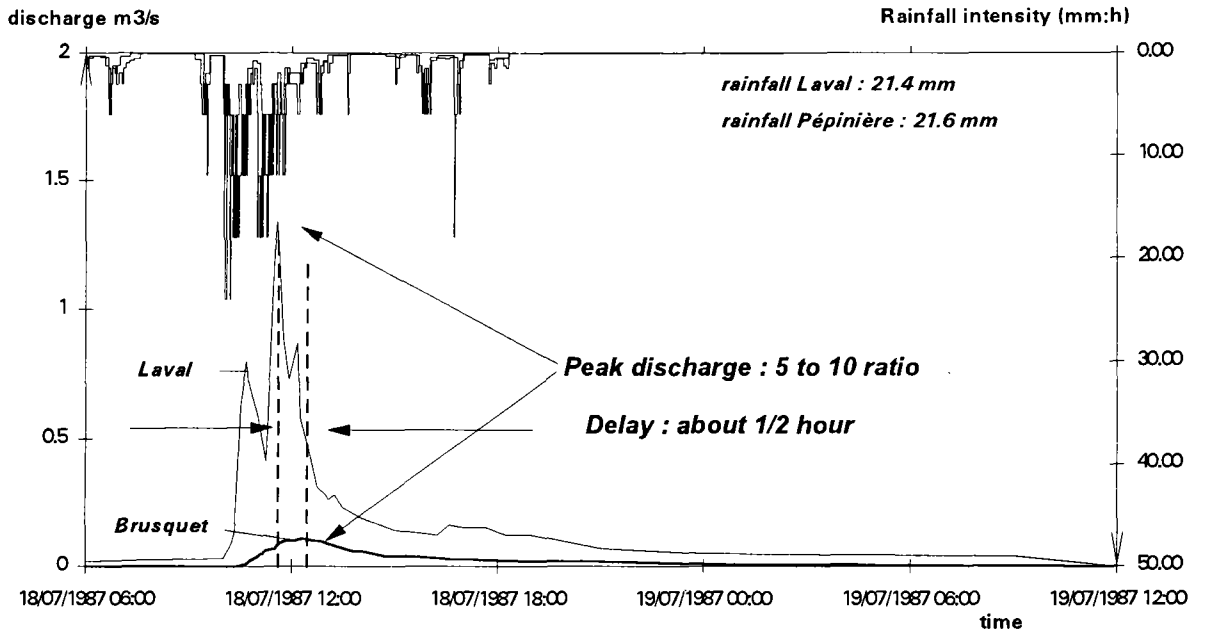

Figure 2: Hydrographs of Laval and Brusquet for similar rainfalls.

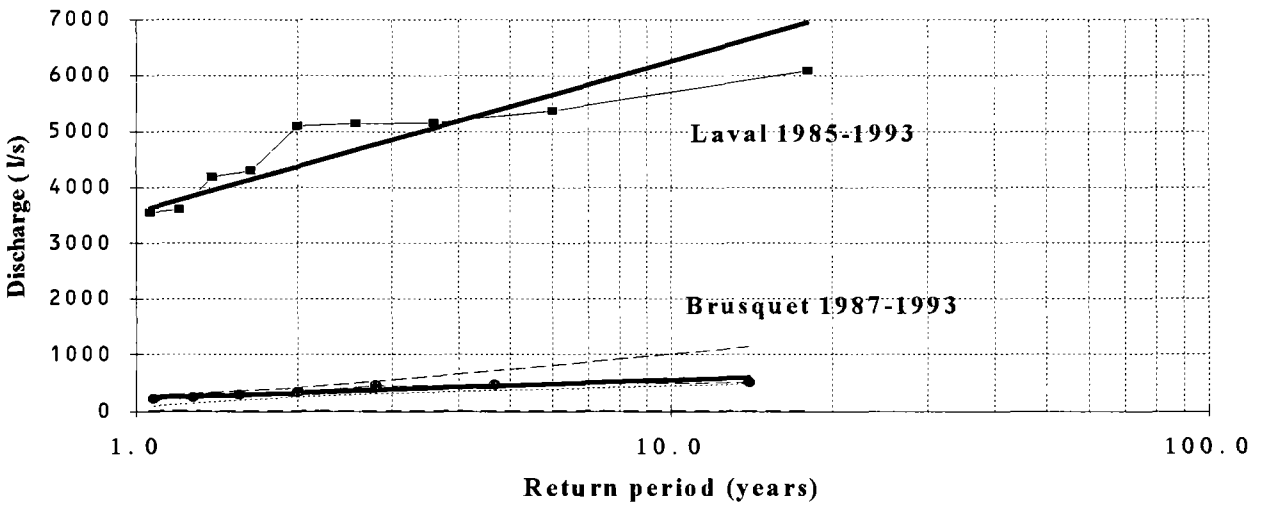

Figure 3 : Statistical results for Laval and Brusquet peak discharges.

3.3 Runoff coefficient

Though runoff coefficient values are not precise (because low discharges are not correctly measured at the gauging stations and because volume calculation limits are difficult to fix) comparison shows that for all the floods the runoff coefficient can reach about 0.9 for Laval and is always under 0.4 for Brusquet. For cases with similar rainfall volumes on the two catchments, the runoff coefficient on the forested area ranges from 10% to 40% of the coefficient of the bare area in the same case (Figure 4).

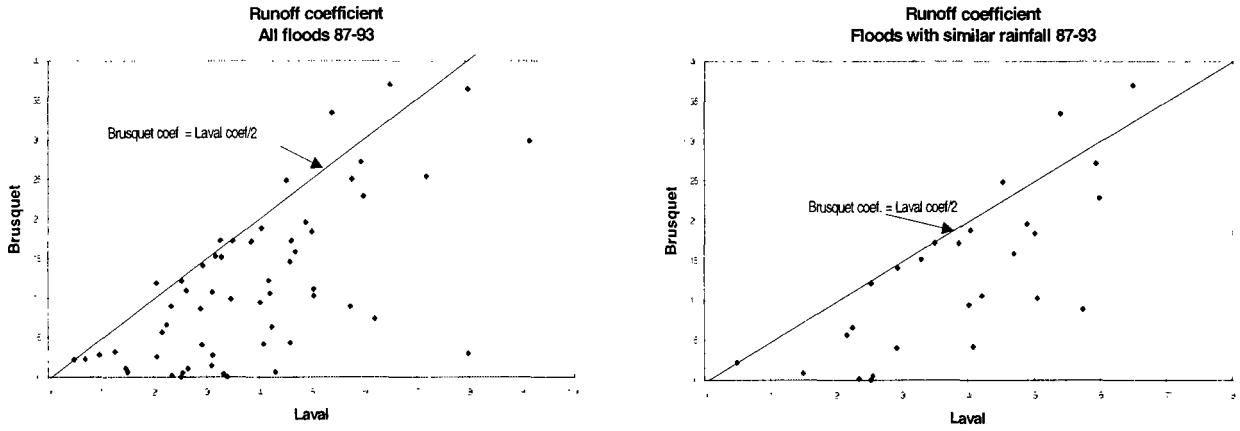

Figure 4: Comparison of runoff coefficients.

3.4 Erosion processes and sediment yield

Sediment production of each flood is the sum of the deposited volume in the sediment trap and the volume transported downstream, through the gauging station. At Brusquet, deposits are very low, so it is only possible to measure the cumulated deposits of several events. Deposits in sediment traps can reach 600 m^3 for one flood at Laval station and is between 5m^3 and 20 m^3 for one year at Brusquet. Sediment concentration of more than 350 g/l has been observed downstream from the Laval sediment trap. It did not exceed 35 g/l at the Brusquet station. The transported volume, calculated with sediment concentration of the samples gathered during the flood, is often greater than 300 m^3 at Laval and was always lower than 5 m^3 at Brusquet during the 1987 - 1993 period. The specific annual sediment yield of Brusquet is about 200 times lower than for Laval (Mathys *et al*, 1996). In terms of loss from the catchment area it is, on average, 40 times lower for Brusquet than Laval, as shown in Table 2.

TABLE 2: Annual sediment yield (T/ha.year) reported to bare area of the catchments

Year	1988	1989	1990	1991	1992	1993	Mean
Brusquet	2	2	2	3	8	7	4
Laval	103	64	181	135	311	176	154

4. Modelling forested and unforested catchment floods

4.1 The calibration of simple rainfall-runoff models

The rainfall-runoff-erosion model ETC (Erosion des Torrents en Crue) was used on the largest floods in these two catchments. For the rainfall-runoff part of this model, we looked among existing models for a simple, global model with few parameters. Two combinations of production and transfer functions were used :

The SCS production function, with initial abstraction So and potential maximum retention S, associated with a triangular unit hydrograph transfer function, with characteristic time Tc and position of the peak parameter k (rising time is Tc/k).

GR2, a two-reservoir model with infiltration reservoir height A, runoff reservoir height B, and Tr initial filling rate of A. (Michel, 1991).

In the calibration stage, we searched for constant values of S, Tc, k (parameters of the SCS model) and of A and B (parameters of the GR2 model). Only one parameter for each model (So or Tr) was made variable in order to take into account previous saturation of the basin. Rainfall threshold curves were successfully used for determining initial conditions (So or Tr) (Brochot, 1995).

4.2 The models parameters of the two basins

Calibrated values of the parameters in the two different models (Table 3) show a clear difference between the two basins which is easy to correlate with forest cover. A and S can be related to the retention ability of the basin and are several times higher in the forested basin. Tc, k and B are related to the runoff velocity and their ranges are coherent with time lapses observed on the two basins floods. The highest value for So is 9 mm at Laval and 26 mm at Brusquet. Tr ranges from 0 to 0.3 at Laval and from 0 to 0.5 at Brusquet. These results have been validated using the same model at Rimbaud catchment of Real Collobrier ERB (before and after fire).

TABLE 3: SCS and GR2 models parameters

	S (mm)	Tc (mn)	k	A (mm)	B (mm) for 5mn time step
Laval	28	30	2	25	7
Brusquet	600	200	10	125	96

The validation stage gave relatively good results with acceptable errors on peak flow values: 26% on Laval and 43% on Brusquet for the SCS validation; and 30% on Laval and 25% on Brusquet for the GR2 validation.

The better shape of the graph of flood decay obtained with GR2 has led us to retain this model for further studies. One example of the GR2 validation is given in Figure 5.

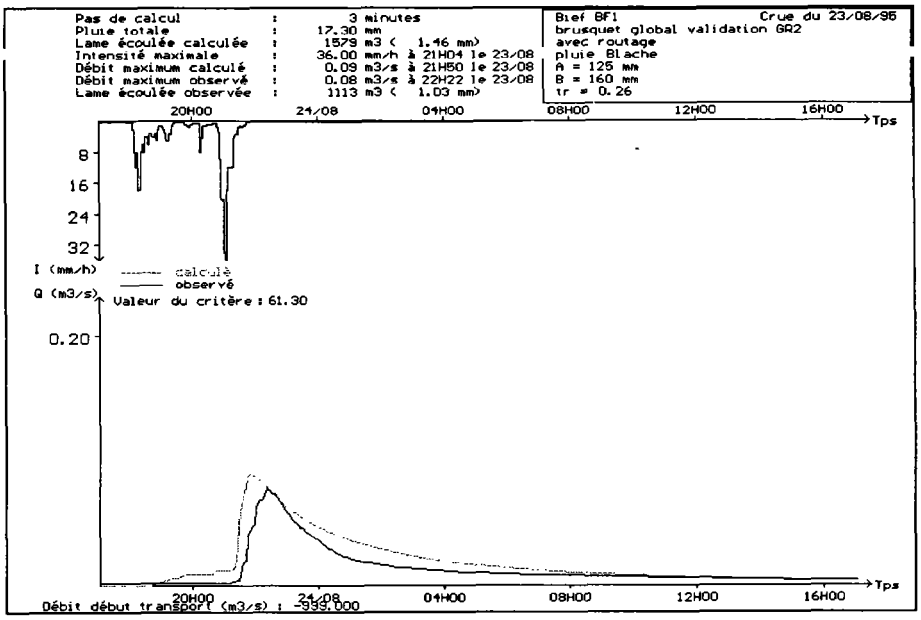

Figure 5: Example of GR2 validation on Brusquet catchment.

5. Discussion

The two catchments which have been compared have similar areas, and similar geological and topographic features. The most important difference is that the vegetation cover of Brusquet is mainly

forest, with only 13% bare area whereas Laval has no vegetation (forest or herbaceous vegetation) over 78% of its area.

Because of its higher runoff threshold, the forested Brusquet basin has fewer floods. This point is important for reducing erosion in this kind of basin. The forest cover effect on erosion is very apparent as all the factors of erosion production are concerned: rain splash effect on the ground; detachment sensitivity of the soil surface; and frequency and volume of floods able to transport sediment. Comparison of hydrograph shapes and peakflows shows that rapid surface runoff is the dominant process for the denuded basin while subsurface runoff characterizes the process in the forested catchment. This difference in hydrological behaviour has been observed in the Rimbaud basin before and after fire (Lavabre *et al.*, 1991).

For medium and high flow events on these two catchments, forest cover has a significant effect on the reduction of the peak and volume of the floods. However, it is not certain that the same pattern of rainfall-runoff can be assumed for high-density and/or longer duration rainfalls. The highest floods of the observed series occurred in autumn 1994. On 8th September, streamflow at the Laval gauging station reached a peak discharge of nearly 20 m^3/s while the Brusquet peak reached only 2.3 m^3/s. Later, after two months of many storms, the Brusquet station registered the second highest maximum of the series with a peak of 1.3 m^3/s while Laval discharge was only 2.5 m^3/s. In this case, initial saturation of the catchment explains the importance of Brusquet flood which is well predicted by the SCS or GR2 model with less than 30% error.

6. Conclusion

Observations on the Draix experimental catchments have shown that in a small forested mountainous catchment peak floods are reduced by a factor of between 5 and 10, flood runoff volume by a factor greater than 2 and the flood peak is delayed in a significant way. This comparison was possible because the two catchments were small with contrasting vegetation cover. Erosion and sediment yield at the outlet of the forested catchment is 200 times lower than that observed downstream from the bare catchment. Hydrological models with few parameters were successfully calibrated on a series of floods and the values of the parameters are coherent with forest cover. Use of these models has shown that rainfall-runoff processes are different in the two catchments which differ only as regards forest cover. Further experimentation on runoff formation will be necessary and separation of hydrograph components using isotopes has already been undertaken.

7. References

BROCHOT S., (1995) 'Desertification in Mediterranean area. European DM2E project.' *Cemagref Grenoble final report.* Project EV5V-CT91-0039. 60 P.

BROCHOT S. and M. MEUNIER (1996) 'Un modèle d'érosion des torrents en crue (ETC).' *Ingénieries - EAT* - N°6, juin 1996, p 9-18.

COSANDEY C. (1991) 'Forêt et écoulement : rôle de la forêt sur la formation des crues et sur le bilan d'écoulement annuel.' *Rapport sectoriel provisoire de fin de contrat CEE*, LA 141, Meudon, 82 p.

HUMBERT J. and G. NAJJAR (1992) 'Influence de la forêt sur le cycle de l'eau en domaine tempéré. Une analyse de la littérature francophone.' *CEREG Strasbourg.* 85 p.

LAVABRE J., D. SEMPERE-TORRES and F. CERNESSON (1991) - Etude du comportement hydrologique d'un petit bassin mediterranéen après la destruction de l'écosystème forestier par un incendie. Premières analyses. *Hydrologie Continentale.* Vol. 6 N°2. 121-132.

MATHYS N., S. BROCHOT and M. MEUNIER (1996) 'L'érosion des Terres Noires dans les Alpes du Sud: contribution à l'estimation des valeurs annuelles moyennes (bassins versants expérimentaux de Draix, Alpes-de-haute-Provence, France).' *Revue de Géographie Alpine* 1996 n°2, p 17-27.

MICHEL C. (1991) 'Hydrologie appliquée aux petits bassins ruraux.' Editions Cemagref Antony. 2 tomes. 411 p.

Hydrograph separation of stormflow components in a small catchment (Strengbach, Vosges) using hydrological measurements, and chemical and isotopic tracers

S. Idir[1], B. Ladouche[2], D. Viville[3], A. Probst[1], M. Loubet[4], J.L. Probst[1] and T. Bariac[2]

[1] *Centre for Geochemistry, Strasbourg, France*
[2] *Laboratory of Isotopic Biogeochemistry, Paris, France*
[3] *Centre for Eco-Geographical Research Studies, Strasbourg, France*
[4] *Laboratory of Geochemistry, Toulouse, France*

1. Introduction

Streamflow generation processes have been the subject of many previous studies in order to determine streamflow components in various catchments under different environmental conditions (e.g. Pinder and Jones, 1969; Pearce, 1990). Generally such studies use chemical tracers in a two or three-component mixing model for hydrograph separation, and are supposed to estimate the contributions from two or three reservoirs (surface runoff, sub-surface flow and groundwater) (Hooper *et al.*, 1990; Ogunkoya and Jenkins, 1993; Buzek *et al.*, 1995). Other studies have used water stable isotopes (^{2}H, ^{18}O) to distinguish pre-event water from event water (as example : McDonnell *et al.*, 1990). Recently, some authors (Kennedy *et al.*, 1986; Wels *et al.*, 1991) have tentatively compared the results obtained using isotopic and chemical tracers.

Since the different tracers used in the above studies do not identify the same streamflow components, the present study has tentatively used simultaneously hydrological measurements, stable isotopes (^{18}O, ^{2}H) and geochemical tracers. The aim was to investigate the origin of the water in a small catchment by identifying the temporal (pre-event and event water) and spatial components (contributing areas) to the total streamflow during a major storm event.

In this paper, hydrograph separation was performed in three different ways: (1) using hydrological measurements of the different tributaries to estimate the subcatchment contributions to the total streamflow; (2) using ^{18}O and ^{2}H to determine the proportion of event water; and (3) using dissolved organic carbon (DOC) and silica which have been selected among several other measured chemical tracers to identify the contributing areas.

2. Material and Methods

The Strengbach forested catchment (80 ha) at Aubure is located at the eastern side of the Vosges mountains (north-eastern France), 58 km south-west of Strasbourg (Probst *et al.*, 1990). It ranges from 883 m at the outlet to 1146 m at the top (Fig. 1). This catchment mainly lies on a base-poor granitic bedrock (the Brezouard granite). Soils are acidic, sandy and stony; brown acid and podzolic soils have developed on the south- and north-facing slopes respectively. In the valley bottom, a small saturated area with permanent hydromorphic conditions covers ~2 % of the basin area (Probst *et al.*, 1992). The catchment is completely forested: Norway spruce covers two-thirds of the catchment area (mainly as old trees), and mixed beech and silver fir take up the rest. The climate is temperate-oceanic-mountainous. The mean annual precipitation (1986-1989) is 1553 mm with 25 % falling as snow (Probst *et al.*, 1992). The mean annual discharge is 1051 mm; the highest flow period generally occurs during snowmelt (spring) and the lowest flow period is always in autumn (September-October).

During the storm event of 18 May 1994, bulk precipitation (PS) and throughfall (TF) have been collected regularly in PVC funnel collectors and in replicate 2 m long open gutters, respectively. Throughfall and zero tension soil solutions (SS) were collected in an old spruce stand. Stream discharge

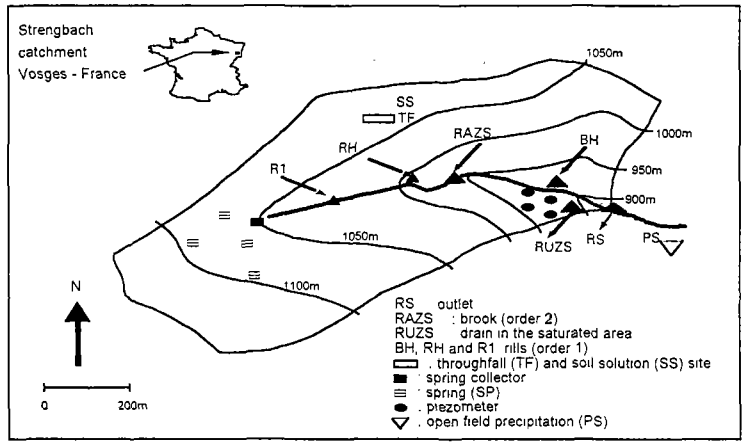

Figure 1: Map of the Strengbach basin and location of different sampling sites.

was monitored at a permanent gauging station (RS) equipped with an H-flume weir and at two non-permanent sites (RAZS and R1). Water samples were frequently and regularly taken simultaneously at the outlet (RS), along the main stream (RAZS, R1) and at the adjacent tributaries (BH, RH). The small saturated area has also been sampled using several piezometers and a gauging pipe (RUZS) (Fig.1). Samples were collected in polyethylene bottles and filtrated through a 0.45 µm Millipore membrane. For pH, electrical conductivity, alkalinity, silica, SO_4^{2-}, NO_3^-, Cl^-, Na^+, K^+, Ca^{2+}, Mg^{2+}, NH_4^+ and dissolved organic carbon (DOC), classical analytical methods were used (Krempp, 1988). Oxygen-18 analysis were carried out by the standard CO_2 equilibration method (Eipsten and Mayeda, 1953) and deuterium analysis by reduction of water to hydrogen over zinc at 540°C following a standard method (Coleman *et al.*, 1982). Results are expressed in per mil (‰) difference relative to the standard mean ocean water (SMOW) as defined by (Craig, 1961). Deuterium analyses have been normalized according to the V-SMOW-SLAP scale (Gonfiantini, 1978).

For both chemical and isotopic tracers, the hydrograph separation was performed using a classical two-component mixing model (Pinder and Jones, 1969). This approach assumes that the mixing of the fluxes coming from different sources is conservative and that there is no chemical interaction between the different components. In the model, equations could be solved at each step of the hydrograph separation by using the concentrations and the discharges measured in the different components.

3. Results and discussion

3.1. Hydrology

At the outlet of the Strengbach catchment, the hydrograph generated by the storm event of 18 May 1994 (40 mm in 19 hours) is characterized by two peaks of discharge (35 l/s and 28 l/s) in response to two successive rainfall events (respectively 26 mm and 14 mm). Figure 2 represents the hydrographs of the main stream (RS, RAZS and R1) and of the different tributaries (BH, RH and RUZS), and the corresponding hyetograph. In Fig. 2, it can be seen that the discharge measured at the pipe of the saturated area (RUZS) reaches its maximum during the first peak of the total streamflow. Whereas RAZS which controls the upper subcatchment presents its maximum discharge during the second peak of the hydrograph. However, the water table measurements in the piezometers of the saturated area indicate an increase of water height during the second period of the storm event which means that the contribution of the deep flow increases. During the first part of the event, the surface flow was important in the saturated area.

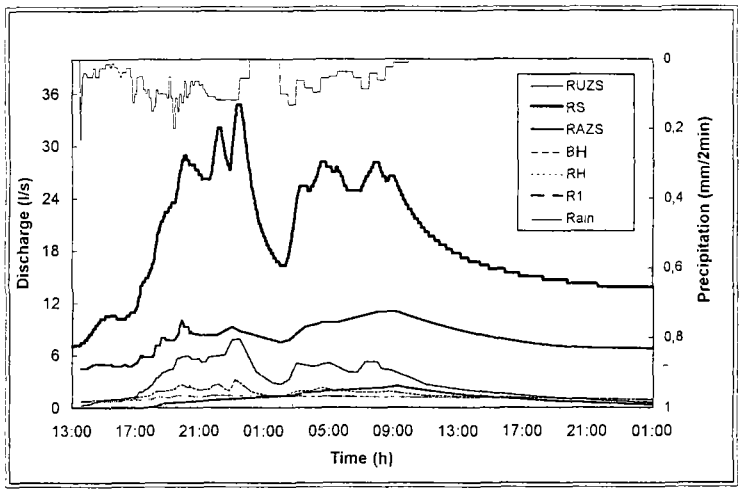

Figure 2: Hydrographs of the stream at the outlet (RS) and of the different tributaries, and corresponding hyetograph during the storm event of 18 May 1994.

For the whole event, the hydrological measurements indicate that the amount of water supplied by the upper subcatchment RAZS represents 40% of the total streamflow with a specific discharge of 3.5 l/s/km^2. The downstream subcatchment (between RAZS and RS) contributes the remaining 60% with a specific discharge of 5.7 l/s/km^2. However on the whole, the hydrological budget indicates that about 40% of the total streamflow could not be gauged because of uncontrollable drainage areas.

This hydrological approach allows determination of the geographical origins of the streamflow but it must be coupled with chemical and isotopic tracers to determine the contribution, in space and in time, of the different reservoirs.

3.2. Isotopic tracers

The isotopic signatures of the rainfall-runoff event show that the initial oxygen-18 content in streamwater (-9.43 ‰) is nearly identical to that of groundwater (-9.49 ‰), considering the uncertainty (Fig. 3). During the event, the temporal variation of oxygen-18 content measured at the outlet (RS) is low but significant compared to that observed in the open-field precipitation. The isotopic content of the streamwater is fluctuating around the mean $\delta^{18}O$ of spring water and returns to the initial value during the recession period. This temporal evolution of $\delta^{18}O$ measured in streamwater is mainly due to a contribution of event water (rainfall). However, these results show that only a very small amount of rainfall contributes directly to the storm runoff.

The temporal isotopic variation of event rainfall may complicate the choice of appropriate signature for hydrograph separation. So, the event water composition has been derived using the incremental weighted mean method in order to integrate the temporal variability of $\delta^{18}O$ in rainfall (McDonnell *et al.*, 1990). The hydrograph separation (Fig. 4) takes into account two distinct rainfall events and a constant pre-event isotopic composition supposed to be equal to that of the mean spring water content which is relatively constant.

The hydrograph separation indicates that pre-event water is the major component for this event. The instantaneous event contributions are not very important, ranging from a minimum value of 2 % at the beginning of the stormflow to a maximum value of 12 % at the main peak flow. The determination of the total event contribution for the entire stormflow period is around 277 m^3 ± 51 m^3. The area contributing new water determinated from the isotopic separation is 0.87 ha ± 0.16 ha. This result suggests that the contributing areas calculated by the isotopic method could represent the saturated areas located in the vicinity of the main stream (1.06 ha before the stormflow). Thus, for this event, it is suggested that nearly all the precipitation on the surface of the saturated areas have contributed to the stormflow.

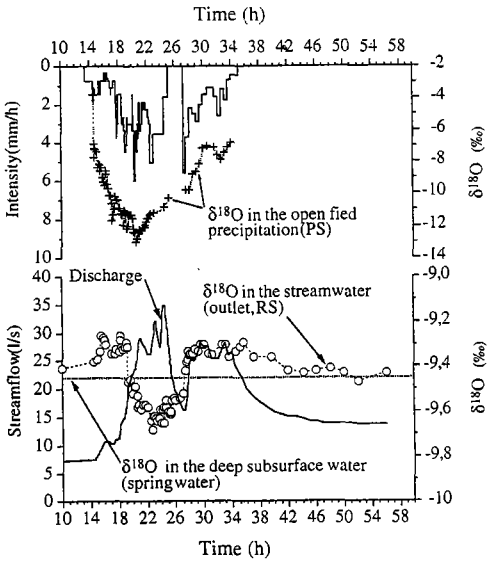

Figure 3: Rainfall intensity and stream discharge at the outlet. Rainfall and streamwater isotopic variations ($\delta^{18}O$) during the storm event of 18 May 1994.

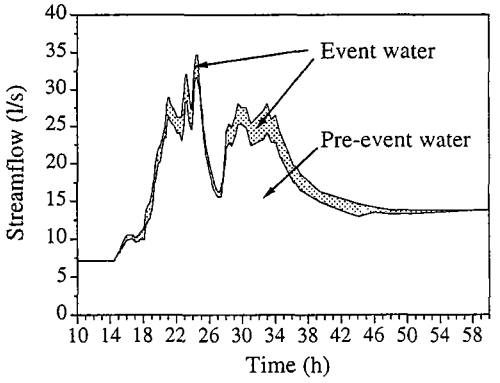

Figure 4: Hydrograph separation performed using isotopic tracer ($\delta^{18}O$).

3.3. Chemical tracers

During the storm event, the rainwater is slightly acidic (pH = 5.1), very diluted and dominated by ammonium, protons, sulfate and nitrate. Concentrations decrease during the first part of the event. During the second part, concentrations were higher (particularly for acid compounds). Throughfall is more acidic (pH = 4.6) and more concentrated than open-field precipitation. Streamwater is circumneutral (pH between 6 and 6.7); calcium and sulfate dominate the chemical composition as previously observed in this catchment (Probst *et al.*, 1990).

According to their concentration behaviour with respect to discharge variations in the mainstream and in the adjacent tributaries, four groups of chemical parameters could be identified during the storm event:

- parameters for which the concentrations are highly diluted with increasing discharge at all sampling stations (conductivity, SO_4, Cl, Na, Ca, Mg and silica);
- elements for which the concentrations are weakly diluted (K, pH and alkalinity);
- dissolved organic carbon (DOC) for which the concentration increases with discharge for all sampling stations; and
- NO_3 which is diluted during the first flow and concentrated in the second part of the storm event.

The linear mixing diagram between DOC and silica (Fig. 5) exhibits the contribution of two obvious end-members to the total streamflow discharge: one is characterized by low silica concentrations and high DOC contents and the other by high silica concentrations and low DOC contents. The first one corresponds to waters draining the upper layers of the saturated area (RUZS pattern) and the second corresponds to waters draining deep layers of the hillslopes (spring water pattern). It is important to note that, as confirmed by mixing diagrams using other major elements, the soil solution (SS), the open-field rain water (PS) and the throughfall (TF) are not on the mixing line. Consequently, they contribute only very weakly to the chemical composition of the stream water.

Because of their clearly identified origin and of the good relationship between concentration and discharge, hydrograph separation was performed using DOC (Fig. 6) and silica. We identified two contributing areas; the hillslopes and the saturated areas. During this storm event, the main water contribution to the total stream discharge is supplied by the hillslope (75% of total stream flow).

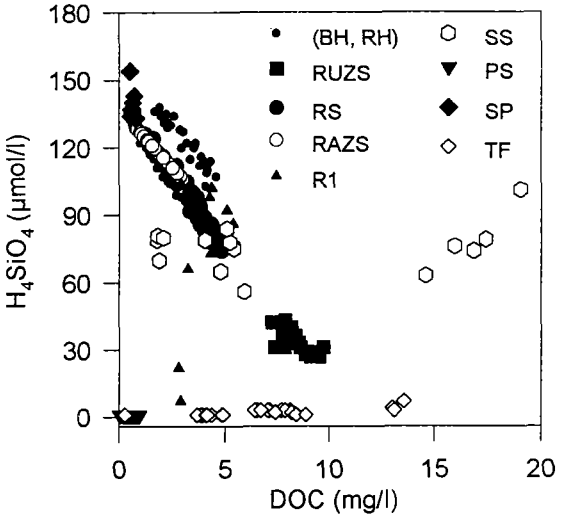

Figure 5: Mixing diagram between DOC and silica in various sampling sites during the storm event of 18 May 1994.

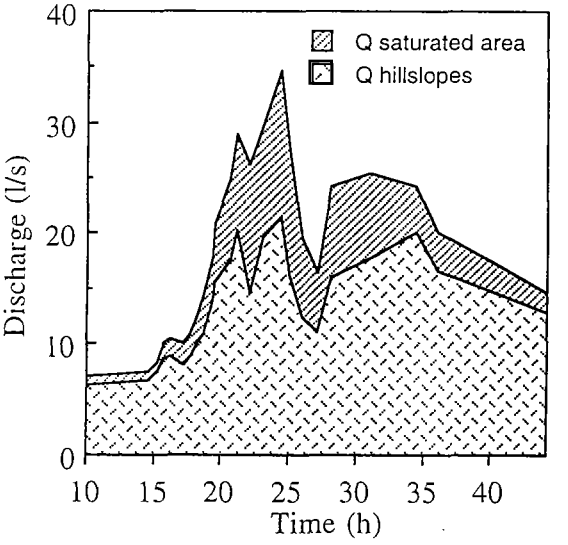

Figure 6: Hydrograph separation using DOC as a chemical tracer.

Nevertheless, this contribution is slightly lower during the first period (70%) than during the second one (77%). The results obtained using DOC and silica as geochemical tracers are very close and are consistent with those obtained using isotopic tracers. We consider that the major part of the hillslope contribution is dominated by pre-event water.

4. Conclusion

Contrary to many comparable studies where event waters were found to highly influence stream water composition, the hydrograph separation of a main storm in the small Strengbach catchment presents a different pattern of results.

The hydrological measurements indicate a major contribution of the upper subcatchment (upstream source area) to total stream flow. The isotopic tracers (^{18}O, ^{2}H) point out that the direct influence of rain water on streamwater is very low (2% to 10%). Among several measured chemical elements, silica and DOC appeared to be the more efficient tracers to identify contributing areas. Streamflow hydrochemistry is highly controlled by a mixing of two contributing areas; the hillslope (75%) and the saturated area (25%). The simultaneous use of geochemical and isotopic tracers shows that pre-event water draining hillslopes was the main contribution to total streamflow.

This approach combining hydrological, geochemical and isotopic measurements is recommended for streamflow component separation in other case studies.

5. Acknowledgments

This work has been carried out within the DBT II « Fleuves et Erosion » research program supported by the INSU/CNRS.The authors are also grateful to all participants in the field and in the laboratory for their contribution which allows this study to progress in good conditions.

6. References

BUZEK, F., J. HRUSKA and P. KRAM (1995) 'Three-component model of runoff generation, Lysina catchment CZEC Republic'. *Water, Air and Soil Pollution*, 79, p. 391-408.

COLEMAN, M. L., T.J. SHEPERD, J.J. DURHAM, J. E. ROUSE and G. R. MOORE (1982) 'Reduction of water with zinc for hydrogen isotope analysis'. *Anal Chem*, 54, p. 993-995

CRAIG, H. (1961) 'Standard for reporting concentrations of deuterium and oxygen-18 in natural waters'. *Sciences.*, 133, p. 1833-1834.

EIPSTEN, S. and T. MAYEDA (1953) 'Variation of 18O content of waters from natural sources'. *Geochimica et Cosmochimica Acta.*, 4, p. 231-224.

GONFIANTINI, R. (1978) 'Standards for stable isotope measurements in natural compounds'. *Nature*, 271, p. 534-536.

HOOPER, R.P, N. CHRISTOPHERSEN and N.E. PETERS (1990) 'Modeling streamwater chemistry as a mixture of soil water end-members- An application to the Panola mountain catchment, Georgia, U.S.A'. *J. of Hydrology*, Vol 116, p. 321-343.

KENNEDY, V. C.; C. KENDALL, G.W. ZELLWEGER, T.A. WYERMAN and R. J. AVANZINO (1986) 'Determination of the components of stormflow using water chemistry and environmental. isotopes, Matolle river basin, California'. *J. of Hydrology*, Vol. 84, p. 107-140.

KREMPP, G. (1988) 'Techniques de prélèvements des eaux naturelles et des gaz associés. Méthodes d'analyse des eaux et des roches'. *Notes Techniques 19*, Institut de Géologie, Strasbourg, France, 79p.

MCDONNELL, J.J., M. BONELL, M. K. STEWART, and A.J. PEARCE (1990) 'Deuterium variations in storm rainfall: implications for stream hydrograph separation'. *Water Resources Research*, Vol. 26, No. 3, p. 455-458.

OGUNKOYA, O. O. and A. JENKINS (1993) 'Analysis of storm hydrograph and flow pathways using a three-component hydrograph separation'. *J. of Hydrology*, Vol. 142, p. 71-88.

PEARCE, A J. (1990) 'Streamflow generation processes: An Austral view'. *Water Resources Research*, Vol. 26, No. 12, p.3037-3047.

PINDER, G.F and J.F. JONES (1969) 'Determination of the groundwater component of peak discharge from the chemistry of total runoff'. *Water Resources Research*, Vol. 5, No 2, p. 438-445

PROBST, A., E. DAMBRINE, D. VIVILLE and B. FRITZ (1990) 'Influence of acid atmospheric inputs on surface water chemistry and mineral fluxes in a declining spruce stand within a small granitic catchment (Vosges massif, France)'. *J. of Hydrology*, Vol. 116, p. 101-124.

PROBST, A., D. VIVILLE, B. FRITZ, B. AMBROISE and E. DAMBRINE (1992) 'Hydrochemical budgets of small forested granitic catchment exposed to acid deposition : The Strengbach catchment case study (Vosges massif, France)'. *Water, Air and Soil Pollution*, 62, p. 337-347.

WELS, C., R.J. CORNETT and B.D. LAZERTE (1991) 'Hydrograph separation: A comparison of geochemical and isotopic tracers'. *J.of Hydrology*, Vol 122, p. 53-274.

Conference "Ecohydrological Processes in Small Basins", Strasbourg, 24 - 26 September 1996

Analysis of water residence times in a prealpine catchment using oxygen-18 measurements (Rietholzbach, eastern Switzerland)

T. Vitvar

Department of Geography, Federal Institute of Technology, Zürich, Switzerland

1. Introduction

Water balance studies of Swiss prealpine catchments have shown high precipitation amounts and groundwater recharge rates (Gronowski and Lang, 1993; Menzel, 1996). The groundwater stored within the local porous aquifers serves as an essential water resource. It is therefore of great importance to obtain information about mixing mechanisms which influence the water residence times and transport of water and solute in representative basins.

One of the crucial steps towards this topic is the estimation of water residence times in aquifers (molasse or Quaternary glacial deposits) contributing mainly to surface outflow. Koenig *et al.* (1994) determined a daily balance of runoff components in the Rietholzbach catchment for the period 1975-1990 but their graphical approach does not allow the calculation of residence times or prove the interconnection between the aquifer and the outflow from the catchment. On the other hand, case studies made in various porous catchment formations using stable isotopes as tracers (e.g. Maloszewski *et al.*, 1992) demonstrate the usefulness of the lumped parameter modelling approach for characterizing the subsurface residence time distribution.

The aim of this paper is twofold. Firstly, the mean residence time of baseflow water at the main Rietholzbach runoff gauging site, and at a subcatchment runoff gauging site, is estimated using ^{18}O measurements and a lumped parameter modelling approach. Secondly, aquifers mainly contributing to the baseflow at both sites are identified.

2. Study area

The Rietholzbach basin (Fig.1) is a small hilly prealpine basin in the middle part of the Thur river basin in north-eastern Switzerland. The catchment covers an area of 3.18 km^2 and is primarily used as pasture land. Approximately25 % of the area is forested and the elevation ranges from 680 to 960 m a.s.l. The geology of the catchment is characterised by the Tertiary deposits of the Upper Freshwater Molasse consisting of consolidated clastic sediments such as conglomerates (Nagelfluh), sandstones, layers of marls and banks of limestone. In the lower parts of the catchment there are also Pleistocene gravel pockets which represent Würm glacier moraines. Particularly the conglomerates and the Quaternary deposits can be regarded as groundwater aquifers with medium to high hydraulic conductivities and relatively large storage capacities. Average annual values of the catchment water balance are: precipitation 1600 mm, runoff 1040 mm, and evapotranspiration 551 mm (Koenig *et al.*, 1994; Menzel, 1996).

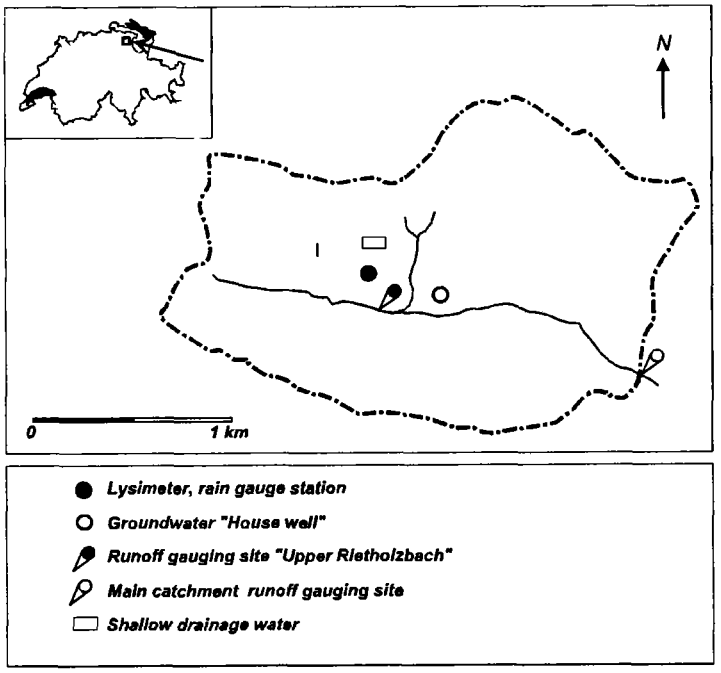

Figure 1: Rietholzbach catchment with sampling sites.

3. Data collection

Several hydrometeorological variables in the Rietholzbach catchment, including evapotranspiration, soil moisture and percolation water from a 2.20 m deep lysimeter, have been measured since 1975 with high temporal resolution. The ^{18}O data input series are derived from monthly rainfall samples collected at the meteorological station Büel. Streamwater was sampled weekly or daily at two locations (the main runoff gauging station Rietholzbach and the gauging station of the upper subcatchment (Oberer Rietholzbach). Weekly samples from two sub-surface water reservoirs referred to in this study, i.e. shallow drainage water and groundwater from a farm-house well, were analysed. Sampling started in January 1994 for rainfall and streamwater, and in June 1994 for the sub-surface water samples. The ^{18}O analyses were carried out at the Stable Isotope Laboratory of the Geological Institute ETH Zurich, using the OPTIMA mass spectrometer. The final values are expressed with reference to Standard Mean Ocean Water (SMOW) in units of parts per thousand.

4. Methods

Lumped-parameter flow and transport models are analytical, steady-state and one-dimensional concepts describing the transformation of a given tracer input (concentration in precipitation C_{in}) into the tracer output (concentration at an outflow site C_{out}) within a continuous flow system (Maloszewski and Zuber, 1982; Amin and Campana, 1996). For stable isotopes as tracers, this expression takes the form of a convolution integral with a system response function representing the expected residence time distribution:

$$C_{out}(t) = \int_0^\infty C_{in}(t-T)\, g(T)\, dT \qquad (1)$$

The function $g(T)$ characterises the type of water mixing, or the model concept itself, and t and T are chronological and residence time respectively. Mixing can range from the piston flow concept (no mixing) to complete exponential mixing. Therefore, for simulating the most probable partial mixing type

occuring in a natural system, a two-parameter exponential-piston flow combination for describing limiting cases or the dispersion model concept (in flow concentration mode, see Parker and van Genuchten, 1984) were used. The mean water residence time is always the main model parameter.

The modelling has been made in monthly steps for the period 1994-1995. The ^{18}O output functions of baseflow consist only of values measured during low flow periods as the purpose is to determine the residence time of stored water. Concerning the input function, two original parametrization steps have been carried out. Firstly, the local ^{18}O monthly record in precipitation was completed for the period 1981-1995 by the use of monthly values from IAEA/WMO stations Bern and Konstanz. Secondly, the complete input function was weighted by monthly values of outflow rates from the lysimeter installed within the Rietholzbach catchment (using the weighting procedure of Maloszewski *et al.*, 1992). As a consequence, the input function incorporates a groundwater recharge factor and eliminates that part of the precipitation which does not contribute to the baseflow.

5. Results and discussion

Fig. 2 shows the ^{18}O input function for the period of measurement from 1994 to 1995. On the left, the relationship between the ^{18}O concentration in precipitation and air temperature is shown. On the right, a comparison between this raw function and its values weighted by lysimeter outflow rates is plotted. It is obvious that the intensity of flow through the lysimeter is generally lower during the summer and autumn dry periods. Thus, in such a case the importance of this recharge period for the baseflow water turnover decreases and the parameterized summer input values are relatively smaller. Experience has shown that the ^{18}O input function is a term influencing essentially the quality of the simulation so that use of the observed input function only leads to doubtful fitting results.

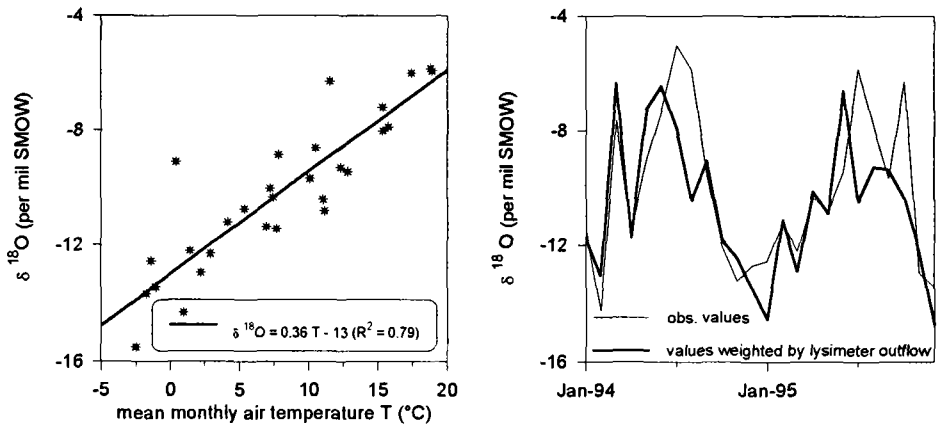

Figure 2: Local ^{18}O input function for the Rietholzbach catchment, 1994-1995. On the left, the relation between ^{18}O content in precipitation and air temperature is presented. On the right, a comparison of the observed input function with a weighted function is given.

Fig. 3 compares the modelled ^{18}O output functions with measured values for two output sites. It can be seen that all calculated functions satisfactorily simulate the measured data. The Oberer Rietholzbach catchment is characterized by a mean residence time of 24.5 months obtained by the exponential model. The ^{18}O output signal within the shallow drainage reservoir is very similar to that in the baseflow samples from Oberer Rietholzbach so that both functions are simulated simultaneously using the same model parameters. The exponential type of residence time distribution shows an essential influence of efficient mixing within the glacier deposits. Simulations using the dispersion concept do not satisfactorily fit the measured data because of the overestimation of components transported by dispersion. Concerning the total catchment baseflow runoff, a larger amplitude of the output function indicates lower mean water residence time. The best fit was obtained for 12.5 months using the exponential-piston flow model. In this case the identical ^{18}O output signal occurs in samples from the Farm-house well site. This means that the eastern catchment, where some parts are formed by steep

slopes, includes a small volume fraction of the piston-flow water transport type. Such a mixing type may be typical for deeper storage reservoirs within the molasse conglomerates. Moreover, the mean residence time of total catchment baseflow indicates that there is also water in the molasse aquifers having a residence time shorter than 12.5 months. Additional observations showed that such a very fast transport exists in the form of hillslope fluxes through small conglomerate formations overlaying the banks of marls and limestones.

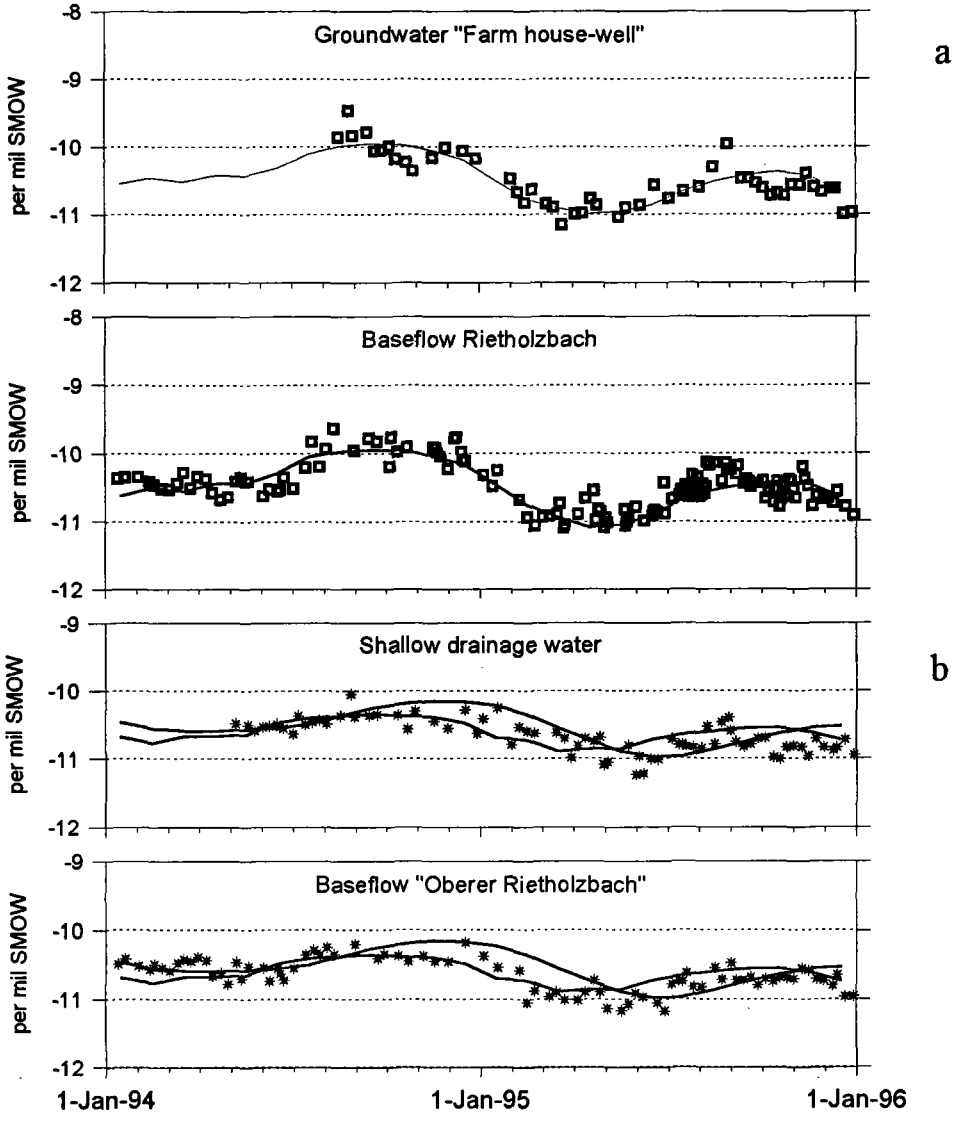

Figure 3: Measured ^{18}O values and simulated ^{18}O output functions. The following best fits were obtained: a) baseflow Rietholzbach and 'Farm house-well', using the exponential-piston flow model (ca. 5% volume fraction of piston flow) for the mean residence time of 12.5 months, and b) baseflow 'Oberer Rietholzbach' and shallow drainage water, using the exponential model (bold) and the dispersion model (thin; dispersion parameter = 0.8) for the mean residence time of 24.5 months.

6. Conclusions

The study has described the interactions between surface water and groundwater within the small prealpine catchment Rietholzbach. Two processes have been identified. Firstly, there are relatively fast hillslope fluxes through deep molasse aquifer with a small fraction of piston flow transport. This system is represented by total catchment baseflow runoff with a mean water residence time of approximately 1 year. The ^{18}O measurements showed an interconnection between the baseflow and the

molasse groundwater aquifer at the farm house-well. Secondly, efficient mixing processes occur in that part where the glacial deposits play an essential role in the mixing. Here the exponential type of residence time distribution with a mean of about 24 months satisfactorily simulates the measured ^{18}O values of baseflow in the upper subcatchment Oberer Rietholzbach and of an interconnected aquifer.

The simulation results obtained using ^{18}O as tracer show a very good applicability of the lumped parameter approach in catchment aquifers characterized by short mean residence times of up to 2 years.

Bibliography

AMIN, I. E. and M. E. CAMPANA (1996). 'A general lumped parameter model for the interpretation of tracer data and transit time calculation in hydrologic systems'. *J. Hydrol.*, 179, p. 1-21.

GRONOWSKI, T. and H. LANG (1993). 'Die natürliche Grundwasserneubildung in einem urban beeinflussten Einzugsgebiet im Voralpenraum'. *Wasser, Energie, Luft*, 85, 48-52.

KOENIG, P., H. LANG and R. SCHWARZE. (1994). 'On the runoff formation in the small prealpine research basin Rietholzbach'. In *Proc. of 2nd Conference on FRIEND, Braunschweig, October 1993,* IAHS Publ. No. 221, p. 391-380., IAHS Press.

MALOSZEWSKI, P. and A. ZUBER (1982). 'Determining the turnover time of groundwater system with aid of environmental tracers, 1. Models and their applicability'. *J. Hydrol.*, 57, 207-231.

MALOSZEWSKI, P., W. RAUERT, P. TRIMBORN, A. HERRMANN, and R. RAU (1992). 'Isotope hydrological study of mean transit times in alpine basin (Wimbachtal, Germany)'. *J. Hydrol.*, 140, 343-360.

MENZEL, L. (1996). 'Modellierung der Evapotranspiration im System Wasser-Pflanze-Atmosphäre'. *Zürcher Geographische Schriften*, 67.

PARKER, J.C. and M.T. VAN GENUCHTEN (1984). 'Flux-Averaged and Volume-Averaged Concentrations in Continuum Approaches to Solute Transport'. *Water Resour. Res.*, 20, 866-872.

Influence of temperature variations on daily runoff in a high mountain catchment

P. Pourrut and J. Patoux

ORSTOM, Antofagasta, Chile

1. Introduction

Urban activities, agricultural demands and the exploitation of the considerable mineral resources of the Atacama desert require a constantly increasing water supply from the upper slopes of the Chilean Andes, the exclusive source of water for the Region of Antofagasta (see Fig. 1). Water withdrawal from this area has thus become extremely intensive.

In the uppermost part of the eastern *altiplano*, in the ecological level known as "la puna", flows the Zapaleri river, which remains one of the last sources free of water abstractions for human consumption. This river is of particular significance because it feeds the small lake of Tara, chosen by the extremely rare Andean flamingoes for nidification. The water abstraction system to be installed in the years to come will have to be designed to yield a maximum of drinkable water without threatening the minimum ecological flow rate necessary to the survival of an endangered species.

In 1993, in order to obtain a good estimate of these limiting values, the Northern Catholic University of Antofagasta and ORSTOM decided to install measurement stations and to initiate a program of study in this area devoid of reliable hydroclimatological information (Araya *et al.*, 1995).

2. Description of the Zapaleri river basin

The Zapaleri river flows out of Bolivia into Argentina before reaching Chile. The Zapaleri catchment is an endoreic watershed of approximately 1000 km^2, which extends between 4250 m and 6000 m altitude. It lies between 22°30' and 23°00' of southern latitude, 66°90' and 67°20' of westwern longitude (see Fig. 2).

Two types of climate, separated by the 5000 m level contour, can be distinguished in the watershed: *altitudinal steppe* and *tundra* (Koeppen classification). Major planetary and topographic features (tropical latitude, South Pacific anticyclone, Humboldt current, relief of the Andes) explain the overall aridity, extremely high incoming solar radiation and low temperatures observed in winter. Along with these factors, is to be considered the southward motion of the low pressure cell centered on the Amazon basin and the Chaco which, during the austral summer, drives warm and humid air masses westwards. It is responsible for the main period of precipitation between December and March, known as the *Bolivian winter*. This precipitation, from 50 to 200 mm per year, displays high interannual irregularity.

The streamflow regime observed on the Zapaleri river is similar to the high mountain glacio-nival regime (Pardé classification) which is characterised during the dry and warm season by higher flow rates resulting from the melting of the snow-ice pack accumulated in the upper basin (Araya *et al.*, 1995). Daily fluctuations also affect these flow rates, the peaks of which follow the maxima of solar radiation and temperature. To some extent, however, the streamflow observed at the Zapaleri station differs from this typical regime. Two causes can be identified :

(a) the extremely high range of temperatures, especially during the austral winter when the temperatures vary widely above and below 0°C during the same day (a maximum range of 30 °C from -13 °C to +17 °C was recorded on the 23rd of August) ; and

(b) the types of input to the hydrographic network.

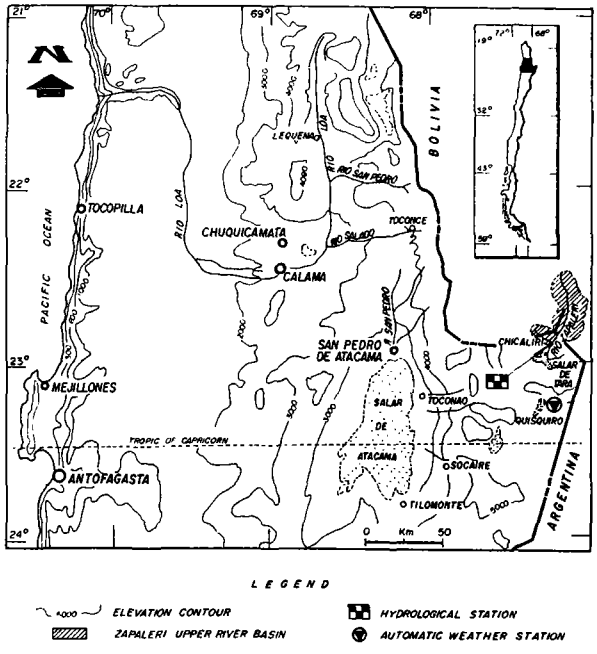

Figure 1: Location of study area.

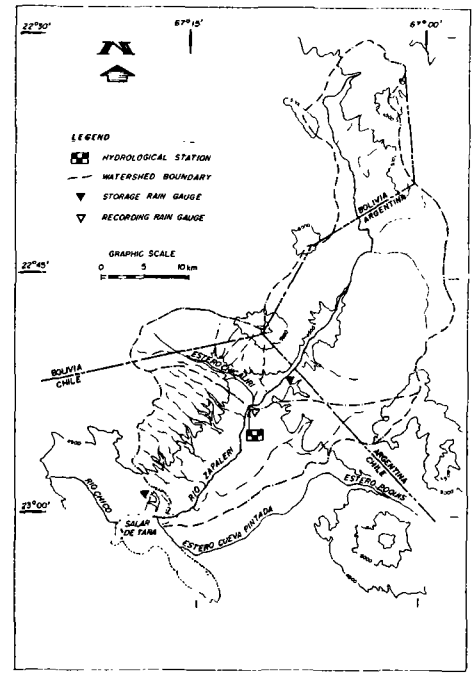

Figure 2: Zapaleri river basin.

Because of the almost total absence of significant rainfall, rain-induced floods are very rare. The numerous poorly consolidated tuffs and major quaternary detritic formations produce a storage and circulation of groundwater which constitute the main inputs to the Zapaleri river. Along with the melting of the *permafrost* (and most probably a few isolated glaciers protected by a rock layer, referred to as "rock glacier"), these water inputs ensure a constant baseflow.

3. Objectives

The examination of the hydrograms of the Zapaleri river after its meeting point with the Chicaliri (S = 680 km^2 - see Fig. 2) reveals the complexity of the daily streamflow regime (see Fig. 3). The highly variable discharge is likely to be produced by ice jamming and break-up processes due to high temperature variations. More than one year of uninterrupted measurement in this area was used to confirm this hypothesis, to identify these streamflow variations and to establish a typology of the daily floods, the respective roles of the inputs to the river and the influence of climatological factors such as solar radiation and temperature variations.

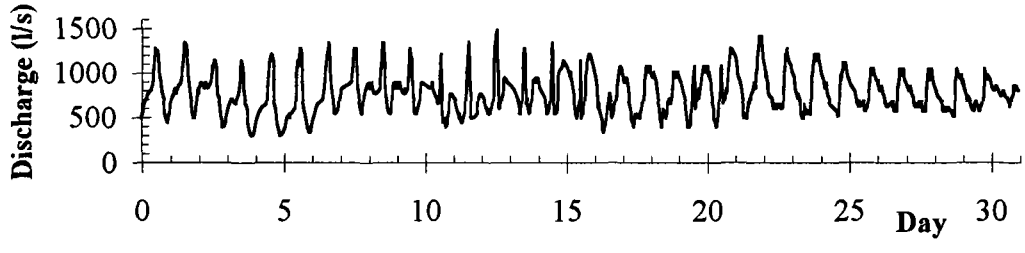

Figure 3: Discharge of Zapaleri River - August 1995.

But the main objective of the study was to obtain a maximum of climatological and hydrological data, in order to establish critical elements for the design of a water abstraction system in accordance with economic and ecological priorities.

4. Equipment - implementation (July - December, 1994)

A calibration and control section was constructed and an ELSYDE LIMNI 92 limnigraph installed immediately downstream of the confluence of the Zapaleri and Chicaliri river (altitude 4300 m). The stage (sensitivity of 1 cm , time step of 15 minutes) and temperature of the water are measured by an SPI probe. Air temperature is measured in the shelter where the recording equipment is stored.

On the shore of the salt lake of Quisquiro (altitude 4250 m), 40 km south of the limnigraphic station, was installed an automatic climatological station (CAMPBELL platform and ISCO sampler). The choice for installing the station outside of the Zapaleri river basin was dictated by the presence of an observer, the unique inhabitant in a 20,000 km^2 area.

5. Results

5.1 Mechanisms of daily streamflow variations

The discharge fluctuations and the associated floods result from a series of *ice jams* and *break-ups* occurring in the different parts of the basin where a potential source of water is liable to be mobilised. An *ice jam* here refers to the freezing of the water inputs or to an accumulation of water behind a temporary dam (Gray and Prowse, 1993); an ice jam upstream of the hydrological station produces a diminution of the observed discharge. *Break-ups* are induced by fracturing which follows the melting of the frozen layers and the sudden rupture of the hanging dams (Gray and Prowse, 1993); the flood wave following a break-up is characterised by a significant increase of flow. The succession of ice jams and break-ups is responsible for the various types of hydrogram observed at the station.

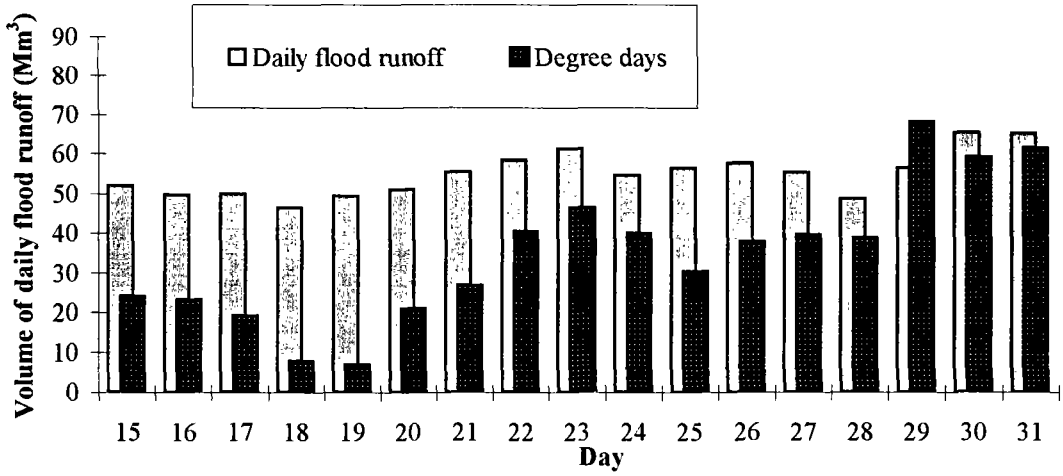

Note : the different floods are identified by the day on which they were initiated, but they can extend to the following day

Figure 4: Zapaleri d.j. Chicaliri -July 15-31, 1995; relation between positive temperatures and daily floods.

The solar radiation and associated air temperatures are the main factors which determine the occurrence and intensity of ice jams and break-ups. The dynamics of the system are driven in particular by the passing above and below 0°C of temperature and the duration of insolation, as is evidenced by the tight relation which links the volume of the daily floods and the range and duration of the positive temperatures, illustrated by the integration in Fig. 4.

5.2 Origin of the water inputs

The upper basin, lying above 4800 m, extends over an area of about 100 km^2. It plays an important role when covered by a significant amount of persistent snow and ice, which melts and contributes to the runoff. To this input from the upper watershed is to be added the melting of the permafrost and glaciers (which are sensitive to high temperatures in summer, in spite of the protection of the rock layers), groundwater return flow, springs, small streams and the melting of water frozen on the river banks. When the snow-ice pack on the upper watershed is reduced or absent, as during the study period, the inputs are limited to these last quantities.

In the lower part of the basin, the upper limit of which is at about 4500 m, the mechanisms responsible for the flow rate variations take place in the reach itself. Reaches of gentle slope, which contains many sections where the water velocity is most of the time reduced, if not zero, enhance freezing processes. This zone is also characterised by significant groundwater inputs resulting from the effluent seepage of the aquifer into the riverbed and from individual sources.

Three hundred meters upstream of the hydrometric station, the Chicaliri river brings in 50 l/s. The zone of confluence, a marshy area extending over more than a hectare, is particularly subject to freezing and acts as a "buffer zone", which strongly influences the constitution and distribution of flood waves over time.

5.3 Formation and typology of daily floods

The streamflow observed at the station is generally complex because it results from the superposition of inputs from the different parts of the basin described above, and produced at distinct moments. It is thus often most difficult to locate and identify the exact origin of the flood waves. For instance, a common standard can hardly be defined for the succession of apparently random small sudden peaks, up to ten per day, which are associated with the repeated rupture of temporary hanging dams, concentrated in the narrower sections of the riverbed where ice blocks accumulate.

However, the similarity of form which characterises particular flood waves, as well as the periodicity which marks their daily rhythm, were used to identify two main types of characteristic flood waves, referred to as *upper basin* and *lower basin flood waves* (see Fig. 5). During the period from the 11th to the 17th of August, a remarkably enhanced lag time between the recording of the two flood waves helped to identify their characteristics.

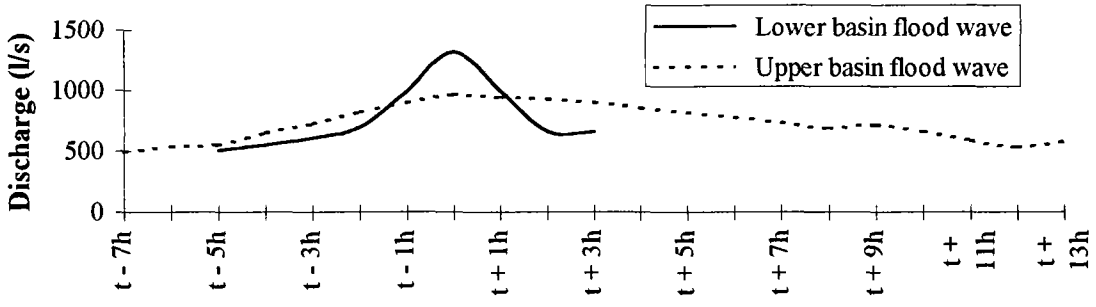

Figure 5: Theoretical Floodwaves (averaged from the August 1995 series).

The very steep rising limb of several hundred litres per second, observed every day systematically between 0730 hrs and 0930 hrs, illustrates the arrival of a turbulent flood wave which is the direct result of the nearly instantaneous emptying of a reservoir nearby. This wave corresponds to the fluxes of the Chicaliri and partly those of the Zapaleri, being set suddenly in motion with the breaking-up of the temporary dam appearing each night at the marshy confluence of the two rivers. During daytime, solar energy contributes to the warming of the hanging dam and induces a break-up

which liberates almost instantaneously a large mass of water and ice blocks arriving suddenly at the station. For clarity, it is here referred to as *lower basin flood wave*.

Another type of flood wave, further spread out in time, can be observed systematically each day with an approximate lag time of twelve hours when compared to the lower basin flood wave. This lag time and the non-turbulent nature of this flow indicate an origin in a fairly long and remote reach. For simplicity, this remote input is here called *upper basin flood wave*. Until the end of June, at the austral winter solstice, the arrival of the wave frequently occurs around 1900 hrs or 2000 hrs. During the month of July, the lag time increases steadily (apparent motion of the sun) and the time of arrival of the wave eventually settles down to 2200 hrs or 2300 hrs.

The typology of the flood waves can however hardly be limited to the two hydrograms described above; complex flood waves are to be observed most of the time, with a unique peak resulting from the superposition of these two types of runoff.

5.4 Characteristic discharge values

For the period of May to September 1995, Table 1 presents the monthly mean, minimum and maximum values for the instantaneous discharge.

TABLE 1: Characteristic discharge values of Zapaleri river (May-September, 1995)

Discharge (l/s)	May	June	July	August	September	May-September
Qmean	623	628	628	783	631	659
Qmin	296	296	296	296	251	251
Qmax	1079	1144	1278	1486	921	1486

Of particular interest are the absolute minimum and maximum reached throughout the whole period of study, 250 and 1490 l/s respectively, and the mean discharge, Qm = 660 l/s. Moreover, on the 27th, 28th of July and 5th of August, variations of the instantaneous discharge in a ratio of one to four (from 296 to 1210 l/) were observed in the same day.

TABLE 2: Characteristics of daily floods of Zapaleri river for a representative decade of August 1995

	Volume of water per daily flood* ($10^3 m^3$)			Discharge (l/s)	
Day	Total flow	Base Flow	Excess Flow	min	max
8	72.9	47.5	25.5	544	1346
9	66.9	43.6	23.3	544	1278
10	69.0	42.0	26.9	390	1211
11	52.9	34.1	18.8	390	1346
12	62.9	47.1	15.8	491	1486
13	72.6	51.9	20.7	544	1278
14	62.1	42.1	20.0	544	1346
15	71.5	42.8	28.7	491	1144
16	70.8	45.1	25.8	491	1211
17	62.4	42.4	20.0	491	1079

* Note : these floods can start on a given day and extend to the following day

The following volumes of water delivered to the system by the ice jams and break-ups were calculated for each flood of several characteristic 10-day periods: The *global flow* or total amount of water; the *base flow* here defined as the amount of water not involved in the ice jamming; and finally the flow corresponding to the flood peak itself, here referred to as *excess flow*. The results are presented in Table 2.

These calculations enable us to isolate the volume of water accumulated and then delivered to the system through the mechanisms induced only by the temperature variations. From the period of May to September, this *excess flow* is about 22 10^3 m^3 and reaches 28.7 10^3 m^3, when the daily mean *base*

flow corresponds to about 35 10^3 m^3. Note that the calculation of the *base flow*, as defined previously, is of higher value for the design of an abstraction system.

6. Conclusions

The present study contributes significantly to the understanding of phenomena driving streamflow variations in a high mountain river, under very low and widely fluctuating temperatures. It shows the limitation of the parameters generally used for the design and construction of abstraction systems, and brings new elements to choose them and then to complement the calculation of their technical characteristics: run-of-river system in the case of a water demand inferior to the absolute minimum discharge; and off-stream storage in a reservoir for a higher demand. Of course, the limiting value of discharge will have to take into account a minimum streamflow to the lake of Tara, in order to respect ecological priorities.

Bibliography

ARAYA, J., A. COVARRUBIAS, P. POURRUT (1995) 'Estudios hidroclimatológicos en la puna chilena'. *Jornadas del PHI/UNESCO*, Antofagasta.

GRAY, D.M. and T.D. PROWSE (1993) 'Snow and floating ice'. In: D.R. Maidment (ed.), *Handbook of Hydrology*. McGraw-Hill, Inc. New York.

Conference "Ecohydrological Processes in Small Basins", Strasbourg, 24 - 26 September 1996

Radar remote sensing for runoff processes; modelling results from the French Coët-Dan catchment

P. Gineste and C. Puech

Remote Sensing Laboratory CEMAGREF, Montpellier, France

1. Introduction

Land surface hydrology has developed in many ways in recent decades. New concepts have emerged to explain how stormflow is generated and what controls the occurrence of some particular processes, such as the influence of topography.

Due to computational advances, hydrological distributed models have flourished and become quite sophisticated as more and more of the spatial physical and geomorphologic characteristics of a watershed can be incorporated. Yet this increase in complexity does not warrant that the spatial information gained about internal flows is reliable. After a brief review of stormflow generation processes, it is argued that calibration of the model parameters on the basis of the global catchment discharge only is not sufficient in this respect.

Multi-configured radar sensors have recently offered some promise of delivering distributed data sets of moisture data which may then be used in the calibration and validation of hydrological models. But serious problems may arise from soil profile heterogeneities given a superficial measurement only. Of special interest however is the mapping of the saturated areas for their key role within the *variable source area* concept.

How can saturated areas be remotely sensed so as to further improve model predictions? An approach is illustrated with the French Coët-Dan catchment surveyed by ERS-1 SAR acquisitions every three days during the winter of 1992.

2. Stormflow generation processes

Up to the 1960s, it was generally accepted that rain water followed a surface route to streams according to the *Hortonian infiltration excess* concept (Horton, 1933). However, water flowing at the soil surface is not very commonly observed except in arid to semiarid landscapes, and wherever the soil surface is particularly degraded. The Horton concept can not explain why some very permeable watersheds can also produce a quick flood runoff. Most isotopic studies conclude that the stream water in response to a storm event is essentially 'old water' initially stored within the soil layer.

Several mechanisms have been proposed to explain the quick subsurface flows observed. Hursh (1936) described a temporary saturated subsurface flow which occurs when infiltrating water encounters an impeding or a much less permeable layer. Also, the macropores that result from decayed roots and the burrowing of animals were thought to favour a quick soil transfer (Hursh, 1944; Beven and Germann, 1982). These two mechanisms nevertheless do not necessarily imply much circulation of the water initially stored within the watershed. It was shown finally that the groundwater may also contribute to the storm runoff because of a rapid elevation of its water table owing to the capillary fringe becoming free water in response to even a little amount of infiltrated water (Vaidhianathan and Singh, 1942; Sklash and Farvolden, 1979).

First proposed by Cappus (1960), the *variable source area concept* (Hewlett, 1961; Hewlett and Hibbert, 1967) describes how the subsurface contributions mentioned previously can be

supplemented by a surface flow which occur when the saturation from below reaches the ground surface. Rain that falls on these exfiltration areas can not infiltrate and flows downslope (saturation overland flow) along with the return flow. Mostly located near the streams where they usually form a riparian waterlogged zone, the saturated areas have the ability to expand dynamically during large storms according to topography and pedology and depending on initial wetness conditions (Quinn and Beven, 1993). But they may be found wherever the soil lateral transmissivity is not sufficient to transmit the water flux from above as a result of a locally shallow effective depth and/or topographic convergence (O'Loughlin, 1981).

3. Spatial modelling and water pathways

A model should carefully be based on the correct processes dominating the watershed response if it intends to represent its internal flows. The problem in humid to temperate climates is rather complex since most of the quick flow travels through the soil itself. The computational capabilities in the late 1980s has led to the development of physical models supposed to describe the flow characteristics accurately enough to allow for assessment of the effects of land-use changes. However, physics-based models have been used quite successfully to explore theoretically the influence, for instance, of topography (Freeze, 1972), revealing great weaknesses when dealing with real catchments and their inherent heterogeneity.

How to account for preferential flows? Which data may be available to describe the soil spatial heterogeneity of a catchment? Transmissivity, for instance, is a particularly problematic parameter for incorporation into distributed models because it may vary by several orders of magnitude on a reasonably small scale (Franks *et al.*, 1996). Accepting our inability to measure it at the catchment scale, it is often lumped. How realistic is the application of the non-linear Richards' equation at the scale of a model elementary cell (of the order of a hundred meters square) while established by the small scale physics of homogenous systems (Beven, 1989)? The same applies to overland flow which may be either treated as a laterally uniform sheet or as a uniform collection of rills for the Saint-Venant equations to be used. A hydraulic resistance law is further required but implies some fitting of the observed discharge hydrograph in order to calibrate an empirical friction factor which is assumed to be constant over the whole catchment (Dunne, 1979).

Physics-based models hence are still lumped conceptual models for which parameters need calibration. The problem is the plethora of parameters owing to the discretization, that yields a group of optimal parameters sets with respect to the flow simulation; but internal flows differ for each set (Grayson *et al.*, 1992).

As an alternative to fully distributed models, simpler models based on the partial area concept are becoming quite popular. TOPMODEL (Beven and Kirkby, 1979) is based on simple approximations to physical theory while retaining the ability to make predictions distributed in space. Although the concept of an index of hydrological similarity reduces the number of lumped parameters required to just a few, the problem is still that many different parameter sets, scattered throughout the parameter space, will reproduce the observed discharges almost equally as well while the saturated area extention will be quite different. Clearly, the outlet discharge alone is not sufficient to constrain a distributed model.

4. Radar remote sensing of the saturated areas

The saturated areas concept has been described above in terms of the natural limits of various hydrological processes. Knowledge of the spatial and temporal pattern of the saturated area would not only allow assessment of where overland flow in its broader sense occurs (with subsequent implications dealing with erosion and the washing out of pollutants adsorbed on soil particles) but may also reflect the subsurface flows acting below.

However, it may be concluded from the last section that the saturated area extension may not be accurately predicted by distributed models. It would be limited to the characterization of positional

waterlogging (Merot *et al.*, 1995) disregarding human influences typical of agricultural catchments such as embanking and surface or subsurface compaction by cattle, harvesting and ploughing.

Remote sensing, on the other hand, offers a unique potential to survey the saturated areas at the catchment scale. The microwave band especially is thought to be very promising because it is not restricted by cloud cover and allows a direct areally averaged measure of the surface dielectric properties which is closely related to water content due to the particularly high dielectric constant of water (Van de Griend and Engman, 1985). It is thus generally accepted that radar backscatter increases with increasing soil moisture content. Unfortunately, most studies have used a limited range of water content below field capacity, whereas soil moisture usually reaches higher values during the wet period of the year.

Theoretical models (Autret *et al.*, 1989) nevertheless show that a saturation of the signal should first occur owing to a saturation of the soil dielectric constant at high water content (of the order of 0.5 g/cm^3). Then, as ponding appears and increases, the soil surface tends to be more specular depending on the ratio between ponding and near-saturated surfaces, and the backscattering coefficient is expected to decrease. Based on a helicopter-borne C-band scatterometer and extensive ground experiments over the Coët-Dan catchment, Brun *et al.* (1990) accordingly proposed the mapping of saturated areas using a threshold on the backscatter coefficient. A threshold value of -7 dB concerning the ERS SAR configuration was found independent of the nature of the field surface. Using a crane-mounted radar and controlled ponding conditions, Merot and Chanzy (1991) further confirmed the decrease of the backscattering coefficient when the percentage of saturated areas increases. The study described in this paper has been an opportunity to test the feasibility of the threshold detection scheme when applied to ERS-1 SAR images.

5. Synthetic results from the Coët-Dan catchment

5.1. Materials

The Coët-Dan is a 12 km^2 catchment located near the town of Naizin in the centre of Brittany, France (Lat : 48° ; Long : 357° 10'); there is a main stream in the middle of the area. Mean annual runoff is 303 mm for 711 mm mean annual rainfall. There are two secondary streams in the upper part, one of which was chosen to survey the saturated area extension simultaneously with the SAR acquisitions. Soils are deep corresponding generally to a silt loam. Gentle concave slopes cover a Brioverian schists substratum overlain by brown acidic soils and underlain by degraded hydromorphic soils and fluvents. Agriculture is intensive yet in winter the vegetation is either sparse with young winter wheat or absent (42% bare soils).

Fifteen ERS-1 PRI scenes ranging from January 28th to March 28th during the so-called ice-phase B in 1992 are considered. This period was covered by radar imagery every 3 days (except for some missing days), all of them in the ascending phase of the satellite. The images have been calibrated using the procedure given by Laur (1992). Because of the scale at which saturation usually develops at the bottom of the typically small fields of this hedged landscape, a filtering procedure has been specifically developed to exploit the multi-temporal information in the SAR images in order to derive a meaningful estimate of the surface reflectivity at the 12.5 m pixel scale (Gineste *et al.*, 1996).

5.2. Mapping saturated areas

Figure 1 presents the saturated area predictions for the ground truth zone when a threshold of -7 dB (Brun *et al.*, 1990) is applied to the filtered images for Julian days 37, 46, and 82. The only rain event of this dry period fell between the first two dates. The maximum extent of the saturated area pattern was observed on day 46. Yet the smallest predicted saturated area extension occurs on this same date and the largest predicted saturated area extension occurs on the driest image. Clearly, the specular effect is dominated by the dielectric effect within the pixels which invalidates the detection scheme that relies on it.

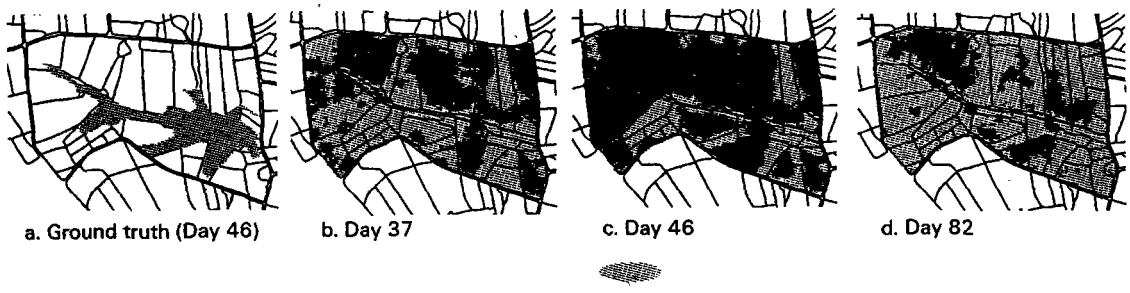

Figure 1: Predicted saturated areas (threshold at -7dB).

Difference images are more instructive for they avoid the drawback of having different absolute backscatter levels due to different vegetation covers and surface roughnesses. It was argued (Gineste *et al.*, 1996) that the backscatter seems to increase with soil moisture up to some value that may be reached before saturation, while varying little above saturation (or even slightly decreasing). This allows identification of the wettest part of the catchment provided that the two images retained bound a marked hydrologic event. Figure 2 illustrates the drying of the catchment except for the areas where the backscatter is nearly constant. A saturation cartography could not, however, be obtained for each date and the use of a pair of images may be further limited by the residual speckle and the slight inaccuracy in the SAR images calibration. Considering the whole temporal backscatter profile would, at the present time, be a safer approach for characterising the areas that are more prone to develop saturation.

An unsupervised classification based on the temporal backscatter profile after normalisation with respect to its maximum observed value has been proposed (Gineste *et al.*, 1996). It allows (Figure3) detection of changing roughness conditions (class 1) and the poorest drained areas (class 5). The rationale for it relies on the fact that saturation develops on parts of the catchment which stay wetter than the other parts because of lateral recharge, so that soil moisture variations in response to the hydrologic forcing conditions are less likely. Consequently, it is instead proposed in the following a quantitative index based on the backscatter standard deviation.

Whatever the method used to identify the saturated areas (difference images, classification technique, or backscatter standard deviation index), they are mainly found in the riparian areas of the streams and in the eastern middle part of the catchment which is a zone of cattle breeding (pers. comm., C. Cann) and perhaps an artefact due to the vegetation cover. Further investigation is necessary to assess the actual nature of the predicted non-positional saturated areas. It is important to note, however, that it is the observed differential backscatter behaviour that tends to support the partial area concept.

5.3. On constraining model predictions

The remotely sensed saturation potential index may not be used directly with hydrological models; they are limited to the characterisation of positional waterlogging while the index on the other hand is a very crude estimator of the saturation likelihood. The best fit of the ground observed saturated areas is in fact achieved through the joint use of the topographic index.

Figure 4 displays a coloured overlay of the two indexes. It shows that the radar index may help correct deficiencies in the topographic index since the red areas better fit the ground truth contour than can be achieved with the topographic index only. Fitting has been achieved through the Lookup Table (LUT) linear stretching of the indexes that allows adjustment of the weights given to each of them; a growing extent of the saturated areas predicted by both indexes is obtained by increasing the upper threshold value of the radar index (ThRsd) at which the LUT is maximum. This visual combination of the two indexes has not yet been exploited in terms of saturated area pattern predictions and it would take some account of factors other than topography.

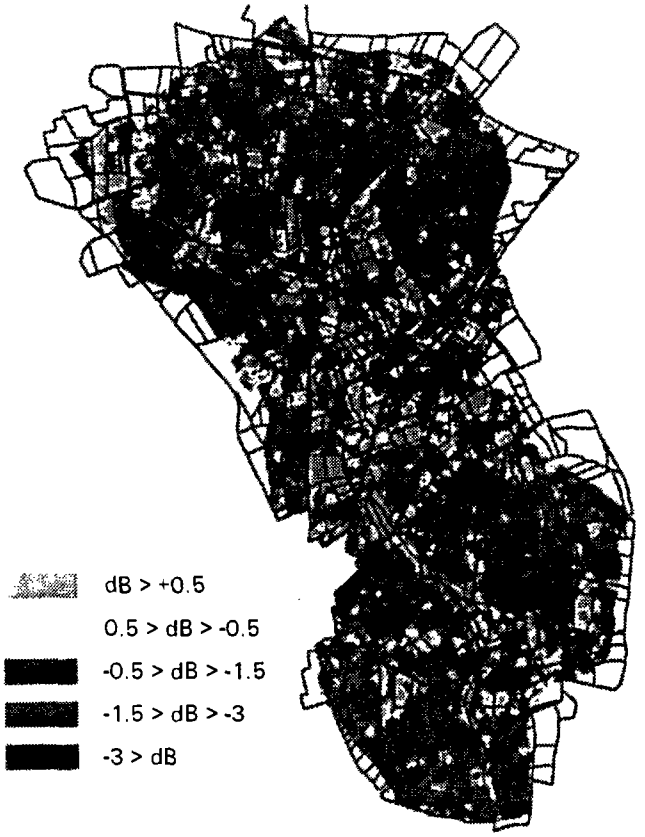

igure 2. Backscatter difference between Julian day 82 and 55

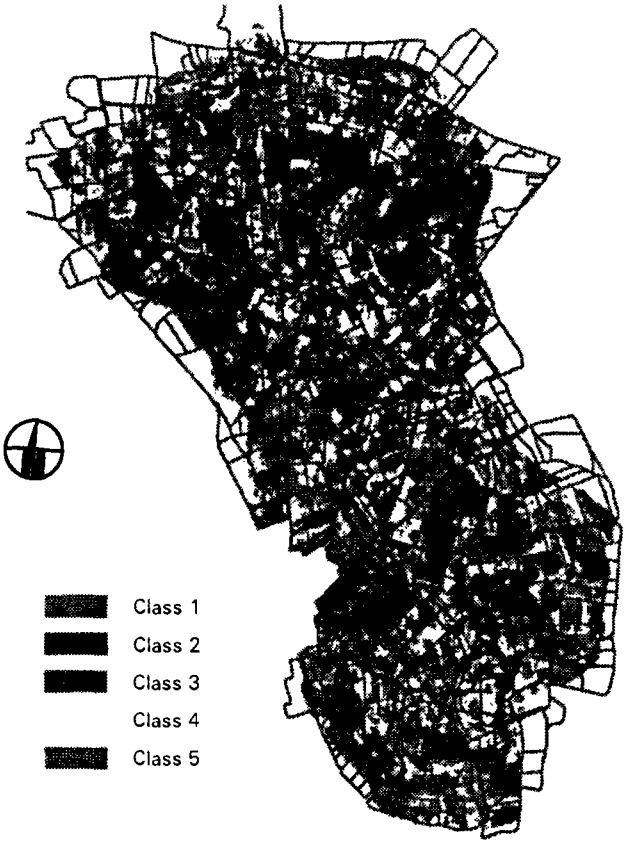

Figure 3. Unsupervised classification based on the backscatter temporal profile

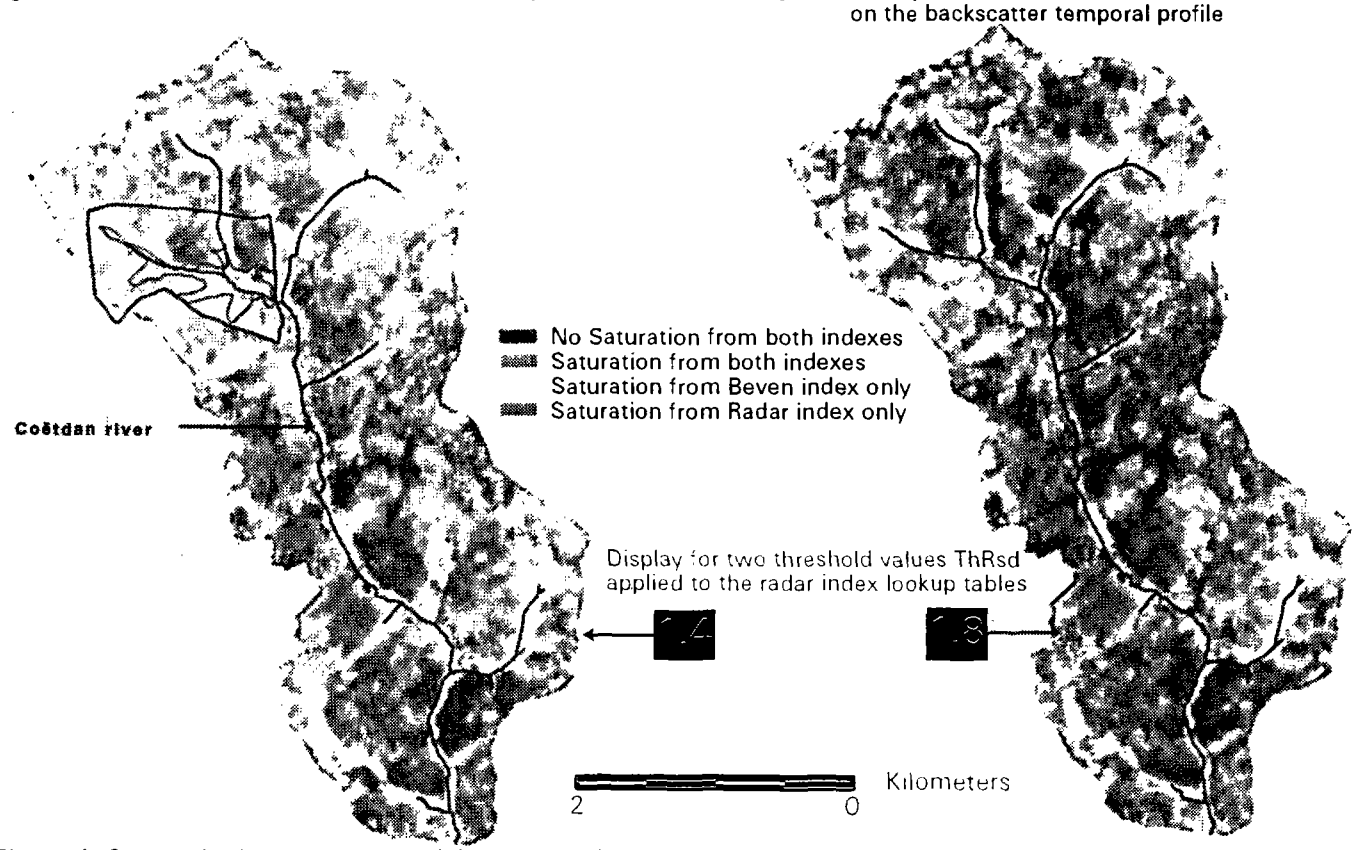

Figure 4. Composite images of potential saturation indexes

In a very recent study (Franks *et al.*, 1996), however, TOPMODEL parametrisations have been conditioned on predictions of the maximum saturated area extent in addition to the discharge data. The catchment-wide saturated area estimates were extrapolated from the correlation between the predictions derived by thresholding both indexes and the observed saturated area on day 46. Their use in constraining TOPMODEL parametrisations has been feasible thanks to the Generalised Likelihood Uncertainty Estimation (GLUE) methodology which was developed as a method for calibration taking account of multiple acceptable parameter sets. It is a Bayesian method based on Monte-Carlo simulations in which the different parameter sets may be ranked according to a subjective likelihood measure reflecting how well each set, when used for prediction, fits the observed data used for comparison. The GLUE methodology further allows updating of the likelihood weights associated with each simulation as more data or different types of data are made available, using Bayes' equation.

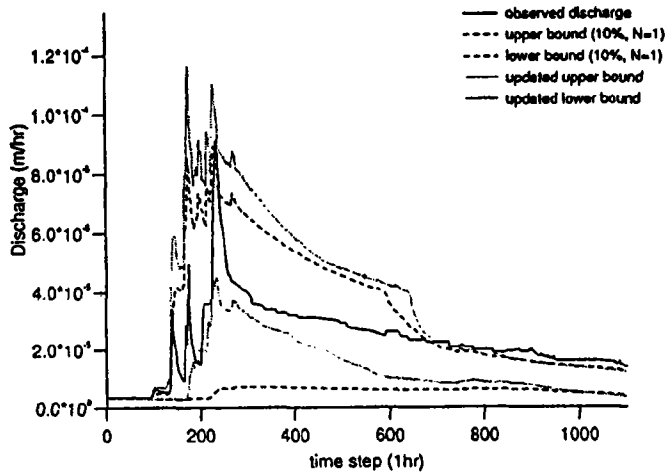

Figure 5: TOPMODEL discharge uncertainty bounds (95%) for the 92 rainfall events conditioned on 1993 - 1994 period (best 10%) then updated with the catchment maximum saturated area extension estimates.

It is shown that although uncertainty is significant in the predictions of saturated area the methodology can reject many previously acceptable parameterisations (acceptable in terms of conditioning on discharge alone). The consequence is a marked reduction in predictive uncertainty (Figure 5) and a feasible range of the catchment average lateral transmissivity parameter (1.35 - 4.95 m^2/h).

6. Conclusion

Central to the variable source area concept is the role of the saturated areas. The modelling and remote sensing approaches applied separately can identify the saturated area patterns but with uncertainty. However, the remote sensing approach has been shown to be able to constrain significantly the uncertainty associated with the modelling approach.

Bibliography

AUTRET, M., R. BERNARD and D. VIDAL-MADJAR, (1989) 'Theoretical study of the sensitivity of the microwave backscattering coefficient to the soil surface parameters'. *Int. J. Remote Sens.*, 10(1), 171-179.

BEVEN, K. (1989) 'Changing ideas in hydrology - The case of physically-based models'. *J. Hydrol.*, 105, 157-172.

BEVEN, K.J. and A.M. BINLEY (1992). 'The future of distributed models: Model calibration and uncertainty prediction'. *Hydrol. Process.*, 6, 279-298.

BEVEN, K. and P. GERMANN (1982) 'Macropores and water flow in soils'. *Water Resources Research* 18 (5), 1311-1325.

BEVEN, K.J., and M.J. KIRKBY (1979) 'A physically based variable contributing area model of basin hydrology'. *Hydrol. Sci. Bull.*, 24(1), 43-69.

BRUN, C., R. BERNARD, D. VIDAL-MADJAR, C. GASCUEL-ODOUX, P. MEROT, J. DUCHESNE and H. NICOLAS (1990) 'Mapping saturated areas with a helicopter-borne C band scatterometer'. *Water Resour. Res.*, 26(5), 945-955.

CAPPUS, P. (1960) 'Etude des lois de l'écoulement: Application au calcul et à la prévision des débits: Bassin expérimental d'Alrance'. *Houille Blanche*, 15(A), 493-520.

DUNNE, T. (1979) 'Field studies of hillslope flow processes'. *Hillslope Hydrology*, Kirkby M. J. (ed.), Wiley, Chichester, U.K.

FRANKS, S., P. GINESTE, K. BEVEN and P. MEROT, (1996) 'On constraining the predictions of distributed models: The incorporation of fuzzy estimates of saturated areas into the calibration process'. *Water Resources Research*, submitted.

FREEZE, R.A. (1972) 'Role of subsurface flow in generating surface runoff. 2.Upstream source areas'. *Water Resour. Res.* 8(5), 929-941.

GINESTE, P., C. PUECH and P. MEROT (1996) 'Radar remote sensing of the source areas from the Coët-Dan catchment'. *Hydrol. Process.*, submitted.

GRAYSON, R.B., I.D. MOORE and T.A. MCMAHON (1992) 'Physically Based Hydrologic Modelling, 1. A terrain-based model for investigative purposes'. *Water Resour. Res.*, 28(10), 2639-2658.

HEWLETT, J. D. (1961) 'Catchment management'. In: *Report for 1961 Southeastern Forest Experiment Station*, U.S. For. Serv., Asheville, N.C.

HEWLETT, J. D. and A.R., HIBBERT (1967) 'Factors affecting the response of small catchments to precipitation in humid areas'. in *Proceedings of the International Symposium on Forest Hydrology*, pp. 275-290, Pergamon, New York.

HORTON, R.E. (1933) 'The role of infiltration in the hydrologic cycle'. *Trans. Am. Geophys. Union* 14, 446-460.

HURSH, C.R. (1936). 'Storm water and adsorption', Report of the Comittee on Absorption and Transpiration, *Trans. Am. Geophys. Union* 17, 301-302.

HURSH, C.R. (1944). 'Report of the sub committee on subsurface flow'. *Trans. Am; Geophys. Union*, 25, 743-746.

LAUR, H. (1992) 'ERS-1 SAR calibration: Derivation of backscattering coefficient s° in ERS-1'. *SAR.PRI products, Issue 1*, Rev. 0, ESRIN, ESA.

MEROT, P. and A. CHANZY (1991) 'Mesure de l'humidité du sol par radar dans des conditions d'excès d'eau'., *paper presented at 5th ISPRS International Colloquium : Mesures physiques et signatures en télédétection, Int. Soc. of Photogramm. and Remote Sens.* , Val d'Isère, France, Jan. 14-18.

MEROT, P., B. EZZAHAR, C. WALTER and P. AUROUSSEAU (1995) 'Mapping waterlogging of soils using digital terrain models'. *Hydrol. Process.*, 9, 27-34.

O'LOUGHLIN, E.M. (1981) 'Saturated regions in catchments and their relation to soil and topographic properties'. *J. Hydrol.*, 53, 229-246.

QUINN, P.F. and K.J. BEVEN (1993) 'Spatial and temporal predictions of soil moisture dynamics, runoff, variable source areas and evapotranspiration for Plynlimon, Mid-Wales'. *Hydrological Processes*, 7, 425-448.

SKLASH, M.G. and R.N. FARVOLDEN (1979) 'The role of groundwater in storm runoff'. *J. Hydrol.*, 43, 45-65.

VAIDHIANATHAN, V.I. and C. SINGH (1942) 'A new phenomenon in the movement of the free water-level in a soil and its bearing on the measurement of the water table'. *Proc. Ind. Acad. sci.*, 15, 264-280.

VAN DE GRIEND, A.A. and E.T. ENGMAN (1985) 'Partial area hydrology and remote sensing'. *J. Hydrol.*, 81, 211-251.

Modelling rainfall - runoff processes in the Hupselse Beek research basin

P.M.M. Warmerdam, J. Kole and J. Chormanski

Department of Water Resources, Wageningen Agricultural University, The Netherlands

1. Introduction

Mathematical modelling is an important tool for increasing the knowledge of rainfall-runoff processes in river basins. In the relatively flat and permeable basins in the eastern and southern part of the Netherlands runoff process studies are generally focused on the interaction between rainfall, evapotranspiration, soil moisture, groundwater storage and runoff. In these permeable basins the process of runoff generation depends largely on the antecedent moisture conditions. If rain intensity and initial soil water content are low all rainwater may infiltrate. Water percolated to the groundwater table may produce a slow response of groundwater outflow. However, continued rainfall with increasing soil water content and groundwater storage may reduce infiltration and some quick flow might be generated. Significant sources of quick flow relate to surface runoff from temporarily waterlogged areas, lateral seepage through the upper zone of cultivation and preferential flow through macropores of river banks. Tiledrains, if present, also contribute to quick flow. For a heterogeneous system, as is apparently a characteristic of all basins, it is usually difficult to trace the quick and slow components of the runoff back to their origins of the typical hydrological processes in the basin. Based upon these considerations the Wageningen rainfall-runoff model was developed in the research basin of the Hupselse Beek in the Netherlands to identify the various components of the runoff process.

The Wageningen model was developed in the 1970s and initially concentrated on the rainfall-runoff studies in the winter season when no special attention for the evapotranspiration process was required. While keeping its structure simple the model has gradually been modified and improved when new data and knowledge of the processes involved became available.

This paper presents results of the overall performance of the model and the functioning of the separate components when using data over the period 1988-1993.

2. Description of the catchment area

The alluvial catchment of the Hupselse Beek is situated in the east of the Netherlands. The area covers 6.5 km^2, and varies in altitude between 24 m and 33 m above mean sea level. The Hupselse Beek stream runs from east to west through this slightly undulating rural landscape.

The top of the underlying thick tertiary formation of marine clays is found at shallow depths in the east and slopes down to the west. These marine clays are covered with younger sandy deposits. The thickness of this sand aquifer varies between 1 m and 8 m from east to west. Consequently the transmissivity and the storage capacity of the soil are relatively small. Land-use is mainly agricultural, with about 70% of the area covered with grass, 20% arable land and 6% covered with trees. The groundwater table in this region is shallow, fluctuating between about 50 cm below the surface in winter and about 1.50 m in summer. The catchment is well drained and about 50% of the area has tiledrains. Lateral seepage and some surface runoff from temporary waterlogged surfaces during prolonged wet periods may contribute to peak discharge.

3. Instrumentation and data collection

In the Hupselse Beek catchment precipitation and discharge data have been collected from 1970. At a central meteorological station radiation, air temperature, humidity and wind speed have been observed with an automatic data collection system since March 1976. Between March 1976 and October 1984 profiles of temperature, humidity and wind were observed to determine the sensible heat flux to the atmosphere as one of the components used in the energy balance. In this period accumulated values of actual evapotranspiration computed with the energy balance method were in good agreement with values derived from the water balance of the catchment. The mean annual actual evapotranspiration in this period amounts to 490 mm. Potential evapotranspiration has been determined according to the method of Thom and Oliver up to 1988 (Thom and Oliver, 1977). Since then the Makkink reference evapotranspiration (De Bruin, 1987) is used to compute potential *ET*. The Royal Dutch Meteorological Institute (KNMI) continued these observations with a new on-line data collection system in 1989.

A recording groundlevel raingauge is used to measure rainfall at intervals of 20 minutes. Streamflow is measured with an *H*-flume. Water stages are observed every 20 minutes and processed to runoff data for time units of 3 hours and 24 hours. Groundwater depths are measured in a network of 18 observation wells.

4. Model description

Based upon the hydrological conditions of the relatively flat and permeable catchment areas in the Netherlands the Wageningen model has two branches, expressing the quick and slow components of the runoff process as shown in Figure 1. The flow process through the quick branch is represented by a convective-diffusion model for physically non-steady flow with upstream inflow (Nes, van de and Hendriks, 1971). The instantaneous unit hydrograph is expressed by

$$u(0,t) = \frac{x}{2\sqrt{\pi D t^3}}\, e^{-(x-At)^2/4Dt} \qquad (1)$$

with D the diffusion coefficient, A the translation coefficient, x the distance along the river and t the continuous time variable. Substituting $E = \frac{x}{2\sqrt{D}}$ and $F = \frac{A}{2\sqrt{D}}$, the equation is simplified to a two parameter model. When the rainfall is expressed as a series of inputs over successive intervals T the response $u(T,t)$ of (1) can be calculated by numerical integration.

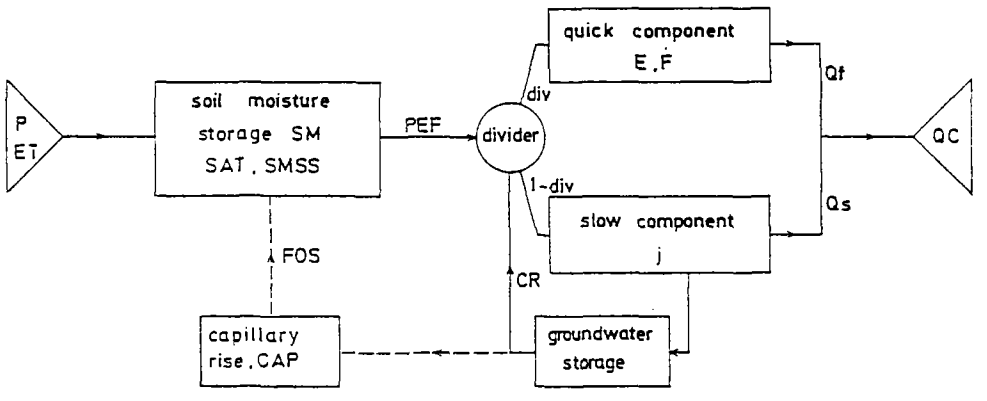

Figure 1: Flow diagram of the Wageningen mode: Qf and Qs are the computed fast and slow runoff components respectively and QC represents the total computed runoff.

For the slow component a model of non-steady groundwater outflow from a horizontal aquifer into the drainage channel is used (Kraijenhoff, 1958). According to the Dupuit-Forchheimer assumption the following instantaneous unit hydrograph of groundwater flow is derived:

$$u(0,t) = \frac{8}{\pi^2}\frac{1}{j}\sum_{n=1,3,5...}^{n=\infty} \exp\,(-n^2\, t / j) \qquad (2)$$

where $j = \frac{1}{\pi^2}\frac{\mu L^2}{kD}$, a characteristic time parameter with m for active porosity of the soil, kD for transmissivity of the aquifer and $1/L$ the density of channel system.

From this instantaneous unit hydrograph the ordinates of the unit hydrograph for successive intervals T can be computed. The effective precipitation (PEF), which is that part of rainfall that contributes to the runoff, is allocated to both runoff components using a divider (DIV) which is functionally (through a parameter CR) dependent on the volume of groundwater stored. A gradual increase of groundwater storage due to continued rainfall implies that an increasing part of the rainfall follows quicker routes towards the channel system.

The model uses a moisture budgeting procedure, based upon a soil moisture storage reservoir to calculate the effective precipitation (PEF) and its time distribution. Precipitation (P) and capillary upward flow (CAP) replenish the reservoir, and actual evapotranspiration (ET) and effective rainfall (PEF) deplete the reservoir. The actual soil moisture storage at time i (SM_i) is then:

$$SM_i = SM_{i-1} + P_i - ET_i + CAP_i - PEF_i \qquad (3)$$

Effective precipitation is computed when the actual level of the soil moisture reservoir exceeds a threshold (SMSS):

$$PEF_i = RESM \bullet \frac{SM_i}{SAT}(SM_i - SMSS) \qquad (4)$$

where SAT is the maximum moisture storage (mm) at saturation, SMSS is the moisture storage between mean groundwater depths in spring and summer, and RESM is a parameter representing the rate of depletion.

When SM values drop below the threshold SMSS, effective rainfall is zero and evapotranspiration may partly be provided by capillary rise which is functionally dependent on soil moisture deficit (SMSS-SM) and the volume of groundwater storage. When the actual soil moisture is above the SMSS threshold capillary upward flow is zero. FOS (Figure 1) is a parameter to be evaluated.

If time series of potential ET data are used as input to the model a cosine reduction function decreases the apparent evapotranspiration from a soil moisture deficit (SM < SMSS).

The six parameters of the model E, F, j, FOS, CR and RESM are optimised using the Marquardt algorithm, where the constants SMSS and SAT are estimated for the whole basin from soil physical characteristics. The goodness of fit or model efficiency is expressed as the percentage of the initial variance F_o^2 of the observed runoff data explained by the model:

$$RE = 100\frac{F_o^2 - F^2}{F_o^2}\% \qquad (5)$$

where F^2 the sum of squares of the residuals between observed and computed flows.

5. Results of model application

The model uses records of rainfall and evapotranspiration to compute the runoff for each time interval. Observed runoff is used to adjust the parameter values of the model so that a best fit is obtained between calculated and actually observed runoff rates. The results of model performance over the period 1988 to 1993 are reported here (Chormanski, 1995). The winter period of 1991 is not fully considered because of ice and snow. Except 1989 this period was relatively wet. In 1993, for example, the total rainfall was 1011 mm whereas the long-term mean (1972-1988) amounts to 780 mm. The total runoff was 445 mm as against 290 mm in a normal year. That year (1993) showed the lowest model efficiency of 81%. The highest efficiency achieved was 92% for the year 1992, for which rainfall and runoff were slightly below average.

Generally, peak flows and the time to peak are simulated quite well. Some peak events show rather large differences in runoff rates, but in general minor differences exist between calculated and observed peak values. The recession limb of the hydrograph is generally in good agreement with the observed one. However, in some cases relatively large differences can be observed.

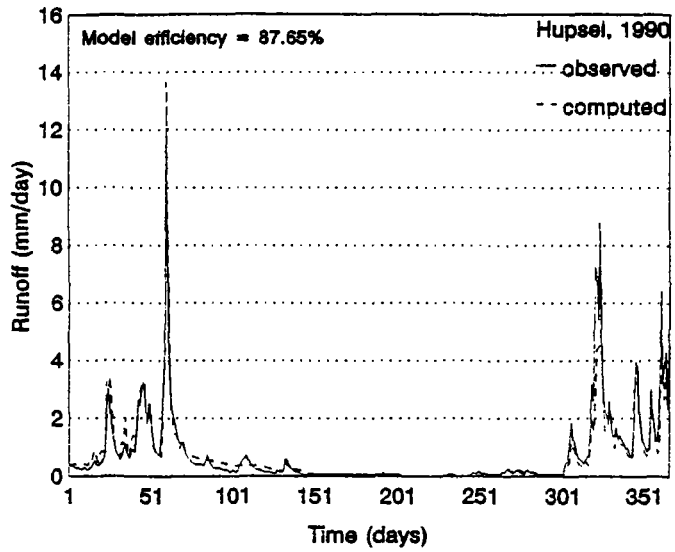

Figure 2: Observed and simulated runoff of the Hupselse Beek catchment from January 1 to December 31, 1990.

Figure 2 shows the observed and simulated hydrographs for 1990. Although most of the peaks are calculated very well, that of day 320 stands out. An error in rainfall is most likely. The quick and slow components of the hydrograph calculated by the model are shown in Figure 3. On average, 40% of rainfall is routed through the quick component. However, depending on the wetness of the catchment, values vary between 28% and 60%.

The autumn period of 1993 was extremely wet as shown in Figure 4. The rising groundwater table induced an increasing percentage of quick runoff. In this wet period computed peaks are slightly overestimated. Due to temporary storage of water on the surface the computed peak of an extreme rainstorm of 45 mm at day 365 considerably exceeds the observed peak value.

Figures 2 and 4 show that the soil moisture budget method as used in this model calculates the time distribution of effective rainfall satisfactorily, even after periods of sustained drought. However, during the relatively wet summer of 1993 the peak discharge of mid-August (Figure 4, around day 220) was considerably underestimated.

Similar results of model performance to these presented here have been obtained with data of other periods and of other catchments in the Netherlands (Warmerdam *et al.*, 1993).

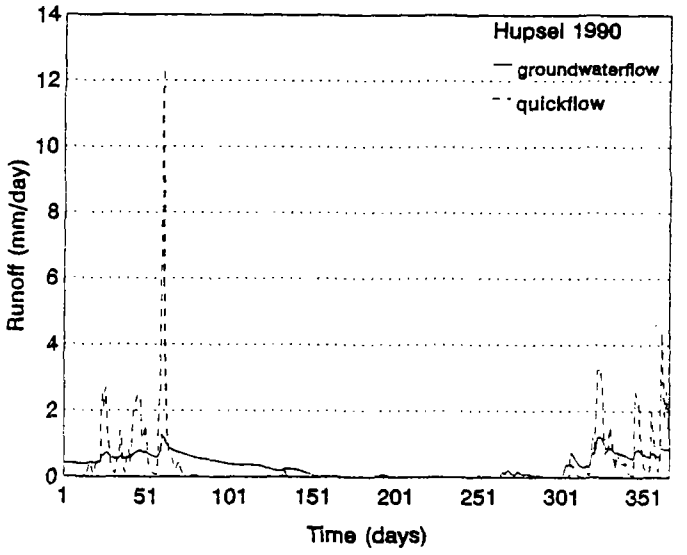

Figure 3: Daily rates of the computed quick and slow components of the runoff in the Hupselse Beek, 1990.

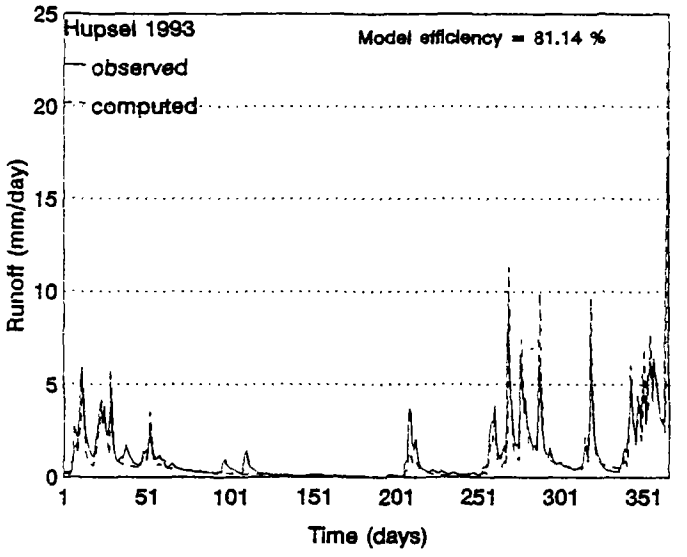

Figure 4: Observed and simulated runoff of the Hupselse Beek catchment from January 1 to December 31, 1993.

6. Conclusions

The physically based conceptual Wageningen model was developed and evaluated in an extensive study in the research basin of the Hupselse Beek in which the separate components of the rainfall-runoff process could be verified by measurements in the field. The model visualizes the interaction between rainfall, evapotranspiration, capillary rise, quick flow and groundwater flow. In general the model performed adequately, both for the wet and dry seasons. In the continued attempts to improve the model attention will be given to a soil moisture flow procedure instead of a budgeting method.

Bibliography

BRUIN, H.A.R. DE (1987) 'From Penman to Makkink'. TNO: Committee on hydrological research, The Hague. *Proceedings of 'Evaporation and weather'*, information No. 39:5-31.

CHORMANSKI, J. (1995). 'A study on application of the deterministic conceptual model - the Wageningen rainfall-runoff model on the Hupselse Beek catchment'. *MSc-thesis.* Dept. of Water Resources. Agricultural University Wageningen. 52 p.

KRAIJENHOFF VAN DE LEUR, D.A. (1958) 'A study of non-steady groundwater flow with special reference to a reservoir coefficient'. *Ingenieur*, Utrecht 70(19), p. 87-94.

NES, TH.J. VAN DE and M.H. HENDRIKS, (1971). 'Analysis of a linear distributed model of surface runoff'. Lab. of Hydraulics and Catchment Hydrology, Wageningen Agricultural University. *Report 1.*

THOM, A.S. and H.R. OLIVER (1977) 'On Penman's equation for estimating regional evaporation'. *Quart. J. Roy Met. soc.* No. 103, 345-357.

WARMERDAM, P.M.M., J. KOLE and J.N.M. STRICKER (1993). 'Rainfall runoff modelling in the research area of the Hupselse Beek'. *International Symposium on Runoff and Sediment yield.* (eds. K. Banasik) Warsaw.

Water balance, runoff formation and components from two rainfall-runoff models for a small agricultural basin with irrigation in quaternary northern Germany

A. Herrmann[1], M. K. Kim[1] and J. Buchtele[2]

[1] *Institute for Geography and Geoecology, Technical University, Braunschweig, Germany*
[2] *Institute of Hydrodynamics CAS, Prague, Czech Republic*

1 Introduction

Conceptual modelling techniques and sophisticated field measurements have been applied in a small study basin in the northern German lowlands to ascertain the influence of agricultural activities on runoff generation and water balances, and to quantify the artificial influences on runoff changes.

The hydrological investigations form part of a comprehensive programme of which the other components have recently been published (Herrmann and Ueberschär, 1993). The experience gained in the foregoing research indicated that the combined experimental works and modelling techniques gave results which are theoretically sound and practically acceptable. In this long-term programme different models of the rainfall-runoff process are being applied, and geophysical and tracer techniques are being used for verification of assumptions regarding flow paths and runoff components (Schwarze *et al.*, 1991). Experiments with two other models have been carried out for the present investigation; the BROOK-TOP model and the SACRAMENTO soil moisture accounting model (SAC-SMA). Time series of about six years are now available for the Eisenbach research basin, thus permitting further analyses in some aspects to those of Herrmann and Ueberschär (1993).

The present study of runoff generation in the agricultural Eisenbach basin largely profits from former research in the well-known forested Lange Bramke basin of 0.76 km² situated in the Harz Mountains (Herrmann *et al.*, 1989). In Lange Bramke, extensive hydrological tracer, geophysical and hydraulic experiments led to some important results about the age and pathways of water, and about runoff generation. Furthermore, the research in Lange Bramke suggests that the proportions of simulated runoff components using two rainfall-runoff models (Buchtele *et al.*, 1996) are in relatively good agreement with the hydrological tracer findings.

A very practical intention of the present study is to ascertain whether it would be possible to evaluate independently the required volumes of irrigation water because these amounts of water are regulated by law, but frequently surpassed by far. The main objective is to see to what extent both rainfall-runoff models selected are suitable tools to describe runoff processes in a sub-drained agricultural area.

2 Study area and models used

2.1 Eisenbach study basin

The Eisenbach agro-ecological study basin of 4.25 km² is between 62 m and 109 m above mean sea level and is situated 70 km north of Braunschweig. The upper shallow aquifer is made up by later Saalian morainic and glaciofluvial sediments. Flat areas near the river channel are mostly drained, and major crops, i.e. winter rye and barley, summer barley, potatoes and sugar beet, are irrigated. Irrigation measures are necessary due to insufficient summer precipitation of 300 mm per half-year on average. Accordingly, annual runoff is considerable, amounting to 535 mm compared to 625 mm of measured precipitation.

The following daily time series have been made available for simulation of rainfall-runoff processes between 1989 and 1994: precipitation, air temperature and discharge. Groundwater levels are measured at about 20 sites, and 12 time series are shown in Fig. 4. The main reason for such detailed observations is to allow statistical assessment of groundwater behaviour and investigation of the relationship between groundwater storages and outflows, i.e. to evaluate the hydraulic consequences of exfiltration as previously published (Herrmann and Ueberschär, 1993). In contrast to the flood events analyzed there, the present experiments concern longer time series, thus allowing evaluation of long-term water regimes.

Evapotranspiration has been assessed in two alternative ways:

(a)the SAC-SMA model uses as input evapotranspiration which represents the requirements of the existing vegetation cover by considering its seasonal development;
(b)the BROOK-TOP model computes actual evapotranspiration using air temperature, solar radiation and wind velocity.

2.2 Models applied

The BROOK90 and SAC-SMA models which are both applied to the Eisenbach basin have recently been tested at different scales in Central Europe. The experiences gained so far with these tools, and comparisons of results from different geomorphological conditions, allow not only the identification of optimal and/or physically realistic parameter values, but also comparison of the proportions and dynamics of the water balance and its runoff components. Both models have been introduced elsewhere (Buchtele *et al.*, 1996), and comprehensive information can be found in the relevant literature (Burnash *et al.*, 1973; Federer, 1993). In the current context, it is worth noting important features with respect to the topic, i.e. the physically-based BROOK model uses a hydraulic concept for description of soil moisture (Clapp and Hornberger, 1978), while the SAC-SMA model assumes that the temporal variations of water content in its soil zones (reservoirs) correspond to a hydrological concept. The groundwater module from TOPMODEL (Beven *et al.*, 1995) has been used instead of the original linear storage concept for more adequate representation of reality with BROOK-TOP.

Runoff is considered by both models to have:

(a) six components in the SAC-SMA model: PRM (primary baseflow [long-term]), SUP (supplementary baseflow [seasonal]), INT (interflow), SUR (surface flow) particularly including direct runoff from temporarily (DIR) and permanently impervious areas (IMP);
(b) four components in the BROOK-TOP model: GWFL (groundwater flow), DLFL (downslope flow), BYFL (bypass flow) and SRFL (surface flow) with (BYFL+SRFL) = direct flow (DIR).

3 Simulation results

3.1 Flow regimes

Flow simulations with the SAC-SMA and BROOK-TOP models compared with observed discharge are shown in Fig. 1. Accuracy of the simulations is not acceptable at all times and this is a specific problem of implementing the models for this basin. Accordingly, by applying just the measured precipitation data and not considering the hydrological effects of the spray irrigation system operated by farmers the resulting errors of simulation are sometimes considerable. The deviations of simulated from observed discharge are more apparent during the vegetation growing season, and less evident in winter. Another problem is the much less steep recession limbs from SAC-SMA compared to BROOK-TOP simulations and to the observations, indicating that the size of the subsurface reservoir has been overestimated.

As a result, large discrepancies are apparent in Fig. 1, and the large errors of simulation in Table 1 reflect this effect caused by irrigation. This assumption is also supported by the fact that the flow

measurements with a Venturi flume and Seba limnigraph should provide rather accurate values, and that the measured precipitation at one station inside the basin should be a reasonable representation of actual areal precipitation in the small and flat catchment area. Despite this situation, several statistical characteristics of simulations are unfavourable as indicated in Table 1.

TABLE 1: Statistical characteristics of simulation accuracy obtained from SAC-SMA for three Central European basins

No.	Basin		Area [km^2]	Accuracy characteristics		
				R	Monthly |_| [%]	Monthly RMS [%]
1	Eisenbach	without irrigation	4.25	0.665	34.5	46.8
2		with irrigation		0.721	25.8	33.1
3	Lange Bramke		0.76	0.914	15.2	19.1
4	Liz-Spulka(*)		0.9	0.817	15.8	23.7

R correlation coefficient of observed and simulated daily discharge
|_| average absolute error of monthly flow [%]
RMS monthly root mean square error [%]
(*) Experimental basin in Sumava Mts. of the Institute of Hydrodynamics, Czech Academy of Sciences

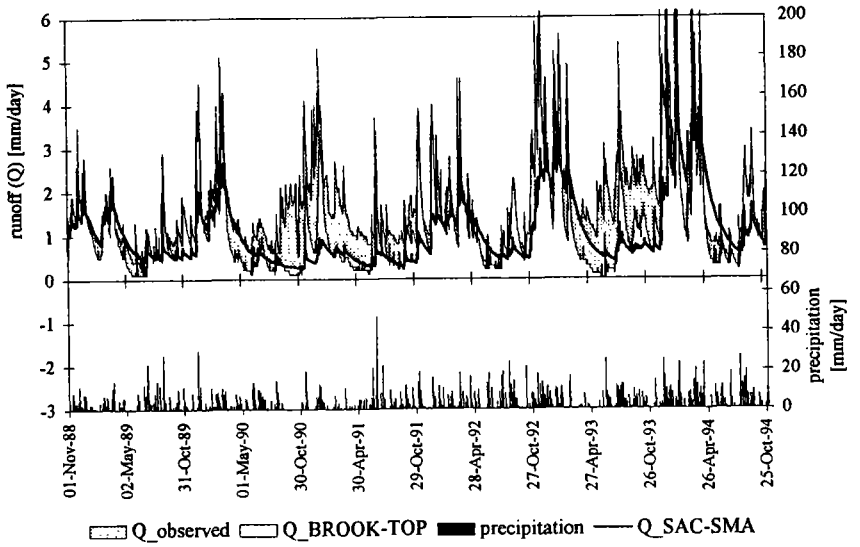

Fig. 1: Observed and simulated discharge of Eisenbach river flows obtained from the SAC-SMA and BROOK-TOP models without considering irrigation.

Unfortunately, there are no reliable measurements available to quantify the volumes of irrigation water. Therefore, rough estimates of irrigation during the period May to September for rainless and rainy periods of P < 0.9 mm/day is 1-2 mm/day. Table 2 provides a summary of water balance components for the whole period from BROOK-TOP simulations. It includes also irrigation water inputs and net groundwater inflows, and measured and simulated monthly runoff with the latter considering also SAC-SMA model outputs and additional fluxes.

TABLE 2: Water balance and runoff components for the Eisenbach basin obtained from SAC-SMA and BROOK-TOP model applications

Total BROOK-TOP model input: 782 [mm/year]			Evapo-transpi-ration	Evapo-ration	Transpi-ration	Total runoff	Direct flow	Inter flow	Groundwater (gw.) flow	
Precipi-tation	Estim. irrigat-ion	Estim. net gw. inflow	249	124	125	534	40	0	494	
623	140	19								
Runoff components of SAC-SMA model [l/s]						63.7	SUR + IMP + DIR 4.5	INT 1.5	SUP 43.4	PRM 14.3
Component runoff in percent of total runoff			SAC-SMA model			100%	7%	2.4%	68.3%	22.3%
			BROOK-TOP model			100%	SRFL +BYFL 7.5%	DSFL 0%	GWFL 92.5%	

Agreement between observed and simulated runoff is still not as satisfactory as for instance for Lange Bramke basin (cf. Table 1). The reasons are as follows.

The poor assessment of the irrigation effect e.g. extraordinary low flows in 1992, indicate that during the vegetation growing period of that year excessive irrigation was probably practised. However, for simulation it was not possible to assume respective increase of inputs, otherwise simulated flows would have been too large. This would mean that irrigation does not affect flow behaviour in the basin in any circumstance. Also, since irrigation is not performed uniformly over the whole area, application of irrigation water on fields far away from river reaches and ditches apparently does not directly contribute to basin runoff due to the hydrogeological structure of the system.This latter point obviously fits the phenomena occurring during flood events as previously discussed in Herrmann and Ueberschär (1993).

3.2 Groundwater storages

The SAC-SMA model also provides as an output the simulated amounts of soil moisture and groundwater storages. In Fig. 2 can be found two alternative graphs: one with, and the other without, assumed irrigation. However, the irrigation effect seems to be more or less negligible. This result is also in agreement with previous findings from the BROOK90 model (Buchtele *et al.*, 1996) where the trials have been made to omit - computationally - summer precipitation. The result then was only a slight change in runoff in comparison to the reverse situation, i.e. of suppressed winter precipitation.

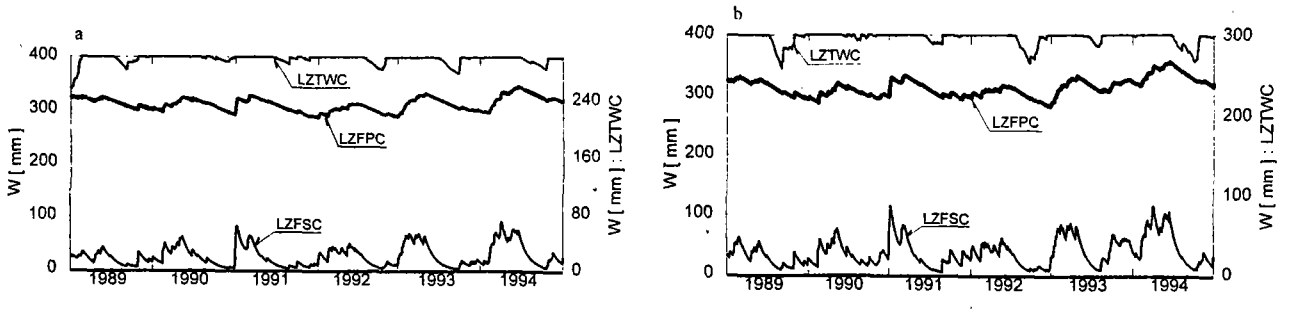

Fig. 2: Soil and groundwater storages (a) without and (b) with irrigation as simulated with SAC-SMA (LZTWC: soil moisture; LZFSC resp. LZFPC: groundwater storages providing seasonal resp. long-term baseflow).

However, even if some increase of water in SAC-SMA model zone LZFSC (Lower Zone Free Supplementary Content - providing seasonal baseflow) is noticeable, it is necessary to consider these results as an approximate picture of reality in the given area for two reasons: the problem is much more complex due to the fact that the irrigation water is abstracted from the same hydrogeological system; and the modelling tool applied is a lumped conceptual model which does not contain any hydraulic algorithm for description of water in motion.

A useful picture of the groundwater situation is provided by Fig. 3 which shows the time series of observed groundwater levels. The variations seem to be quite synchronous implying that the study area is relatively homogenous at macroscale. However, in Fig. 4 data series are also displayed for the groundwater storages LZFPC (Lower Zone Free Primary Content - i.e. the source of long-term baseflow) as computed from the SAC-SMA model. Similar tendencies in both kinds of series are visible. Furthermore, the observed groundwater level exhibits in some cases an exceptional shape contrary to usually quick rise and slow recession. The uncommon quick decrease of the recession limb cannot be explained by pumpings of water for irrigation purposes during summer months because it is taken from a second lower aquifer at 12-13 m below surface, or by any other field hydraulic effect. The reason for the unusually rapid recession limb is suspected to be an artefact of the model concept itself.

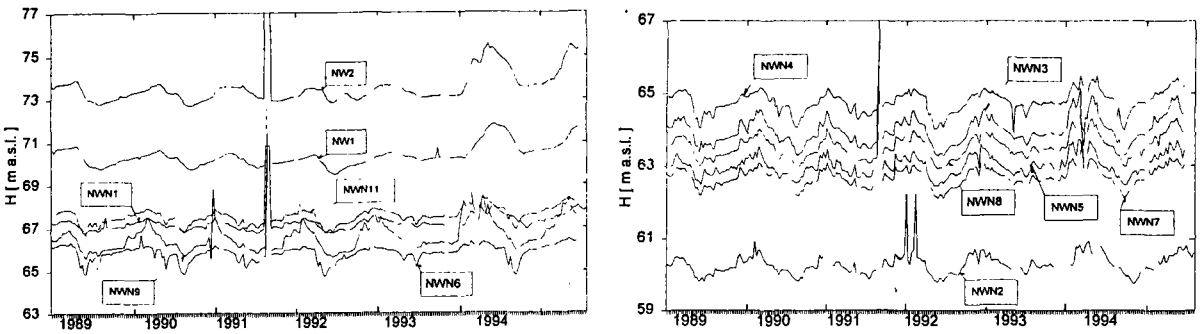

Fig. 3: Development of groundwater tables in several observation wells in the Eisenbach basin.

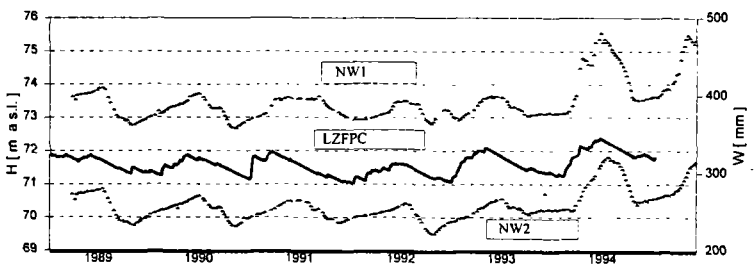

Fig. 4: Comparison of observed groundwater tables in two observation wells and simulated groundwater storages LZFPC in the Eisenbach basin.

3.3 Runoff components

Fig. 5 illustrates the runoff components simulated by the SAC-SMA model. It shows also the results obtained for the mountainous basins of Lange Bramke in the Harz Mountains, and Kosatky Creek in the Cretaceous area of Central Bohemia. In both cases, the groundwater sources are very important for runoff generation. However, in the flat Quaternary Eisenbach basin the proportion of runoff which could be

attributed to overland flow, i.e. including surface runoff and runoff from impervious parts of basin, are nearly negligible. This is the reason why different time ranges were used for presentation of basin outputs here. If a whole year for the Eisenbach were to be displayed in one graph, the three upper (short-term) runoff components would not be noticeable. The average balance of a whole year's cycle is shown in Table 2.

In addition to the comparison with the Lange Bramke area of fractured Paleozoic bedrock the outputs of simulations are available for the Cretaceous north-eastern Bohemian Metuje River basin, which allows comparison of the proportions of long-term baseflow (PRM) and seasonal baseflow (SUP) (Buchtele *et al.*, 1996). For instance, the ratio PRM:SUP is quite opposite: instead of approximately 70:20 for Lange Bramke it is 20:70 there (Table 2). From BROOK-TOP, GWFL=92.5%, DSFL=0%, and DIR=7.5% are found (Table 2 and Fig. 6).

One could suppose that in the Eisenbach basin the groundwater changes would be similar to those of the Cretaceous area. However, it seems that the conditions which have been discussed during the initial stage of the research by Herrmann and Ueberschär (1993) are again confirmed, i.e. exfiltration phenomena affected by pulse pressure transmission etc.

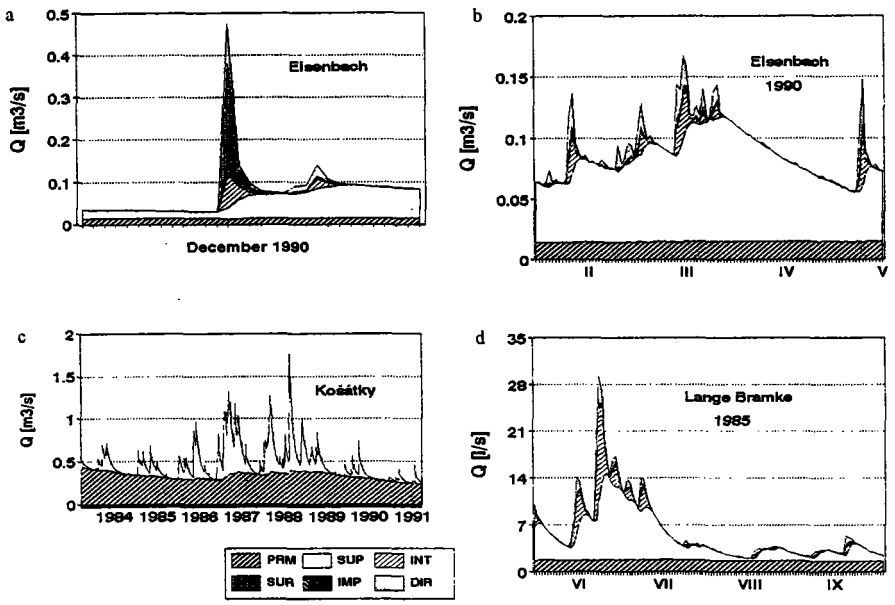

Fig. 5: Runoff components as simulated by the SAC-SMA model: Eisenbach basin (a) including surface flow during winter and (b) with prevailing seasonal baseflow; (c) Kosatky river, Central Bohemia; and (d) Lange Bramke, Harz Mts.

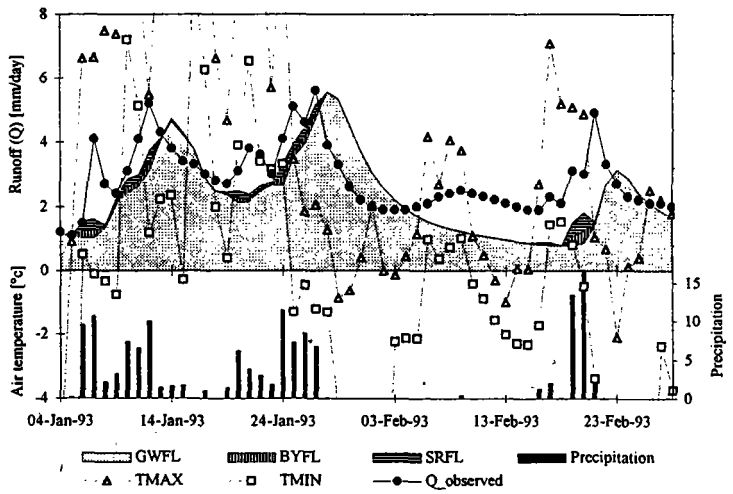

Fig. 6: Example for runoff components for the Eisenbach basin as simulated with BROOK-TOP model.

4 Conclusion

Runoff and groundwater level analyses and hydrological simulations carried out for the Eisenbach agro-ecological research basin in the lowlands of northern Germany, which had as a main goal to evaluate the dynamics of rainfall-runoff process in these specific conditions, have indicated the influence of irrigation on flow regime and areal water balance.

The experiments confirmed the dominant role of groundwater storage in runoff generation in the whole year's cycle. Comparison of observed groundwater levels and simulated groundwater storages exhibits similar tendencies, indicating the ability of simulations to provide the basis for the assessment of groundwater resources development over several years.

Bibliography

BEVEN, K., LAMB, R., QUINN, P., ROMANOWICZ, R. and J. FREER (1995) 'TOPMODEL'. In: V.J. Singh (ed.) *Computer Models of Watershed Hydrology*. Water Resour. Publ., Littleton Col., USA.

BUCHTELE, J. (1993) 'Runoff changes simulated using a rainfall-runoff model'. *Water Resour. Management* Vol. 7, No. 8, p. 273-287.

BUCHTELE, J., V. ELIAS, M. TESAR and A. HERRMANN (1996) 'Runoff components simulated by rainfall-runoff models'. *Hydrol. Sci. J.*, Vol. 41, No. 1, p. 49-60.

BUCHTELE, J., J. KESL and Y. CISSE (1996) 'Evaluation of dynamics of groundwater storages using the water balance simulations'. *J. Hydrol. Hydromech.*, Vol. 44.

BURNASH, J.C.R., R.L. FERRAL and R.A. McGUIRE (1973) 'A Generalized Streamflow Simulation System'. *NWS and California Dept. of Water Res.* Sacramento, California, USA, 204.

CLAPP, R.B. and G.M. HORNBERGER (1978) 'Empirical equations for some soil hydraulic properties'. *Water Resour. Res.* Vol. 14, p. 601 - 604.

FEDERER, C.A. (1993) '*BROOK 90* - A Simulation Model for Evapotranspiration, Soil Water and Streamflow'. *USDA Forest Service*, Durham NH, USA.

HERRMANN, A., J. KOLL, Ch. LEIBUNDGUT, P. MALOSZEWSKI, R. RAU, W. RAUERT, M. SCHÖNIGER and W. STICHLER (1989). 'Wasserumsatz in einem kleinen Einzugsgebiet im paläozoischen Mittelgebirge. Eine hydrologische Systemanalyse mittels Umweltisotopen als Tracer (Turnover of water in a small basin of the paleozoic highlands. A hydrological system analysis using environmental isotopes as tracers).' *Landschaftsökologie und Umweltforschung*, Vol. 17, Braunschweig, 305 p.

HERRMANN, A. and R. UEBERSCHÄR (1993) 'Quick exfiltration response of porous aquifer to actual basin input and consequences for transport modelling: the case of Eisenbach study catchment area'. *Modeling Geo- Biosphere Processes*, Vol. 2. p. 25-40, Cremlingen.

SCHWARZE, R., A. HERRMANN, A. MÜNCH, U. GRÜNEWALD and M. SCHÖNIGER (1991) 'Rechnergestützte Analyse von Abflußkomponenten und Verweilzeiten in kleinen Einzugsgebieten' (Computer-aided analysis of runoff components and residence times in small basins). *Acta hydrophys.*, Vol. 35, No. 2, p. 143-184, Berlin.

Runoff modelling in a mountain catchment

L. Holko[1], Z. Kostka[1], J. Buchtele[2] and A. Lepistö[3]

[1] *Institute of Hydrology SAS, Liptovsky Mikulas, Slovakia*
[2] *Institute of Hydrodynamics CAS, Prague, Czech Republic*
[3] *Finnish Environment Agency, Helsinki, Finland*

1. Introduction

Rainfall-runoff models are often used to simulate hydrological processes in catchments. TOPMODEL (Beven and Kirkby, 1979) has become very popular in recent years. In this paper the model is used in the study of runoff generation in the mountain catchment of the Jalovecky creek (Western Tatra Mountains, Slovakia). Since TOPMODEL is a "topography driven" model, we were interested in testing its performance in this catchment where topography is definitely one of the most important factors. The same input data series were used with the Sacramento soil moisture accounting model SAC-SMA (Burnash *et al.*, 1973) coupled with a snow model. The results provided by both models were compared in order to assess their potential for the description of hydrological processes. The analysis focuses on the simulation of catchment runoff (comparison of simulated and measured runoff) and runoff components (comparison of simulated runoff components with the results of runoff separations).

2. Catchment

The Jalovecky creek catchment, situated in north Slovakia, is representative of the highest part of the Western Carpathians. The catchment area is 22.2 km^2 and mean elevation is 1500 m a.s.l. (800-2178 m a.s.l.). Fractured metamorphic and igneous rocks covered by Quaternary glacio-fluvial sediments form 93% of catchment area. The remaining 7% of the catchment is made up of limestone and dolomite. Slopes in the catchment are steep (mean 27°). Vegetation cover is represented by forests (44% of catchment area) with prevailing spruce, dwarf pine (32%), and alpine meadow and bare rocks (24%).

Hydrological measurements in the catchment started in 1986. Catchment runoff is measured continuously at the outlet. Monthly precipitation is measured at 6 sites, weekly precipitation is measured at two sites, and hourly rainfall is measured in warm seasons at two sites. Additional measurements include air temperature, radiation, wind speed and velocity, soil moisture and temperature, and snow water equivalent and depth.

3. Models and data

Two mathematical rainfall-runoff catchment models were used.

TOPMODEL has a simple structure that takes the topography of the catchment into account. The model has a low number of parameters which is an advantage for use in mountain catchments. Runoff components simulated by TOPMODEL include subsurface and overland flow.

The SACRAMENTO model is a well structured conceptual model with the ability to solve the water balance in medium-sized catchments. Due to its structure, SACRAMENTO has more parameters.

Runoff components include primary base flow (long-term), supplementary baseflow (seasonal), interflow, surface flow and direct runoff (from permanently and temporarily impervious areas).

Input data included daily series of precipitation, runoff, air temperature and potential evapotranspiration from January 1989 to September 1993. Parameters of the models were calibrated for the same period and were kept constant during the whole period of simulation, i.e. they were not optimised for particular events. Validation was not performed due to the lack of additional data.

4. Results and discussion

The aim of the modelling was to find out how well both models simulate the total catchment runoff and what information on runoff components they provide. Although TOPMODEL incorporates information on terrain configuration, it was created using catchments with much more moderate slopes than those in the Jalovecky creek catchment. Therefore, we wanted to check if the model can provide reasonable results in our catchment. We were also interested in comparison of results provided by the well structured SACRAMENTO and parametrically less demanding TOPMODEL. Runoff components computed by TOPMODEL and SACRAMENTO were compared with runoff components calculated by three other independent methods.

4.1 Simulation of catchment runoff

Both models gave similar results. Table 1 shows the comparison of measured and simulated runoff for particular hydrological years. Runoff simulation was rather successful, except for the TOPMODEL simulation in hydrological year 1992 when the runoff was remarkably underestimated. The reason is revealed by the analysis of hydrographs and precipitation. Figure 1 shows the comparison of simulated and measured monthly runoff. It can be seen that in hydrological year 1992, TOPMODEL simulated very low runoff during the summer months (August, September). Summer 1992 was extremely dry. In August, the measured catchment runoff reached minimum values which typically occur in February when all the precipitation is accumulated in snow cover and the runoff is contributed only by catchment storage. Despite high rainfalls in September 1992, TOPMODEL simulation was underestimated and it recovered only in October. SACRAMENTO provided better simulation for these extreme conditions.

TABLE 1: Comparison of runoff simulations (total annual cumulated runoff) by TOPMODEL and SACRAMENTO expressed in % of the measured runoff.

PERIOD	SIMULATED RUNOFF [% of the measured runoff]	
	TOPMODEL	SACRAMENTO
Jan 1989-Oct 1989	91	89
Nov 1989-Oct 1990	102	108
Nov 1990-Oct 1991	103	111
Nov 1991-Oct 1992	76	99
Nov 1992-Sep 1993	95	97

The analysis of monthly results also shows that the runoff simulated by both models during the main phase of snowmelt periods (May) was usually overestimated. It reflects problems with modelling floods caused by combined effects of snowmelt and rainfall. TOPMODEL has a very simple snow subroutine which is based on the degree-day method. Only three parameters determine the water content of the snow cover and the release of the water from it; the snowfall correction factor, degree-day factor and air temperature control the start of melting. However, the more sophisticated snow model PACK coupled with SACRAMENTO leads to better results. The major parameters of the PACK model include maximum and minimum values of the degree-day factor, a snowfall correction factor and a

parameter characterising regional wind conditions. Another eight parameters characterise the influence of air temperature on precipitation structure and snowmelt, the amount of water contained in the snowpack and average areal snow depletion. Generally better simulation of catchment runoff was achieved in summer months.

In about one half of months the simulated runoff did not differ more than 10% from the measured runoff. The range of the differences was higher for TOPMODEL than for SACRAMENTO.

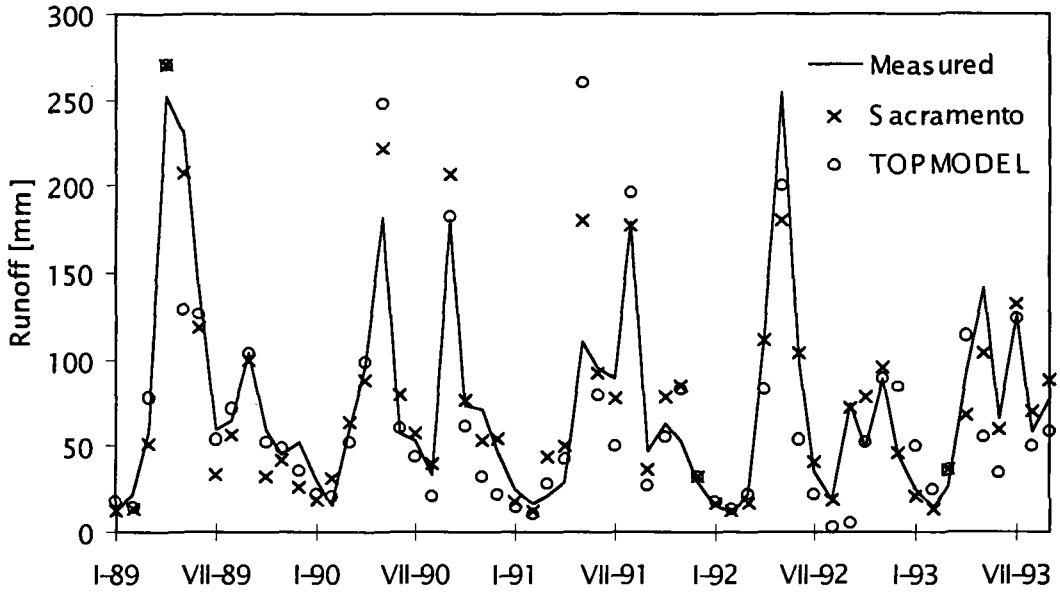

Figure 1: Measured and simulated monthly runoff from January 1989 to September 1993.

4.2 Runoff components

Different methods of runoff separations were used in the Jalovecky creek catchment:

- The separation method based on the relationship between groundwater table and stream discharge (Kliner and Knezek, 1974) was applied for the whole catchment of the Jalovecky creek including the foothill part (46 km^2). Separations were performed for daily data. The mean monthly contribution of groundwater to total runoff in the period May 1988 - February 1992 was 56% (minimum and maximum values are 33% and 93%, respectively).
- The long-term groundwater contribution (hydrological years 1979-1988) for the same area calculated by the method of Kille (1970) was 54%. The method is based on the assumption that the stream is supplied mainly by groundwater during the periods of minimum discharge. Thus, the input data file contains only the average minimum daily stream discharges in a particular month.
- A two-component isotopic runoff separation (deuterium based) was used during two snowmelt seasons and one summer stormflow (Holko, 1995). Old water contribution during the snowmelt varied between 51 and 97%. The mean contribution of the old water during the summer stormflow was 90%. The method is based on natural labelling of water molecules in the hydrologic cycle.

The above mentioned methods are based on different principles, but they are all rather objective, i.e. the separation criteria are relatively clearly defined (and physically justified). The results given by these methods indicate the active role of groundwater in the catchment, although they are not directly comparable.

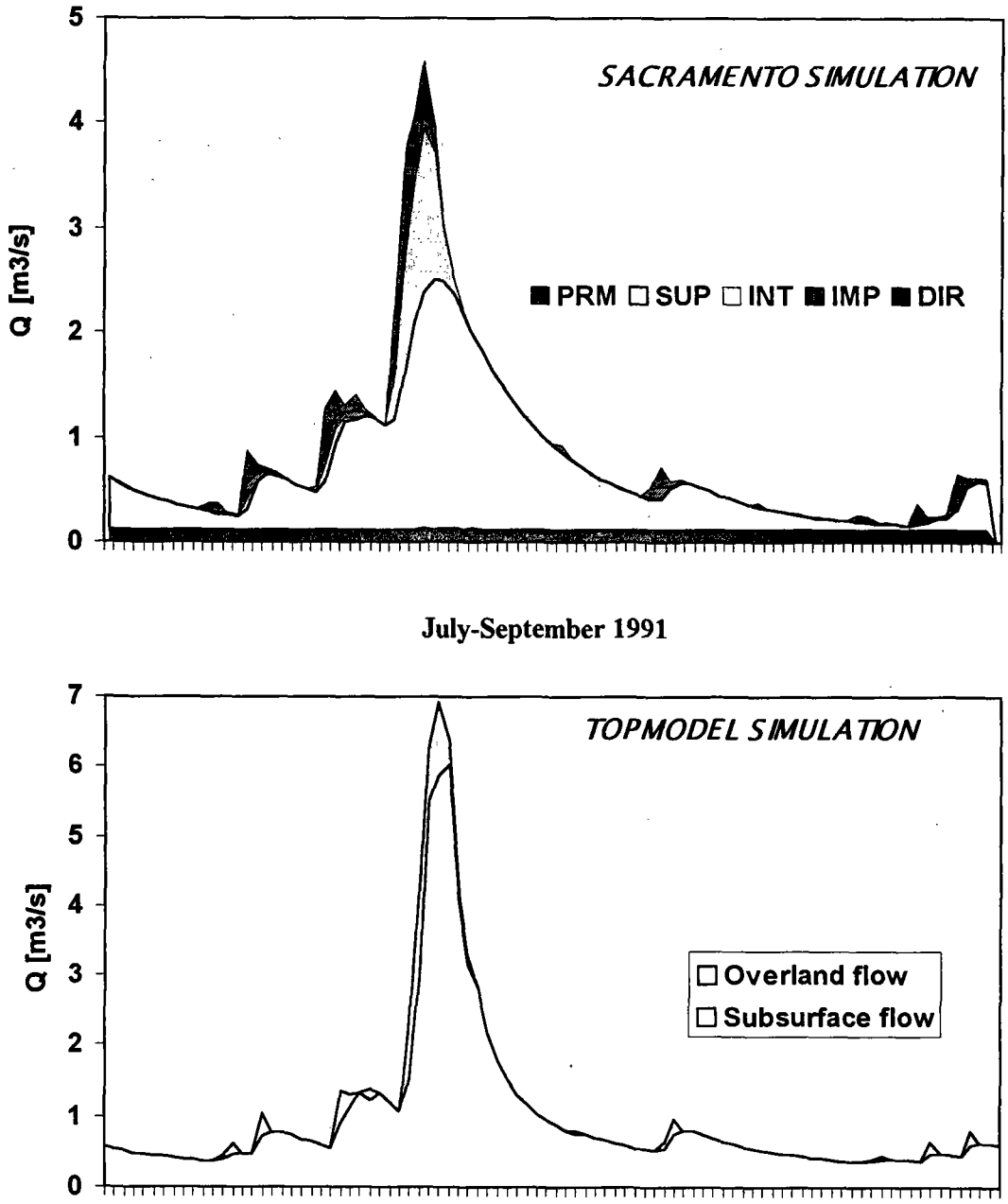

Figure 2: Comparison of runoff components simulated by SACRAMENTO and TOPMODEL for daily data in summer 1991; PRM - primary baseflow, SUP - supplementary baseflow, INT - interflow, IMP - overland flow from impervious areas, DIR - direct runoff.

TOPMODEL and SACRAMENTO provided the following information on runoff components. About 16% of total runoff simulated by TOPMODEL was contributed by overland flow. SACRAMENTO computed the following contributions from different reservoirs: PRM (primary baseflow) 19%, SUP (supplementary baseflow) 70%, INT (interflow) 3%, IMP (overland flow from impervious areas) 3%, DIR 5% (direct runoff) and SUR (surface runoff) 0%. If we consider that the overland flow in SACRAMENTO is represented by the last three reservoirs, the result is similar to that given by TOPMODEL. This similarity is demonstrated in Figure 2 which shows runoff components in summer 1991. The above mentioned numbers represent the whole simulation period. Proportions of different runoff components for particular flood events were not evaluated separately because of lack of data for verification of modelled results. Of the above mentioned three separation methods, only the

isotopic separation is suitable for short time separations but the isotopic data in the catchment is limited. Therefore, at present it can be concluded that both mathematical models provide similar information on proportions of overland\subsurface runoff. High contributions of subsurface runoff modelled by TOPMODEL and SACRAMENTO agree with the results obtained by runoff separation methods.

5. Conclusions

Both models provided similar results in runoff simulation as well as in simulation of runoff components. Despite the low number of parameters, TOPMODEL simulations are comparable with those achieved with the well structured SACRAMENTO model. However, SACRAMENTO could be better adjusted to simulate most of the highest flood peaks and the very low runoff following the extremely dry conditions. Considering the results of runoff separations, runoff components simulated by both models seem to be reasonable.

The simulations showed that TOPMODEL can also provide reasonable results in a mountain catchment with steep slopes.

6. References

BEVEN, K.J. and M.J. KIRKBY (1979) 'A physically based variable contributing area of basin hydrology'. *Hydrol.Sci. Bull.*, 24, 43-69.

BURNASH, J.C.R., R.L. FERRAL and R.A. MCGUIRRE (1973) 'Generalized streamflow simulation system'. *NWS and California Dept. of Water Res., Technical Report*, California, USA.

HOLKO, L. (1995) 'Stable environmental isotopes of ^{18}O and ^{2}H in hydrological research of mountainous catchment'. *J. Hydrol. Hydromech.*, 43, 4-5, 249-274.

KILLE, K. (1970) 'Das Verfahren MoMNQ, ein Beitrag zur Berechnung der mittleren langjährlichen Grundwasserneubildung mit Hilfe der monatlichen Niederigwasserabflüsse'. *Z. Deutsch. geol. Gessel.*, 89-95.

KLINER, K., and M. KNEZEK (1974) 'The underground runoff separation method making use of the observation groundwater table'. (in Czech with English abstract), *J. Hydrol. Hydromech.*, 22, 5, 457-466.

Topography-based modelling at different scales

W. Lahmer, D.-I. Müller-Wohlfeil, V. Krysanova and A. Becker

Institute for Climate Impact Research, Potsdam, Germany

1. Introduction

1.1 General

Lateral flow components play an important role for both the redistribution of precipitation into various flow components and the spatially distributed dynamics of soil moisture patterns. Up to now, ecosystem models applied to large areas rarely account for lateral water flow and only a few studies including this flow component have been undertaken.

Topography-based models like TOPMODEL (Beven and Kirkby, 1979) provide a simple way to introduce lateral flow components into regional ecosystem models. They may help to improve the regional representation of moisture patterns (Famiglietti and Wood, 1991) and to enable independent runoff calibration. TOPMODEL is based on the assumption that local soil moisture dynamics strongly depend on i) the size of the upslope area a draining through an observed catchment point, ii) the local topographic surface slope $tan\beta$ representing the hydraulic gradient for saturated water flow, and iii) the downslope soil transmissivity T which decreases exponentially with depth below the soil surface.

Up to now, TOPMODEL has rarely been applied to large landscapes, because (a) the model was developed for the hillslope/catchment and not for the drainage basin scale and (b) the mesh size of single spatial units for TOPMODEL applications should not exceed 100 m (Quinn *et al.*, 1995a). Only a few examples exist where the mesh size of topography-based approaches exceeds 100 m (i.e. Wigmosta *et al.* 1994, Hutchinson and Dowling 1991).

1.2 Objectives

We decided to apply TOPMODEL at the basin/regional scale, since investigations of the potential limits in coarse and large scale applications are necessary. Regional modelling approaches have to cope with available data (currently, the spatial resolution of world-wide available Digital Elevation Model (DEM) data is not better than 1 km (Arnell, 1993)), and global ecosystem models often operate on grid cell sizes not smaller than 0.1° - 0.5°.

TOPMODEL was applied to various German catchments in order to study its operational applicability for regional and large scale investigations. Advantages of the model for such investigations are the simple model structure and the need to calibrate only a few parameters. Moreover, in contrast to many other runoff schemes, TOPMODEL provides spatially and time distributed soil moisture patterns.

The main goals of the study were to

(a) investigate to what extent low resolution DEMs can be used for topography-based hydrological studies and to determine potential errors in neglecting detailed relief features,

(b) study the influence of relief type on the simulation results and possible limitations of model applicability, and
(c) extend previous investigations focused on the scaling behaviour of TOPMODEL towards larger grid sizes.

2. Topography-based modelling

2.1 Study areas

To study the effects of area and topographic characteristics on the simulation results, analyses were performed for catchments of different size differing in geomorphology and relief: the German part of the Elbe drainage basin (96,000 km²); the Stör catchment (1,780 km²) and its sub-catchment Buckener Au (58 km²), located in the center of Schleswig-Holstein/northern Germany (lowland region); and the Vils catchment (756 km²) and its sub-catchment Frankenohe (45.1 km²) located in southern Germany (dry hilly upland region).

The simulations in the Stör and Vils catchments are based on DEM data sets with a spatial resolution of about 33 m x 33 m and 29 m x 29 m respectively (Federal Armed Forces Geographic Office FAFGO, Euskirchen, Germany). For the simulation runs in the Elbe basin a 30'' x 50 '' (~ 1000 m x 1000 m) DEM was used (Institute for Applied Geodesy IFAG, Frankfurt, Germany).

2.2 Methods

From the large number of existing TOPMODEL versions (Beven *et al.*, 1994; Beven *et al.*, 1995) the distribution version TOPMOD9403 (pers. comm. K.J. Beven) was chosen for the simulation calculations. Input data are DEMs and time series data for precipitation and potential evapotranspiration. Measured discharges can be used for validation. Output data include simulated discharges, actual evapotranspiration, and information on the build up of soil moisture.

The simulation program requires $ln(a/tan\beta)$ distributions for each sub-catchment, which were calculated from DEM data sets by a modified version of the GRIDATB program (pers. comm P.F. Quinn). To suppress the generation of very large $ln(a/tan\beta)$ values, the upslope drainage area for each cell can be limited by a channel initiation threshold (CIT) which, in turn, supports the creation of a virtual river net (Quinn *et al.*, 1995b).

In order to ensure potential flow from each grid cell to its neighbours, local sinks and plateaus had to be removed from the raw elevation data. A modified version of the program SINKS (Dr. Quinn/ADAS, Wolverhampton) was used for this purpose. Modifications of the original data sets caused by the cleaning procedure were studied carefully, since they play an important role in flatter region applications. Topography may be changed dramatically, both with respect to the maximum elevation change and the percentage of manipulated catchment area.

2.3 Analyses of the topographic index

To study scaling effects, the influence of catchment size, topographic conditions, spatial resolution, and channel initiation threshold (CIT) on the $ln(a/tan\beta)$ distributions the simulation results were analysed in detail for the Stör and Vils catchments. Since no discharge time series data were available for the Elbe basin, the aim of the simulation runs was focused on studies of the topographic index to extend the analyses in the Stör and Vils catchments to a whole landscape.

Influences of the CIT on the $ln(a/tan\beta)$ distributions were studied based on the recommendation of Quinn *et al.* (1995b), who suggest that starting from high CIT values, the mean $ln(a/tan\beta)$ value significantly decreases and the number of virtual river points significantly increases when the CIT is chosen to be too small. The CIT used in the simulation runs depends on the catchment size and the spatial resolution and takes values between 0.1 km² (equal to 100 pixels) for the Buckener Au at 33 m, and 30 km² (equal to 100 pixels) for the Stör and Vils at 1000 m spatial resolution. In Fig. 1 the effect

of the threshold CIT on the *ln(a/tanß)* distributions is demonstrated for the case of the Stör catchment. For all spatial resolutions this threshold reduces the mean of the distributions by suppressing very large *ln(a/tanß)* values, which in turn alters the response of runoff in TOPMODEL.

In order to study the influence of spatial resolution on the *ln(a/tanß)* distribution functions, simulations were performed at different resolutions for the Buckener Au sub-catchment (32 m, 110 m and 250 m), the Stör catchment (250 m, 500 m and 1000 m) and the Vils catchment (50 m, 100 m, 250 m, 500 m and 1000 m). In all cases, DEM aggregation was performed by the GRID resampling procedure of the Geographic Information System (GIS) ARC/INFO using the nearest neighbour relationship. Generally, minimum, mean, and maximum of the distributions increase with decreasing spatial resolution, due to increasing grid cell area and decreasing slope related to smoothing effects (smaller *tanß* values). Since the number of samples contributing to the distributions decreases with decreasing resolution, distributions of high resolution DEMs are smoother than those of low resolution DEMs for the same area. These effects of spatial resolution are also shown in Fig.1.

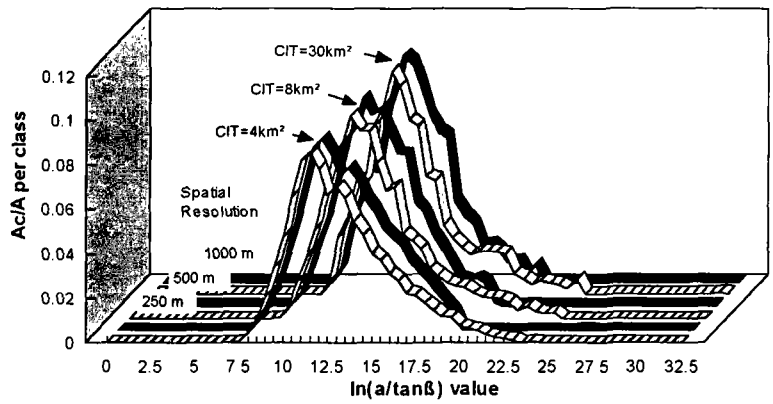

Figure 1: Effects of the channel initiation threshold (CIT) on the ln(a/tanß) distributions for the Stör catchment at 250 m, 500 m and 1000 m resolution (bright: without CIT, dark: with indicated CIT).

Fig. 2 demonstrates how catchment size influences the *ln(a/tanß)* distributions. For the same spatial resolution (250 m) and the same CIT value (4 km^2), the distributions obtained for the four catchments do not show a general trend.

The effects of topography and area size on the *ln(a/tanß)* distributions are most evident for the 57 rather different sub-catchments of the Elbe basin, derived by the *r.watershed* function of the GIS GRASS. The mean *ln(a/tanß)* values vary between 11.73 in the southern mountainous regions and 14.94 in extremely flat areas (i.e. the Elbe outlet).

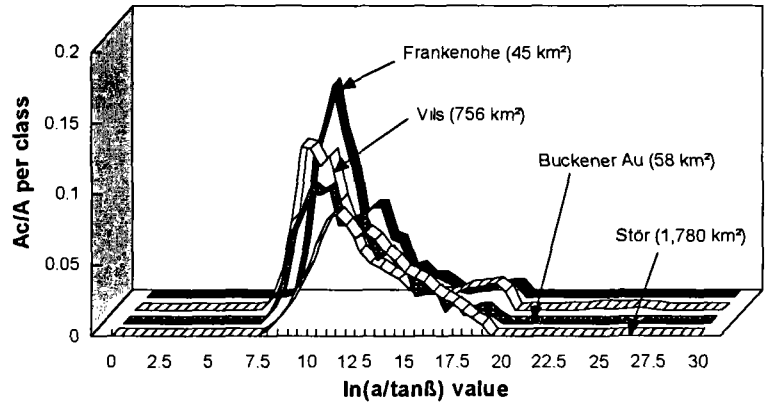

Figure 2: Effects of catchment size on the ln(a/tanß) distribution for a common spatial resolution of 250 m and a CIT of 4 km².

3. Scaling effects

Changes in spatial resolution and area cause changes in the predicted runoff behaviour via the *ln(a/tanβ)* distribution function. Our simulation results confirm conclusions drawn by Wolock and Price (1994) according to which the predicted base flow to total flow ratio Qb/Qtot decreases for all catchments with decreasing spatial resolution, when the same parameter set is used in the simulation runs. Simultaneously, the efficiency/objective function ε (Nash and Sutcliffe, 1979) is reduced by up to about 35% (see Table 1).

TABLE 1: Scaling effects on the TOPMODEL simulation results. Changes of efficiencies ε and base flow to total flow ratio Qb/Qtot for a) identical parameter sets and b) calibrated parameter sets used in the simulation runs.

			a) identical parameter set			b) calibrated parameter set		
catchment	**resolution [m]**	**mean ln(a/tanß)**	**ln(T0)**	**Δε [%]**	**ΔQb/Qtot [%]**	**ln(T0)**	**Δε [%]**	**ΔQb/Qtot [%]**
Buckener Au	33	8.94	1.72	-20.1	+21.4	0.25	-0.1	+0.7
	110	10.41	1.72	0	0	1.72	0	0
	250	11.22	1.72	-5.9	-13.4	2.53	+0.5	-0.3
Stör	250	12.56	4.36	-1.3	+1.1	3.84	-7.2	-5.7
	500	13.08	4.36	0	0	4.36	0	0
	1000	13.77	4.36	-15.1	-10.2	5.05	-0.1	+3.0
Franken-ohe	29	8.01	0.32	-22.4	+31.6	-1.64	+0.2	+0.4
	110	9.97	0.32	0	0	0.32	0	0
	250	10.16	0.32	-5.6	-4.4	0.51	-3.1	-0.6
Vils	50	9.23	0.20	-15.6	+26.7	-1.35	-0.4	-2.0
	100	9.78	0.20	-8.5	+18.6	-0.80	+0.6	-0.2
	250	10.78	0.20	0	0	0.20	0	0
	500	11.85	0.20	-10.8	-23.9	1.27	-1.4	-2.7
	1000	12.67	0.20	-34.7	-40.8	2.09	-1.8	-4.5

Recalibration of the model parameters is possible by shifting just the parameter ln(T0) according to the mean *ln(a/tanβ)* values, resulting in almost identical efficiencies and flow ratios (small deviations of ε and Qb/Qtot, respectively), i.e. predicted discharges. The emboldened resolution values in Table 1 were taken as a bench mark (differences in ε and Qb/Qtot are always zero for that resolution).

The results given in Table 1 indicate that discharge differences can be largely compensated by changing the mean transmissivity T0 and that after this compensation other discharge simulation results are almost independent of scale, which confirms results of Wolock and McCabe (1995), Bruneau *et. al* (1995) and Quinn *et al.* (1995a).

In Fig. 3 time series data of precipitation, and measured and simulated discharges are shown for the Buckener Au sub-catchment. The simulated discharges reproduce the measured ones quite well, particularly for the winter periods. The efficiency of about 68% approaches the highest efficiencies ever reached (85%).

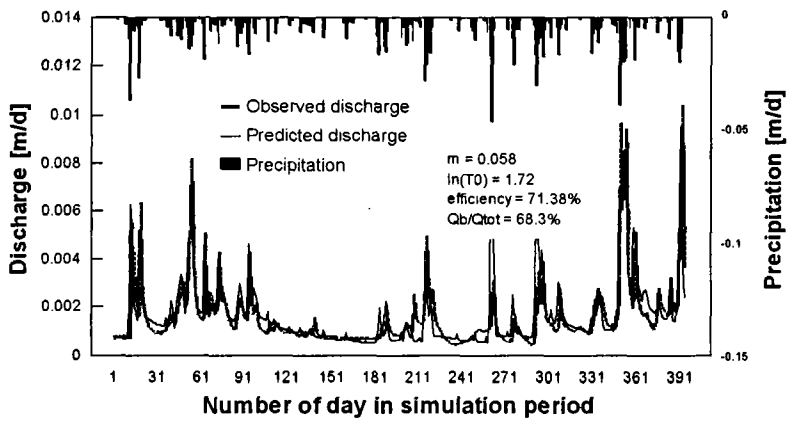

Figure 3: TOPMODEL runoff simulation results for the Buckener Au catchment (time period of 14 months)

4. Conclusions and outlook

The simulations performed for various German catchments demonstrate that even simple models including only key factors of system behaviour can be effective tools for the analysis of the hydrological cycle in a watershed. The results show that a topography-based approach can be applied even in lowland regions, if high resolution DEMs are available and the limits of application are carefully studied. Runoff estimations are scale dependent, but differences in discharge can be compensated for all regions and resolutions after a simple recalibration by a shift of the mean transmissivity T0 - even at the 1000 m grid scale.

Thus, TOPMODEL applications allow the use of information gained at one scale in making predictions at another scale. This potential behaviour can be integrated into regional ecosystem models to improve the regional representation of soil moisture patterns like those shown in Fig. 4 for the Vils catchment. The spatially and time distributed soil moisture patterns (representing single pixel saturation counts) provided by TOPMODEL are almost identical for all spatial resolutions. Moreover, the saturation patterns obtained for the Buckener Au sub-catchment are comparable to patterns of soil texture, which supports observations of Merot *et al.* (1995).

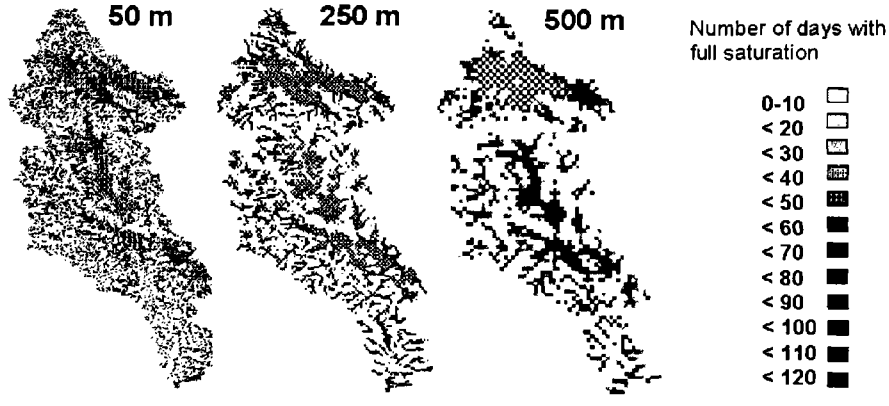

Figure 4: Soil moisture patterns of the Vils catchment for spatial resolutions of 50 m, 250 m, and 500 m (519 days simulation period).

The advantages of the TOPMODEL approach are included in the river catchment model EGMO (Becker, 1975; Becker and Pfützner, 1987) which is characterised by more sophisticated features to account for heterogeneous landscape properties, which according to Avissar (1991) and Bruneau *et al.* (1995) are particularly important in large-scale modelling. The coupling of the two models can be achieved in two ways:

1. Use of the topographic index as an additional basic cover within the GIS pre-processing stage of the applying EGMO, to include this information during the creation of hydrological response units (HRU). By this means, areas characterised by shallow and deep groundwater table can be localised.
2. Direct integration of the topographic index into EGMO, in order to describe directly the dynamics of areas with shallow groundwater. In this case the topographic index takes into account intra-patch heterogeneities by a respective distribution function.

Bibliography

ARNELL, N. W. (1993) 'Data requirements for macroscale modelling of the hydrosphere'. In: Wilkinson W.B. *Macroscale modelling of the hydrosphere*. Proceedings of an international Symposium held at Yokohama, Japan 21 July 1993. IAHS Publications 214, 139-150.

AVISSAR, R. (1991) 'A statistical-dynamical approach to parameterize subgrid-scale land surface heterogeneity in climate models'. Surv. Geophys. 12, 155-178.

BECKER, A. (1975) 'EGMO-Einzugsgebietsmodelle zur Abflußberechnung, -vorhersage und -simulation'. *WWT* 25, 9, S. 316-322.

BECKER, A. and B. PFÜTZNER (1987) 'EGMO - system approach and subroutines for river basin modelling'. *Acta Hydrophysica* 31, pp. 125-141.

BEVEN, K.J. and M.J. KIRKBY (1979) 'A physically based variable contributing area model of basin hydrology'. *Hydrol. Sci. Bull.*, 24, 43-69.

BEVEN, K.J., P.F. QUINN, R. ROMANOWICZ, J. FREER, J. FISHER and R. LAMB (1994) "TOPMODEL and GRIDATB. A users guide to the distribution version'. CRES Technical Report TR 110/94, Centre for Research on Environmental and Biological Sciences, Institute of Environmental and Biological Sciences, Lancaster University, UK.

BEVEN, K.J., P.F. QUINN, R. ROMANOWICZ, J. FREER, J. FISHER and R. LAMB (1995) 'TOPMODEL'. In: Singh V.P.(Ed.): *Computer Models of Watershed Hydrology.* Water Resources Publications, 627-668.

BRUNEAU, P., C. GASCUEL-ODOUX, P. ROBIN, PH. MEROT and K. BEVEN (1995) 'Sensitivity to space and time resolution of a hydrological model using digital elevation data'. *Hydrol. Process.*, 9, 1, 69-81.

FAMIGLIETTI, J.S. and E.F. WOOD (1991) 'Evapotranspiration and runoff from large land areas: Land surface hydrology for atmospheric general circulation models'. *Surveys in Geophysics* 12, 179-204.

HUTCHINSON, M. F. and T.I. DOWLING (1991) 'A continental hydrological assessment of a new grid-based digital elevation model of Australia'. *Hydrol. Process.*, 5, 45-58.

MEROT, PH., B. EZZAHAR, C. WALTER and P. AUROUSSEAU (1995) 'Mapping waterlogging of soils using digital terrain models'. *Hydrol. Process.* 9, 1, 27-34.

NASH, J.E. and J.V. SUTCLIFFE (1979) 'River flow forecasting through conceptional models, 1. A discussion of principles'. *J. Hydrol.*, 10, 282-290.

QUINN, P.F., K.J. BEVEN and R. LAMP (1995a) 'The In(a/tan ß) index: how to calculate it and how to use it within the TOPMODEL framework'. *Hydrol. Process.* 9, 2, 161-182.

QUINN, P.F., K.J. BEVEN and A. CULF (1995b) 'The introduction of macroscale hydrological complexity into land surface - atmosphere transfer models and the effect on planetary boundary layer development'. *J. Hydrol.*, 166, 421-445.

WIGMOSTA, M.S., L.W. VAIL and D.P. LETTENMAIER (1994) 'A distributed hydrology-vegetation model for complex terrain'. *Water Res. Research.* Vol. 30. 6, 1665-1679.

WOLOCK, D. M. and G. J. MCCABE (1995) 'Comparison of single and multiple flow direction algorithms for computing topographic parameters in TOPMODEL'. Water Res. Research, 31, 5, 1315-1324.

WOLOCK, D.M. and C.V. PRICE (1994) 'Effects of digital elevation model and map scale and data resolution on a topography-based watershed model'. *Water Res. Research*, 30, 11, 3041-3052.

A model for determining flood waves in small basins

P. Mita and C. Corbus

National Institute of Meteorology and Hydrology, Bucarest, Romania

1. Introduction

The model proposed in the present paper is based on using certain analytical functions in order to compute the hydrograph of the flood wave in small basins up to 5 km^2. This hydrograph is considered to be made up of surface runoff (including near-surface runoff) and baseflow. The parameters of the analytical functions proposed for computing the two component hydrographs are determined using certain characteristics of the flood waves.

In the first part of the paper, results regarding the dependence of the flood wave characteristics on the rainfall characteristics are presented. In the second part, an analytical method for determining the flood waves in small basins is presented.

Data have been used from two representative basins in Romania with hydrometeorological records longer than 25 years and where at least two or three major floods have occurred.

The study has been carried out in order to specify, theoretically, the problem and also as a response to the interest which hydrological practitioners have shown in floods in small basins.

2. Dependence of the flood wave characteristics on rainfall characteristics and on morphohydrographical factors

The dependence of the flood wave characteristics (e.g. increase and decrease durations, maximum discharge, increase and decrease volumes for the hydrograph of the surface runoff, and the final baseflow discharge of the hydrograph) on the rainfall characteristics (e.g. amount, duration, time distribution) was first analysed separately for hydrometric sections in the representative basins identified according to surface, slope and vegetation.

On the basis of the data from all the analysed sections, characterised by a large diversity of the factors mentioned, the influence of these factors on the flood waves has been emphasised. In this way, synthesis relations were obtained. These characteristics actually represent the main parameters of the proposed model.

2.1 Analysis of the dependence of flood wave characteristics on rainfall characteristics

The flood wave and rainfall characteristics, taken into account in the study and schematically presented in Figure 1, are the following:

Δt - the time interval between the beginning of the rainfall and the beginning of the flood;

t_{cr}, t_d, T_v - flood increase, decrease and total duration;

Q_{max} - maximum discharge of the flood;

ΔQ_{max} - the maximum discharge of the surface runoff;

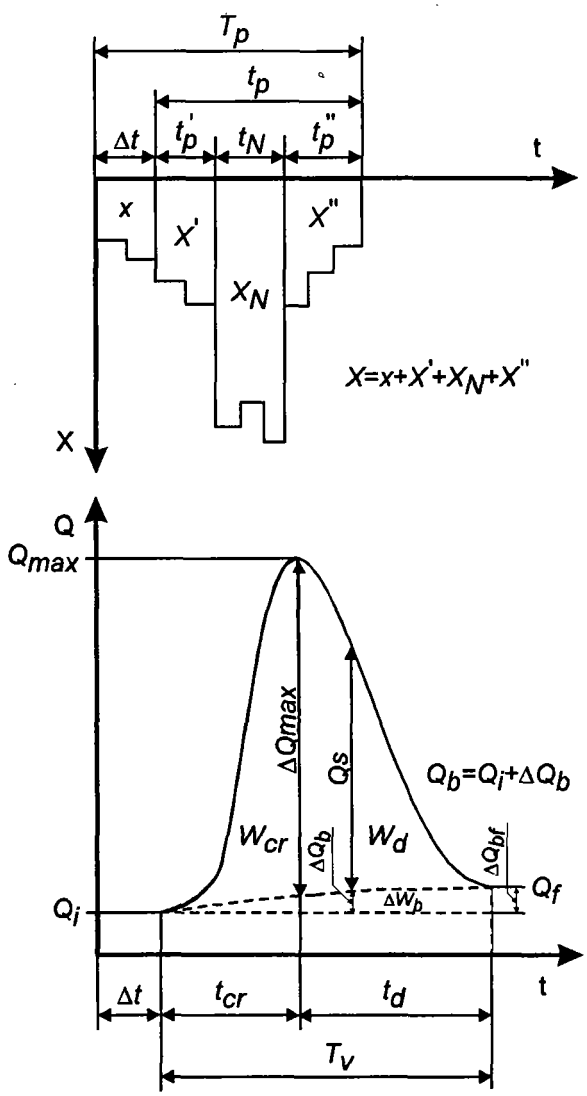

Figure 1: Flood wave and rainfall characteristics.

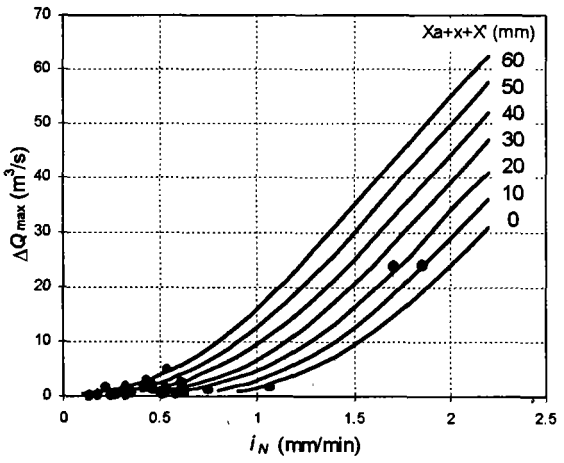

Figure 2: The $\Delta Q_{max} = f(i_N, X_a + x + X')$ *relation for the section upstream the confluence with the Caprita river*

Q_i, Q_f - initial and final discharge;

ΔQ_{bf} - variation of the basic discharge with Q_i, at the end of the flood;

W_{cr}, W_d - increase and decrease volume of the surface runoff;

ΔW_b - variation of the volume of baseflow with the volume corresponding to Q_i;

t'_p- the time interval between the beginning of the rainfall and the beginning of its nucleus;

t_N - duration of the rainfall nucleus;

t''_p - the time interval between the end of the rainfall nucleus and the end of the rainfall;

t_p - the time interval between the beginning of the flood and the end of the rainfall;

T_p - total duration of the rainfall;

x, X', X_N, X'' - amount of rain fallen during the time interval Δt, t'_p, t_N and t''_p respectively;

X - total amount of the rainfall registered during the time interval T_p;

Other elements necessary to model the hydrograph of the flood, as shown in Figure 1, at a certain moment are:

Q_s - surface runoff discharge;

Q_b - baseflow discharge;

ΔQ_b - variation of baseflow with Q_i.

The dependency of the flood wave characteristics on precipitation characteristics was investigated for seven hydrometric sections within the Iedut and Fântâna Galbena representative basins, located in the mountain area in the north-western part of Romania. For each of these sections, 20 to 40 floods between 1969 and 1995 were analysed. The morphometric and vegetation characteristics of the sub-basins corresponding to the seven sections are as follows: area between 0.15 km^2 and 3.33 km^2; basin slopes between 20% and 30%; and afforestation coefficients between 20% and 85%.

The Δt interval is a reference element in the flood evolution which depends on the x parameter and on the soil humidity before the flood, expressed by the rainfall registered 5 days before, X_a. For the normal rainfalls, the flood will start after 15-20 minutes.

t_{cr} was analysed depending on $t_p^{'}+t_N$. Generally, for the analysed rainfalls, the nucleus is most frequently situated in the middle of the interval or in its second part. At values for $t_p^{'}+t_N$ of 20-40 minutes (most frequently), the value of t_{cr} is 2-3 times larger. Larger values of the $t_p^{'}+t_N$ tend to equal the value of t_{cr}.

t_d was analysed for each sub-basin depending on $t_p^{''}$ and i_N, where i_N represents the intensity of the rainfall nucleus: $i_N = \frac{X_N}{t_N}$

ΔQ_{max} was analysed depending on i_N and $X_a + x + X^{'}$. Figure 2 presents, as an example, the graphical relation obtained for the section upstream of the confluence with the Caprita river in the representative basin of Iedut. This sub-basin, located in the mountain area of Romania (the Bihor mountains), has the following morphometric and vegetation characteristics: area - 2.41 km^2; sub-basin slope - 25% and afforestation coefficient - 22%.

W_{cr} was calculated depending on $x + X^{'} + X_N$.

W_d was calculated depending on X.

ΔQ_{bf} and ΔW_b was analysed depending on X and i_N.

2.2 Regionalization of the flood wave characteristics

From an analysis of data from all the studied sections, characterised by a large diversity of environmental factors, graphical synthesis relationships were obtained which are valid for an approximately 1500 km^2 area in the north-western part of Romania.

For Δt the relation with $\frac{F}{\sqrt{I_b}}$ parameter was established, considering X_a.

For t_{cr} the relation with $\frac{F}{\sqrt{I_b}}$ parameter was established, considering $t_p^{'}+t_N$.

For t_d the relation with $\frac{F}{\sqrt{I_b}}$ parameter were also established, but considering T_p and X.

In order to determine ΔQ_{max} coaxial synthesis relations were established, considering basin surface F (km^2), afforestation coefficient C_p (%), precipitation $X_a + x + X^{'}$ (mm) and rainfall nucleus i_N (mm/min) (Figure 3).

For W_{cr} the relation with $\frac{F}{\sqrt{I_b}}$ parameter was established, considering $X_a + x + X^{'} + X_N$.

For W_d, ΔQ_{bf} and ΔW_b the relation with $\frac{F}{\sqrt{I_b}}$ and C_p parameters was established, considering $X_a + x$.

3. Determination of the form of flood wave hydrographs in small basins

In order to determine the form of flood waves in small basins, geometric models (based on analytical functions), type models (defined by real registered floods) or unit hydrograph models can be adopted.

In the literature (Alexeev, 1955; Sokolovski 1959; Mustata, 1964; Lauterbach, 1965; Cadariu, 1979; Serban and Pretorian, 1989) there are many analytical models, made up either of one function which describes the whole flood or of two functions which describe the increase and decrease phases of the flood. Sometimes, however, the drafts include errors and this has determined the intensification of efforts to elaborate better flood forms and to improve their practical application.

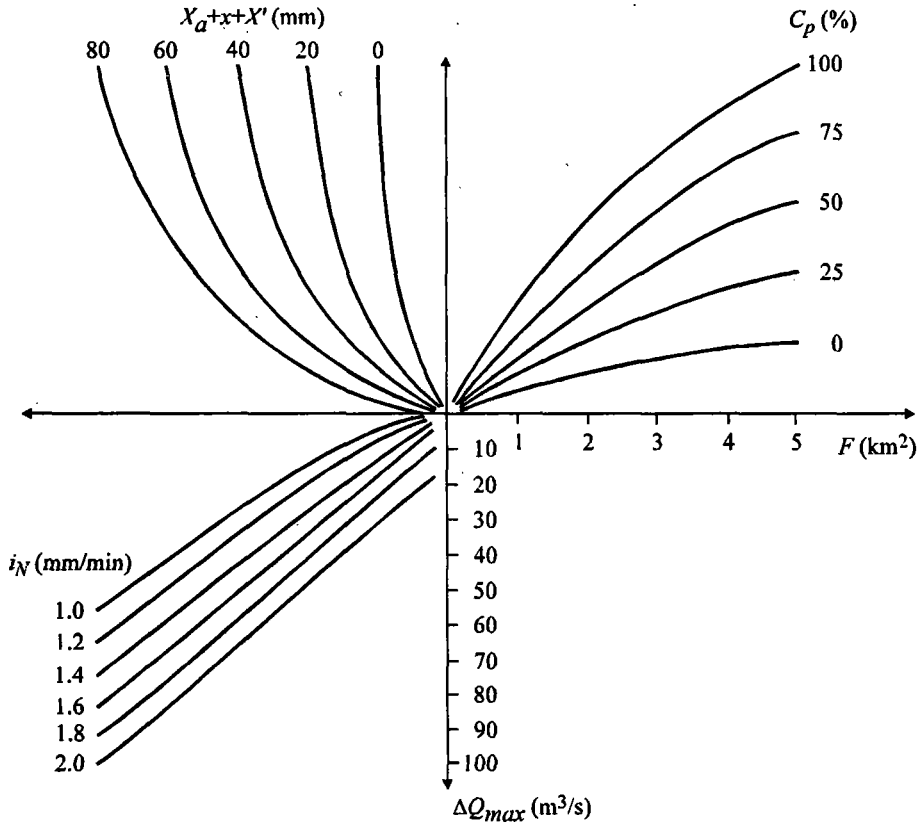

Figure 3 : Coaxial synthesis relation $\Delta Q_{\max} = \mathrm{f}(i_N, X_a + x + X', F, C_p)$

The present paper proposes a new model based on analytical functions from which two components of the hydrograph of flood wave can be simulated: surface (and near-surface) runoff; and baseflow.

4. Modelling of the surface runoff hydrograph

In order to model this hydrograph, a model based on a rational function (in combination with the polynomial and exponential functions) unique for the whole flood is proposed:

$$Q_s(t) = \frac{At(T_v - t)}{e^{Bt+C}}$$

where t is time and parameters A, B and C determine the form of the surface runoff hydrograph.

The proposed analytical model can be used in computing the ordinates of the hydrograph of the surface runoff given that the following elements which characterise the flood are specified: t_{cr}, t_d, $\Delta Q_{\max}$, W_{cr} and W_d.

Parameters A, B, C are determined by solving an equation system which has the following three conditions:

- the function graph has to pass through the point of co-ordinates: $t = t_{cr}$ and $Q_s(t) = \Delta Q_{\max}$;
- the abscissa of the maximum point of the analytical function is $t = t_{cr}$;
- the defined integral $\int_0^{T_v} Q_s(t)dt$ is equal to the volume of the surface runoff calculated by the formula $W_{cr} + W_d$.

In order to model the hydrograph of the basic runoff a polynomial function was used:

$$Q_b(t) = Q_i + \Delta Q_b(t)$$

with

$$\Delta Q_b(t) = at^2 + bt$$

where: t is time; and a and b are parameters which determine the form of the baseflow hydrograph.

The proposed analytical model can be used in computing the ordinates of the baseflow hydrograph given that the following elements which characterise the flood are known: t_{cr}, t_d, ΔQ_{bf} and ΔW_b.

Parameters a and b are determined by solving the equation system which has the following conditions:

- the function graph has to pass through the point of co-ordinates: $t = T_v$ and $\Delta Q_b(t) = \Delta Q_{bf}$;
- the defined integral $\int_0^{T_v} \Delta Q_b(t)dt$ is equal to the variation of the volume of baseflow given by ΔW_b.

Solving the above mentioned equation system, the final form of the baseflow hydrograph is:

$$Q_b(t) = Q_i + \left(\frac{t}{T_v}\right)^2 \left(T_v \Delta W_b - \Delta Q_{bf}\right) + \frac{t}{T_v}\left(-T_v \Delta W_b + 2\Delta Q_{bf}\right)$$

5. Application

An example of a practical application of the proposed model is presented as follows for the flood of 14 July 1991, 1330 hours, registered in the Iedut basin in the section upstream of the confluence with the Caprita river.

Given the rainfall characteristics, and using the relationships in Figure 2, the elements which characterise the two component hydrographs corresponding to baseflow and surface runoff were computed. The rainfall characteristic elements, from which different elements of the flood necessary for determination of its form were computed, are given in Table 1.

TABLE 1: The elements which characterise the flood of 14 July 1991, registered in the Iedut basin, computed with the use of the rainfall characteristic elements.

Computed elements (flood)	Measured elements (rainfall)							
	X_a=0 mm	x=6.7 mm	X'=3.7 mm	t'_p=5 min	X_N=36.5 mm	t_N=20 min	X''=25.1 mm	t''_p=30 min
Δt=46 min	✓	✓	-	-	-	-	-	-
t_{cr}=65 min	-	-	-	✓	-	✓	-	-
W_{cr}=17200 m^3	-	✓	✓	-	✓	-	-	-
ΔQ_{max}=25 m^3/s	✓	✓	✓	-	✓	✓	-	-
t_d= 76 min	-	-	-	-	✓	✓	-	✓
W_d=18800 m^3	-	✓	✓	-	✓	-	✓	-
ΔW_b=5300 m^3	-	✓	✓	-	✓	✓	✓	-
ΔQ_{bf}=0.66 m^3/s	-	✓	✓	-	✓	✓	✓	-

Using the flood characteristic elements, the hydrographs of the baseflow and surface runoff are then computed analytically. Gathered together, the two hydrographs form the total hydrograph of the flood. The result is presented in Figure 4.

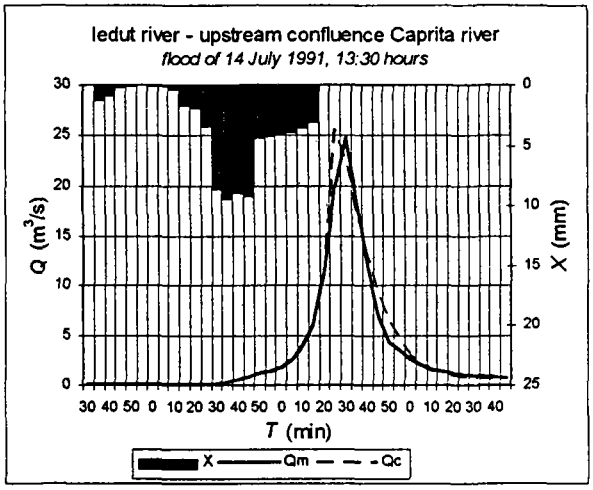

Figure 4: Measured (Q_m) and calculated (Q_c) discharges using the proposed model.

For the example presented here, the value of the Nash-Sutcliffe error criterion (Nash and Sutcliffe, 1970) is 0.95. Generally, for the simulated floods, the values of this criterion are between 0.85 and 0.97.

6. Conclusions

The proposed model can be successfully used in forecasting floods in small basins. The results will be better the smaller the remaining part of the total rainfall. Therefore, the best results are obtained after reaching the maximum nucleus of the rainfall when the only forecasted elements are X'' and t_p''.

The mathematical function model, proposed in the paper for describing the flood, is a possible solution, together with the other established models, and does not have to be considered as unique. The selection, for each analysed representative basin, of the optimum analytical function model is a mandatory process. Furthermore, if for a representative basin several models give approximately the same good results, and if their manner of application can be specified, the use of all the models can be considered.

The practical use of the proposed function for determining the form of flood wave hydrographs can provide advantages, especially for computer modelling in the field of hydrology and water management.

References

ALEXEEV D. L. (1959) 'Calculation of the river flow at the high waters.' *Ghidrometeorologhiceskoe izdatelstvo*, Leningrad.

CADARIU R. (1979) 'Non-dimensional analytical model for the form of single theoretical floods.' *Hidrotehnica*, vol. 24, no. 6, Bucharest.

LAUTERBACH D. (1965) 'Ein Verfahren zur Berechnung von Hochwasserganglinien fur die Bemessung von Speicherraumen.' *Besondere Mitteilungen zum Gewasserkundlichen Jahrbuch*, nr. 3, Berlin.

MUSTATĂ L. (1964) 'The analysis of forming and computing method of the hydrograph of pluvial floods on the rivers of Romania' *Hydrology studies*, vol. XI, Bucharest.

NASH, J. E. and I. V. SUTCLIFFE (1970) 'Flood-wave formation.' *Technical Note, no. 92, W.M.O*, Geneva, Switzerland.

SOKOLOVSKI D. L. (1959) 'River flow.' *Ghidrometeorologhiceskoe izdatelstvo*, Leningrad.

SERBAN P. and R. PRETORIAN (1989) 'The automatic composition of the flood waves'. *Hydrology studies and research,* no. 3 (58), National Institute of Meteorology and Hydrology, Bucharest.

Conference "Ecohydrological Processes in Small Basins", Strasbourg, 24 - 26 September 1996

Hydrological networks and digital elevation models (DEM): comparison with ground data

C. Puech and A. Adam

Remote Sensing Laboratory CEMAGREF, Montpellier, France

Introduction

Development of spatial techniques such as remote sensing and GIS (geographical information systems) provide new opportunities for hydrological modelling. The focus is no longer on catchments as a whole, seen as a black box; the interest is now on internal differences within the catchment and we try to use them in an adapted model. To characterise and validate the internal computations, we need a good localisation of the different areas, a good understanding of flow processes and a good elementary flow computation. In particular, the sub-catchment productions and transfers are linked to the behaviour of water through the drainage network. So, automatic computation of drainage network using a digital elevation model (DEM) is important.

Since the development of DEM, there has been a proliferation of automatic procedures for extracting channel networks (Blöschl and Sivalapan 1995). For research in hydrology using DEM, the calculation is both the easiest part and the departure point. The drainage network is indeed necessary to improve knowledge in transfers, in separating slow and rapid flows (as in slopes and rivers). Source areas are defined on a criterion of network distance assuming that the nearest zones are the more productive ones. But these areas strongly depend on the mapped length of the river, so the quality of the network becomes important.

Here, we try to estimate the DEM and network quality in relation to hydrological criteria. Indeed, the DEM and network quality are usually estimated using numerical or computable criteria, and it occurs that these criteria can be opposite. In this case, the quality of the DEM-derived network may not be reliable. To avoid this problem, we present a comparison between networks derived from a DEM, cartographic data and ground observations.

First we recall the usual way of creating a DEM, and then deriving the drainage network from a DEM. Then we discuss the accuracy of drainage network calculated by a DEM and its coherence versus the observed drainage network.

1 Drainage network determination using a DEM

1.1 DEM processing

To create a DEM, it is possible to use satellite data, but the resulting quality is lower than using maps at 1/25000. The mean error is about 10m in altitude (using SPOT panchromatic with 10m resolution), with local variations perturbing slope calculation and consequently drainage directions. Contour lines are more useful for creating an accurate DEM.

Determination of a DEM uses the following stages: 1) taking points, 2) selection, 3) interpolation, and 4) storage. At each stage, we can use various methods. The accuracy of a DEM is strongly linked to the method used (for example a regular or irregular storage) but also from the resolution used (size of ground information).

1.2 Extracting the drainage network from a DEM

We distinguish between 'local' and 'global' algorithms, i.e.

local — determining the local flow direction, using altitude, slope or aspect layers,
global — determining first particular points as passes or summits, then progressing along thalwegs.

Local algorithms are more common. They start from an *altitude layer* of the DEM and use a structural element (3x3 or 5x5) which moves along the image. A first step determines a *flow directions layer* using 4-neighbours (or 8-neighbours), where each pixel value ranges from 1 to 4 (or 8) defining which neighbour receives the flow. Starting from upstream pixels (cases without flow) and progressing downstream, we sum the number of pixels to calculate the *accumulated drainage area layer*.

The simplest extracting techniques use a threshold *So* on the accumulated drainage area which is considered as a **critical area** (Montgomery and Dietrich, 1988), or a **support area** (Blöschl and Sivalapan , 1995) and represents the area where flows begin: if $S > So$, the pixel is a drain-pixel, if not it is a hillslope pixel.

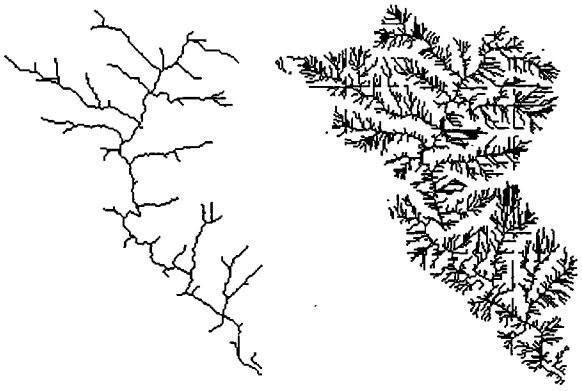

Threshold = 100 pixels Threshold = 5 pixels
Site : REAL COLLOBRIER (Var)- Mauret catchment

Figure 1: Examples of determination of the drainage network using DEM. Which threshold can we choose? (1 pixel = 0.04 ha).

Accuracy of results depends on pixel size (Moussa, 1991). But there is a more immediate effect due to the threshold *So*. The mapped network can be just one point (the outlet, when *So* equals the catchment area) or it can be the whole image (each pixel is a drain pixel when *So* = 1 pixel). Every intermediate solution is possible, as illustrate by Figure 1 (Adam, 1996). Two points are very important here.

Is it possible (what is the significance) to fix such a value to define the network? "The fixation of getting a number, or a fit, can hide the comprehension of what is done choosing a single value" (Blöschl and Sivapalan, 1995).

If so, what value of the critical area *So* should be chosen? The choice is often made " in a subjective manner as insufficient guidance is available based on physical considerations" (Blöschl and Sivapalan, 1995).

2 Quality and meaning of drainage network

The focus here is on the differences between the computing and thematic points of view. The first requires simple and constant criteria for the calculations, the second needs hydrologically consistent criteria.

When using the accumulated drainage area, we have a parameter which is very easy to calculate using a DEM (with some errors, see 2.2) but the pertinence of the criteria which defines the point where flow begins is not clear. Hydrologists do know that the beginning of flow depends on climate, rainfall and local characteristics, e.g. morphology (slope) and geology. Some texts are very critical: " There is a considerable debate as to whether the use of a support area is the best method to define channel initiation, considering the spatial non uniformity of geology, soils and rainfall over large geographical regions" (Blöschl and Sivapalan, 1995). But, too often, users of DEM techniques do not consider these remarks and take rough thresholds for the network computation. A few papers indicate that the problem exists for "large regions" as there is no problem on small areas where the variance of the critical area is assumed to be low and, consequently, the use of a drainage area parameter becomes valuable.

In order to assess the quality of the DEM and of the associated drainage network, and to investigate the variability of the critical area, we have compared the DEM with ground observations for a small domain (100km²) in a geologically uniform mountainous area.

2.1 Study Area

The study area is the Real Collobrier Catchment, Var, France, where we have a DEM (at 20 m resolution, from IGN maps at 1/25000). The *drainage area layer* has been calculated at 20 m resolution and, for each pixel, we can estimate the upstream area.

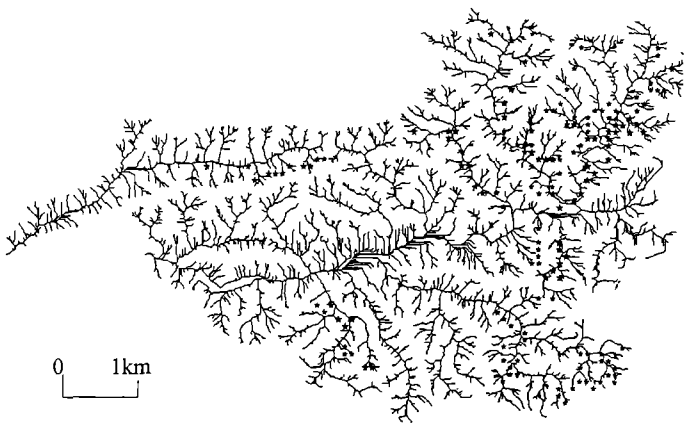

Figure 2: Experimental scheme for discharge meausurements.

Ground observations (local slope, discharge or no discharge) have been taken in two periods in April 1996 in nine sub-catchments with different landcovers, slopes and geology: 4th to 5th April — 70 points of observation; and 29th April to 3rd May — 115 points of observation. Because observations were made during a wet period, in April 1996, a large number of small drains were running. Figure 2 shows the measurement points.

2.2 Is the mapping of flow paths correct ?

First, we have to keep in mind that a DEM calculated from topographical maps may not be more accurate than maps. A computed DEM appears interesting because the approach is systematic and automatic, but not because results are more accurate. Each calculation stage has its artefacts, and accuracy decreases. Second, the standard DEM uses algorithms whose priorities are computational efficiency. This gives good results in many uses of DEM, but can produce a poor determination of flow paths, for example in flat areas. In fact, these computational criteria can be opposite to hydrological ones.

For example, in the selection stage, the number of selected points is generally high in mountainous zones (rapid variations in altitude), and low in flat zones. But, to define the hydrological network, we need the opposite; a few points in mountainous zones and a high density in flat ones. Another example concerns the interpolation stage which often uses statistical algorithms such as linear interpolation or spline functions. Then, the calculated DEM may present many local holes and hills due to calculation artefacts, leading possibly to poor hydraulic consistency. Before network calculation it is necessary to clean-up the DEM using specific algorithms to eliminate any holes. But these procedures add complementary errors. However, it is obvious that the initial contour lines are consistent hydraulically. It is possible to define by hand the flow direction in every point of a map. That is why some interpolation methods based on water path notions such as lines of maximum slope have been developed (Proy, 1986 ; Soille, 1997). They give DEM with less holes and hills than commercial DEMs (Puech, 1993).

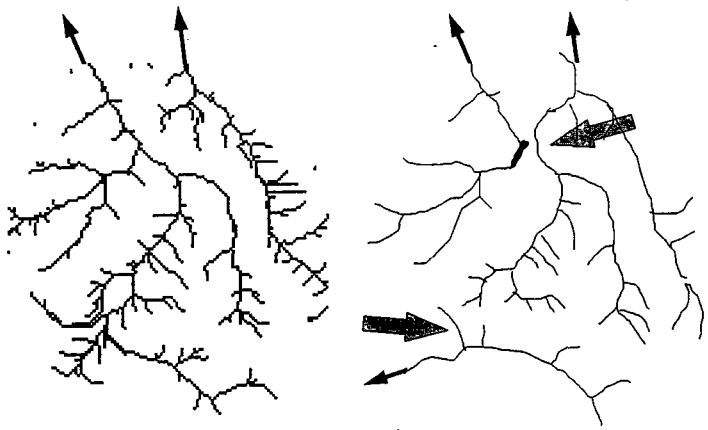

Figure 3: Errors of drawing using DEM (point of geological capture indicated by arrow).

Comparing ground observation, maps and the computed DEM gives the following results. In mountainous areas (Maurets and Valescure catchments, with slopes of about 25%), no errors are noticed. The network is well detected and well mapped. In flat areas serious errors have been detected. For example, in the Rimbaud catchment, with slopes of about 5%, two small drains have been associated with the wrong catchment, so the catchment area has been reduced by 10% (Adam, 1996). In the Meffrey catchment we have noticed the same phenomenon of 'flow captures' in flat areas (Fig. 3). These observations are consistent with previous work. In fact, creating a good DEM requires the use of 'structure lines' such as cliffs, crests and river beds in the interpolation stage (Labbe, 1992). Moreover, defining the true directions of flow paths needs a high quality DEM, which implies it has been created using these lines. The initial knowledge of the drainage network is the best guarantee to define a good DEM, in order to calculate a good drainage network!

2.3 Validity of the threshold for critical area *So*

2.3.1 Observed flow rate versus drainage area

On each observed plot, we have two groups of information: (a) *discharge* or *lack of flow, slope* and *bed distance* from observed ground data; and (b) *upstream area* calculated by its position in the DEM.

For a given upstream area, the discharge varies strongly from one catchment to the other. For example on 29th April 1996, for an upstream area of 30ha, 90% of the discharge values ranges from 1 l/s to 10 l/s (Figure 4).

Comparing these two data we notice that, for a given day, the discharge value seems well linked to the upstream area if the studied zone is small, i.e. inside a sub-catchment. In fact, on each stream the upstream area corresponding to commencement of flow is slightly different from the neighbouring

streams. But, for a given sub-catchment, it is possible to estimate a mean critical area, i.e. a mean value for the area at which flow begins.

To define the mean critical area *So* for a given day we used a statistical method. For each value of the threshold, the DEM separates drain-pixels and hillslope-pixels. Then we can number how many plots with flow are hillslope-pixels (error1) and how many pixels with no flow are drain-pixels (error2). When *So* increases, error1 decreases and error2 increases. We chose *So* corresponding to error1 <10% of plots.

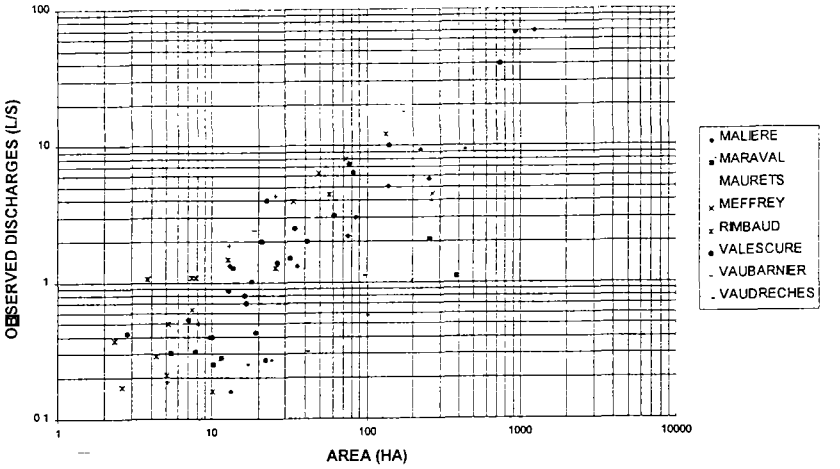

Figure 4: Observed discharges on 29.04.96 versus upstream area.

We have calculated the critical area for the different days of measurements (4th April and 29th April 1996) and each sub-catchment. Even if the discharge is strongly different (from 1 to 10 l/s for an area of 30ha), the position where flow begins is less variable. We have noticed a few differences in the critical area, perhaps due to the presence of multiple springs.

Results for critical area on 29th April 1996 are given in Table 1.

TABLE 1: Critical area 29th April 1996

Sub-catchment name	critical area (ha) 29th April 1996	Geology	Mean Slope	forest cover
Rimbaud	1	gneiss	5%	bushes
Maliere	6	mixed	15%	oaks
Maraval	5	schistes	20%	pines
Maurets	6	phyllades	25%	oaks
Meffrey	6	phyllades	20%	pines + oaks
Valescure	7	mixed	40%	oaks
Vaudreches	15	phyllades	35%	oaks
Vaubarnier	4	mixed	20%	chestnuts

Between sub-catchments we notice great differences. The critical area estimated on 29th April 1996 varies from about 1 ha in the Rimbaud catchment to about 15 ha in the Vaudreches catchment. These large differences in the same zone (the distance between these two sub-catchments is about 3 kilometres) indicates that the solution using a unique threshold to define a drainage network from a DEM is not acceptable. The variations of the critical area from one catchment to the others seem to be linked to local conditions such as geology, pedology, slopes and land cover. Montgomery and Dietrich (1988) have noticed a link between local slope and critical area. Crave (1995) indicates probable links with climate, land cover and permeability. We first tried to use these characteristics to explain the differences.

First we used, instead of the *upstream area*, the *topographic index* ATB (Beven and Kirkby, 1979) which is an index including both slope and upstream area:

$$ATB = Log(A) / \tan(s)$$ where A is the upstream area and s the local slope.

But, the difference between catchments still ranges from 1 to 10 when comparing the observed discharges for a given *topographic index* value. So, slope does not explain all the differences.

Geology seems more significant, but the Real Collobrier zone is very complicated, most of the area being a geological patchwork. Furthemore, we have too few data. The most interesting catchment, Rimbaud (1 km²), is quite different from the other catchments. There, slopes are low, geology is gneiss, land cover is poor and discharges are high with streams starting near the crest marked by the catchment boundary (less than 1 ha for upstream area). But which characteristic is important? We cannot, with these data, determine a strong link between descriptive attributes and discharges.

This work also questions the real meaning of a hydrological drain. For a given day it is possible to separate drains and slope. In the field, we have also noticed differences between dry drain (visible but no flow) and wet drain (visible with flow). But the limits are variable in time. Some approaches suppose that this limit can go upstream and reach the very crest. With this idea, every point may become a drain-pixel if the rainfall is sufficient. In usual rain events, such as during our ground observations, the response is clear. Drains only appear after a few hectares (from 0.5 to 5 depending on the location). So, every point of the catchment can not be a drain.

When considering large areas (regional scale) we observe the largest rivers and channels. Then the description scheme of network appears to be fractal, with similar patterns from one scale to the other. But considering small areas (local scale or hillslope scale) the network representation appears scale dependent. Indeed, the network changes nature when approaching springs. There, the vertical dimension versus the horizontal dimension becomes important and can not be neglected. Slopes, geology, soil depths, become important to define the flow paths which cannot be explained only by the morphology. In this case the fractal scheme is broken and the network on slopes is not similar to the regional network.

How, then, can the drainage network at hillslope scale be determined? We are convinced that to define the network precisely we need to add ground information to DEM, indicating where flows begin. The easier way is to use the networks drawn on topographic maps, because these include the memory of observed flows.

2.3.2 Comparison with map at 1/25000

In order to be sure that this way is correct, we have compared our ground data with topographic maps. Using a DEM, each mapped end of river can be characterised by its upstream area. We have analysed the statistical distributions of these upstream areas, assuming that the median value is representative of each sub-catchment. We observe large differences between the different sub-catchments, as indicated in Table 2.

TABLE 2: Distribution of upstream area from 1/25000 map

Sub-catchment name	upstream area frequency 0.10	upstream area frequency 0.50 (Median value)	upstream area frequency 90%
Rimbaud	0.8	3.5	4
Maliere	0.8	3	8.8
Maraval	2.4	1.8	7.2
Maurets	1.6	2	5.6
Meffrey	0.8	1.6	4
Valescure	0.8	3	6.4
Vaudreches	2.4	3	11.2
Vaubarnier	2.4	4	5.6

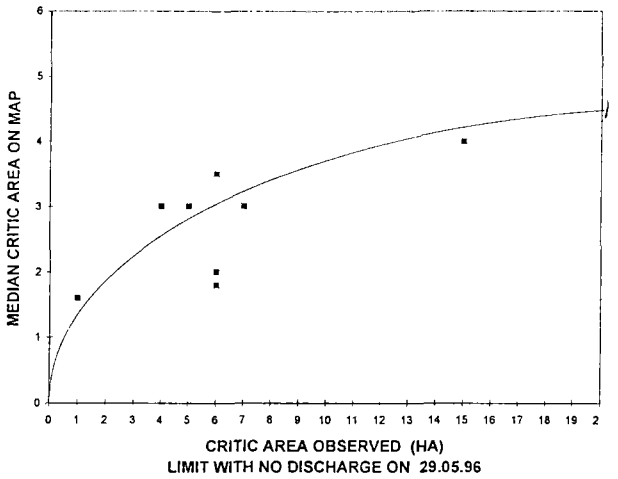

Figure 5: Comparison between observed critic area on 29.04.96 and map critic area.

Comparing the critical areas, the one observed on 29th April 1996 and the median critical area given by maps, a good link is observed (Fig. 5). This confirms that the ends of rivers on precise maps are significant. This information is not perfect. We have noticed some errors, in particular some streams with flow where the map indicates no river. But, generally, using map information appears more precise than using a unique threshold for the critical area.

Conclusion

The use of automatic procedures for processing DEMs and extracting a drainage network is growing. Accuracy is not always indicated but hydrologists use these tools more and more. In this paper we have discussed the drainage network accuracy through a comparison with ground data.

For hydrological purposes, automatic procedures for creating a DEM and extracting drainage networks do not give sufficient accuracy. First, creating a good DEM requires the use of structure lines including the drainage network itself. Otherwise, serious errors may appear in flat areas. Even with 5% slopes, the drawing of flow paths becomes erratic. Secondly, upstream limits of the drainage network are not defined by a unique value of accumulated drainage area. Even in small zones, due to the local context (slopes, geology, etc.), this value ranges by more than an order of magnitude. To define a good network, the morphology (given by a DEM) appears to be insufficient. We need additional information corresponding to the points where flow begins. No covariate parameter (geology, slope, etc.) easily gives this information. To improve it by means other than ground observations, the only way remaining is the determination of the start of the streams marked on maps. Precise maps (1/25000 if possible), which merge a part of subjective drawings and a part of true observations, remains the less bad way, certainly better than extraction from a DEM alone.

So, the use of automatic procedures to extract the drainage network from a DEM does not give a better accuracy on morphology. The interest lies in the automatic and systematic use of information. These new tools also permit a new description of space with new criteria which are easy to calculate and pertinent for the analysis, e.g. the accumulated drainage area. But flows are complex due to their natural origin. The hydrological catchment behaviour (and the network extremities) can not be defined only through geometric criteria derived from a DEM. Other data are needed, which can be obtained from a field survey or a simple map due to the fact that " in hydrology, bad ground data often give more information than long calculation" (Roche, 1964).

References

ADAM, A. (1996) 'Extraction du réseau hydrographique d'un MNT et confrontation au terrain. Application au bassin versant du Réal Collobrier.' *DEA Université Montpellier I*, 50p.

BEVEN, K. and M.J. KIRKBY (1979) 'A physically-based variable contributing area model of basin hydrology'. *Hydrol. Science Bull.* (24), 43-69.

BLÖSCHL and SIVAPALAN (1995) 'Scale issues in hydrological modelling : a review.' *Hydrological processes.* Vol 9 251-290.

CRAVE, A. (1995) 'Quantification de l'organisation des réseaux hydrographiques.' *Thèse Univ. Rennes 1.* 200p.

LABBE, S. (1992). 'Intégration télédétection et systèmes d'information géographique. Algorithme des corrections d'image utilisant les modèles numériques de terrain'. *DEA Univ. Montpellier II*, 83 p.

MOUSSA, R. (1991) 'Variabilité spatio temporelle et modélisation hydrologique'. *Thèse Univ. de Montpellier II.*

MONTGOMERY, D.R. and W.E. DIETRICH (1988) 'Where do channels begin ?' *Nature 336.* 232-234.

PUECH, C. (1993) 'Détermination des états de surface par télédétection pour caractériser les écoulements des petits bassins versants - application à des bassins en zone méditerranéenne et en zone tropicale sèche'. *Thèse, Université Joseph FOURIER, Grenoble I*, 217 p.

PROY, C. (1986) 'Intégration du relief aux traitements d'images de télédétection.' *Thèse de docteur-ingénieur. Institut National Polytechnique de Toulouse,* 173 p.

ROCHE, M. (1964) 'Hydrologie de surface'. *Gauthier Villars Paris.* ORSTOM. 430 p.

SOILLE, P. (1997) 'Analyse d'images par la morphologie mathématique.' Thèse HDR. Univ. Montpellier II.

Names and adresses of the authors

ABRIL, M. : Institute of Earth Sciences Jaume Almera (CSIC), Solé i Sabaris s/n
ES-08028 Barcelona
Spain

ADAM, A. : LCT CEMAGREF-ENGREF
500, rue J.F. Breton
34093 Montpellier Cedex5
France.
Tél (33) 04 67 54 87 54
Fax (33) 04 67 54 87 00

AMBROISE, B. :Centre d'Etudes et de Recherches Eco-Géographiques, URA 95 CNRS, ULP
3 rue de l'Argonne
67083 Strasbourg Cedex, France
Tél (33) 03 88 45 64 41
Fax (33) 03 88 41 13 59
E-mail ambroise@geographie.u-strasbg.fr

ANDRIEUX, P., : INRA Science du Sol,
2 place Viala,
34060 Montpellier Cedex1
France
Tél (33) 04 67 61 23 09
Fax (33) 04 67 63 26 14
E-mail andrieux@montpellier.ensam.inra.fr

BARIAC, T. : Laboratoire de Biogéochimie Isotopique, BGCI (UPMC/CNRS/INRA), Case 120, 4 place Jussieu,
75252 Paris
France
Tél (33) 01 44 27 59 98
Fax (33) 01 44.27 41 64
E-mail bariac@ccr.jussieu.fr

BECKER, A. :Potsdam Institute for Climate Impact Research (PIK)
P.O.Box 601203
Telegrafenberg
D-14412 Potsdam
Germany

BIRON, P. : Centre d'Etudes et de Recherches Eco-Géographiques, URA 95 CNRS, ULP
3 rue de l'Argonne
67083 Strasbourg Cedex
France
Tél (33) 03 88 45 64 35
Fax (33) 03 88 41 13 59
E-mail biron@geographie.u-strasbg.fr

BOUZIGUES, R. : INRA, UFR de Science du Sol
2 Place Pierre Viala
34060 Montpellier Cedex1
France

BRAUD, I. : LTHE/IMG
(URA 1512 CNRS-INPG-UJF)
BP 53
38041 Grenoble Cedex 9 France.

BROCHOT, S. :Cemagref Grenoble, Division Protection contre les Erosions
BP 76
38402 St Martin d'Hères
France

BUCHTELE, J. : Institute of Hydrodynamics, Czech Academy of Sciences
166 12 Prague 6
Czech Republic
Tél (42) 2 24310671
Fax (42) 2 2322 181

BURCH, H. : Section of Forest Hydrology at the Swiss Federal Institute for Forest, Snow and Landscape Research (FSL)
Zürcherstrasse 111
CH-8903 Birmensdorf
Switzerland
Tél (41) 1 739 24 80
Fax (41) 1 739 24 88
E-mail burch@wsl.ch

BUCEK, J. : Czech Hydrometeorological Institute,
Na sabatce 17
143 06 Praha,
Czech Republic

CANN, CH. : CEMAGREF
17, avenue de Cucillé
F-35044 Rennes Cedex
France

CEBALLOS, A. : Dept. of Geography Universidad de Extremadura
Avda. de los Quijotes s/n
10.003 Cáceres
Spain
Tél (34) 27 24 96 00
Fax (34) 27 24 88 58
E-mail aceballo@unex.es

CORBU, C. : National Institute of Meteorology and Hydrology
Soseaua Bucuresti-Ploiesti 97
77551 Bucharest
Romania

DAMBRINE, E. : Centre de Recherches Forestières
INRA Nancy-Champenoux,
54280 Seichamps
France

DEMUTH, S. : Department of Hydrology, University of Freiburg
Werderring 4
D-79085 Freiburg
Germany

DIJKSMA, R. : Department of Water Resources
Nieuwe Kanaal 11
6709 PA Wageningen
The Netherlands
Tél (31) 317 482778
Fax (31) 317 484885l
E-mail roeldijksma@whh.au.nl

ETZENBERG, CH. : International Graduate School Institute
Markt 23
D-02763 Zittau
Germany
Tél (49) 03583-771518
Fax (49) 03583-771534
E-mail etzenber@novell1.ihi.htw-zittau.de

FEGER, K.H.: Albert-Ludwigs-Universität, Institute for Soil Science and Forest Nutrition
Bertoldstrasse 17
D-79098 Freiburg,
Germany

FISCHER, L. : Centre d'Etudes et de Recherches Eco-Géographiques, CNRS/ULP
3 rue de l'Argonne
67083 Strasbourg Cedex
France

FOUCHE-ROGUIEZ, S. : Centre d'Etudes et de Recherches Eco-Géographiques, URA 95 CNRS, ULP
3 rue de l'Argonne
67083 Strasbourg Cedex
France
Tél (33) 03 88 45 64 32
Fax (33) 03 88 41 13 59
E-mail fouche@geographie.u-strasbg.fr

FRITSCHE, V. : DR/HGT, BRGM,
BP 6009
45060 Orléans Cedex2
France

FRITSCHI, B. : Section of Forest Hydrology at the Swiss Federal Institute for Forest, Snow and Landscape Research (FSL)
Zürcherstrasse 111
CH-8903 Birmensdorf
Switzerland

GALLART, F. : Institute of Earth Sciences Jaume Almera (CSIC)
Solé i Sabaris s/n
ES-08028 Barcelona
Spain
Tel (34) 3 3302800
Fax (34) 3 4110012
E-mail fgallart@ija.csic.es

GINESTE, P. : Remote Sensing Laboratory CEMAGREF-ENGREF
500, rue J.F. Breton, 34093
Montpellier Cedex5
France.
Tél (33) 04 67 54 87 54
Fax (33) 04 67 54 87 00
E-mail
philippe.gineste@teledetection.fr

GRANIER, A.: Centre de Recherches Forestières, INRA Nancy-Champenoux
54280 Seichamps
France

HERRMANN, A. : Institute for Geography and Geoecology, Technical University
Langer Kamp 19c
D-38106 Braunschweig
Germany.
Tél (49) 531 391 8170
Fax (49) 531 8170
E-mail herrmann@ifgug.nat.tu-bs.de

HOLKO,L. : Institute of Hydrology SAS, Ondrasovecka 16
031 05 Liptovsky Mikulas
Slovakia

IDIR, S. : Centre de Géochimie de la Surface / CNRS,
1 rue Blessig
67084 Strasbourg Cedex, France
Tel (33) 03 88 35 85 56
Fax (33) 03 88 36 72 35
E-mail sidir@illite.u-strasbg.fr

JOSEPH, C. : URA CNRS Géofluides, Bassin et Eau, Place E. Bataillon,
34095 Montpellier Cedex2
France

KIM, M.K.: Institute for Geography and Geoecology, Technical University,
Langer Kamp 19c,
D-38106 Braunschweig, Germany.

KOLE , J.W. : Department of Water Resources,
Nieuwe Kanaal 11,
6709 PA Wageningen,
The Netherlands

KONICEK, A. : Institute of Hydrology SAS
Racianska 75
P.O. Box 94
83008 Bratislava, Slovakia
Tél (42) 7 259 346
Fax (42) 7 259 346
E-mail pekarova@uh.savba.sk

KOSTKA, Z. : Institute of Hydrology SAS, Ondrasovecka 16
031 05 Liptovsky Mikulas
Slovakia

KRYSANOVA, V., Potsdam Institute for Climate Impact Research (PIK)
P.O.Box 601203 Telegrafenberg
D-14412 Potsdam
Germany
Tél (49) 331 288 2524
E-mail lahmer@pik-postdam.de

LADOUCHE, B. : Laboratoire de Biogéochimie Isotopique, BGCI (UPMC/CNRS/INRA), Case 120
4 place Jussieu
75252 Paris
France
Tél (33) 01 44 27 51 81
Fax (33) 01 44.27 41 64
E-mail ladouche@ccr.jussieu.fr

LAHMER, W. : Potsdam Institute for Climate Impact Research (PIK)
P.O.Box 601203, Telegrafenberg
D-14412 Potsdam
Germany

LATRON, J. : Institute of Earth Sciences Jaume Almera (CSIC)
Solé i Sabaris s/n,
ES-08028 Barcelona
Spain
Tel (34) 3 490 05 32
Fax (34) 3 4110012
E-mail:jlatron@ija.csic.es

LEIBUNDGUT, CH., : Department of Hydrology, University of Freiburg, Werderring 4
D-79085 Freiburg, Germany

LEPISTÖ, A. : Finnish Environment Agency, Kesäkatu 6,
00260 Helsinki
Finland

LLORENS, P. : Institute of Earth Sciences Jaume Almera (CSIC), Solé i Sabaris s/n, ES-08028 Barcelona Spain Tel (34) 3 3302800 Fax (34) 3 4110012 E-mail pllorens@ija.csic.es

LOUBET, M. : Laboratoire de Géochimie (UPS/LMTG) 38 rue des 36 Ponts 34100 Toulouse France

MATHYS, N. : Cemagref Grenoble, Division Protection contre les Erosions BP 76 38402 St Martin d'Hères, France Tél (33) 04 76 76 27 57 Fax (33) 04 76 51 38 03 E-mail nicolle.mathys@ grenoble.cemagref.fr

MEUNIER, M. :Cemagref Grenoble, Division Protection contre les Erosions BP 76, 38402 St Martin d'Hères, France

MENZEL, L. : Department of Geography, Hydrology Section, Federal Institute of Technology ETH, Zürich Switzerland Tél (41) 1257 52 34 Fax (41) 1362 5197 E-mail menzel@geo.umnw.ethz.ch

MESZAROS I. : Institute of Hydrology SAS, Racianska 75, P.O. Box 94, 831 01 Bratislava Slovakia, Tel (+427) 259 311 E-mail meszaros@uh.savba.sk

MIKLANEK, P. : Institute of Hydrology SAS, Racianska 75 P.O. Box 94 83008 Bratislava, Slovakia Tél (42) 7 259 311 Fax (42) 7 259 311 E-mail ncihp@uh.savba.sk

MITA, P. : National Institute of Meteorology and Hydrology Soseaua Bucuresti-Ploiesti 97 77551 Bucharest Romania Tél (40) 1 31 29842 Fax (40) 1 31 29843 E-mail relatii@meteo.i.n.m.h.ro

MOLNAR, L. : Institute of Hydrology SAS Racianska 75 P.O. Box 94 831 01 Bratislava Slovakia tel (+427) 259 311 E-mail meszaros@uh.savba.sk.

MOUSSA, R. : INRA, UFR Science du Sol, 2 Place Viala 34060 Montpellier Cedex1 France Tél (33) 03 67 61 24 56 Fax (33) 03 67 63 26 14 E-mail moussa@ensam.inra.fr

MÜLLER, G. : International Graduate School Institute, Markt 23 D-02763 Zittau Germany

MÜLLER-WOHLEIL, D.I. Potsdam Institute for Climate Impact Research (PIK) P.O.Box 601203 Telegrafenberg D-14412 Potsdam Germany

NAJJAR, G. : Centre d'Etudes et de Recherches Eco-Géographiques, CNRS/ULP, 3 rue de l'Argonne, 67083 Strasbourg Cedex France Tél (33) 03 88 45 64 35 Fax (33) 03 88 41 13 59 E-mail najjar@geographie.u-strasbg.fr

NOILHAN, J. : Météo-France/CNRM 42 av. Coriolis 31057 Toulouse Cedex France.

PATOUX, J. :ORSTOM Casilla 34 - Correo 2 Antofagasta Chile

PAUWELS, H. : DR/HGT, BRGM BP 6009 F-45060 Orléans Cedex 2 France

PEKAR, J. : Department of Numerical and Optimising Methods, Comenius University Bratislava, Slovakia

PEKAROVA, P. : Institute of Hydrology SAS Racianska 75 P.O. Box 94 83008 Bratislava Slovakia Tél (42) 7 259 346 Fax (42) 7 259 346 E-mail pekarova@uh.savba.sk

PESCHKE, G . : International Graduate School Institute Markt 23 D-02763 Zittau Germany

PFISTER, L. : Centre d'Etudes et de Recherches Eco-Géographiques, URA 95 CNRS, ULP 3 rue de l'Argonne 67083 Strasbourg Cedex France Tél (33) 03 88 45 64 36 Fax (33) 03 88 41 13 59

PINAULT, J.L. : DR/HGT, BRGM, BP 6009 F-45060 Orléans Cedex 2 France Tél (33) 02 38 64 39 73 Fax (33) 02 38 64 47 30 E-mail jlpinault@brgm.fr

POCH, R. : Institute of Earth Sciences Jaume Almera (CSIC) Solé i Sabaris s/n, ES-08028 Barcelona Spain

POURRUT, P. : ORSTOM
Casilla 34 - Correo 2
Antofagasta
Chile
Fax (56 55) 24 53 18
E-mail
ppourrut@socompa.cecun.ucn.cl

PRAZAK, J. : Institute for Thermomechanics,
Dolejskova 5
182 00 Praha 8
Czech Republic

PROBST, A. : Centre de Géochimie de la Surface / CNRS,
1 rue Blessig
67084 Strasbourg Cedex
France
Tel (33) 03 88 35 85 39
Fax (33) 03 88 36 72 35
E-mail aprobst@illite.u-strasbg.fr

PROBST, J.L. : Centre de Géochimie de la Surface / CNRS,
1 rue Blessig
67084 Strasbourg Cedex
France
Tel (33) 03 88 35 85 73
Fax (33) 03 88 36 72 35
E-mail jlprobst@illite.u-strasbg.fr

PUECH , C. : Remote Sensing Laboratory CEMAGREF-ENGREF
500, rue J.F. Breton
34093 Montpellier Cedex 5
France
Tel (33) 04 67 54 87 54
Fax (33) 04 67 54 87 00
E-mail
christian.puech@teledetection.fr

RIBOLZI, O. : INRA, Unité de Science du Sol, Domaine Saint-Paul, Site Agroparc
84914 Avignon Cedex 09,
France

RICHARD, S. : Centre d'Etudes et de Recherches Eco-Géographiques, CNRS, ULP,
3 rue de l'Argonne
67083 Strasbourg Cedex
France
Tél (33) 03 88 45 64 36
Fax (33) 03 88 41 13 59

ROGG, M. : Department of Hydrology, University of Freiburg
Werderring 4
D-79085 Freiburg,
Germany

ROLKE, A., : Department of Hydrology, University of Freiburg,
Werderring 4
D-79085 Freiburg,
Germany
Tél (49) 0761 203 3539
Fax (49) 0761 203 3594

RONCAK, P. : Slovak Hydrometeorological Institute,
Bratislava
Slovakia

SALVANY, M.C. : Institute of Earth Sciences Jaume Almera (CSIC),
Solé i Sabaris s/n
ES-08028 Barcelona,
Spain

SCHNABEL, S. : Dept. of Geography,
Universidad de Extremadura,
Avda. de los Quijotes s/n
10.003 Cáceres
Spain

SIR, M. : Institute of Hydrodynamics,
Podbabska 13
166 12 Praha 6,
Czech Republic

TESAR, M. : Institute of Hydrodynamics,
Podbabska 13
166 12 Praha 6
Czech Republic
Tél (42) 2 342 590
Fax (42) 2 322 181

TRAMBOUZE, W. : INRA Science du sol
2 Pl.Viala
34060 Montpellier Cedex I
France

VAN DE WEERD, B. : Department of Water Resources,
Nieuwe Kanaal 11
6709 PA Wageningen,
The Netherlands

VAN LANEN, H.A.J. : Department of Water Resources,
Nieuwe Kanaal 11
6709 PA Wageningen
The Netherlands

VITVAR, T. :Geographical Institute, Hydrology Section,
Swiss Federal Institute of Technology, Winterthurerstrasse 190
CH-8057 Zurich
Switzerland
Tél (41) 01 257 54 09
Fax (41) 01 362 51 97
E-mail
tomas@geo.umnw.ethz.ch

VIVILLE, D. : Centre d'Etudes et de Recherches Eco-Géographiques, URA 95 CNRS, ULP
3 rue de l'Argonne,
67083 Strasbourg Cedex
France
Tél (33) 03 88 45 64 36
Fax (33) 03 88 41 13 59
E-mail viville@geographie.u-strasbg.fr

VOLTZ, M., : INRA Science du Sol
2 place Viala
34060 Montpellier Cedex 1
France
Tél (33) 04 67 61 23 40
Fax (33) 04 67 63 26 14
E-mail voltz@ensam.inra.fr

WALDNER, P. : Section of Forest Hydrology at the Swiss Federal Institute for Forest, Snow and Landscape Research (FSL)
Zürcherstrasse 111
CH-8903 Birmensdorf
Switzerland

WARMERDAM, P.M.M.:
Department of Water Resources,
Nieuwe Kanaal 11
6709 PA Wageningen,
the Netherlands
Tél (31) 317 482778
Fax (31) 317 4848851
E-mail
roeldijksma@users@whh.au.nl

WEGEHENKEL, M. : ZALF e.V.,
Institute for Landscape modeling
Eberswalder Strasse 84
D-15374 Münchenberg
Germany
Tél (49) 33432 82 275
Fax (49) 33432 82 334
E-mail mwegehenkel@zalf.de

ZIMMERMANN, L. : Albert-
Ludwigs-Universität, Institute
for Soil Science and Forest
Nutrition,
Bertoldstrasse 17
D-79098 Freiburg am Breisgau,
Germany
Tél (49) 0761 203 3621
Fax (49) 0761 203 3618
E-mail lziml@ruf.uni-
freiburg.de